FEVALUATION OF SYMPTOMATIC AND NEUROPROTECTIVE EFFICACY OF CERTAIN PHYTOCHEMICALS IN *DROSOPHILA* MODEL OF PARKINSON'S DISEASE

By

Mr. MOHAMAD AYAJUDDIN, *M Phil*

Registration No 636/2015

Submitted to

NAGALAND UNIVERSITY

(A Central University)

In fulfillment of requirements for the Degree

of

DOCTOR OF PHILOSOPHY IN ZOOLOGY

DEPARTMENT OF ZOOLOGY
NAGALAND UNIVERSITY
LUMAMI-798627
NAGALAND, INDIA

2022

NAGALAND UNIVERSITY

(A Central University)

DEPARTMENT OF ZOOLOGY

Headquarters: Lumami, Zunheboto District-798627, Nagaland, India

---

DECLARATION

I, **Mr. Mohamad Ayajuddin**, hereby declare that the subject matter of this thesis is the record of work done by me, that the contents of this thesis did not form basis for the award of any previous degree to me or to the best of my knowledge and to anybody else, and that the thesis has not been submitted by me for any research degree in any other university.

This is being submitted to Nagaland University for the degree of Doctor of Philosophy in Zoology.

Date:
Place: Lumami

Mohamad Ayajuddin, *M. Phil.*
(Candidate)

Head of Department

(Dr. Bendang Ao)
Professor
विभागाध्यक्ष / Head
प्राणि विज्ञान विभाग / Department of Zoology
नागालैंड विश्वविद्यालय / Nagaland University
लुमामी / Lumami - 798627

Supervisor

(Dr. Sarat Chandra Yenisetti)
Professor

Dr. Sarat Chandra Yenisetti, Ph.D
Professor
Department of Zoology
Nagaland University Lumami-798627
Nagaland, India

NAGALAND UNIVERSITY

(A Central University)
OFFICE OF THE HEAD OF DEPARTMENT
DEPARTMENT OF ZOOLOGY
Headquarters: Lumami, Zunheboto District-798627, Nagaland, India

---

CERTIFICATE

This is to certify that the thesis entitled "**Evaluation of Symptomatic and Neuroprotective Efficacy of Certain Phytochemicals in Drosophila Model of Parkinson's Disease**" is a record of original research work done by **Mr. Mohamad Ayajuddin**. He is a registered research scholar bearing **Regd. No. 636/2015** of the Department and has fulfilled all the requirements of Ph.D. regulations of Nagaland University for the submission of the thesis. The work is original and neither the thesis nor any part of it has been submitted elsewhere for the award of any other degree or distinctions. The thesis is therefore, forwarded for adjudication and consideration for the award of degree of **Doctor of Philosophy in Zoology** under Nagaland University.

Date:
Place: Lumami

Head of Department

(Dr. Bendang Ao)
Professor
विभागाध्यक्ष / Head
प्राणि विज्ञान विभाग / Department of Zoology
नागालैंड विश्वविद्यालय / Nagaland University
लुमामी / Lumami - 798627

Supervisor

(Dr. Sarat Chandra Yenisetti)
Professor

Dr. Sarat Chandra Yenisetti, Ph.D
Professor
Department of Zoology
Nagaland University Lumami - 798627
Nagaland, India.

Acknowledgments

All glory to Almighty!!!

This study was conducted at the Drosophila Neurobiology Laboratory, Department of Zoology, Nagaland University (Central), Lumami campus, Nagaland. I had the privilege of carrying out my research work under the supervision of ***Dr. Sarat Chandra Yenisetti****. His knowledge of the broad fields of neuroscience and genetics is truly admirable. Albeit working on several demanding projects simultaneously, he always gave time for discussions on scientific and non-scientific matters. I am truly grateful for his patience and support during the ups and downs of this project. Without his positive attitude, this thesis would never have been completed. His patience and enthusiasm for neuroscience provided the initial spark for my motivation to produce this thesis. His creativity and efficacy in designing and conducting experiment are something that I admire the most. I thank him for spending his valuable time in teaching me everything about experiments starting from scratch. I thank him for his tireless support and help in various successful experiments and for providing motivation after failed ones during the course of my work. I learned a great deal of myself while staying with him.*

I extend my humble and sincere gratitude to my respected faculties at the Department of Zoology: Prof. Pardeshi Lal (Honourable vice chancellor), (L) Prof. Sharif U. Ahmed, Prof. L. N. Kakati, Dr. Bendang Ao, Mr. P. Rajesh Singh and Dr. Pranay P. Pankaj for their constructive discussions, advice and support.

I had the honour of working with the following persons in the Drosophila Neurobiology Laboratory: Dr. Bovito Achumi, Dr. Limamanen Phom, Dr. Zevelou Koza, Mrs. Priyanka

Modi, Mr. Abhik Das, Mr. Rahul Chaurasia, Ms. Abuno Thepa, Ms. Nukshimenla Jamir and Mr. kelevikho Neikha. They are acknowledged for creating a fruitful scientific atmosphere in the group as well as for many interesting non-scientific discussions. After a tight and hectic schedule in the laboratory, the time we spent together outside the laboratory is truly memorable too.

I thank my father, mother and siblings for their unconditional love and support and motivating me with soft comforts during the hard times.

It is truly said that "Most women want an established man but a strong woman supports in establishing him". I extend my warmest and deepest gratitude to my beloved wife Dr. Sultana Parveen without whose understanding and support, I could not have completed my work. Thank you for being you!!

I would like to acknowledge DBT for Junior Research Fellowship and UGC and NU for Non NET Fellowship provided to me during the initial course of my work. I would also like to deeply acknowledge ICMR, New Delhi for granting Senior Research Fellowship during the final stage of my work. Without their financial assistance, this thesis would not have come into shape. Last but not the least; I would like to acknowledge the authors of different publications for allowing me to reproduce their works.

Mohamad Ayajuddin, M. Phil.
July 2022, Nagaland

Dedicated to:

My supervisor for his tireless, constant and enthusiastic guidance

My family members for their constant support and prayer

LIST OF FIGURES AND TABLES **Page No**

Chapter 1

Chapter 2

Chapter 3

Chapter 4

LIST OF ABBREVIATIONS

α-syn: α-synuclein

3-MT: 3-Methoxytyramine

6-OHDA: 6-Hydroxydopamine

AADC: Aromatic L-Amino acid Decarboxylase

AchE: Acetylcholine Esterase

AD: Alzheimer's Disease

ADH: Aldehyde Dehydrogenase

ALP: Autophagy Lysosome Pathway

ALS: Amyotrophic Lateral Sclerosis

APBA: Aminophenylboronic Acid

ATP: Adenosine Triphosphate

BBB: Blood Brain Barrier

BDNF: Brain-Derived Neurotrophic Factor

BSA: Bovine Serum Albumin

CaMKK: Calcium/calmodulin-dependent protein Kinase Kinase

CAT: Catalase

CMA: Chaperone-Mediated Autophagy

CNS: Central Nervous System

COMT: Catechol-O-Methyltransferase

CREB: cAMP-Response Element Binding protein

CRISPR: Clustered Regularly Interspaced Short Palindromic Repeats

CUR: Curcumin

DA: Dopamine

DA-ergic: Dopaminergic

DN: Dopaminergic Neuron

DAPI: 4′,6-Diamidino-2-Phenylindole

DAT: Dopamine Transporter

DBS: Deep Brain Stimulation

DJ-1: Daisuke-Junko-1

DMSO: Dimethyl Sulfoxide

DNA: Deoxyribonucleic Acid

DOPAC: Dihydroxyphenyl Acetic Acid

DOPAL: 3,4-Dihydroxyphenylacetaldehyde

DR: Dopamine Receptor

ECD: Electrochemical Detector

ER: Endoplasmic Reticulum

ERK: Extracellular signal-Regulated Kinase

ETC: Electron Transport Chain

FDA: Food and Drug Administration

FOXO: Forkhead Box Transcription Factors

GABA: Gamma-Aminobutyric Acid

GBA: Beta-Glucocerebrosidase

GFP: Green Fluorescent Protein

GRP: Glucose-Regulated Protein

GSH: Glutathione

GST: Glutathione S-Transferase

GWASs: Genome-Wide Association Studies

HD: Huntington’s Disease

HLA: Human Leukocyte Antigen

HPLC: High Performance Liquid Chromatography

HVA: Homovanillic Acid

IFN: Interferon

IIS: Insulin/Insulin-like growth factor-1 (IGF-1) Signaling

IL: Interleukin

iNOS: inducible Nitric Oxide Synthase

iPSC: induced Pluripotent Stem Cells

JAK/STAT: Janus kinase/Signal Transducers and Activators of Transcription

JNK: c-Jun N-terminal Kinase

LB: Lewy Body

L-DOPA: Levodopa OR l-3,4-Dihydroxyphenylalanine

LID: Levodopa-Induced Dyskinesia

LNs: Lewy Neurites

LRRK2: Leucine Rich Repeat Kinase

MAO: Monoamine Oxidase

MAPK: Mitogen-Activated Protein Kinase

MD: Mitochondrial dysfunction

MDA: Malondialdehyde

Mefs: Mouse Embryonic Fibroblasts

MHC: Major Histocompatibility Complex

MKK: Mitogen-Activated Protein (MAP) Kinase Kinase

MMP: Mitochondrial Membrane Potential

MPTP: 1-Methyl-4-Phenyl-1,2,3,6-Tetrahydropyridine

Mtdna: Mitochondrial DNA

Mtor: Mammalian Target of Rapamycin

NADPH: Nicotinamide Adenine Dinucleotide Phosphate

NBT: Nitroblue Tetrazolium

NDD: Neurodegenerative Disease

NGS: Normal Goat Serum

NHP: Non-Human Primates

nIRF: near Infrared Fluorescence

NSAID: Non-Steroidal Anti-Inflammatory Drug

Nurr: Nuclear receptor related

OS: Oxidative Stress

PAL: Protocerebral Anterior Lateral

PAM: Protocerebral Anterior Medial

PBS: Phosphate-Buffered Saline

PD: Parkinson's Disease

PERK: Protein Kinase R (PKR)-like Endoplasmic Reticulum Kinase

PINK1: PTEN-Induced Kinase 1

PKA: Protein Kinase A

PPD: Protocerebral Posterior Deutocerebrum

PPL: Protocerebral Posterior Lateral

PPM: Protocerebral Posterior Medial

PQ: Paraquat

RGS: Regulator of G-protein Signaling

RNA: Ribonucleic Acid

ROS: Reactive Oxygen Species

ROT: Rotenone

SDH: Succinate Dehydrogenase

SNCA: α-Synuclein gene

SNpc: *Substantia Nigra pars compacta*

SOD: Superoxide Dismutase

TALEN: Transcription Activator-Like Effector Nucleases

TH: Tyrosine Hydroxylase

TNF: Tumor Necrosis Factor

TRAP: Tumor necrosis factor Receptor-Associated Protein

TRPM: Transient Receptor Potential Melastatin

UAS: Upstream Activation Sequence

UCH: Ubiquitin C-terminal Hydrolase

UDP: Uridine Diphosphate

UPR: Unfolded Protein Response

UPS: Ubiquitin Proteasome System

VMAT: Vesicular Monoamine Transporter

VPS35: Vacuolar Protein Sorting

VUM: Ventral Unpaired Medial

XBP: X-box Binding Protein

CONTENTS

CHAPTER-1

Review of Literature

1.1. Introduction:

Neurodegenerative diseases (NDDs) are a cluster of disorders that are categorized by continuous degeneration of the nervous system resulting in a gradual deterioration in a person's quality of life. This degeneration is either due to the death of the neurons or structural changes that prevents neurons from functioning normally. NDDs pose a risk to human health as these diseases are becoming more prevalent in recent years (Parenti *et al.* 2020). Though neurodegeneration is frequently multifactorial in origin, gene-environment factors and the ageing processes are believed to play an important role. The pathological hallmarks of NDDs consist of oxidative stress (OS), mitochondrial dysfunction (MD), proteasomal impairment, and aggregation of abnormal proteins. Another factor for neurodegeneration is the inability of the central nervous system (CNS) neurons to regenerate cells on their own, once death or damage occurs, creating a major threat to the human lifespan (Cooke *et al.*, 2022; Fawcett, 2020). Some of the common NDDs are Huntington's disease (HD), Amyotrophic Lateral Sclerosis (ALS), Alzheimer's disease (AD) and Parkinson's disease (PD). Despite several years of research, the etiology and pathogenesis of these diseases remain uncertain. Hence, developing efficient therapeutic strategies for such diseases is challenging but a necessity for researchers working in this field.

1.2. Parkinson's Disease (PD)

Among the various NDDs, PD is the most common NDD affecting the movement in the ageing human population (Zhu *et al.*, 2022; Aarsland *et al.*, 2021) and the second most common NDD affecting about 1% of the population over 50 years (Ayajuddin *et al.*,

2018), 1.5% to 2% over the age of 60 years and 4% of the elderly individual over the age of 80 years (Marino *et al*., 2020). More than 6 million individuals across the globe are suffering from PD (Armstrong and Okun, 2020). It is a multifactorial disorder in which the etiology is mostly not known. Progressive impairment of voluntary motor control is the clinical hallmark of this disease (Heidari *et al*., 2022). The characteristic pathological feature of PD is the selective degeneration of dopaminergic neurons (DNs) in the *Substantia Nigra pars compacta* (SNpc) leading to motor dysfunction, bradykinesia, tremors and rigidity (Khairnar *et al*., 2022). Other non-motor symptoms of PD include depression, sleep disturbances, fear, anxiety, fatigue, weight changes, energy loss, psychosis, memory loss, attention deficits, sexual dysfunction, gastrointestinal issues, and pain affecting the quality of their life (Khairnar *et al*., 2022).

Another pathological feature of PD is the cytoplasmic proteinaceous inclusion called Lewy bodies (LBs). Among the multiple proteins such as α-synuclein (α-syn), ubiquitin, parkin and neurofilaments present in LB, fibrillar deposits of misfolded α-syn lead to neuronal damage (Zhu *et al*., 2022). The precise mechanisms of how α-syn and other proteins lead to neuronal damage are unknown but considered to have engaged in oxidative modifications. Along with DA-ergic neuronal degeneration in SNpc, cell loss and neuropathology occurs in other parts including the nucleus basalis of Meynert, raphe, locus coeruleus, cerebral cortex, dorsal motor, olfactory bulb, the nucleus of the vagus and autonomic nervous system (Giguère *et al*., 2018). Hippocampal and cortical neurodegeneration may also lead to dementia which is again associated with PD. These statements show that not only the DA-ergic but also non-DA-ergic pathways are involved in the PD pathology.

1.2.1. Types of PD

Though the decisive cause of PD is yet to understand, epidemiological studies indicate two major types of PD. In most populations, 3–5% of PD cases are known to be caused by genetic factors linked to known PD genes that signify monogenic PD whereas the remaining 90-95% cases are believed to be sporadic, implicating the role of environmental factors (Bloem *et al.,* 2021). The role of neurotoxicants in the pathogenesis of nigrostriatal degeneration has been reported, showing a strong association between environmental factors in PD (Schildknecht *et al.,* 2017). Furthermore, the identification of the mutated α-synuclein gene (SNCA) involved in familial PD (Polymeropoulos *et al.,* 1997) provides a genetic background for the disease. Genetical studies implicate the involvement of mitochondrial, endolysosomal and synaptic vesicles in both sporadic and familial PD (Nalls *et al.,* 2019; Nguyen *et al.,* 2019; Burbulla *et al.,* 2017).

Not only the toxin-induced or genetic models of PD, but other models of PD have also been developed to investigate the pathogenesis of PD. Using induced Pluripotent Stem Cells (iPSC) methods, *in vitro* midbrain organoids have been generated for disease modelling and drug screening (Kim *et al.,* 2019). These iPSCs-derived midbrain organoids from the PD patient or genetically modified healthy controls may replicate the pathogenesis of PD patients (Chlebanowska *et al.,* 2020). This model may help in understanding the mechanisms of DA-ergic neuronal loss/degeneration and in screening drugs to intervene in disease progression. Discoveries on the involvement of the immune system in the pathogenesis and association of human leukocyte antigen (HLA) with PD have also shown a new direction of the disease (Sulzer *et al.,* 2017). Inducing inflammation or autoimmunity in the midbrain using different methods leading to DA-ergic neuronal degeneration may offer novel animal models which would help in

identifying the role of the immune system in causing PD. This knowledge would eventually help in finding a treatment for this disease.

1.2.1.1. Genetic forms of PD

Along with environmental factors, genetic mutations are also associated with PD. Environmental chemicals can affect the DNs with MD, redox cycling and oxidative damage, unfolded protein response, neuro-inflammation, ubiquitin-proteasome system (UPS) dysfunction and metabolic disruption leading to cell death. A better understanding of the effects caused by pesticides is gained through transcriptional and proteomic networks (Cao *et al.*, 2019).

The mutation is an important factor in the development of NDDs in humans. The difficulties in the study of neuronal cell death in the progressive development of PD led to the development of *in vitro* models of DNs (Fricker *et al.,* 2018). In such cases, transgenic models are proved to be a potential alternative for studying the role of mutant genes in the pathophysiology and pharmacological intervention in PD (Xiong and Yu, 2018). The first gene that has been reported to cause autosomal dominant PD is SNCA and to date, five other missense mutations of SNCA have been identified (A30P, G51D, E46K, A53E, and H50Q) (Pasanen *et al.,* 2014; Lesage *et al.,* 2013; Proukakis *et al.*, 2013; Zarranz *et al.*, 2004; Krüger *et al.,* 1998; Polymeropoulos *et al.,* 1997). Other autosomal dominant genes such as LRRK2 and VPS35 are also implicated in PD. In autosomal recessive inheritance, genes such as PINK1, PARKIN, DJ-1 and FBXO7 are implicated (Blauwendraat *et al.,* 2020). Meta-analysis of genome-wide association studies (GWASs) indicates other genes such as LRRK2, SNCA, GBA1, CTSB and SH3GL2 as risk factors for PD (Nalls *et al.,* 2019). The level of expression of these genes plays a role in PD progression (Selvaraj and Piramanayagam, 2019). The genes implicated in PD are summarized in **Table 1.1**.

Symbol	**Gene locus**	**Gene**	***Drosophila* homolog**	**Inheritance**	**Nature of PD**	**Status and remarks**
PARK1	4q21-22	SNCA (Polymeropoulos *et al.*, 1997)	no homolog	AD	Early-onset parkinsonism	Confirmed
PARK2	6q25.2-q27	PARK2 encoding Parkin (Kitada *et al.*, 1998)	parkin	AR	Early-onset parkinsonism	Confirmed
PARK3	2p13	Unknown	-	AD	Classical parkinsonism	Unconfirmed
PARK4	4q21-q23	SNCA	no homolog	AD	Early-onset parkinsonism	Erroneous locus (identical to PARK1)
PARK5	4p13	UCHL1	*Uch*	AD	Classical parkinsonism	Unconfirmed
PARK6	1p35-p36	PINK1 (Valente *et al.*, 2004)	pink1	AR	Early-onset parkinsonism	Confirmed
PARK7	1p36	PARK7 encoding DJ-1 (Bonifati *et al.*, 2003)	*DJ-1α* and *DJ-1β*	AR	Early-onset parkinsonism	Confirmed
PARK8	12q12	LRRK2 (Paisán-Ruíz *et al.*, 2004)	*LRRK*	AD	Classical parkinsonism	Confirmed
PARK9	1p36	ATP13A2 (Ramirez *et al.*, 2006)	CG32000	AR	Kufor-Rakeb syndrome, a form of juvenile-onset atypical parkinsonism with dementia	Confirmed
PARK10	1p32	Unknown	-	RF	Classical parkinsonism	Confirmed susceptibility locus
PARK11	2q36-27	Unknown (maybe GIGYF2)	-	AD	Late-onset parkinsonism	Not independently confirmed
PARK12	Xq21-q25	Unknown	-	RF	Classical parkinsonism	Confirmed susceptibility locus
PARK13	2p12	HTRA2	*HtrA2*	AD or RF	Classical parkinsonism	Unconfirmed

PARK14	22q13.1	PLA2G6 (Paisán-Ruíz *et al.*, 2009)	*iPLA2-VIA*	AR	Early-onset dystonia-parkinsonism	Confirmed
PARK15	22q12-q13	FBXO7 (Shojaee *et al.*, 2008)	no homolog	AR	Early-onset parkinsonian-pyramidal syndrome	Confirmed
PARK16	1q32	Unknown (maybe RAB7L1)	-	RF	Classical parkinsonism	Confirmed susceptibility locus
PARK17	16q11.2	VPS35	*Vps35*	AD	Classical parkinsonism	Unconfirmed
PARK18	6p21.3	EIF4G1	*eIF4G*	AD	Late-onset parkinsonism	Unconfirmed
PARK19	1p31.3	DNAJC6 (Edvardson *et al.*, 2012)	auxillin	AR	Juvenile-onset parkinsonism	Confirmed
PARK20	21q22.11	SYNJ1 (Krebs *et al.*,2013; Quadri *et al.*, 2013)	*Synj*	AR	Early-onset parkinsonism	Confirmed

Table 1.1: Genes implicated in PD and its fly homolog(s): AD- Autosomal Dominant; AR- Autosomal Recessive; RF- Risk Factor (adapted from Modi *et al.*, 2016)

1.2.1.2. Sporadic forms of PD

The etiology of sporadic PD is not precisely understood. PD cases are mostly considered to be sporadic indicating the involvement of environmental factors. Studies have shown that rural people using pesticides on fields, consuming well water and occupations like mining over a long period have an increased risk of PD (Elbaz *et al.,* 2009; Ritz *et al.,* 2009). Mimicking these effects, several neurotoxins are in use to produce different models of PD. Some of the commonly used neurotoxins are 6-Hydroxydopamine (6-OHDA), 1-methyl-4-phenyl-1,2,3,6-tetrahydropyridine (MPTP), rotenone, N,N-dimethyl-4-4-4-bipyridinium (paraquat), maneb and dieldrin (Segura-Aguilar and Kostrzewa, 2015). Though the mechanisms of action are different for all the neurotoxins, the ultimate result is the degeneration of DNs which is indicated by aggregation of α-syn to neurotoxic oligomers, mitochondria dysfunction, OS and neuroinflammation. Some of the commonly used toxin-mediated animal models of PD are described in the following paragraphs.

***MPTP*:** The neurotoxic nature of MPTP was first reported in 1983 among drug addicts who have injected themselves with a derivative of meperidine containing MPTP (Langston *et al.*, 1983). After crossing the blood-brain barrier (BBB), MPTP is converted to its active form MPP+ by monoamine oxidase-B (MAO-B) (Mei *et al.,* 2019). MPP+ specifically targets DNs through the dopamine transporter (DAT) and inhibits the complex I in mitochondria leading to the generation of reactive oxygen species (ROS) and consequently neuronal death (Martí *et al.,* 2017). This toxin degrades vesicular monoamine transporter-2 (VMAT-2) causing auto-oxidation of DA leading to neurotoxicity (Lohr *et al.,* 2015). MPTP also causes gastro-intestinal abnormalities which is an important feature of PD (Poirier *et al.*, 2016). MPTP-induced Parkinsonian symptom looks very similar to PD patients (Langston, 2017). Hence, it is an attractive

neurotoxin to develop animal PD models (Rai and Singh, 2020; Zeng *et al.*, 2018). MPTP is primarily used in nonhuman primates, dogs, cats and mice (Yun *et al.*, 2015). This toxin model is also used to study non-motor symptoms of PD (Choudhury and Daadi, 2018) since it degenerates both the nigrostriatal DA-ergic system as well as the peripheral nervous system (Mingazov *et al.*, 2018). One of the major drawbacks of this model is its inability to form LBs, an important feature of PD (Blesa and Przedborski, 2014). Other disadvantages include the resistance of rats to MPTP while mouse strain shows variable sensitivity to this toxin (Meredith and Rademacher, 2011) and its inability to replicate in clinical studies to develop PD drugs (Lindholm *et al.*, 2016).

***6-OHDA*:** The toxicity of 6-OHDA was first evident in 1963 when a significant decrease in noradrenaline levels was observed in the mouse heart after intraperitoneal administration (Porter *et al.*, 1963). It is used as an exogenous neurotoxin to study neurodegeneration in various animal models (Zeng *et al.*, 2018; Lindholm *et al.*, 2016). Among the various 6-OHDA-animal PD models, the rat is the most commonly used model. It is always given through unilateral injection as it is impermeable through Blood Brain Barrier (BBB) (Zeng *et al.*, 2018). This mode of injection could degenerate 60% of DNs in the striatum of rats (Perlbarg *et al.*, 2018). The damage caused by 6-OHDA to DNs depends on the amount of toxin used, site of injection and species. This model could replicate many features of PD like loss of DNs and depletion of dopamine (DA) (Ghatak *et al.*, 2018). Interestingly, this model neither forms LBs nor affects other regions of the brain except for the degeneration of the nigrostriatal pathway (Jiang and Dickson, 2018). This toxin fails to produce motor deficits even after marked DA-ergic degeneration in *Caenorhabditis elegans* (Harrington *et al.*, 2011). The main drawback of this model is the absence of motor deficits related to PD and the inability to cause DA-ergic denervation (Hou *et al.*, 2017). Other disadvantages include its inability to cross BBB

and hence needs to be injected directly into the brain (Zeng *et al.,* 2018). This model fails to form LB, an important feature of PD (Jiang and Dickson, 2018). Hence, this model is neither suitable to study the mechanism of PD pathogenesis nor to examine the efficacy of drugs against PD (Lindholm *et al.,* 2016; Park and Stacy, 2015).

***Paraquat*:** The herbicide paraquat (PQ) resembles the structure of MPP+ and thus can induce parkinsonian symptoms (Vaccari *et al.,* 2017; Jayaraj *et al.,* 2016). An important feature of this model is its longer half-life period causing chronic PD in animal models (Hisahara and Shimohama, 2010). Degeneration of DNs in the striatum and neurobehavioral changes are observed in PQ induced mouse model (Breckenridge *et al.,* 2013). PQ has been shown to induce Parkinsonian symptoms in *Drosophila* in a dose-time-dependent manner (Phom *et al.,* 2014). PQ is shown to damage the macromolecules like proteins, lipids, RNA and DNA through OS (Berry *et al.,* 2010). Similar to structure of MPP+, PQ crosses the BBB causing degeneration of the DNs in the SNpc (Zeng *et al.,* 2018). It also inhibits complex I of the electron transport chain (ETC) and reduces ATP production causing a neurotoxic effect in the DNs and glial cells as well (Cannon and Greenamyre, 2010). There are contradictory shreds of evidence of PQ toxicity as it causes motor dysfunctions only in higher doses in mice models (Blesa *et al.,* 2012). A study on mice demonstrated that systemic administration of PQ reduces motor activity and dose-dependent loss of DNs (McCormack *et al.,* 2003) whereas others showed no changes in the ventral tegmental area (Thiruchelvam *et al.,* 2000). The main drawbacks of this model are the inability to cause significant motor impairment (Blandini and Armentero, 2012) and restrictions on the LB pathology (Hisahara and Shimohama, 2010). The exact mechanism of neurodegeneration induced by this toxin is unclear (Cannon and Greenamyre, 2010). Hence, this model is not suitable to study idiopathic PD but only toxin-induced sporadic PD (Thompson and Zhang, 2016).

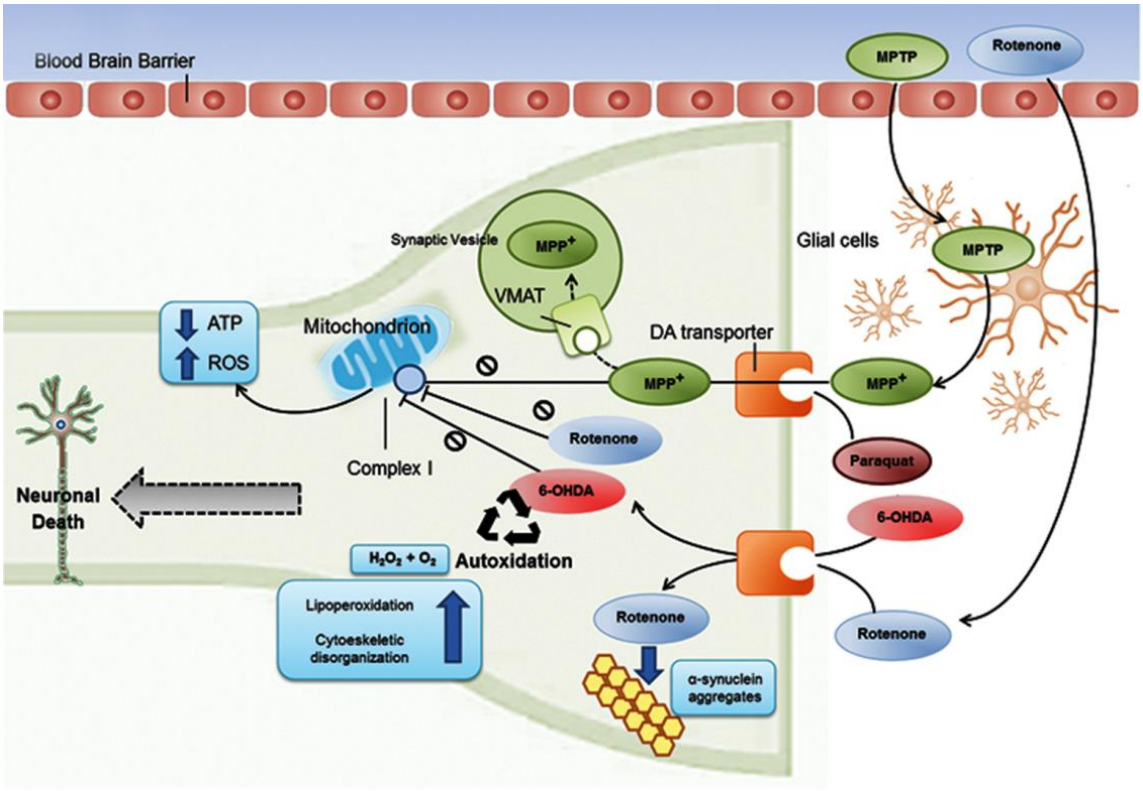

Figure 1.1. Schematic representation of pathogenesis of toxin-induced PD models: ROT and MPTP can easily cross the blood-brain barrier and metabolized into their toxic forms. These compounds inhibit complex I of the mitochondrial electron transport chain producing ROS and reducing ATP leading to activation of programmed cell death molecular pathways. Paraquat, similar to MPP+ and 6-OHDA, crosses the cell membrane through the DAT and exerts partial toxicity in mitochondria with the subsequent production of ROS and quinones. All these compounds ultimately degenerate DNs leading to PD (Copied from Blesa *et al*., 2016).

***Rotenone*:** Rotenone (ROT) is a neurotoxin extracted from the plant of the rotenoid family (Johnson and Bobrovskaya, 2015). Because of its high lipophilic nature, it can readily cross the BBB and hence highly toxic (Fuzzati-Armentero *et al.*, 2019). It inhibits complex I of ETC in the whole system and is not limited to catecholaminergic neurons (Bisbal and Sanchez, 2019), and hence neurodegeneration is not very specific to DNs of

SNpc (Hisahara and Shimohama, 2010). The compound ROT has been extensively used in multiple animal PD models. Intravenous administration of ROT in male Lewis rats induces nigrostriatal DA neuronal loss, α-syn aggregation and gastrointestinal problems (Cannon *et al.,* 2009). Intraperitoneal injection of ROT once daily for four weeks induces PD in male Wistar rats with a significant decrease of DNs in the SNpc, increase in nitrite levels, oxidative injury by losing anti-oxidant enzymes and activation of proinflammatory cytokines and inflammatory mediators (Javed *et al.,* 2016). Comparable with human PD patients, ROT intoxication leads to a reduction of 35% serotonergic, 29% cholinergic, and 26% noradrenergic neurons causing degeneration of the nigrostriatal pathway (Höglinger *et al.,* 2003). This model is used in a wide range of species that can undergo genetic manipulation to understand gene-environment interactions (Cannon and Greenamyre, 2010). ROT increases the intracellular and mitochondrial ROS levels and activates caspase-3/caspase-9 activity leading to apoptotic cell death in a time-dose-dependent manner in SH-SY5Y cells (Wang *et al*., 2020). Among different multicellular animal models of PD available, *Drosophila melanogaster* is one of the most appreciated and extensively used models for studying genes and proteins implicated in PD (Thao, 2020). Exposing the *Drosophila* to 500 μM ROT showed impaired climbing ability and increased malondialdehyde levels assayed by lipid peroxidation in the brain tissues (Siima *et al.,* 2020). Rotenone (500 μM) is shown to induce time-dose-dependent effect on mobility and survivability and significantly reduced the DA and its metabolites in the *Drosophila* model of PD (Pandareesh *et al.,* 2016). The drawbacks of the ROT-animal model are the non-availability of well-documented ROT-induced human PD cases with which it can be compared (Bové *et al.,* 2005) and its less specificity to DNs (Blesa *et al.,* 2012). Another disadvantage of this model is its ability to show motor impairments without DA neuronal loss in rats

(Hisahara and Shimohama, 2010). Overall, ROT-mediated PD models exhibit all the pathological features of PD and are hence an attractive model of PD.

Additionally, there are other pesticides or agricultural chemicals like Maneb (manganese ethylene bisdithiocarbamate) or ziram known to cause neurotoxicity in SH-SY5Y cells (Huang *et al.,* 2019) and rat models (Colle *et al.,* 2018). Epidemiological studies have also shown the cases of PD in rural people consuming well water containing heavy metals. These studies point toward the fact that environmental factors are involved in the pathogenesis of PD (**Figure 1.1**). However, substantial studies on the mechanism of action of these toxins are the need of the hour to determine the accurate involvement of these compounds in the pathogenesis of PD.

1.3. ROT exposure in PD: A chemical of epidemiological relevance

Epidemiological studies have shown that the use of ROT as piscicide started in the US in the 1930s (Dawson *et al.,* 1983) but gardeners have been using the root extract containing ROT in East Indies as early as 1848 (La Forge *et al.,* 1933). The use of this pesticide has been banned in the USA and Canada in 2006 and 2008 respectively (EPA, 2015; Pest Management Regulatory Agency-Canada, 2008). Epidemiological studies have shown the co-relation between ROT exposure and a higher risk of developing PD in humans (Pouchieu *et al.,* 2018; Furlong *et al.,* 2015; Tanner *et al.,* 2011, 2009; Dhillon *et al.,* 2008; Hancock *et al.,* 2008; Kamel *et al*., 2007).

One case-control study has shown the inhibition of mitochondrial complex I upon using ROT in humans leading to PD (Tanner *et al.,* 2011). Another case-control study to assess the use of protective gloves has shown a co-relation between ROT use and PD with or without gloves (Furlong *et al.,* 2015). Another cohort study of 181,842 agriculture

workers (4916 of whom were exposed to ROT) was found to increase the risk of developing PD with prolonged exposure to ROT (Pouchieu *et al.*, 2018). Evidence of clinical and epidemiological studies supporting the linkage between ROT exposure and Parkinson's disease is shown in **Table 1.2**.

Type of Study	**Location**	**Year Published**	**Subjects**	**Results - Relative Risk or Odds ratio (95% CI)**	**Reference**
Cohort Study	France	2017	181,842 agricultural workers (4916 exposed to ROT)	1.57 (1.08, 2.29), with past exposure to ROT	Pouchieu *et al.*, 2018
Case-Control Study	USA	2015	69 cases and 237 controls	3.7 (1.7, 8.1), 3.8 (1.5, 9.6), 5.5 (2.0, 15.3) with exposure to ROT	Furlong *et al.*, 2015
Case-Control Study	USA	2011	110 PD cases and 358 controls	2.5; 95% CI, 1.3–4.7 with past exposure to ROT	Tanner *et al.*, 2011
Case-Control Study	USA	2009	519 cases and 511 controls	0.82 (0.05-13.34) with past ROT use	Tanner *et al.*, 2009
Case-Control Study	USA	2008	319 cases and 296 relative and other controls	5.93 (0.63-56.10) with the use of ROT	Hancock *et al.*, 2008
Case-Control Study	USA	2008	100 cases and 84 controls	10.0 (2.9-34.3) with the use of ROT	Dhillon *et al.*, 2008
Case-Control Study	USA	2007	83 prevalent cases and 79,557 controls	1.7 (0.6-4.7) with past ROT use	Kamel *et al.*, 2007

Table 1.2. Evidence of clinical and epidemiological studies supporting a link between ROT and Parkinson's disease

1.4. ROT-mediated animal models of PD

PD is a late-onset disease and hence it progresses gradually. Hence, one cannot easily use human subjects to study the mechanisms of its pathogenesis. In the last few decades, many PD models have been established either using genetic modulations or neurotoxin-induced means (Sulthana *et al.,* 2022; Fodor *et al.,* 2020; Pandareesh *et al.,* 2016). Some of these models are discussed below.

Cell line model: DNs are mainly affected in PD. Since the maintenance of the DA-ergic neuronal primary cells is difficult, research in the field of PD is mostly done using established neuronal cell models, such as neuroblastoma SH-SY5Y lineage. This cell line is commonly used because of its human origin, easy maintenance and its catecholaminergic neuronal properties. However, there is no consensus on the fundamental aspects relating to its use, the effects of culture media composition and variations in differentiation protocols (Xicoy *et al.,* 2017). ROT is shown to cause cytotoxicity, OS and MD, increase BAX and downregulate the Bcl2 expression as well as cytochrome c release and also caspases activation in SH-SY5Y cells which could be attenuated by pretreatment with PIASA, a novel peptide (Sulthana *et al.,* 2022). ROT increases the intracellular and mitochondrial ROS levels and activates caspase-3/caspase-9 activity leading to apoptotic cell death in a time-dose-dependent manner in SH-SY5Y cells (Liu *et al.,* 2013). Treatment of N27 DA-ergic neuronal cell line with ROT (10-2000 nM) for 24h has been shown to affect the cell in a dose-dependent manner (Pandareesh *et al.,* 2016).

Nematode model*:* Completely sequenced genome and multiple offspring in a short period for high throughput screening make *Caenorhabditis elegans* an ultimate model for genetic studies on PD. Among the total cells in adult wild-type worms, about 320 are neurons of which 8 are DNs which play a role in mechanosensation, habituation, basal

motor activity, egg-laying and defecation. *C. elegans* possess orthologues of the genes required for neurotransmission including the enzymes involved in DA biosynthesis and metabolism, despite its simplicity at the molecular level (Nass *et al.,* 2002). The phenotypic characteristics like blebbing of DA-ergic neuritis and rounding of cell bodies occur before apoptotic cell death showing its sensitivity to neurotoxins (Ved *et al.,* 2005; Braungart *et al.,* 2004; Nass *et al.,* 2002). An important characteristic of DA-ergic dysfunction in *C. elegans* is the loss of basal slowing response and reduction of bending frequency while feeding (Sawin *et al.,* 2000), and other characteristics like coiling and freezing have also been noted (Braungart *et al.,* 2004). Nevertheless, the loss of the DNs and the toxin-induced behaviours are not clearly correlated. To mention, 6-OHDA produces marked degeneration without motor deficits while MPP+ produces motor deficits even at lower doses inducing cell death (Harrington *et al.,* 2010), while dopamine agonists could rescue the altered phenotypes (Braungart *et al.,* 2004). Similar with *Drosophila*, many of the PD-associated genes are also conserved in *C. elegans* making this worm a genetic model of PD. Though this organism lack orthologues of α-syn, models produced by overexpressing wild-type or mutant human α-syn show DA-ergic neuronal degeneration along with loss of the basal slowing response (Kuwahara *et al.,* 2006). Mutations in PD-associated genes like parkin and DJ-1 have been shown to increase the susceptibility to ROT (Ved *et al.,* 2005) while the survival in response to PQ and ROT was increased upon overexpression of wild-type LRRK2 (Saha *et al.,* 2009), demonstrating that LRRK2 mutations may increase the vulnerability in PD. Hence, *C. elegans* provides an opportunity for assessing the combined effects of environmental and genetic factors associated with PD.

Zebrafish model*:* Zebrafish have been used for several years to study development. It is also used as a potential model of PD for *in vivo* drug screening. DNs in the posterior

tuberculum of the ventral diencephalon of this vertebrate ascend towards the striatum which is anatomically comparable with the nigrostriatal tract of mammals. Environmental toxins such as 6-OHDA and MPTP induces Parkinsonism leading to reduced levels of neurotransmitters in the brain within 2 days of injection but the symptomatic bradykinesia and the chemical alterations are shown after the 8^{th} day (Wen *et al.,* 2008; Anichtchik *et al.,* 2004). Contrastingly, the same model but with different toxins like ROT or PQ did not show PD symptoms (Bretaud *et al.,* 2004). Recently there has been more focus on creating genetic models of PD in the zebrafish. Genetic manipulations and high-throughput screening can be conducted in zebrafish. Knocking down of PD-related genes in the zebrafish embryo using morpholino-oligonucleotide approaches has created a wide range of phenotypes. For instance, knocking down DJ-1 produces no loss of TH-positive neurons by itself but augments susceptibility to OS (Bretaud *et al.,* 2007). A specific 20% loss of DNs in the posterior tuberculum and impaired complex I activity has been shown in Parkin-knockdown zebrafish but no alteration in swimming behaviour (Flinn *et al.,* 2009). Surprisingly, PINK1 knockdown did not effect in loss of DNs but altered their projection modes and resulted in decreased swimming ability (Xi *et al.,* 2010). Interestingly, knockdown of LRKK2 in this model has been shown to reduce the TH-positive cells by 25–30% and swim half the distance (Xi *et al.,* 2010). This model seems to be a promising vertebrate model to examine some aspects of the genetics of PD.

Snail model: *Lymnaea stagnalis*, commonly known as a snail, has simple characteristic features such as locomotion, respiration and feeding. An important characteristic of this model is that the exposure to toxins takes place through absorption of the skin or swallowing during feeding which replicates some of the most probable routes of ROT exposure in humans (Fodor *et al.,* 2020). Exposure of *L. stagnalis* to a concentration of

0.1-5 µM ROT showed a decrease in DA content in the circumoesophageal complex and the paired buccal ganglia. It also showed a decreased spontaneous locomotor activity and feeding behaviour in a time and dose-dependent manner where a concentration of 5 µM ROT could kill all the snails in 4 days of exposure (Vehovszky *et al.,* 2007). Exposing *L. stagnalis* to 0.1-5 µM concentrations of ROT showed a significant decrease in DNs, reduced locomotor activity and feeding behaviour in a time and dose-dependent manner but concentrations above 5 µM could kill all the snails in 4 days of exposure (Vehovszky *et al.,* 2007). Absorption through skin and swallowing during feeding in *L. stagnalis* are the critical characteristics of this model which replicates some of the most probable routes of ROT exposure in humans (Fodor *et al.,* 2020).

Rodent model: ROT induces neurotoxicity in Lewis rats when administrated directly in the brain (Alam *et al.,* 2004), oral administration (Inden *et al.,* 2007), intragastric (Pan-Montojo *et al.,* 2010) and intraperitoneal injection (Alam *et al.,* 2004). The cognitive function, oxidative defence and mitochondrial complex (II and III) enzymes activities are significantly altered in the ROT-administered mouse model for a period of 3 weeks when compared to the normal group (Khatri and Juvekar, 2016). Intravenous administration of ROT in male Lewis rats induces nigrostriatal DA neuronal loss, α-syn aggregation and gastrointestinal problems (Cannon *et al*., 2009). Intraperitoneal injection of ROT once daily for four weeks induces PD in male Wistar rats with a significant decrease of DNs in the SNpc, increase in nitrite levels, oxidative injury by losing anti-oxidant enzymes and activation of pro-inflammatory cytokines and inflammatory mediators (Javed *et al.,* 2016). Multiple doses of ROT (1.5, 2, or 2.5mg/kg) daily for 5 weeks caused a dose-dependent elevation in α-syn and a significant decrease in the number of DNs in the SNpc and DA in the striatum of male Wistar rats (Zhang *et al.,* 2017). Interestingly, the medium dose of 2mg/kg dose did not affect the body weight but it showed MD and

decreased rearing and shorter latency to fall from a rotarod (Zhang *et al.,* 2017). Additionally, ROT increased nitrate levels, caused oxidative injury by losing antioxidant enzymes and induced activation of pro-inflammatory cytokines and inflammatory mediators (Javed *et al.,* 2016).

***Non-human primates*:** Animal models of non-human primates (NHP) are very important in drug discovery. MPTP was shown to cause Parkinsonism in the rhesus macaque (*Macaca mulatta*), and it became the first MPTP-lesioned NHP model of PD (Burns *et al*., 1983). Later it was reported to induce similar symptoms in many other species of NHP like squirrel monkey (Langston *et al.,* 1984), common marmoset (Jenner *et al.,* 1984), cyomolgus macaque (Bédard *et al.,* 1986), African green monkey (Elsworth *et al.,* 1987), capuchin monkey (Gaspar *et al.,* 1993) and baboon (Todd *et al.,* 1996). Subcutaneous administration of MPTP in marmoset monkeys at a dose of 6mg/kg for 9 days leads to a 75% reduction in DNs in SNpc and a 95% reduction in DA (van Vliet *et al.,* 2008). NHPs like marmoset, macaque and squirrel monkey have been used for assessing the effects of experimental drugs on psychosis, dyskinesia and Parkinsonism (Veyres *et al.,* 2018). The severity of dyskinesia depends on the dose of L-DOPA administered and the co-administration of anti-dyskinetic agents making this model ideal for identifying potential anti-dyskinetic molecules (Koprich *et al.,* 2011; Morin *et al.,* 2010). The identification of this anti-dyskinetic molecule before going to clinical trials serves several advantages and appears compulsory for ethical reasons (Veyres *et al.,* 2018). The NHP models are also useful in studying other features like activity counts or the duration of L-DOPA antiparkinsonian action (Huot *et al.,* 2011; Johnston *et al.,* 2011).

1.4.1. ROT-mediated *Drosophila* model of PD

The disheartening results obtained from other PD animal models have inspired an interest in searching for alternative multicellular model organisms. Studies on single-gene mutations, that are responsible for rare and heritable forms of PD, provide a prospect to gain insights into the molecular mechanisms of PD (Whitworth *et al.,* 2006). Those genetic models show a high level of reproducibility although the quantity and outline of DA-ergic neuronal deficit may differ among models.

Genetic models of *Drosophila* are greatly in use. A loss-of-function or a gain-of-function in LRKK2 mutant *Drosophila* showed decreased climbing ability and reduced TH expression and DA-ergic neuronal number (Liu *et al.,* 2008). L-DOPA could somewhat restore the behavioural defects in those flies (Liu *et al.,* 2008). Knockdown of PINK1 in *Drosophila* leads to behavioural defects and DA-ergic neuronal loss (Park *et al.,* 2006; Wang *et al.,* 2006) whereas DJ-1 mutant *Drosophila* does not have a consistent PD-like phenotype (Park *et al.,* 2005). Parkin mutant *Drosophila* also exhibits a similar mobility defect and loss of DNs along with a ~60% reduction in brain dopamine levels (Wang *et al.,* 2007; Cha *et al.,* 2005; Whitworth *et al.,* 2005; Greene *et al.,* 2003). All these studies highlight that the fly PD model mimics human PD condition and hence it can be used as a powerful tool to study PD.

The review of literature illustrates that the first ROT-mediated fly model of PD was developed by Coulom and Birman, (2004) and to date (June 2022), 50 research articles were published where different laboratories developed/used ROT-mediated *Drosophila* models of PD. **Table 1.3** summarizes ROT-mediated *Drosophila* models of PD.

Sl no	Strain / transgenic lines	Age/Sex	Exposure Paradigm	PD related phenotypes	Nutraceutical intervention strategies (if any)	Rescue, if any	Reference
1	W-, UAS-*CncC*, UAS-*CncC* RNAi and *da*-GAL4)	1day/ Male	515 µM for 7 days in diet	Motor deficit; Neuronal loss; Reduced ATP content, Complex I and II activity; Enhanced ROS, HP	Ginsenosides Type: Re	Rescued. Re mediated protection through *CncC*	Qiao *et al*., 2022
2.	Harwich	1-3days/Both the sexes	250 and 500 µM in filter disc for 7 days.	Reduced survival, motor performance, fecundity, AchE, Cell viability; PC, HP, MDA, NO Reduced CAT, GST, THS, non-protein THS	Trans-astaxanthin	Rescued.	Akinade *et al*., 2022
3	w^{1118}	1day/Male	ROT 250 µM in media for 7 days	Reduced locomotor activity and survival; Enhanced ROS in fly head	Anthocyanin-Rich Extract from Sweet Cherry	Rescued	Filaferro *et al*., 2022
4	*Elav*-GAL4 and repo-GAL4, UAS-*CncC* and UAS-*CncC* RNAi	1day/ Female	1, 10, and 100 µM in media 3 and 4 weeks	Reduced survival and mobility	CDDO-Me; *CncC* overexpression	Rescued	Guo *et al*., 2021
5	*D. melanogaster*	2-8 days/ Male	500 µM ROT for 7 days.	Mobility defects and reduced survival; Impaired mitochondrial morphology and synaptic vesicles	Acteoside	Rescued	Aimaiti *et al*., 2021
6	Harwich	1-4d	500 µM in media for 7 days	Mobility defects, and reduced survival; Reduced DA, TH level, impaired AchE activity and SOD, GST, TBA reactive substances level	lutein-loaded nanoparticles	Rescued	Fernandes *et al*., 2021
7	Oregon-K	8-10 days/ Male	500 µM in media for 7 days	Mobility defects and decrease in DA level, ETC complexes and increase in ROS production and cholinergic activities in head and body of the fly	Chitosan	Rescued	Pramod and Prashanth, 2020

8	w^{1118}, TH-GAL4/UAS-Parkin-RNAi	1-4 days/ Both the sexes	500 µM in diet for 7 days	Mobility defects; Increased MDA levels assayed by LP in the brain tissues; Expression levels of mRNA of SOD and CAT were elevated	Flavonoids and Polyketides	Rescued	Siima *et al*., 2020
9	w^{1118}, UAS-*dmfrn*, *Fer3HCH* RNAi and *dmfrn* RNAi	2 days/ Male	2 mM in food media	Impaired climbing ability and survival	-----	-----	Wan *et al*., 2020
10	w^{1118}, *Elav*-GAL4, UAS-EGFP, UAS-*Tsf1* RNAi, UAS-*Tsf1*-EGFP	2 days/ Male	250 µM in food for 7 days	Mobility defects and decreased survival; Decreased mitochondrial complex 1, ATP level; Neuronal death in PAL, PPL1 and PPM3 cluster; Enhanced CAT, SOD activity and ROS generation	-----	-----	Xue *et al*., 2020
11	w^{1118}, $PINK1^{B9}$	1 day/ Male	250 µM for 10 days in media	Both strains showed enhance climbing latency, decreased Jump or flight activity; Wild type showed decreased neuronal number in PPL1	Eigallocatechin -3-gallate	Rescued	Xu *et al*., 2020
12	w^{1118}, $PINK1^{B9}$	3 days/ Male	5 mM in media	Reduced survival of WT fly	Ginseng total protein	Survival enhanced	Liu *et al*., 2020
13	Canton S, *Elav*-GAL4, UAS-*park*, UAS- *MUL1 Elav*-GAL4 > UAS-*park*, *Elav*-GAL4 > UAS-*MUL1*	1 day/ Male	Cotton soaked in 500 µM ROT for 7 days	In non *Park* and *MUL1* overexpressing flies: Impaired motor and DA-ergic neurodegeneration Negatively affected synaptic proteins, including Synapsin, Synaptotagmin and Disk Large1, as well as the structure of synaptic vesicles	-----	------	Doktór *et al*., 2019
14	Oregon-K	10 days/ Male	500 µM for 7days on filter paper	Decreased survival for all concentration; Decreased locomotor activity; Increased ROS, Peroxide; decreased GSH, DA, DOPAC in both head and body but enhanced DOPAC/DA	APAU (no neutraceutical)	Rescued.	Lakkappa *et al*., 2019
15	Harwich	1-4 days/ Both the sexes	500 µM in diet for 7 days	Increased mortality and mobility defects; DA and selenium down; more ROS and LP, Lower SOD, CAT activity, increased	7-chloro-4-(phenylselanyl) quinoline (4-	Rescued	de Freitas Couto *et al*., 2019

				cholinergic profile	PSQ)		
16	w^{1118}, *Elav*, α-syn	0 to 2-days/ Male fly	0.25 µM for 5 days in media	Mildly influenced insoluble α-syn aggregates	-------	-----	Prasad *et al*., 2019
17	STR-5	0-1 day/ Male	Rot 500 µM on filter disc.	Reduced climbing ability	Levodopa; Mucuna pruriens Extract	Rescued	Johnson *et al*., 2018
18	w^{1118}	1 day, 10 days, 20 days/ Both the sexes	50, 100, and 200 µM of ROT 1-day, 10-day, and 20-days in media	Reduced survival; Aging flies were more vulnerable to ROT-induced stress; DA neuron death; Enhanced ROS; Induces dSARM and inflammatory gene *Eiger* and *Relish* expression; Upregulation of *JAK/STAT* signalling mediated immune and stress response genes.	N-acetylcysteine Reserveratrol	Decreased ROS; Improved motor ability; Decreased and normalized gene expression	Sur *et al*., 2018
19	Canton-S	8-10 days/ Male	Rot 500 µM for 7 days	Reduced climbing ability, impaired muscular coordination, gait disturbances, memory decline; DA-ergic neuronal degeneration; DA depletion, Enhanced LP, SOD, CAT and GPx activity, reduced GSH level and enhanced expression of apoptosis marker BAX.	Myricetin	Rescued	Dhanraj *et al*., 2018
20	UAS-synuclein-WT, UAS-LRRK2-G2019S, UAS-Parkin-Q311X	0-last day of survival/ Both the sexes	100 µM in food till all the flies died	Observed shorter lifespan; Gradual worsening of climbing behaviour with continuous exposure (Observed till 1 week to 5 weeks)	Morphine	Rescued	Wang *et al*., 2018
21	Harwich	1-3 day/ Both the sexes	250 µM for 7 days in diet.	Locomotor deficit; Reduced number of fly emergence; Increased HP generation, AcHE activity and NO; Inhibited CAT and GST activities and depleted total thiols level	Kolaviron	Rescued	Farombi *et al*., 2018
22	20xUAS-IVSmCD8::GFP	3 days/ Male	0.5 mM on blotting paper	Induced mobility defects in a time-dependent manner; No change in neuronal number;	-----	-----	Stephano *et al*., 2018

	or UAS-*arm*, TH-GAL4 driver			Higher expression of genes regulating cell death and neuronal functions; Higher activities of the MAPK/EGFR- and TGF-β signalling pathways but not Wnt pathway			
23	Oregon-K	10 days/ Male	500 µM for 7 days on filter disc	Reduces the DA and DOPAC; DOPAC/DA is lower in ROT group	PTUPB	Restored DOPAC/DA to normal	Lakkappa *et al*., 2018
24	*Ddc*-GAL4, *24B*-GAL4, *yw*, w1118, UAS-LRRK2 G2019S, UAS-mito-GFP, parkin and pink1 null	15 days/ Female	50 µM ROT for 15 days	Mobility defects, reduction in life span, DA neuron loss	-----	-----	Basil *et al*., 2017
25	CHCHD2, c.182C>T, c.434G>A, and c.5C>T	2-3days/ Both the sexes	500 µM	Mobility defects, DNs degeneration, reduction in lifespan, MD, OS, and impairment in synaptic transmission	Ebselen	Rescued	Tio *et al*., 2017
26	w^{1118}; *Da*-Gal4	Age/sex not mentioned	15 µM for 24 h in isolated cells	Production of ROS was not affected by PTP1B inhibition; Neuroprotective effect of the PTP1B inhibitor is not associated with ROS production, MG132-induced toxicity involving proteasome inhibition	Protein tyrosine phosphatase 1B (PTP1B)	Rescued	Jeon *et al*., 2017
27	Oregon-K	10 days/ male	500 µM for 7 days in diet	Dose-dependent lethality; mobility defects; higher ROS and HP levels; DA, DOPAC and HVA down (*); (DOPAC+HVA)/DA higher compared with control	curcumin and curcumin monoglucoside (CMG)	Rescued; DA upregulate but not DOPAC and HVA; (DOPAC+HVA)/DA reduced compared to Rot group	Pandareesh *et al*., 2016
28	Oregon-K	9–10 days/	500 µM for 7	Higher levels of ROS, HP, NO, PC levels;	saffron	Rescued	Rao *et al*.,

		Male	days	Reduced levels of reduced GSH and TSH; MDs, elevated the activity of AChE, exhibited severe impairment of locomotor activity, reduced complex I activity; Depleted the DA levels	methanolic extract (SME) and its active constituent, crocin (CR)		2016
29	w^{1118}; *Ddc*-GAL4 and *Elav*-GAL4	3, 30 days/ Male	125 µM for 14 days	Impairment of motor function, reduced the level of TH	Tianma Gouteng Yin	Rescued	Liu *et al*., 2015
30	Harwich	1-5 days/ Both the sexes	500 µM for 7 days in diet	Mobility defects; inhibition of AChE activity; Decrease in MTT cell viability and mitochondria, increases ROS, increases in LP and MDA, inhibition of SOD, CAT and GST activity	γ-orizanol	Rescued	Araujo *et al*., 2015
31	Oregon-K	8-10 days/ Male	500 µM for 7 days in diet	Induce motor deficits and mortality, increase in the levels of ROS, LPO and HP; Depletion in the levels of GSH and non-protein thiols, SDH and MTT; Inhibition of complex I–III and complex II–III; Enhanced activity of AChE and BchE; Decrease in DA levels in whole-body homogenate	Withania somnifera	Rescued	Manjunath and Muralidhara, 2015
32	Park and pink1 mutant;	3 days/ Male	1 µM for 48 hr in isolated neurons	Inhibition of mitochondria complex I activity induces BNIP3L degradation and interferes with mitophagy	BNIP3L	Rescued	Gao *et al*., 2015
33	*VPS35*-line	20 days and 60 days/ Female	500 µM	Late-onset loss of TH-positive DNs, poor mobility, shortened lifespans and increased sensitivity to ROT	-----	-----	Wang *et al*., 2014
34	Canton-S	1-3 days/ Male	125, 250 and 500 µM for 3 days	Defect in startle-induced locomotion, defect in spontaneous locomotion,	-----	-----	Liao *et al*., 2014
35	Canton-S, w^{1118}	3rd instar larvae	0-100 µM	A53T mutant larvae showed locomotion deficits and also loss of DNs; Expression of mutant α-syn and exposure to ROT do not cause olfactory defects	-----	-----	Varga *et al*., 2014
36	α-synuclein,	10, 20, 30,	500 µM for 6	No loss in DNs; Reduction in signal intensity	-----	-----	Navarro *et*

	PINK1, PARKIN	40, and 55 days/ Male	days				*al*., 2014
37	UAS-*hucp2* line	10 days/ Female	500 nM for 24 hr in isolated neurons	hucp2 expression attenuates mitochondrial fragmentation and lethality, increases intracellular cAMP levels,	-----	-----	Hwang *et al*., 2014
38	UAS-LRRK2 overexpressing *Vps35* or *Vps26*	5, 10, 20 days/ Both the sexes	1 mM	Overexpression protects against mobility defects induced by ROT, increases life span,	-----	----	Linhart *et al*., 2014
39	*D. melanogaster*	1-3 days/ Both the sexes	500 µM for 7 days in diet	Mobility defects, higher mortality, decrease in total thiol, increase in the mRNA expression of SOD and catalase CAT and also in the TH gene.	*V. officinalis*	Reverse the effects caused by ROT	Sudati *et al*., 2013
40	Canton-S and *Sin3Alof* line	1-5 days/ Sex not mentioned	62.5, 125 and 250 µM for 3 and 7 days	Selective degeneration of DNs, mobility defects, and early mortality; Sin3Alof were resistant to ROT-induced locomotor impairment and early mortality	Sodium butyrate	Reverse the effects caused by ROT	Laurent St. *et al*., 2013
41	Oregon-K	9-10 days/ Male	500 µM for 7day in diet	Elevation in the levels of ROS, PC and HP in both head and body regions of fly; Increased activities of antioxidant enzymes; DA depletion	*Selaginella delicatula*	Reverse the effects caused by ROT	Girish and Muralidhara, 2012
42	Oregon-R; *TRAP1* expressed fly	7 and 28 days/ Male	200 µM ROT for 24 hr in isolated neurons	Decreased expression of TRAP1 lead to mobility defects, and more sensitive to OS; Lowers the neuronal number and DA content induced by ROT; Overexpression reverses the effects	----	----	Butler *et al*., 2012
43	$w^{1118}$and *hucp2*-expressed line	10 days/ Female	500 µM	DA neuron degeneration, head dopamine depletion, locomotor impairment and ATP deficiencies in wild type	----	hucp2 expression rescues	Islam *et al*., 2012
44	w^{1118}, CS10, UAS-DVMAT	3-7 days/ Both the sexes	250 µM for 10 days	Dose-dependent climbing defects, reduced survival, neuronal loss in wild type	----	Overexpression of DVMAT rescues	Lawal *et al*., 2010

45	UAS-IR-*ple*-1 and UAS-IR-*ple*-2; w^{1118}	3 days/ Male	0.5 mM ROT on filter paper	Reduced DA levels; Reduced Complex 1 activity; Reduced neuronal survival	----	----	Bayersdorfer *et al*., 2010
46	Oregon-K	10 days/ Male	500 µM ROT for 7 days	Locomotor defects, Increased mortality; Diminution Levels of MDA and HP, PC, GSH, GSH; increased activity of CAT, SOD, GST; Reduced DA level	Bacopa monnieri	Rescue the behaviour and biochemical changes	Hosamani and Muralidhara, 2009
47	$w^{1118}$and mutant human LRRK2	10, 30, 50 days/ Both the sexes	100 µm for 1 month	Age-dependent locomotory defects; Significant loss DNs in both the groups of fly; Ubiquitous expression of hLRRK2 increases life span and fertility but more sensitive to ROT	----	----	Venderova *et al*., 2009
48	e03680 (dLRRK mutant)	3–5, 20 days/ Sex not mentioned	250 µM ROT, 5 mM PQ and 2 mM β-ME	Normal life span; unchanged number and pattern of DNs; Selectively sensitive to HP-induced stress but not to PQ, ROT and β-mercaptoethanol	----	----	Wang *et al*., 2008
49	parkin null, mutant human parkin (R275W or G328E)	3,7,10,15, 20 days/ Female	50 µ M	Parkin R275W mutant fly exhibit locomotor deficits; Susceptible to ROT-induced neurotoxicity; Exhibits pleiomorphic mitochondrial abnormalities	----	Overexpression of parkin R275W reverses the effects	Wang *et al*., 2007
50	*y, w* strain	14 days/ Females	250,500 µM for 7 days	Severe locomotor deficits and loss of DN in all the quantifiable clusters	Melatonin (5mM) L-Dopa (1mM)	Rescued	Coulom and Birman, 2004

Table 1.3: A review of ROT-mediated *Drosophila* models of PD. AChE: acetyl choline esterase; CAT: Catalase; DA: dopamine; GST: Glutathione S-transferase, HP: hydrogen peroxide; DNs: Dopaminergic neurons; MDA: Malondialdehyde: NO: Nitric Oxide; PC: Protein Carbonyls; PQ: Paraquat, ROT: Rotenone; ROS: reactive oxygen species; OS: Oxidative stress; TBA: thiobarbituric acid; TSH: Total Thiol

1.5. Potential mechanisms involved in the ROT-mediated neurodegeneration

ROT selectively inhibits mitochondrial complex I causing mitochondrial dysfunction (MD), oxidative stress (OS), nitrative stress, microglial activation, protein aggregation and degradation, affecting apoptotic pathways, neurotrophic factors, *etc*. leading to selective degeneration of striatal DNs (Norazit *et al.,* 2010). Some of the potential mechanisms are discussed below:

***Mitochondrial Dysfunction*:** It is established that decrease in complex I activity and lower ATP levels are correlated with mitochondrial complex I inhibition in animal models of PD (Abdin and Hamouda, 2008). ROT induces MD and inhibits the mitochondrial apoptotic pathway in SHSY5Y cell model (Qiao *et al*., 2022). A case-control study has demonstrated a strong relation between MD and exposure to environmental toxins including ROT (Tanner *et al*., 2011). The rate of mitochondrial fission and fusion is increased at the early stage of chronic exposure to ROT (Arnold *et al*., 2011). Inhibition of fission protects against neuronal loss showing that aberrant mitochondrial dynamics are related to the pathologic mechanism of ROT-induced PD. The inhibition of complex I of the ETC decreases mitochondrial membrane permeability (MMP) thus forming mitochondrial membrane permeability transition pores leading to ROT-induced apoptosis (Isenberg and Klaunig, 2000). Chronic exposure to ROT is shown to induce caspase-3 activation and mitochondrial membrane depolarization leading to neuronal death (Moon *et al*., 2005).

Oxidative stress: Inhibition of complex I by ROT generates ROS and reactive nitrogen species leading to an anaerobic state and contributing to its neurotoxicity. These pathological features could be reversed by antioxidants showing that these changes are caused by OS (Wang *et al.*, 2010; Tantucci *et al.*, 2009). ROT induces OS by activating

the nuclear factor erythroid 2 related factor 2 (Nrf2), an anti-oxidant pathway, which could be abolished by RNA interference-mediated knockdown of Nrf2 in SH SY5Y cell lines (Qiao *et al*., 2022). Chronic exposure to ROT also caused oxidative damage to proteins, increased NO, TBA reactive substances levels that could be reversed by the antioxidant vitamin E (Testa *et al*., 2005). The effects of ROT on the ETC could cause an increase in oxygen-free radicals, thereby resulting in OS and ultimately leading to severe damage to the DNs. Complex I inhibition not only results in ROS production or lesser ATP generation but also impacts the complex downstream signal transduction processes (Kotake and Ohta, 2003).

***Apoptotic pathways*:** ROT is known to induce the apoptotic markers, such as MMP dissipation, Bax expression, caspase-3/caspase-9 activity, and cytochrome c release (Condello *et al.*, 2011; Xiong *et al.*, 2009). OS caused by ROT induces lipid peroxidation and protein misfolding affecting apoptosis through the members of the Bcl-2 family while the activation of Bax and Bak helps mitochondrial outer-membrane permeabilization causing apoptotic cell death (Ethell and Fei, 2009). Chronic exposure to ROT leads to overexpression of anti-apoptotic protein Bcl-2 leading to DA neurodegeneration indicating the role of mitochondrial-apoptotic pathways in the pathogenesis of PD (Abdin and Hamouda, 2008). A higher voltage-dependent anion channel mRNA and protein levels were consistent in ROT-induced apoptosis (Xiong *et al.*, 2009). Furthermore, translocation of nuclear factor-κB and subsequently activation of caspase-3 are also reported in ROT-mediated apoptosis (Wang *et al.*, 2002).

***Microglial activation*:** Activation of microglial cells in the SN via NF-κB pathway is related to the ROT-mediated PD model (Hu *et al.*, 2010). The neurodegeneration process is significantly enhanced in microglial enriched neuronal cultures because of its increased susceptibility to ROT (Gao *et al*., 2002). The release of superoxide from

microglia upon ROT stimulation could be reduced by inhibiting the NADP oxidase thereby reducing the ROT-induced neurotoxicity (Gao *et al*., 2002). Though the neuroprotection of NaHS is attributed to its anti-inflammatory activity, it is actually due to the suppression of microglial cell stimulation in ROT-mediated PD models (Hu *et al.*, 2010).

***Protein aggregation and degradation*:** The ability to trigger LB formation and α-syn aggregation is the most important advantage of ROT-mediated PD models. Among 950 mitochondrial proteins, 110 proteins showed significant changes in abundance in ROT-mediated DA cell line model (Jin *et al*., 2007). In ROT-mediated cells and animal models, not only protein aggregation, but also increased levels of α-syn and ubiquitin (Sherer *et al*., 2002), oxidant-mediated alternative splicing of α-syn, translocation of over-expressed DJ-1 (Lev *et al*., 2008), and oxidation of mitochondrial proteins (Ramachandiran *et al*., 2007) are observed. The house-keeping proteins such as GAPDH are also affected resulting in the formation of intracytoplasmic aggregates of GAPDH under ROT-mediated conditions (Huang *et al*., 2009).

Among the various mechanisms of protein repair, UPS and autophagy-lysosome pathways are known to play a very important role in PD pathogenesis (Pan *et al*., 2008). OS, MD and microtubule proteasome inhibition are prospective mediators of ROT-mediated proteasome inhibition. A reduction in 20S proteasome activity and immunoreactivity indicates a higher degradation of proteasome components due to oxidative damage and microtubule dysfunction (Chou *et al.*, 2010; Ethell and Fei, 2009). The aggregation of the proteasome with other oxidized proteins led to the reduction of proteasome activity in ROT-mediated conditions. This mechanism is responsible for the accumulation of modified proteins in the apoptosis of the DNs in PD (Ren *et al*., 2003).

However, rapamycin reduces the levels of cytochrome C in cytosolic and mitochondrial fractions suggesting its molecular therapeutic strategy in PD (Pan *et al.*, 2009).

Neurotrophic factor depletion**:** Neurotrophic factors play a vital role in NDDs such as PD. The expression levels of vascular endothelial growth factor (VEGF) are prominently decreased in the midbrain of ROT-mediated animal models of PD (Xiong *et al.*, 2010). The neuroprotective efficacy of human umbilical cord mesenchymal stem cells could be significantly enhanced by expression of VEGF in rotenone-lesioned striatum of hemiparkinsonian rats (Xiong et al., 2010). Human retinal pigment epithelial cells can secrete neurotrophic factors derived from glial cells and brain-derived neurotrophic factors and protect DNs against ROT-mediated cell injury showing that depletion of neurotrophic factors is involved in the ROT-mediated DA neurodegeneration (Xiong *et al*., 2011).

Neurotransmitter factors: Dopamine itself contributes to neurotoxicity due to its high vulnerability to oxidation. ROT is shown to cause dose-dependent loss of cortico-striatal field potential amplitude due to the development of a membrane depolarization current along with a higher release of excitatory amino acid and DA in the striatal neurons (Abdin and Hamouda, 2008). ROT induces DA redistribution from the vesicle to cytosol by the stimulation of ROS and protein carbonylation which could be reverted by preventing the DA from being expelled from vesicle and inhibiting the ROT-mediated apoptosis upon administration of an anti-oxidant. This phenomenon indicates that ROT-mediated generation of ROS is involved in DA redistribution to the cytosol (Watabe and Nakaki, 2007). A decrease in cellular DA levels is shown to reduce the neurotoxicity and protect the DNs (Bayersdorfer *et al*., 2010). These results indicate that DA homeostasis plays an important role in the susceptibility of DNs to environmental and genetic factors in *in vivo* models of PD (Bayersdorfer *et al*., 2010).

1.6. Available therapeutic strategies for PD and their limitations

Healthy ageing and longevity are complicated phenotypes affected by environmental factors such as health habits, physical activities, psycho-social situations and genetic factors. Diet and caloric restriction have a crucial role in healthy ageing (Zia *et al.*, 2021). Postponing the ageing process is more effective and less expensive than treating particular age-related diseases. Hence, modern medication targeting a specific pathway will doubtfully be beneficial in preventing or treating these diseases (Bordoloi *et al.*, 2016). Therefore, more attention is paid in developing novel drugs derived from natural products by employing modern technology (Daimary *et al.*, 2020; Parama *et al.*, 2020). Natural products possess diverse biological activities and drug-like properties, making them the most important resources for drug discovery for treating human diseases (Kashyap *et al.*, 2021). To date, treatment with Levodopa remains the main therapy for PD. However, chronic use of L-DOPA for a longer period causes irrepressible movement disorders called Levodopa-induced dyskinesia (LID) in a majority of PD patients (Lane, 2019) making it difficult to manage (Blosser *et al.*, 2020). L-DOPA is readily transformed into highly reactive semiquinone and quinone derivatives contributing to more OS and causing neurotoxicity (Smith *et al.*, 1994). Hence it becomes important to find an alternative therapy for this disease. Some of the other currently available FDA-approved drugs are Sinemet CR, Rytary, Duopa or Duodopa, CVT-301, Ropinirole, Pramipexole, Pergolide, Bromocriptine, Apomorphine, etc. Therapies including DA agonists, MAO-B inhibitors, COMT inhibitors and other Levodopa formulations like the continuous duodenal infusion of Levodopa/carbidopa intestinal gel and apomorphine subcutaneous pumps are used as a substitute for Levodopa therapy limitations (Armstrong and Okun, 2020). Rather than dopamine-replenishing and symptomatic therapeutic strategies, the current trend of PD research has shifted to personalized

treatments targeting the refurbishment of anatomical, molecular and functional integrity of disease-specific brain circuits (Ntetsika *et al.,* 2021). Recently developed techniques targeting to relieve the disease symptoms include gene therapy in which DNA- or RNA-editing enzymes or antisense oligonucleotides are inserted into specific cells using a vector to initiate gene expression (Haggerty *et al.,* 2020; Hudry and Vandenberghe, 2019). Deep brain stimulation (DBS) is another technique which is shown to alter disease progression in patients with severe motor dysfunctions who are not responsive to drugs (Armstrong and Okun, 2020). In preclinical studies, chronic stimulation of the sub-thalamic nucleus electrically was shown to protect of SNpc DNs in rat models (Spieles-Engemann *et al.,* 2010; Harnack *et al.,* 2008). Though animal models have shown the neuroprotective role of DBS, a clinical study has shown that DBS could neither alter DA-ergic neuronal degeneration nor α-syn aggregation in PD patients (Pal *et al.,* 2017). Despite all the beneficial roles of the available therapeutic strategies for PD, there are limitations such as the wearing-out effect of oral drugs and narrow therapeutic strategies for advanced patients which led to instigating the researchers to review currently available methods (Cedarbaum, 2018).

Because of the reasons cited above, there is a need to find alternative therapeutic strategies for PD using natural products/phytochemicals as an alternative medicine.

1.7 Phytochemical mediated alternative therapeutic strategies for PD

Several phytochemicals with anti-oxidant and anti-inflammatory properties have been shown to confer neuroprotective efficacy by multiple experimental studies (Abrahams *et al.,* 2021; Zhao *et al.,* 2021). These phytochemicals offer neuroprotection in animal models of PD by inhibiting the α-syn aggregation (Briffa *et al.,* 2017). These

phytochemicals showed limited success in clinical trials (Cedarbaum, 2018). Hence, in order to develop new drugs for PD, it is very important to identify the plant products that specifically target the site of action (Javed *et al.,* 2019a). Some of the commonly used phytochemicals that have neuroprotective efficacy are listed in **Table 1.4**. Nevertheless, in-depth studies are highly recommended for the therapeutic intervention of plant products in humans.

Small molecules/ phytochemicals	ROT-animal PD models	Dose of ROT	Age of the animal	Mode of action of phytochemicals	Reference
5,6,7,4′-tetramethoxyflavone	*Drosophila*	500 µM for 7 days in diet	1-4 day	Rescues mobility defects, reduces OS, higher expression of mRNA of anti-oxidant enzymes like SOD, catalase	Siima *et al.*, 2020
α-Bisabolol	Albino Wistar rat	2.5 mg/kg for 4 weeks	280-300 g	Prevents loss of DNs, reduces ROS, improves SOD and catalase, attenuates MD	Javed *et al.*, 2020
α-Mangostin	Sprague Dawley rats	2 mg/kg/day for 21 days	250 ± 20 g	Restores the locomotor activity, memory deficits, and improves the levels of anti-oxidant enzymes, reduces the levels of phosphorylated α-syn	Parkhe *et al.*, 2020
Apigenin	Sprague Dawley rats	6 µg/µL	3 months (200-250 g)	Improves behavioral, biochemical and mitochondrial enzymes; attenuates pro-inflammatory cytokines release; enhances dopamine receptor expression	Anusha *et al.*, 2017
Acteoside	*Drosophila*	500 µM for 7 days	2-8 day	Improves locomotion, restores correct morphology of mitochondria and synaptic vesicles	Aimaiti *et al.*, 2021
Bacopa monnieri	*Drosophila*	500 µM for 7 days in diet	8-10 day	Protects against OS and improves DA level; improves mobility and reduces mortality	Hosamani and Muralidhara, 2009
Baicalein	C57BL/6J mice	2.5 mg/kg for 2 weeks	20-22 g	Alleviates the depression-like behavior, reduces α-syn aggregation, inhibits neuroinflammation, maintains neurotransmitters homeostasis, activates the BDNF/TrkB/CREB pathway	Zhao *et al.*, 2021
Biochanin A	Swiss albino	1 mg/kg for	9-10 weeks	Enhances locomotor activity, increases anti-oxidant	El-Sherbeeny *et*

	mice	3 weeks		defenses, lessens pro-inflammatory cytokines, increases phosphorylation of PI3K/Akt/mTOR proteins and upregulates beclin-1	*al.,* 2020
Centella asiatica	Wistar rat	2.5 mg/kg for 20 days	8-week old	Increases number and intensity of DNs; protected against mitochondrial complex I inhibition, decreases MDA levels and increases SOD and catalase activity	Teerapattarakan *et al.,* 2018
Carthamus tinctorius	Sprague Dawley rats	2 mg/kg/day	280–320 g	Improves body weight, rearing behaviour and grip strength; reverses the decreased expression of TH, DA transporter and DJ-1 and increases the levels of DA	Ablat *et al.,* 2016
Chlorogenic acid	C57BL/6J mice	2.5 mg/kg/day for 4 weeks	7 weeks of age	Protects nigral DA-ergic and intestinal enteric neurons; upregulates the antioxidative molecules	Miyazaki *et al.,* 2019
Curcumin and mitochondria-targeted curcumin	Swiss albino mice	3 mg/kg, for 60 days	3-4 month	Reverses the depressive-like behaviour; improves neurotransmitter levels	Hasan *et al.,* 2020
Curcumin monoglucoside	*Drosophila*	500 µM for 6 days	10 day	Shows better survival rate and locomotor activity and exerts anti-oxidant effects by replenishing cellular glutathione levels; restores mitochondrial complex I and IV activities	Pandareesh *et al.,* 2016
Demethoxycurcumin	Wistar rats	2.5. mg/kg/day for 45 days	225-250 g	Attenuates the motor and non-motor deficits; eases the protein expression of DA-ergic and apoptotic indices	Ramkumar *et al.,* 2019
Epigallocatechin-3-Gallate	Rat	0.5 mg/kg for 21 days	3 months	Improves motor ability, anti-oxidant activity, inhibits MD, promotes anti-apoptotic effect	Tseng *et al.,* 2020
Ferulic acid	Wistar rats	2.5 mg/kg for 4 weeks	6-7 months	Restores anti-oxidant enzymes, prevented depletion of glutathione, and inhibited lipid peroxidation; reduces the	Ojha *et al.,* 2015

				inflammatory mediators	
Gallic acid/ ellagic acid	Wistar rats	1.3 mg/kg for 35 days	6 weeks	Inhibits α-syn fibrillation and also disaggregates preformed α-syn amyloid fibrils	Kujawska *et al.*, 2019
Ginsenosides	C57BL/6J mice	30 mg/kg for 6 weeks	18-22 g	Decreases the climbing time and increases the latency, increases the number of TH-positive neurons and DA content	Han *et al.*, 2021
Kolaviron	Wistar rats	3 µg/µl infusiion	240-280 g	Attenuates the loss of nigrostriatal DNs and perturbations in the striatal GRP78 and XBP1 levels	Farombi *et al.*, 2020
Lycopodium	Wistar rats	2.5 mg/kg for 4 weeks	11-12 months	Increases the DNs; reduces activation of microglia and astrocytes	Jayaraj *et al.*, 2019
Morinda citrifolia	Sprague-Dawley rats	1 µg/1 µl infusion	12–15 months	Augments the levels of Bcl2 and blocks the release of cytochrome c and lessens the ROT-induced DN loss	Kishore Kumar *et al.*, 2017
Naringin	Wistar albino rats	2 µl for 14 days into SNpc	6-8 weeks	Reduces behavioral abnormalities, DA-ergic toxicity, mitochondria-dependent apoptosis	Garabadu and Agrawal, 2020
Quercetin	Albino rats	2 ml/kg/day for 4 weeks	180-200 g	Improves behavior, enhances autophagy, attenuates OS and ER stress-induced apoptosis	El-Horany *et al.*, 2016
Resveratrol	Albino Wistar rat	2 mg/kg for 35 days	180-250 g	Improves behavior, attenuates biochemical and histological changes, diminishes OS and MD	Palle and Neerati, 2018
Saffron	*Drosophila*	500 µM, for 7 days in media	9-10 days	Rescues the locomotor phenotype and diminished the enhanced levels of OS markers; attenuates MDs; restored the DA levels	Rao *et al.*, 2016
Selaginella delicatula	*Drosophila*	500 µM for 7 days in media	5-10 days	Protects against lethality; improves climbing ability; restores elevated levels of ROS, hydroperoxides and anti-oxidant enzymes	Girish and Muralidhara, 2012

Spondias mombin	zebrafish	3.0 µg/L for 4 weeks	4-6 months old	Prevents OS, inflammation; increases on the CAT, SOD and GSH and decreases the GST and NADPH oxidase activities	Santo *et al.*, 2021
Thymol	Wistar rats	2.5 mg/kg for 4 weeks	280-300 g	Attenuates DN loss, preserves of endogenous anti-oxidant defense networks and attenuation of inflammatory mediators including cytokines and enzymes	Javed *et al.*, 2019b
Tianma Gouteng	*Drosophila* (w1118 fly)	125 µl for 7 days	4-6 days	Enhances fly survival and locomotion; reduces the loss of DNs and cytotoxicity; inhibits α-syn aggregation	Liu *et al.*, 2015
Vicia faba	Swiss albino mice	1 mg/kg 9 injections	15-20 g	Improves motor activity, enhances striatal dopamine level, and decreases the striatal malondialdehyde as well as the expression of the inflammatory markers	Abdel-Sattar *et al.*, 2021
Withania somnifera	*Drosophila*	500 µM for 7 days in media	8-10 days	Protects lethality, improves locomotion, reduces stress, increased SDH, normalizes the DA level	Manjunath and Muralidhara, 2015

Table 1.4: List of plant extracts and phytochemicals and their neuroprotective efficacy in different ROT-induced PD models and their mode of action

1.6.2. Advantages of phytochemicals over pharmaceutical drugs

During the early days, when humans started hunting and gathered food from the natural environment, they might have consumed poisonous plants that might even lead to death. This is how early humans were able to develop knowledge about edible foods and natural medicines and hence the natural medicines have no side-effects because of the known toxicity of the plants as compared to pharmaceutical drugs. It needs no clinical trial because of the traditional knowledge. Another advantage of nature-based therapeutics is the "synergism" in which multiple components in natural products/phytochemicals play a cumulative role which is better than that of the individual drug. Also, the concept of "1 disease, 1 target, 1 drug" cannot treat complex multifactorial neurological diseases like AD and PD effectively. Hence, the new treatment system is shifted to the "multi-drugs and multi-targets" concept for combination therapies (Yuan *et al.,* 2016). This concept is quite applicable in the case of phytochemical mediated therapies. **Table 1.4** highlights the potential of phytochemical mediated therapeutic strategies for PD. Hence, natural products and traditional medicine based therapeutics are becoming more popular than pharmaceutical drugs because of the higher diversity in chemical structures and biological activities of plant-derived natural products (Yuan *et al.,* 2016). Also, natural products are inexpensive as compared to pharmaceutical drugs and it is available anywhere and anytime.

Though there is no evidence of Hippocrates himself stating **"LET THY FOOD BE THY MEDICINE AND THY MEDICINE BE THY FOOD"**, yet this philosophy is becoming very popular and applicable in today's world of complementarity of nutrition and pharmacology (Witkamp and van Norren, 2018).

1.7. Importance of life stage-matched animal models for late-onset NDDs

PD is a late-onset NDD. However, several researchers developed *Drosophila* PD model using young (5-20 day) animals (Akinade *et al.,* 2022; Maitra *et al.,* 2021; Sur *et al.,* 2018; Nguyen *et al*., 2018; Pandareesh *et al*., 2016; Cassar *et al*., 2015; Coulom and Birman, 2004). Studies regarding susceptibility genes and pathways of PD under neurotoxin treatment have also been conducted mostly using young flies (**Table 1.3)** (Maitra *et al*., 2021; Sur *et al*., 2018; Cassar *et al*., 2015). Pre-clinical studies on NDDs should mimic the characteristic features of the disease such as late-onset for developing therapeutic strategies. Most of the previous studies on the neuroprotective efficacy of phytochemicals and small molecules are mainly based on young animals (**Table 1.4**). No concrete data is available on the later phase of life span which is an important paradigm in finding the therapeutic strategies for PD. The adult life of *Drosophila* is categorized into health (no natural death occurs), transition (slight decline in the mortality curve showing 10% death) and senescence stage (steady decline in mortality curve represented by the window between the end of the transition phase till maximum life span of the fly) (Arking *et al*. 2002). Analysis of the adult life stages in model organisms has revealed that they are characterized by different patterns of gene expression (Arking, 2015, 2009; Pletcher *et al*., 2002), which is similar to that of the equivalent life stages of humans. A transcriptomic analysis using microarrays to compare the gene expression profiles of different life stages of *Drosophila melanogaster* has identified 1184 genes with marked differences in expression level between young and old age groups (Bordet *et al*., 2021). The life stages of *Drosophila* are believed to have both common and unique complex processes and can be influenced independently by a relatively large number of stages associated pathways (Soh *et al*., 2013).

Hence, it is important to study the neuroprotective efficacy of phytochemicals in the later stages of the life span of model organisms. This is the first study to develop an adult life phase-specific (early health phase, late health phase and transition phase) ROT-mediated *Drosophila* model. I shall be using this model to understand the neuroprotective efficacy of curcumin.

1.8. Objectives of the present study are as following:

1. To develop adult health and transition stage-specific rotenone-mediated *Drosophila* model of Parkinson's disease

2. To evaluate the dopaminergic neuroprotective efficacy of curcumin in rotenone-mediated life phase-specific *Drosophila* model of PD

CHAPTER 2

Materials and Methods

2.1. Fly stock:

The animal used in this experiment was the Oregon K strain of *Drosophila melanogaster* obtained from the National Stock Centre, University of Mysore, Karnataka, India. Only male flies were used in the present study.

2.2. Fly husbandry:

The flies were housed in a controlled incubator (Percival DR41VL, USA) with a constant temperature of 22 ± 2^0C and humidity of 65 ± 5%. They were fed on normal media (Section 2.3). The flies were transferred to a fresh vial containing media every 3 days. The mortality of the flies was noted whenever they were transferred to a fresh media vial. The circadian rhythm was maintained at alternate 12 Hour (Hr) light and dark cycles.

2.3. Preparation of Media:

Materials: Sucrose (SRL, India, Cat: 84973), Yeast (Angel, India, Cat: 5331A202008), agar-agar (Himedia, India, Cat: GRM666) and propionic acid (MERCK, Cat: 8006050 500 1730) were used for media preparation.

Methods: The media was prepared following the protocols of Phom *et al.* (2014).

The constituents such as 27 g of sucrose, 16 g of yeast and 1.5 g of agar-agar were dissolved in double distilled water for a few minutes. The mixture was boiled on an induction cooker for 12 minutes with intermittent stirring every 4 minutes. 1.78 mL of propionic acid was added after cooking the media. The media was then poured into the vials.

2.4. Collection and aging of fly:

Materials: Diethyl ether (MERCK, Cat: 1.00923.0521), glass bottle, vials containing media, glass plate, brush and stereo zoom microscope were used for collecting the fly.

Methods: The flies in the propagation vials were tapped and transferred into a glass bottle. They were mildly anaesthetized using a few drops of diethyl ether and the bottle was tapped gently so that the flies were not hurt. Once the flies slept, they transferred to a glass plate. Males and females were isolated using a brush under a microscope. A total of 25 male flies were transferred to a fresh vial containing media. Care was taken to avoid the fly from sticking on the media. The flies were aged by transferring to fresh vials containing media every 3 days till it was used for the experiments.

2.5. Preparation of rotenone stock:

Materials: Rotenone (ROT, Sigma, Cat: R8875); DMSO (Sigma, Cat: D8418) were used for preparing the rotenone stock.

Methods: ROT stock was prepared by dissolving 3 mg in 100 µL of DMSO giving a stock concentration of 76 mM. Further dilution of desired concentration was made in a 5% sucrose solution.

2.6. Rotenone susceptibility assay:

Materials: Rotenone (ROT, Sigma, Cat: R8875); DMSO (Sigma, Cat: D8418) and sucrose (SRL, India, Cat: 84973) were used for feeding the fly. Whatman filter paper no.1 cut in the form of a disc was used as a feeding medium for the experiment.

Methods: For feeding the flies on filter paper, a solution of 5% sucrose was prepared by dissolving 500 mg of sucrose in 10 mL of double-distilled water. Different concentrations of ROT *viz*. 10, 25, 50, 100, 250, 500 and 1000 µM were used to check the susceptibility in early health phase, late health phase and late transition phase flies. A serial dilution of the above-mentioned concentrations was prepared in 5% sucrose. An amount of 250 µL of the ROT solution was added onto the filter disc placed at the bottom of the 100x30 mm glass vial. A minimum of 100 (25 X 4) flies of the same group were exposed to each concentration. Flies were transferred to a fresh vial containing the solution every 24 Hr to avoid desiccation. Mortality and climbing ability of the fly was noted every 24 Hr till all the flies were dead.

2.7. Preparation of Curcumin stock:

Materials: Curcumin (CUR, Sigma, Cat: 1386); DMSO (Sigma, Cat: D8418) and Sucrose (SRL, India, Cat: 84973) were used for feeding the fly. Whatman filter paper no.1 disc was used as a feeding medium in the experiment.

Methods: CUR stock was prepared by dissolving 4 mg in 20 µL of DMSO giving a stock concentration of 543 mM. Further dilution of desired concentration was made in a 5% sucrose solution.

2.8. Curcumin toxicity study:

Materials: Curcumin (CUR, Sigma, Cat: 1386) and DMSO (Sigma, Cat: D8418) and Sucrose (SRL, India, Cat: 84973) were used for feeding the fly. Whatman filter paper no.1 cut in the form of a disc was used as a feeding medium for the experiment.

Methods: A volume of 250 µL of 5% sucrose was fed to the control flies and 250 µL of different concentrations of CUR (10 µM, 25 µM, 50 µM, 100 µM, 250 µM, 500 µM, 1 mM, 1.5 mM, 2 mM and 2.5 mM) prepared in 5% sucrose solution were pipetted onto the filter disc placed at the bottom of 100x30 mm glass vial for CUR treated flies. Twenty-five male flies were put in each vial for the treatment and a total of 100 (25 X 4) flies were used for each concentration in the experiment. Flies were transferred to vials containing fresh solution every 24 Hr to avoid desiccation. Mortality and climbing were noted every 24 Hr till all the flies were dead.

2.9. Negative geotaxis assay:

Materials: Glass vials, plastic tubes with cap, 10 mL graduated glass or plastic pipettes, stopwatch, mouth aspirator, sponge pad (at least 2.5 cm height) and test tube stand were used for negative geotaxis assay.

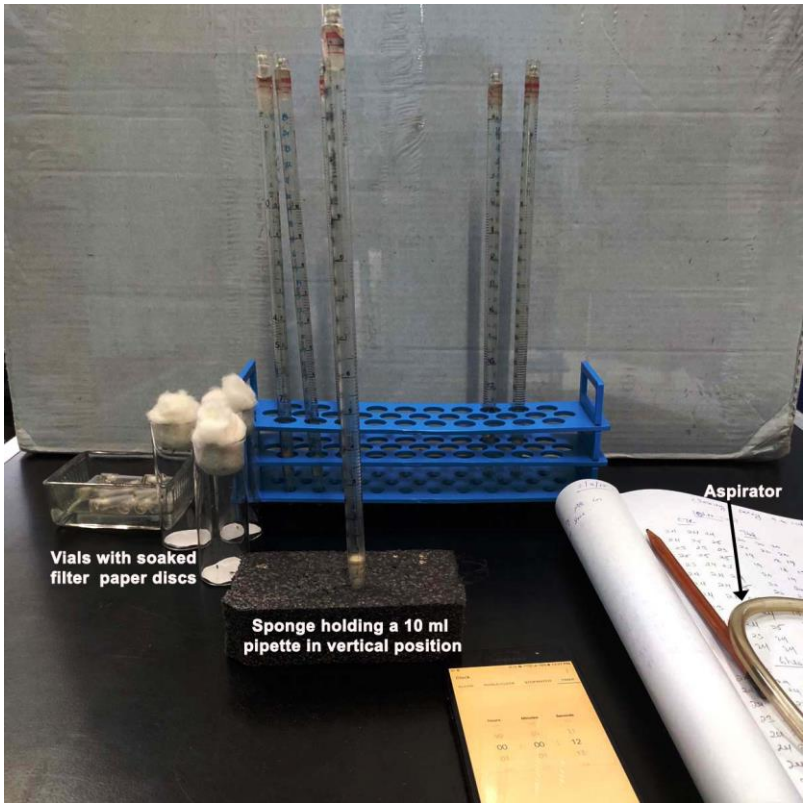

Figure 2.1: Experimental set-up for negative geotaxis assay (From Phom *et al.*, 2021).

Methods: The climbing ability was assessed with minor modifications from Botella *et al*. (2004).

1. A graduated 10 mL pipette was fixed vertically on a sponge and gently drop a single control or experimental fly with an aspirator into the pipette. The open end of the pipette was closed with a cap.

2. The fly was acclimatized for 2 min

3. After 2 min, it was gently tapped to the base of the pipette.

4. The distance it could climb on the wall of the pipette in 12 sec was recorded. Each fly was given three chances.

5. The same procedure was followed for all the flies and at least 12-15 flies were used for each treatment group (**Figure 2.1)**.

2.10. Extraction of mitochondria from fly head and body:

Materials: Mannitol (SRL, India, Cat: 134889); Sucrose MB grade (SRL, India, Cat: 1944115); EDTA (SRL, India, Cat: 54959); HEPES (SRL, India, Cat: 84023) and Tris (SRL, India, Cat: 2049170) were used for mitochondrial extraction.

Methods: Mitochondrial extraction buffer was prepared using the following protocols of Moreadith and Fiskum, (1984) and Trounce *et al.* (1996) with minor modifications.

Preparation of buffers:

(I) **Buffer A**: 50 mM HEPES stock was prepared by dissolving 0.1192 g of HEPES in 10 mL MilliQ water and pH was adjusted to 7.4. To this, 1.82 g of mannitol, 1.195 g of sucrose and 10 µL of 0.5 M EDTA were added. The final volume was adjusted to 50 mL with MilliQ water.

(II) Buffer B: 4.275 g of sucrose was dissolved in 25 mL of MilliQ water and 100 µL of 1 M Tris (1.211 g of Tris in 10 mL of MilliQ water and adjusted the pH to 7.4) was added. The final volume was adjusted to 50 mL.

Extraction: The head and body of the fly were dissected. 500 heads or 200 bodies were taken in an Eppendorf tube and homogenized in 500 µL of extraction Buffer B. Proper care was taken so that the sample was not heated while homogenizing. After crushing, the pestle was rinsed with another 500 µL of the same buffer making a total of 1 mL. The sample was centrifuged at 5000 rpm for 10 min at 4^0C. The supernatant was collected and centrifuged again at 8000 rpm for 10 min at 4^0C. The supernatant was collected for cytosolic fraction while the pellet was dissolved in 1 mL of mitochondrial Buffer A. It was then centrifuged at 9800 rpm for 10 min at 4^0C. The pellet thus obtained was again dissolved in the same mitochondrial Buffer A. For 500 heads, 125 µL of Buffer A was used for dissolving finally while 400 µL of the same buffer was used for dissolving 200 bodies.

2.11. Quantification of mitochondrial protein:

Materials: Bovine serum albumin (BSA; Sigma, Cat: A-2153), Bradford dye (Biorad, Cat: 5000006) and Phosphate-buffered saline (PBS, HiMedia, India, Cat: ML-023) were used for protein quantification.

Methods: Quantification of protein was done using the Bradford method. BSA stock was prepared by dissolving 2 mg/mL PBS for normal protein quantification. A working concentration of 0.2 µg/µL was prepared by dissolving the 100 µL of stock solution in 900 µL PBS. For mitochondrial protein quantification, BSA stock was prepared in extraction

Buffer A for mitochondrial fraction and Buffer B for the cytosolic fraction. A working concentration of 0.2 µg/µL was prepared by dissolving the 100 µL of stock solution in 900 µL PBS. A serial dilution of 0.5, 1, 1.5, 2, 2.5, 3 and 3.5 µg/mL standard BSA solution was prepared by diluting the BSA working solution in PBS and 500 µL Bradford dye (**Table 2.1**). After 5 min of incubation at room temperature (RT), the absorbance was read at 595 nm using NanoDrop 2000C (Thermo Scientific). Mitochondrial samples were quantified using the same standard graph.

BSA (µg/mL)	Working solution (µL)	PBS (µL)	Bradford (µL)
0.5	2.5	497.5	500
1	5	495	500
1.5	7.5	492.5	500
2	10	490	500
2.5	12.5	487.5	500
3	15	485	500
3.5	17.5	482.5	500

Table 2.1: Preparation of serial dilutions using standard BSA

2.12. Assessment of Complex I-III activity:

Materials: Phosphate-buffered saline (PBS, HiMedia, India, Cat: ML-023), KH_2PO_4 (MERCK, Cat: 6.175460.5001730); K_2HPO_4 (MERCK, Cat: 1.93630.0521); Nicotinamide adenine dinucleotide hydrogen (NADH, SRL, India Cat: 44018); Potassium ferricyanide (KFeCN, HiMedia, India, Cat: GRM627); Cytochrome C (SRL, India, Cat: 34015) were used for mitochondrial complex I-III activity assay.

Methods: Mitochondrial NADH-Cytochrome C reductase (complex I-III) was assayed using the modified protocol of Navarro *et al.* (2004).

The dissected heads and bodies of the flies were homogenized in mitochondrial extraction buffer. For complex I-III activity, 60 µg of the isolated mitochondria were mixed with phosphate buffer (0.1 M, pH 7.4). To this sample mixed with buffer, NADH (0.2 mM) and KFeCN (1 mM) were added and mixed for 10 sec. The reaction was initiated with the addition of cytochrome C (0.1 mM) and the absorbance was recorded at 550 mm for 7 min. The total reaction volume was 1 mL. The activity was expressed as nmol cytochrome C reduced/min/mg protein (MEC = 19.6 mM^{-1} cm^{-1}).

2.13. Co- and pre-feeding regimen:

Materials: Rotenone (ROT, Sigma, Cat: R8875); Curcumin (CUR, Sigma, Cat: 1386); DMSO (Sigma, Cat: D8418) and Sucrose (SRL, India, Cat: 84973) were used for feeding the fly. Whatman filter paper no.1 disc was used as a feeding medium in the experiment.

Methods: For understanding the efficacy of CUR in the *Drosophila* model of PD, two treatment regimens were employed i.e., Co-feeding regime and Pre-feeding regime

The concentrations of ROT used for the experiments were 500 µM, 25 µM and 10 µM for early health phase, late health phase and transition phase flies respectively. All these concentrations were selected with utmost care in such a way that they did not affect the viability, however, caused mobility defects in *Drosophila* as explained in the following

chapters. CUR concentrations were selected in such a way that they showed no mobility defects and did not affect the survival of the fly.

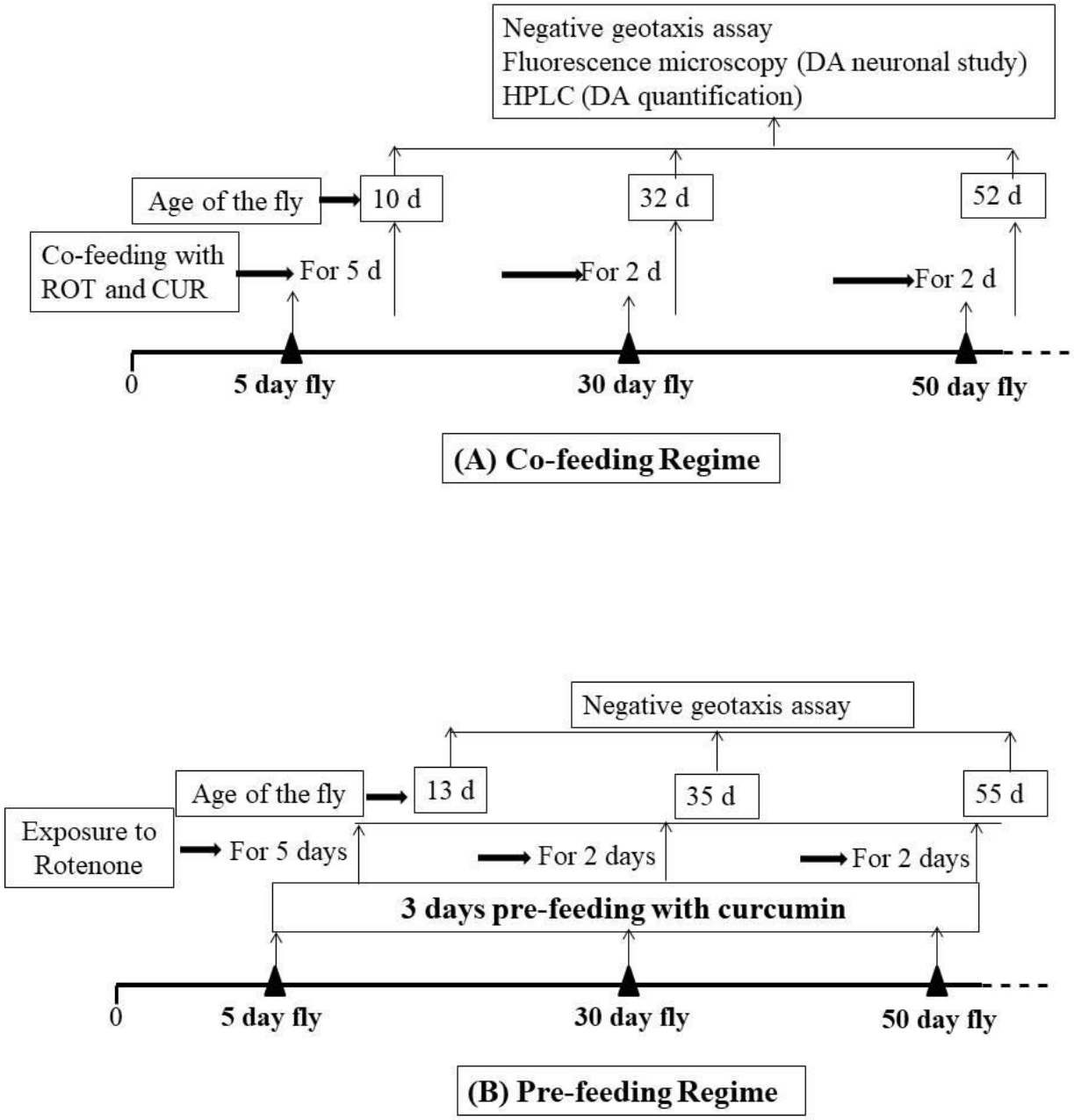

Figure 2.2: Co-feeding and pre-feeding regimen using *Drosophila*: (A) **Co-feeding**: Flies belonging to different life phases (5 days: Early health span; 30 days: Late health span; and

50 days: transition phase) were fed with ROT alone or ROT and CUR for 5 days in case of early health phase and 2 days in case of late health phase and transition phase flies. Control fly remained in 5% sucrose only while the CUR (500 µM) *per se* group was fed with CUR only. The negative geotaxis assay (NGA) was performed on the 4^{th} and 5^{th} day of exposure to ROT in the case of early health phase fly and on 1^{st} and 2^{nd} day of exposure to ROT in case of the late health phase and transition phase flies respectively. (B) **Pre-feeding regimen**: Flies of different life stages (Early health phase; late health phase; and transition phase) were pre-fed with CUR for 3 days. Control and the group to be treated with ROT remain in 5% sucrose during this period. The fly was then exposed to ROT for 5 days in case of the early health phase and 2 days in case of the late health phase and transition phase flies. Control and CUR (500 µM) per se group remain in 5% sucrose. NGA was performed on 4^{th} and 5^{th} day after exposure to ROT in case of the early health phase fly and on 1^{st} and 2^{nd} day of exposure to ROT in case of the late health phase and transition phase flies.

(A) Co-feeding regime: In the co-feeding regimen, the fly was fed with ROT alone for ROT treatment group and a combination of ROT along with CUR (100 µM, 250 µM, 500 µM and 1000 µM) for the co-feeding group while the control fly remain in 5% sucrose only.

(B) Pre-feeding regime: In the pre-feeding regimen, fly was fed with CUR (100 µM, 250 µM, 500 µM and 1000 µM) for 2, 3 and 5 days and then switched to ROT. For the ROT treatment group, fly was fed with 5% sucrose for 2, 3, 4 and 5 days and then transferred to ROT while the control fly was fed with 5% sucrose only. Climbing ability was assessed on the 4^{th} and 5^{th} day of feeding with ROT for the early health phase; while it was on 1^{st} and 2^{nd} day for the late health span and transition phase flies (**Figure 2.2**).

2.14. Quantification of dopaminergic neurons and fluorescence intensity using fluorescence microscopy:

Materials: Paraformaldehyde (Sigma, Cat: I58127); Phosphate-buffered Saline (HiMedia, Cat: ML023); Triton X-100 (TX-100, Sigma, Cat: T8787); Normal Goat Serum (NGS; Vector Lab, Cat: S1000); VECTASHIELD mounting medium (Vector Labs, CA, USA, Cat: H1000); Rabbit anti-Tyrosine hydroxylase (anti-TH) polyclonal primary antibody (Millipore, MA, USA, Cat: Ab152); Goat anti-rabbit IgG H&L (TRITC labelled) polyclonal secondary antibody (Abcam, MA, USA, Cat: Ab6718); Cover glass (Electron Microscopy Sciences); Rotospin test tube rotator (Tasons, Cat: 3070) and Disk for 24x1.5ml tube (Tarsons, Cat: 3071); Fluorescence microscope fitted with 100W Mercury lamp (Carl Zeiss, Axio Imager 2) were used for fluorescence microscopy.

Miscellaneous: Sterilized Eppendorf tubes; Pipette (cleaned with 70% ethanol before and after use); Sterilized pipette tips; Stereo-binocular microscope and other fly handling items are some of the miscellaneous items used in the present study.

For understanding the neurodegeneration in the fly model, the following four steps were followed:

A) Immunostaining of the brain

B) Acquisition of the image

C) Quantification of the dopaminergic neurons

D) Quantification of neurodegeneration through fluorescence intensity

A) Immunostaining of *Drosophila* brain

Immunostaining of the *Drosophila* brain was done using a modified protocol of Bayersdorfer *et al*. (2010). The following steps were followed for immunostaining:

Methods

1. Fly brains were fixed in 4% paraformaldehyde (PFA) containing 0.5% Triton X-100 (TX-100) for 2 Hr at RT.

2. PFA was washed off with PBS containing 0.1% TX-100 (0.1% PBST) 3 times for 15 minutes each at RT.

3. Brains were dissected in PBS.

4. The brains were washed with 0.1% PBST 5 times for 15 minutes each at RT.

5. The brains were blocked in 5% NGS in PBS containing 0.5% TX-100 (0.5% PBST) for 120 minutes at 4° C.

6. The brains were incubated in primary anti-TH antibody (1:250 dilution) for 72 Hr at 4° C.

7. In order to remove the excess primary antibody, the brains were washed 5 times for 15 minutes each in 0.1% PBST.

8. The brains were incubated in secondary antibody (1:250 dilution) for 24 Hrs in dark conditions at RT.

9. The excess secondary antibody was removed by washing the brains 5 times for 15 minutes each in 0.1% PBST.

10. The brains were mounted in Vectashield ® and covered with a cover slip.

11. The edges were sealed using clear fingernail polish.

12. The samples were ready for image acquisition.

DOs and DON'Ts

1. Fixing was done properly using Rotospin at constant velocity (10RPM) for thorough fixing of brain tissue

2. The samples were washed using a rotator at constant velocity (10RPM).

3. Incubation with primary and secondary antibodies was done using Rotospin (Constant 10RPM) to mix the tissue gently and thoroughly.

4. Care was taken while mounting the brain using a cover slip so that the brains were not crushed.

5. Sealing of the edges was done properly to avoid drying of the samples.

6. Image acquisition was done on the same day to avoid bleaching.

B) Acquisition of the image

The images were acquired using a fluorescence microscope fitted with a 100W Mercury lamp (Carl Zeiss, Axio Imager 2) through ZEN 2012 SP2 by using the following steps:

Methods

1. The stained brains were viewed under a fluorescence microscope at 40X objective lens.

2. Monochromatic camera with a Rhodamine fluorescence filter was used for capturing the images.

3. For image acquisition, a red dot test was performed for visibility of neurons for the control brain and reuse the same exposure time for other samples.

4. Z-stack programming was performed with a constant interval.

5. From the Z-stack gallery, only clear images were selected for further processing.

6. For creating a 2D merged image, maximum intensity projection (MIP) and x-y Plane were selected.

7. The 2D images were exported in .jpg format for image presentation.

DOs and DON'Ts

1. Care was taken to capture images from the samples with the same orientation.

2. Care was taken while performing the red dot test.

3. The same setting was always reused for all the images.

4. Care was taken while taking Z-stack so that no neuron is left out of scanning.

After the images were acquired through Z-stacking, the following steps were followed:

C) Quantification of the number of DNs

D) Characterization of neurodegeneration through quantification of fluorescence intensity

C) Quantification of the number of dopaminergic neurons

Multiple models of *Drosophila* have been developed to find a deeper understanding of the mechanisms of PD pathogenesis (Akinade *et al*., 2022; Navarro *et al.,* 2014; Whitworth, 2011; Coulom and Birman, 2004). A pioneering report by Feany and Bender (2000) showing the loss of DNs in α-syn mediated *Drosophila* PD model initiated the excitement of this model. However, many *Drosophila* laboratories could not reproduce the same data as reported by Feany and Bender (Navarro *et al.,* 2014; Botella *et al.,* 2009; Pesah *et al.,* 2005). These contradictory observations gave rise to uncertainties and concerns about the reliability of the *Drosophila* PD models (Navarro *et al*., 2014). Hence, researchers started re-looking into the number of DNs.

A cartoon showing the position of the DNs in the fly brain is depicted in **Figure 2.3** while the number of DNs and their locations in the *Drosophila* brain is summarized in **Table 2.2**.

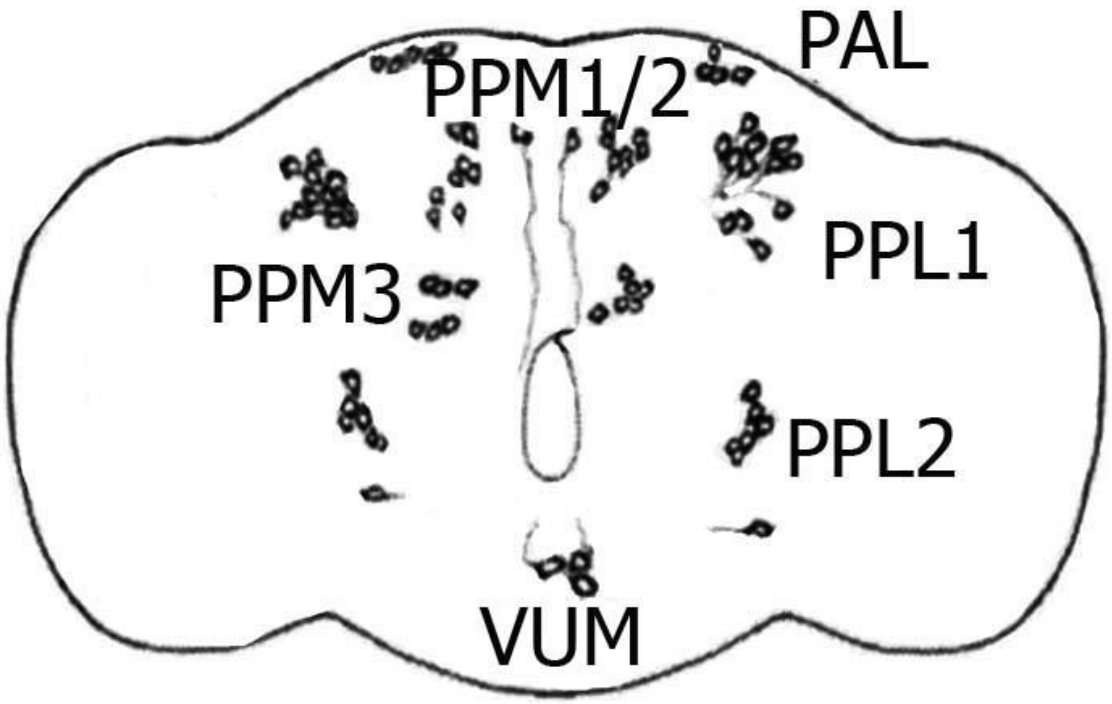

Figure 2.3: Cartoon of *Drosophila* brain showing the position of DAnergic neuronal clusters. The brain of *Drosophila* has around 141 DNs in each hemisphere which are arranged into different clusters. Some of them are PAL (~5 neurons), PPL1 (~12 neurons), PPL2 (~7 neurons), PPM1/2 (~8-9 neurons), PPM3 (~6 neurons) and VUM (3 neurons). These DNs are easily countable using a fluorescently labelled secondary antibody against the anti-TH primary antibody. There are other regions like PAM with around 100 neurons which are not easily quantifiable with a fluorescence microscope. (PAM: Protocerebral Anterior Medial; PAL: Protocerebral Anterior Lateral; PPM: Protocerebral Posterior Medial; PPL: Protocerebral Posterior Lateral; VUM: Ventral Unpaired Medial)

Clusters	Abbreviated as	Number	Location	Remark
Protocerebral anterior medial	PAM	~100	Medial tips of and areas posterior to horizontal lobes	Not countable using fluorescence microscopy
Protocerebral anterior lateral	PAL	4-5	Optic tubercle, superior posterior slope, ventral medial protocerebrum	Easily countable
Protocerebral posterior medial	PPM1	1-2	Ventrally along midline	Easily countable, too close and usually clubbed together as PPM1/2
	PPM2	7-8	Subesophageal ganglion, ventral medial protocerebrum	
	PPM3	5-6	Central complex	Easily countable
Protocerebral posterior lateral	PPL1	11-12	Mushroom bodies and vicinity, superior arch	Easily countable
	PPL2	6	Calyx, lateral horn, posterior superior lateral protocerebrum, Lobula	Easily countable
Ventral unpaired medial	VUM	3	Lower subesophageal	Easily countable
Protocerebral posterior deutocerebrum	PPD	0-1	Posterior slope	Too low or absent
Protocerebral posterior dorsomedial	PPM4	0-1	Central complex	Too low or absent
Protocerebral posterior lateral	PPL3	0-1	Superior posterior slope, dorsal edge of the lateral horn	Too low or absent
	PPL4	0-1		
	PPL5	0-1		

Table 2.2: Anatomical location and number of DNs in *Drosophila* brain: There are approximately 284 DNs arranged in different clusters in each hemisphere of the brain. These neurons can be stained using secondary antibody against primary anti-TH antibody. Most of these clusters are easily countable using fluorescence microscopy while the PAM cluster is not countable (Modified from Nässel and Elekes, 1992).

Method	**Paraffin section / light microscopy**		**Whole-mount / confocal microscopy**		**References**
Cluster/ Model	PPL1	PPM1/2	PPL1	PPM1/2	
α-syn	No	Yes	-	-	Feany and Bender, 2000
	Yes	Yes	-	-	Auluck *et al.*, 2002
	-	Yes	-	-	Auluck and Bonini, 2002
	-	Yes	No	No	Auluck *et al.*, 2005
	-	Yes	-	-	Chen and Feany, 2005
	-	-	-	No	Pesah *et al.*, 2005
Parkin	No	No	-	-	Greene *et al.*, 2003
	-	-	-	No	Pesah *et al.*, 2004
	-	No	-	-	Yang *et al.*, 2003
	-	-	Yes	No	Whitworth *et al.*, 2005
	-	No	-	-	Cha *et al.*, 2005
DJ-1α	-	-	No	No	Menzies *et al.*, 2005
	-	-	No	No	Meulener *et al.*, 2005
	-	Yes	-	-	Yang *et al.*, 2005
DJ-1β	-	-	No	No	Meulener *et al.*, 2005
	-	-	No	No	Park *et al.*, 2005
Rotenone	PPL1	PPM1/2	PPL1	PPM1/2	
50 µM	-	-	Yes	Yes	Wang *et al.*, 2007
250 µM	-	-	Yes	No	Lawal *et al.*, 2010
250 µM 500 µM	-	-	Yes	Yes	Coulom and Birman, 2004
500 µM 500 µM	-	-	Yes	Yes	Coulom and Birman, 2004
	-	-	No	No	Meulener *et al.*, 2005
	-	-	No	No	Navarro *et al.*, 2014
Paraquat	PPL1	PPM1/2	PPL1	PPM1/2	
100 µM	-	-	No	No	Meulener *et al.*, 2005
10 mM	-	-	Yes	No	Lawal *et al.*, 2010
20 mM	-	-	Yes	Yes	Chaudhuri *et al.*, 2007
20mM	-	-	No	No	Navarro *et al.*, 2014

Table 2.3: Difference in the number of DNs in different clusters as shown by different laboratories

For the quantification of the DNs, the following steps were followed:

Methods

1. From the Z-stack image, identify the cluster by going through the slices of the image

2. Enlarge the image to see the clear cell body.

3. Number of DNs was counted for each cluster in a blindfolded manner.

4. A minimum of 5 to 6 brains were quantified for each group of treatments.

D. Characterization of neurodegeneration through quantification of fluorescence intensity of fluorescently labelled secondary antibodies

Though there is a difference in observation regarding the loss of DNs (**Table 2.3**), the decrease in fluorescence signal intensity of GFP reporter (driven by TH-gal4) is proportional to the diminished levels of TH reflecting the condition of "neuronal dysfunction" (Navarro *et al.,* 2014), leading to the DA-ergic degeneration. Here, I tried to look into the DA-ergic neurodegeneration/neuroprotection by quantifying the fluorescence intensity of the fluorescently labelled secondary antibody targeted against the anti-TH primary antibody (TH is the rate-limiting enzyme for dopamine synthesis) using a reliable, repeatable method under a fluorescence microscope developed in our laboratory as described below.

Methods

1. From 3D images of Z- stack, PAL, PPL1, PPL2, PPM1/2, PPM3 and VUM (quantifiable DA neuronal clusters in the fly brain) regions of the brain were selected.

2. The images were enlarged to see clear neuritis.

3. Appropriate tools (draw spline contour) were selected from graphics and a line was drawn around the neuron.

4. Upon right-clicking inside the neuron, more measurement options were opted and the intensity sum was selected and checked.

5. From the measure option; list, view all and create document were selected.

6. The fluorescence intensity sum for each stack was recorded in .xml format.

7. The .xml sheet was opened and selected the slices with the highest intensity and 5 values upper and lower to the max value were taken.

8. An average of the slides was taken.

9. The same procedure was followed for all the neurons.

10. The sum of the averages gave the intensity sum of all the neurons of the particular region (cluster-wise) (**Figures 2.4 and 2.5)**.

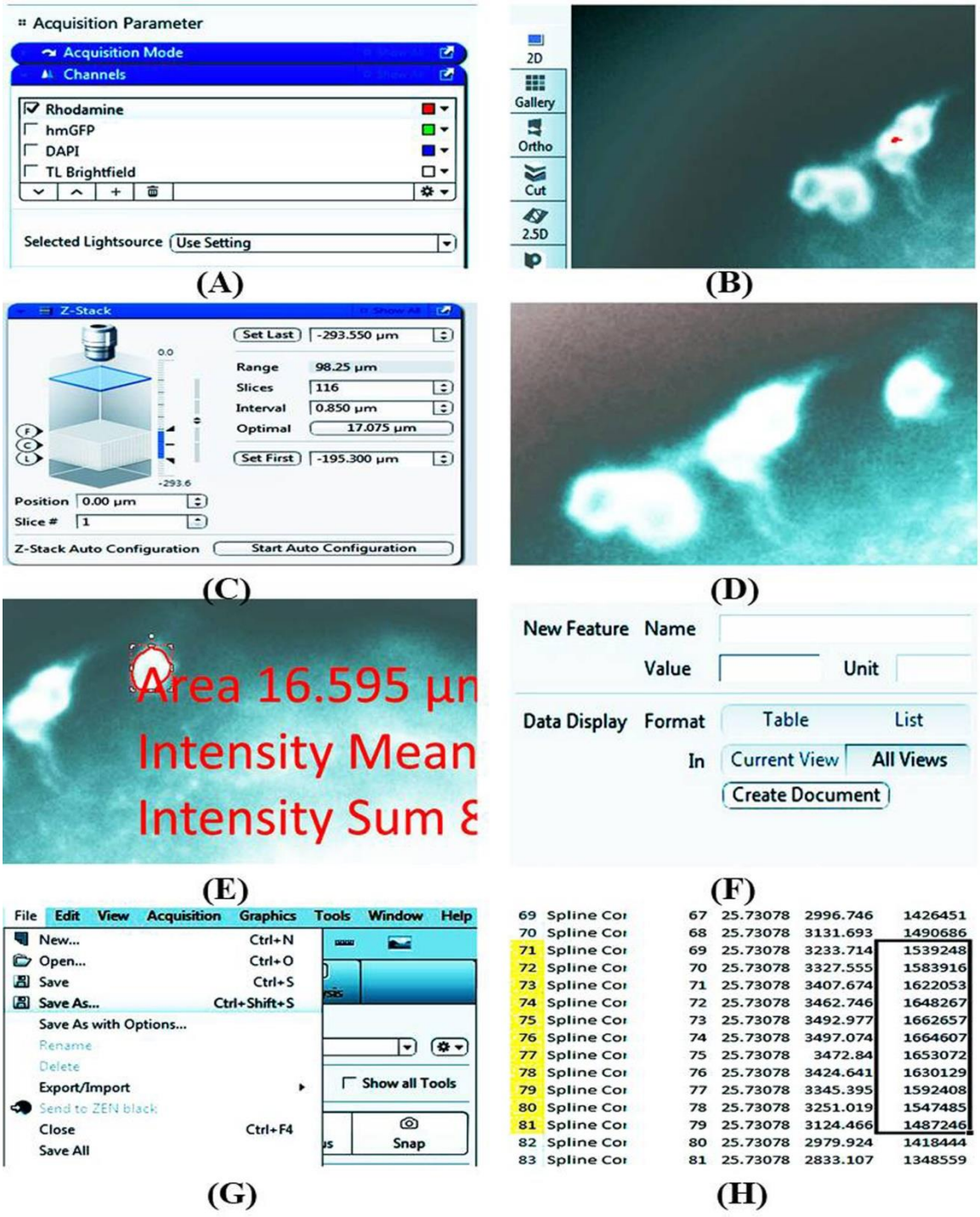

Figure 2.4: Description of the different steps involved in the quantification of fluorescence intensity of DNs using Carl Zeiss-ZEN 2012 SP2 software. Selection of the channel of choice (A), selection of the exposure time (B), capturing Z-stack images (C), selection of slices where the neurons are clearly visible (D), making spline contour around the cell body

of the neuron to measure the fluorescence intensity of the fluorescently labelled secondary antibody (E), creating a document of the fluorescence intensity (F), saving or exporting the document in .xml format (G), selection and quantification of fluorescence intensity from the excel sheet (H).

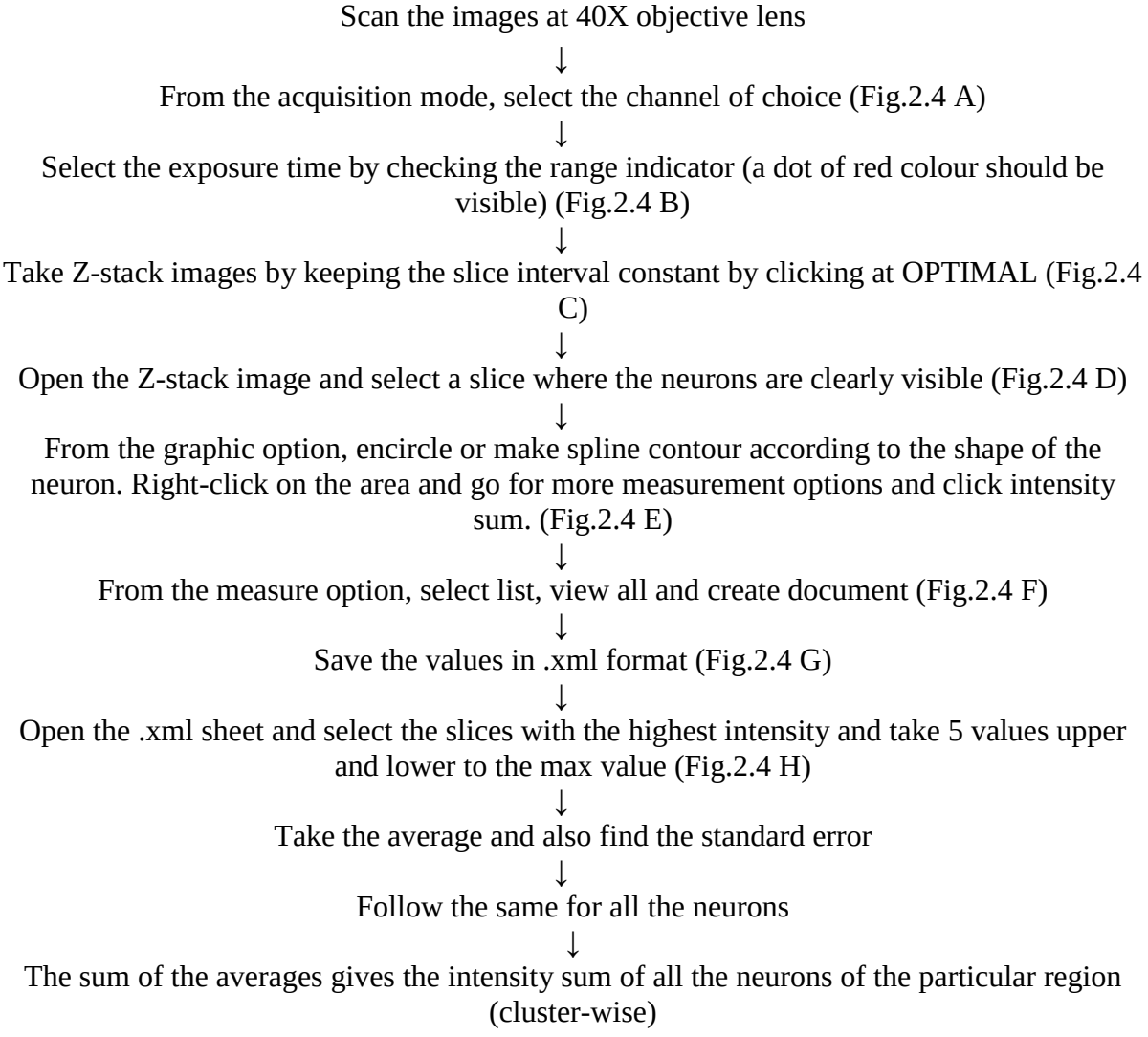

Figure 2.5: Flowchart showing the method for quantification of fluorescence intensity of DNs.

2.15. Quantification of dopamine and its metabolites using High Performance Liquid Chromatography (HPLC):

The HPLC-ECD (Electro Chemical Detector) is the most steadfast process to measure the level of catecholamines in a model system. For catechol-modified proteins, SDS-Page (Rees *et al.,* 2007) and the protein pull-down assay (Plotegher *et al.,* 2017; Liu *et al.,* 2014) is used for quantification. The nIRF scanning is also used to detect and quantify the o-quinones and other modified proteins in cells and tissues (Jinsmaa *et al.,* 2018; Burbulla *et al.,* 2017). All other techniques except for HPLC-ECD are less sensitive, thus making HPLC-ECD the best option for the quantification of catecholamines. The advantages of HPLC-ECD lie in its time efficiency, accurate detection of brain-specific catecholamines and higher flexibility to modify for detection of other related catecholamines (Allen *et al*., 2017).

Hence, I quantified the levels of brain DA and its metabolites using the HPLC-ECD (Thermo-scientific, Dionex Ultimate 3000RS) system. For quantification of catecholamines in the tissue samples, standard DA and metabolites were quantified which gave a specific retention time with which samples were compared (**Figure 2.6**).

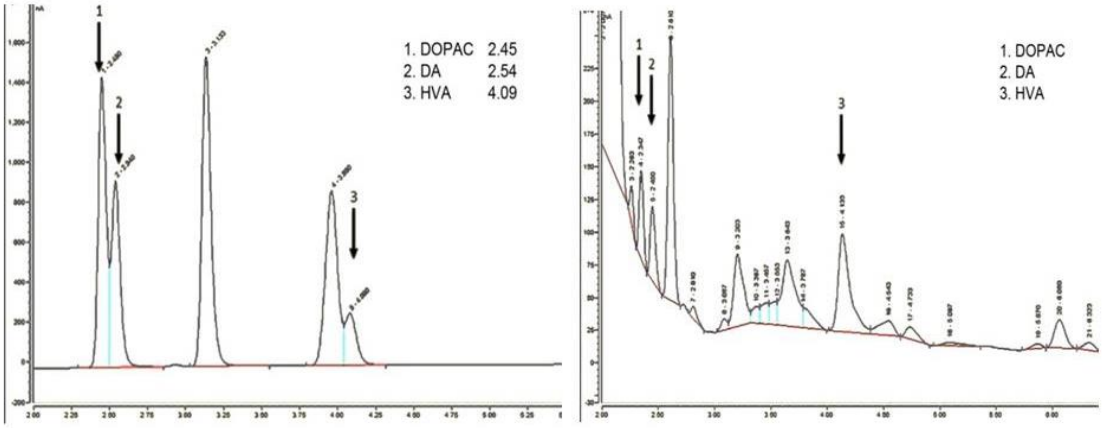

Figure 2.6: Characterization of retention time (RT) of standard DOPAC, DA and HVA (A) and brain-specific catecholamines levels (B): Chromatogram of the standard catecholamines gives a particular RT comparing with which the catecholamines in the fly brain sample is analyzed.

Materials: Dopamine (DA, Sigma-Aldrich, Cat: H8502); 3,4-Dihydroxyphenylacetic acid (DOPAC, Sigma-Aldrich, Cat: 11569); Homovanillic acid (HVA, (Sigma-Aldrich, Cat: 69673); Phosphate-buffered saline (PBS, HiMedia, Cat: ML-023); MDTM mobile phase (Thermo-scientific, Cat: 701332); HPLC grade water (JT Baker, Cat: 4218-03); Acetonitrile (JT Baker, Cat: 9017-03); Methanol (JT Baker, Cat: 9093-68) were used for quantification of DA and its metabolites using HPLC-ECD 3000 RS system (Thermo-scientific, Dionex Ultimate 3000).

Miscellaneous: Sterilized Eppendorf tubes, Pipette (cleaned with 70% ethanol before and after use), Sterilized pipette tips.

Methods: Quantification of DA and metabolites were done following the protocols of Ayajuddin *et al.*, (2021) modified from Yang and Beal, (2011). The procedures are as follows:

A. Fly tissue sample

Head tissues of wild-type Oregon K male *Drosophila* were used for the experiment. The procedures are described below.

B. Preparation of Catecholamine Standard and Brain tissue extract

i. Preparation of Standards

Standards were prepared by dissolving 2 mg of catecholamines (procured commercially) in 2 mL PBS. It was further diluted to get varying concentrations as mentioned in **Table 2.4**. The concentration of 200 ng/µL was taken for loading the standard.

Standard	PBS	Concentration	Stock Name
2 mg	2 mL	1000 µg/mL	S
100 µL of **S**	900 µL	100 µg/mL	S1
100 µL of **S1**	900 µL	10 µg/ mL	S2
100 µL of **S2**	900 µL	1000 ng/ mL	S3
200 µL of **S3**	800 µL	200 ng/ mL	S4
150 µL of **S3**	850 µL	150 ng/ mL	S5
100 µL of **S3**	900 µL	100 ng/ mL	S6

Table 2.4: Preparation of multiple concentrations of standard catecholamines

ii. Sample preparation

1. 15 heads of adult flies were taken in 300 µL 1x PBS (prepared in HPLC grade water).

2. It was then homogenized and sonicated for 20 sec with 5 sec intervals and 30% amplitude.

3. The samples were centrifuged at 6000 rpm for 10 min at 4°C.

4. The supernatant was collected.

5. 200 µL of supernatant (leave the remaining for protein quantification) was taken and 200 µL of 5% TCA was added (before using, centrifuge the 5% TCA at 6000 rpm for 10 min at 4°C to remove any undissolved solute particles).

6. It was then centrifuged two times at 5000 rpm for 10 min each at 4°C.

7. The supernatant was collected for the assay.

Precautions

- The tissues were homogenized and sonicated on ice (to avoid heat generation and prevent degradation).

● The tissue extract and standard solution were kept on ice between the steps to avoid any degradation of the standard molecules and components of the tissue extract.

● Fresh pipette tips were used for preparing serial dilutions of the standard and for transferring tissue extract.

● All the reagents were prepared in HPLC grade or Milli-Q water to avoid any contaminant molecules which may produce a false positive peak in the chromatogram.

Quantification of protein

Protein quantification was done using the Bradford method. BSA stock was prepared by dissolving 2 mg/mL PBS. A working concentration of 0.2 µg/µL was prepared by dissolving the 100 µL of stock solution in 900 µL PBS. The serial dilution was done as mentioned in **Table 2.1**. After 5 min of incubation at RT, the absorbance was read at 595 nm using NanoDrop 2000C (Thermo Scientific) to give a standard graph. 3 µL of the pure extract was used for protein quantification. The concentration of total protein thus obtained was µg/mL. However, this protein content came from 3 µL of extract that was mixed with PBS and Bradford reagent. Hence, the total µg of protein was divided by 3 µL to give the actual protein concentration per µL of the tissue extract.

C. Setting up the HPLC system

i. Solvent Reagents Required

Load the solvent tubing ports of the HPLC-ECD system with the following reagents

1. 100% HPLC grade Methanol

2. 80% Acetonitrile (Prepared in HPLC grade water)

3. 20% Acetonitrile (Prepared in HPLC grade water)

4. MDTM Mobile phase

The following “Pre loading instructions” was followed for solvent reagents

Preloading instructions for solvent reagents

"Preloading of the solvent reagents" refers to the process of placing solvent reagent bottles on the HPLC solvent rack and attaching the respective tubings to the bottle. "Preloading Instructions" given below is a guide for handling the solvent reagents and their containers while preparing solutions, placing the containers on the solvent rack and attaching them to the tubing ports of the HPLC platform.

1. All the reagent bottles were adequately filled (minimum 350 mL in each).

2. While filling, the bottle was tilted and poured the reagents slowly to avoid bubble formation.

3. Mobile phase was filtered with 0.22 micron filter paper and then poured onto the respective reagent bottle as mentioned on point 2 (Miscibility of the components of the mobile phase is a concern when running through the column. Even the readymade mobile phases might have undissolved salt residues and suspended material due to minute level coagulation of organic components of the mobile phase. Filtering through 0.22 micron nylon membrane ensured separation of such residues which might otherwise choke the C18 column fitted with the HPLC-ECD system)

4. All the reagent bottles were sonicated in a bath sonicator at an ultrasonic frequency of 40 kHz for 15 min at RT before attaching them to the HPLC system.

ii. System/ Column cleaning

Columns and electrodes of the detectors may contain tissue debris from the previous experiment with the HPLC platform. Further, the components of the HPLC platform such as

column, ECD and tubing were filled and stored in 100% methanol after completion of an experiment to avoid any fungal growth. Therefore, it is important to clean the system when it is turned on with the flow of the mobile phase to discard any left-over tissue debris and methanol. The cleaning also ensures the removal of any air bubble during the idle phase of the HPLC platform. The following steps were used for system/ column cleaning:

1. The system was cleaned by purging (each solvent port is put into a high flow rate from the pump to outside the system) from all the ports for 5 min each to discard any trapped air bubble.

2. After purging, the purge knob was closed (to divert the flow from the pump to column) and give 100% flow with 20% acetonitrile for 30 min at 0.5 mL/min flow rate to start cleaning the column.

3. A 100% mobile phase was made to flow through the column at the same flow rate for another 30 min after which the mobile phase may be recycled (drainage pipe outlet from the column will be wiped with a tissue soaked in the mobile phase and will be inserted back into the mobile phase container bottle).

iii. Setting up the HPLC parameters

Detection of catecholamine through ECD is best when the oxidation potential is in between the range of 340 mV (Yang and Beal, 2011). With the DIONEX ULTIMATE ECD 3000 system, I found that the catecholamines are best detected at reduction and oxidation potential ranges of -175 mV and 225 mV respectively. The reduction potential provides an equal state for all the catecholamines inside the HPLC platform irrespective of their physiological redox

state in the tissue. The optimum oxidation potential acts as a common threshold for the excitement of all concerned catecholamines inside the HPLC platform.

The following parameters were set for efficient detection and analysis of catecholamines

Oxidation potential	:	+225 mV
Reduction potential	:	-175 mV
Omni cell	:	+500 mV (For noise reduction)
Gain range	:	1 μA
Data collection rate	:	5 Hz
Detection Filter	:	2.0 (for all cells)
Column temperature	:	Room temperature
Auto sampler temperature	:	4^0C
Flow rate	:	0.5 mL/min

iv. ECD priming

1. Once the mobile phase is put on recycle mode, priming of the ECD was started.

2. After setting up the required parameters for ECD, the system was kept on acquisition mode for at least 2 Hr to check the status of the baseline.

3. The two lines (denoted as ECDRS 1 and ECDRS 2) were checked to run in parallel denoting equilibrium while fluctuation was denoted by non-parallel line over time.

4. The baseline was considered to be stabilized if the drifting was less than 2nA/Hr.

D. Standard and Sample loading

A 20 µL of Standards first and then 50 µL of the sample was loaded for analysis. 20 µL of 200 ng/mL concentration of DOPAC and DA showed an optimal peak, but HVA showed a quantifiable peak. However, HVA showed a clearer peak without saturation at a higher concentration of 10 µg/mL.

Note: Standard metabolites were dissolved in PBS and the same PBS was used for sample preparation. A minimum amount of 300 µL was kept in the vial for loading.

E. Analysis

1. The chromatogram acquired with ECDRS2 was used for analysis.

2. Peak integration was inhibited with the "Inhibit Integration range" function that was set on the whole solvent front section of both the standard and sample chromatograms.

3. The chromatogram obtained from ECDRS2 was used and the sample chromatogram was overlaid with the standard chromatogram.

4. Upon comparing the two chromatograms, one could deduce the peaks of the particular catecholamine in the sample.

5. If two peaks were co-eluted or joined together as if a single peak, then the peak was split to make it into two peaks.

6. The peaks were made more accurate by using software tools like the automatic tool, delimiter tool, peak tool, baseline tool etc.

7. After the peak was accurately set, one could further process for quantitative analysis (Quantitative analysis was performed using Chromaleon Version 6.8 software provided along with the HPLC system).

8. Note: The area of the peak was compared with that of the standard for calculation.

E. Calculation of concentration of catecholamines in sample

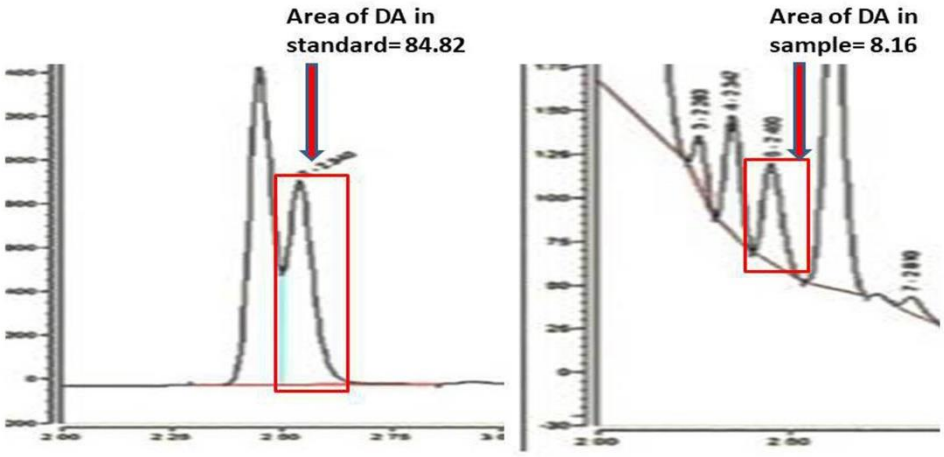

Figure 2.7: Images of chromatogram showing the area of the DA in standard and sample (fly brain tissue)

i. The concentration of the standard catecholamines: DA (DA_{Std}), DOPAC ($DOPAC_{Std}$) and HVA (HVA_{Std}) used in the HPLC assay was 200 ng/mL each.

ii. Injection volume of all standard catecholamine to the HPLC column was I_{Std} = 20 µL

iii. Area of the peak of the standard catecholamines (DA, DOPAC and HVA) in the chromatogram (**Figure 2.7**) was

A_{DA_Std} = 84.82, A_{DOPAC_Std} = 90.21 and A_{HVA_Std} = 60.41

iv. Injection volume of tissue extract to the column was I_{Samp} = 50 µL

v. Area of the peak of catecholamines (DA, DOPAC and HVA) in the tissue sample chromatogram was A_{DA_Samp} = 8.16, A_{DOPAC_Samp} = 12.41 and A_{HVA_Samp} = 12.99

vi. Suppose, a particular tissue extract from an experimental group used for HPLC assay, that was quantified beforehand for total protein was TP_{Samp} = 0.12 µg/ µL

vii. The following steps were followed for calculating the actual amount of the catecholamines in tissue extract (**Table 2.5**).

Calculation

Calculation Steps	Metabolites		
	DA	DOPAC	HVA
Step I: Concentration of standard catecholamines in 20 µl	DA_{Std} X I_{Std}/1000 i.e. (200 X 20)/1000 = 4 ng	$DOPAC_{Std}$ X I_{Std}/1000 i.e. (200 X 20)/1000 = 4 ng	HVA_{Std} X I_{Std}/1000 i.e. (200 X 20)/1000 = 4 ng
Step II: Concentration of catecholamines in brain tissue extract	(A_{DA_Samp} X 4)/ A_{DA_Std} i.e. (8.16 X 4)/84.82 = 0.38 ng	(A_{DOPAC_Samp} X 4)/ A_{DOPAC_Std} i.e. (12.41 X 4)/90.21 = 0.55 ng	(A_{HVA_Samp} X 4)/ A_{HVA_Std} i.e. (12.99 X 4)/60.41 = 0.86 ng
Step III: Determining the total protein in 50 µl that was injected into column	(TP_{Samp} X I_{Samp}) i.e. (50 X 0.12) = 6 µg	(TP_{Samp} X I_{Samp}) i.e. (50 X 0.12) = 6 µg	(TP_{Samp} X I_{Samp}) i.e. (50 X 0.12) = 6 µg

Step IV: Determining the catecholamine in total protein that was injected and normalizing in 1 mg of total protein	[0.38 X (1000/6)] = 63.33 ng	[0.55 X (1000/6)] = 91.66 ng	[0.86 X (1000/6)] = 143.33 ng
Step V: Determining the actual amount of catecholamine as injected tissue extract solution had brain tissue extract + TCA in 1:1 ratio	63.33/2 = 31.66 ng in 1 mg of protein	91.66/2 = 45.83 ng in 1 mg of protein	143.33/2 = 71.66 ng in 1 mg of protein

Table 2.5: Steps for calculation of the amount of catecholamines in 1 mg protein of tissue sample.

2.16. Statistical analysis:

Statistical analysis was performed and graphs were prepared using GraphPad Prism 5.0 software and expressed as the mean ± standard error of the mean (SEM). Statistical significance was determined using a two-tailed unpaired t-test for data with two experimental groups. For data with more than two groups, a one-way analysis of variance (ANOVA) followed by the Newman-Keuls Multiple Comparison Test was performed. P-value < 0.05 was considered significant.

CHAPTER 3

Adult Health and Transition Stage-specific Rotenone-Mediated *Drosophila* Model of Parkinson's Disease: Importance of Life Phase-Specific Animal Models for Late-onset Neurodegenerative Diseases

3.1. Introduction:

Developing an animal model is critical for understanding the pathophysiology of late-onset neurodegenerative diseases such as PD and screening potential neuroprotective molecules for developing novel therapeutic strategies. An animal model of a human disease should exhibit pathophysiological features of the disease; at a life stage during which the disease onsets in humans. Developing a PD model should mimic the characteristic features of PD such as mobility defects, degeneration of DNs along with a significant reduction in the DA level of the brain. The devastation of the nigrostriatal DA and its pathway is the basis of PD animal models. The model organism should also manifest motor symptoms of human PD and be responsive to L-DOPA or any other anti-PD drug therapy. Moreover, the disease onset in the model organisms should be in the later stage of life as in the case of humans.

3.1.1. *Drosophila* mimicking human PD symptoms

Among animal model systems, *Drosophila melanogaster* has been paid more attention because of its simpler morphology, simpler nervous system and highly conserved disease-causing genes with humans. Comparative analysis of whole-genome sequencing revealed that 77% of human diseases causing genes have fly homologues/orthologues (Tello *et al*.,

2022; Reiter *et al.,* 2001), and 40% of overall similarity at nucleotide or protein level with 80-90% or higher in the conserved domain (Pandey and Nichols, 2011). These features emphasize the utility of the "little fly" to understand and address human disease.

Although the physiological differences between humans and flies are very obvious, the central pathology observed in human PD can be reproduced in a commendable way by toxin-induced or transgenic modification. Similar to human PD conditions, age-dependent neurodegeneration and hallmarks of PD biomarkers i.e. the LBs and Lewy neurites (LNs) inclusions are observed in the transgenic *Drosophila* model (Feany and Bender, 2000). Upon exposure to environmental toxins such as rotenone (ROT), *Drosophila* mimics pathological and biochemical features of sporadic PD such as mobility defects, MD and DA-ergic degeneration (Maitra *et al*., 2021; Nguyen *et al*., 2018; Sur *et al*., 2018; Pandareesh *et al*., 2016; Cassar *et al*., 2015; Coulom and Birman, 2004). *Drosophila* also executes complex behavior such as mating, conditioning to fear, aggression, learning and motor behaviors such as flying, walking and climbing (Lessing and Bonini, 2009) which are affected by the PD onset and progression like humans. This multitude of behavior is very much helpful in characterizing different features of PD.

All the genes reported to date in humans associated with Parkinsonism, be it familial or sporadic, are available in *Drosophila* as a homolog except for the SNCA which produces LBs and LNs at the extracellular matrix of the brain, a typical hallmark biomarker for genetic PD condition in the mammalian brain. This adds up to the advantages of genetic manipulation and recapitulating the PD phenotypes. However, PD is a late-onset NDD and hence, it is important to characterize the life stages of the model organisms wherein the disease sets in.

3.1.2. Adult life stages of *Drosophila*

The life stages of *Drosophila* are believed to have both common and unique complex processes and can be influenced independently by a relatively large number of stage-associated pathways. The efficacy of genotropic compounds depends on the availability of the particular target molecules at that particular life stage of the organism when the compound is tested (Soh *et al.,* 2013). Therefore, the adult life stage-specific model of human diseases such as PD is important because this particular disease onsets in the later stage of life. Hence, it is also important to understand the mechanism of action of toxins and drugs in all the life stages of the model organisms. The adult life stages of *Drosophila* have been broadly categorized into three phases i.e., health phase, transition phase and senescence phase (Arking *et al.,* 2002).

The Health Phase*:* As soon as the fly is eclosed, the health phase begins. This stage of life phase is indicated by low mortality and a high survival rate resulting in a significant increase in both the mean and maximum life phase of the *Drosophila*. The survivability starts with 100% and is maintained for some time until the survival rate declines to 90% or below, or when there is a negative sign in the survival curve whichever comes first (Arking, 2005; Arking *et al.,* 2002). In *Drosophila* (Oregon K), this stage lasts for 30 days starting from the day of eclosion (Phom *et al.*, 2014).

The Transition Phase*:* The transition phase is indicated by a period of the life phase wherein the survival rate is between 89% and 81%. The transition phase shows an increased early survival that leads to a significant increase in mean, but not in the maximum life phase. The duration of the transition phase is variable. Some strains of *Drosophila* show a continuous decline in the survival curve, suggesting that these organisms are somewhat

weakened and have a relatively higher age-specific mortality rate from eclosion onwards (Arking, 2005; Arking *et al.*, 2002). The transition phase of life phase ranges from 31 days to 60 days in the case of Oregon K male *Drosophila* (Phom *et al.*, 2014).

The Senescence Phase*:* The senescent phase is indicated by a drastic change in physiology and loss of function, resulting in declining survivability. This period of life phase is commonly referred to as ageing. The organisms undergo a gradual death during this stage of their life phase. The accelerated mortality, decline in reproduction, slow movements, cardiovascular dysfunction, abnormal growths, oxidative damage and neuronal loss are some of the common patterns of this life stage. The senescence phase ends with the death of the organism or cohorts (Arking, 2005; Arking *et al.*, 2002). The senescence phase of the life phase ranges from 61 days to 120 days in the case of Oregon K male *Drosophila* (Phom *et al.*, 2014).

3.1.3. Importance of adult life phase-specific animal models for late-onset neurodegenerative diseases such as PD

The review of the literature (**Chapter 1**) illustrates that most of the studies have used young animals to develop models for late-onset NDD such as PD (Akinade *et al.*, 2022; Maitra *et al.*, 2021; Liu *et al.*, 2020; Sur *et al.*, 2018; Coulom and Birman 2004) and they further screened drugs/natural products during the early phase of their life and concluded their efficacy/inefficacy (Liu *et al.*, 2020; Siddique *et al.*, 2019). Meaning the insights developed using these model systems may not have any relevance to the human condition as PD is a

late-onset NDD. Therefore, here lies the necessity of age-specific models that match the human condition.

The gene expression in different life stages of model organisms reveals that they are characterized by different gene expression profiles (Arking, 2015, 2009) similar to that of the corresponding life stages of humans. There is a significant change of about 23% in genomic transcript profiles with age in *Drosophila* (Pletcher *et al.*, 2002). A transcriptomic analysis using microarrays to compare the gene expression profiles of different life stages of *Drosophila melanogaster* has identified 1184 genes with marked differences in expression level between young and old age groups (Bordet *et al*., 2021). The transcriptome profile of human brain samples of different ages has identified significant changes in the whole transcriptome underlying the age-associated cognitive decline (Ham and Lee, 2020). Genes involved in stress response and oogenesis indicated age-dependent changes in expression depending upon life stage-specific factors (Pletcher *et al.*, 2002). Since the animal models are indispensable for disease progression studies and therapeutic approaches, it is equally important to follow the age-specific study while developing an animal model for NDD such as PD. The adult life stage-specific model of PD is important because a particular target may be active at one stage of life but inactive in another stage and therefore genetic targets of compounds such as curcumin may not be present in all stages of life. As such, the compound will be effective in the organism only during those phases when its target molecules are present (Soh *et al.*, 2013) which is an important and interesting paradigm. Our laboratory has previously demonstrated in the *Drosophila* PD model that nutraceutical curcumin's DA-ergic neuroprotective efficacy is adult life stage-specific (Phom *et al*., 2014), which further signifies the importance and necessity of developing life stage-specific animal models for late-onset NDDs such as PD. Research considering the age-specific stages will greatly

enable the early identification of markers, providing timely interventions in the initial course of disease progression and in developing an effective drug for PD. Therefore, the researcher must evaluate the susceptibility/resistance of the model system to neurotoxicants and the efficacy of drugs in a life-stage-specific fashion.

3.1.4. Mitochondrial complex I inhibitor ROT mediated fly model of PD

Multiple environmental toxins have been shown to provoke neurotoxicity in various animal models of PD. Among those toxins, the compound ROT has been broadly used as a toxin in experimental animal models for PD. Though ROT has been in use as a piscicide in the United States since the 1930s (Dawson *et al.,* 1983), root extracts containing ROT were used by gardeners in the East Indies as early as 1848 (La Forge *et al.,* 1933). In many rural areas of the country including Nagaland, root extracts containing ROT have been used for fishing in streams. ROT is a classical mitochondrial complex-I inhibitor that impairs oxidative phosphorylation of the electron transport chain (ETC) and produces ROS (Swarnkar *et al.*, 2010). Because of its high lipophilic nature and its ability to cross the blood-brain barrier, ROT is highly toxic. The ROT model is very attractive since it replicates the crucial features of PD including MD, OS and DA degeneration (Sherer *et al.,* 2003). Using the animal models, the neuroprotective efficacy of compounds with antioxidant and anti-inflammatory properties may be tested which may later be used for clinical trials (Harkavyi and Whitton, 2010). Surprisingly, there has been no effective and clinically proven neuroprotective or disease-modifying strategy developed from these animal models. Here, comes the need to select appropriate experimental conditions in which the model organisms show the symptoms of the disease but do not affect the survivability. Also, it is important to develop

new protocols to produce animal models of PD that have mixed pathology, late-onset and progressive nature that reflect the disease process more closely and definitely the genetic basis of PD or genes associated with the disease in humans.

3.1.5. Dopaminergic neurodegeneration and altered dopamine metabolism in PD

Dopaminergic neurons are in the frontline when neurodegenerations are concerned. In order to understand the DA-ergic neuronal dysfunction, I tried to look into the number of DNs and fluorescence intensity of the (TRITC labelled) secondary antibody tagged against the anti-TH primary antibody.

There is a consensus that altered DA metabolism, α-syn aggregation, MD, OS and neuro-inflammation are involved in the degeneration of DNs (Franco-Iborra *et al.,* 2016; Moors *et al.,* 2016) resembling the pathophysiological conditions of PD patients (Herrera *et al.,* 2017). Similar to other vertebrates, neurotransmitters like DA perform parallel functions including locomotion, drug response, circadian rhythms, aggression, etc. in *Drosophila* (Kasture *et al*., 2018). DA is synthesized from the amino acid tyrosine through two enzymatic processes: (a) rate-limiting step through tyrosine hydroxylase (TH) converting to L-DOPA and (b) conversion of L-DOPA to DA by aromatic amino acid decarboxylase (AADC) (Yamamoto and Seto, 2014). TH and AADC together with vesicular monoamine transporter-2 form a complex in the membrane of monoaminergic vesicles and prevent the free DA from auto-oxidation. The stable DA accumulates inside monoaminergic vesicles for neurotransmission from the axon of presynaptic neurons to receptors of postsynaptic neurons through the synaptic cleft (Segura-Aguilar *et al*., 2014). The DA is then catabolized to DOPAC by MAO-B and aldehyde dehydrogenase (ADH) which is finally converted to the product HVA

by COMT (Segura-Aguilar *et al.*, 2014). A schematic diagram of DA metabolism is shown in **Figure 3.1**.

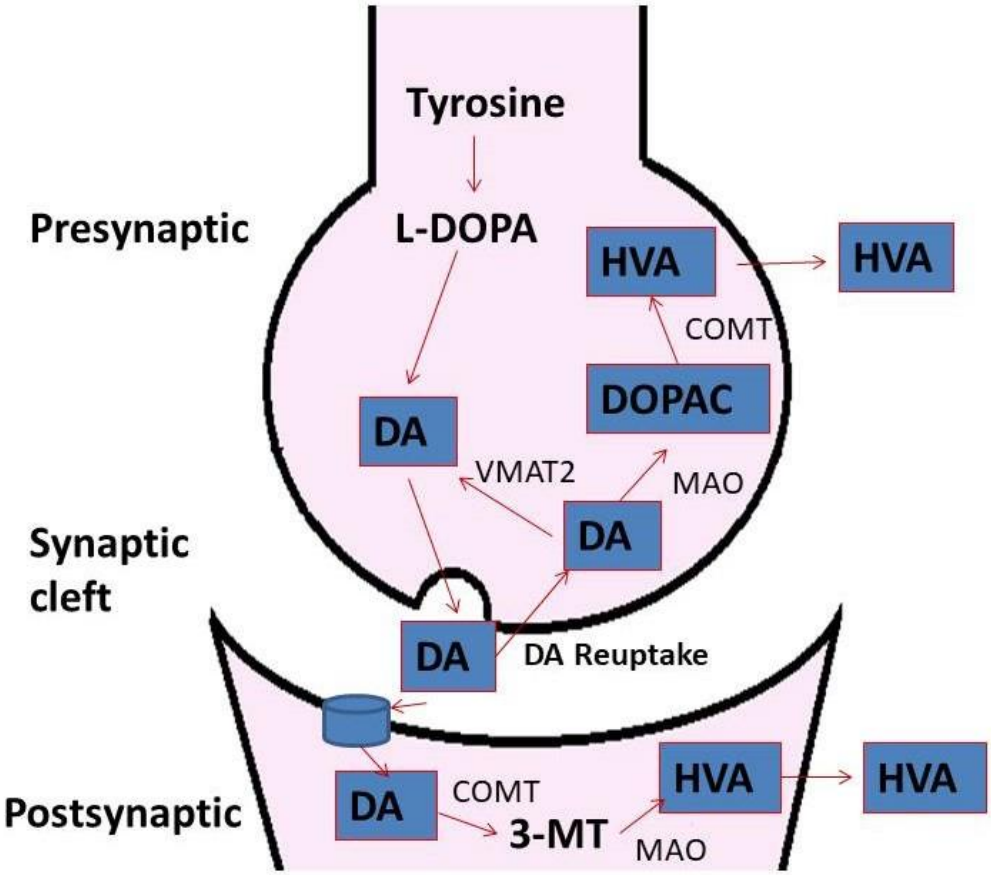

Figure 3.1: Schematic representation showing DA metabolism in presynaptic and postsynaptic neurons: DA is synthesized in the presynaptic neurons by tyrosine hydroxylase (the rate-limiting enzyme) from L-DOPA. DA is released into the synaptic cleft from where it is re-uptaken by the presynaptic neuron again through DAT. This DA is either metabolized into DOPAC by MAO or is restored to its original DA form by VMAT2. DOPAC is further metabolized to HVA by COMT and transported outside the neuron. DA is also taken up by the postsynaptic neuron and metabolized to 3-MT by COMT which is further catabolized to HVA by MAO and transported outside the postsynaptic neuron.

A better understanding of the DA metabolism in PD would help in designing more targeted and successful therapeutic strategies for PD (Masato *et al.*, 2019). Hence, I tried to look into DA metabolism by quantifying the levels of DA, DOPAC and HVA using HPLC to understand its biological significance in the *Drosophila* model of PD.

Taken together, I made an effort to develop neurotoxin ROT (which inhibits mitochondrial complex I of ETC) mediated life stage-specific *Drosophila* model of sporadic PD in three different life stages of *Drosophila*: (a) two health phases [5 days old (early health phase); 30 days old (late health phase)] and (b) transition phase (50 days old), (late-onset NDDs set in during transition phase in humans). Those adult life stage-specific models will be a good tool to screen potential therapeutic compounds and identify their molecular targets of activity. This knowledge will assist in developing novel therapeutic strategies for PD.

3.2. Materials and methods:

3.2.1. Preparation of ROT stock

Refer to section 2.5 of chapter 2

3.2.2. ROT susceptibility assay

Refer to section 2.6 of chapter 2

3.2.3. Negative geotaxis assay

Refer to section 2.9 of chapter 2

3.2.4. Extraction and quantification of mitochondria protein from fly

Refer to sections 2.10 and 2.11 of chapter 2

3.2.5. Complex I-III activity

Refer to section 2.12 of chapter 2

3.2.6. Quantification of DNs and fluorescence intensity using fluorescence microscopy

Refer to section 2.14 of chapter 2

3.2.7. Quantification of dopamine and its metabolites using HPLC

Refer to section 2.15 of chapter 2

3.2.8. Statistical analysis:

Refer to section 2.16 of chapter 2

3.3. Result:

3.3.1. Survival of male *Drosophila* in normal media

Oregon K strain of *Drosophila melanogaster* survived a maximum life span of 120 days with a median life span of 90 days in regular culture media under favourable environmental conditions. Mortality was recorded till all the flies were dead. Phom *et al.,* (2014) categorically classified the windows for the three life stages as follows (1) health phase (window wherein there is no natural death) extends from 1 to 30 days; (2) Transition phase (wherein 10% of death occurs) extends from 31 to 60 days and (3) Senescent phase (wherein a steady decline in survival curve occurs) extends from 61 to 120 days.

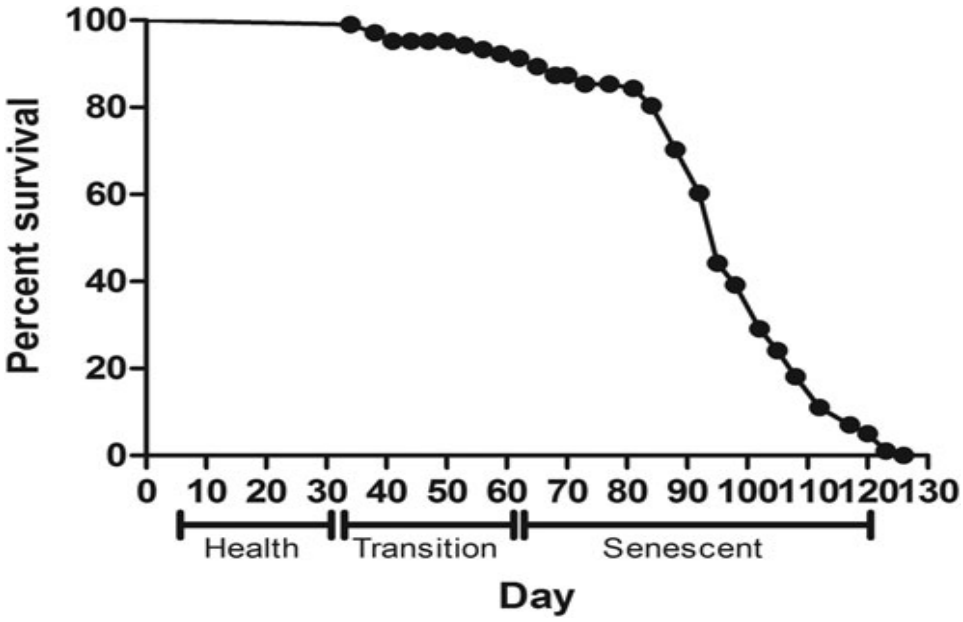

Figure 3.2: Survival of newly eclosed *Drosophila melanogaster* (OK) male fly in regular culture media: Adult *Drosophila* survived for approximately 120 days in regular culture media which are categorized into health phase (0-30 days), transition phase (31-60 days) and senescent phase (from 61 days till the fly dies) (From Phom *et al.,* 2014).

Present study indicates that the health phase in the life stages of the fly comprises the days counting from the day of eclosion till the 30th day. In this phase, there is no natural death of the fly. The transition phase comprises the days when 10-15% of the fly start dying. This phase ranges between 31-60 days of the life stage. The senescent phase of the life stage is that stage wherein the fly starts dying at a very fast rate. It ranges from 61 days to the death of the fly which is approximately 120 days (**Figure 3.2**).

3.3.2. Male *Drosophila* is susceptible to ROT in a dose-dependent manner

In order to understand *Drosophila* susceptibility to ROT, male OK flies of three life stages/phases (5 days: early health phase; 30 days: late health phase; and 50 days: transition phase) were exposed to multiple concentrations (10, 25, 50, 100, 250, 500 and 1000 µM) of ROT. The survivorship of fly was observed and recorded every 24 Hrs.

The results showed that the early health phase fly was susceptible to ROT in a time-dose-dependent manner. The least concentration of 10 µM could survive for 44 days with LD_{50} at 30 days while the fly in the highest concentration of 1000 µM survived for 16 days and showed LD_{50} at 10 days. The fly in the concentrations of 500 µM and 1000 µM started showing significant mobility defects starting from the 4th day onwards but the defect was highly significant (~30% decline in climbing ability as compared to control) on the 5th day (***$p<0.0001$). No mortality was observed at the exposed concentration of 500 µM up to the seventh day (**Figure 3.3**). Hence, the concentration of 500 µM ROT at an exposure window of 5 days was selected for early health phase fly for further studies. No mobility defects were observed in lower concentrations ranging from 10 µM to 100 µM till the 5th day.

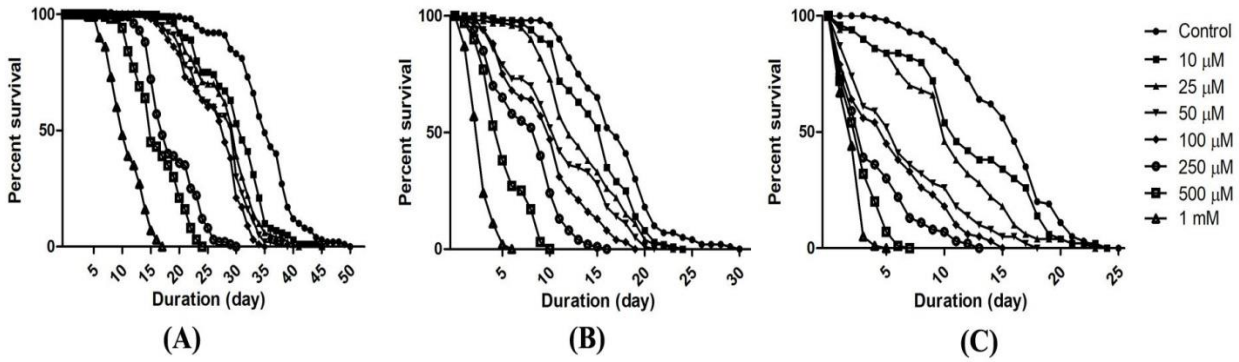

Figure 3.3: Dose and time-dependent mortality of OK male fly exposed to ROT during different phases of adult life. Mortality pattern among adult male fly of the early health phase (**A**), late health phase (**B**) and transition phase (**C**), exposed to seven different concentrations of ROT (10, 25, 50, 100, 250, 500 and 1000 μM) showed concentration-dependent lethality. Mortality data were collected every 24 Hr for each group till all the flies were dead. There was no mortality up to the 6th day for the early health phase fly and the 3rd day for the late health and transition phase flies. Comparison of survival curves reveals a significant difference in response among different tested concentrations (log-rank [Mantel–Cox] test. $p < 0.0001$.

While modelling the PD pathology in animal systems including *Drosophila*, it is essential to avoid the toxic concentration that kills the animal before the DNs degenerate. In such a situation, mechanistic insights researcher generates using such animal models, may not have relevance to the disease condition (Phom *et al*., 2014). Hence it was determined to expose the fly belonging to the early health phase to 500 μM ROT, late health phase to 25 μM ROT and transition phase to 10 μM ROT and characterize the behavioural, biochemical, cytological and molecular markers associated with PD at 5 days feeding window (in case of health phase fly) and 2 days feeding window (in case of late health phase and transition

phase flies). At these time points, with these feeding protocols, no mortality was observed in all the stages of adult *Drosophila*. Hence, these models mimic the human PD condition (behavioural symptoms and DA-ergic neurodegeneration but no mortality).

3.3.3. ROT induces locomotor defects in time and concentration-dependent manner

To establish the effect of ROT on *Drosophila* mobility, fly was fed with multiple concentrations of ROT (10, 25, 50, 100, 250, 500 and 1000 µM) prepared in 5% sucrose and the control fly remain in 5% sucrose using filter disc method. Flies of different age groups showed mobility defects after particular time points. Mobility defects were quantified using a negative geotaxis assay. Under normal conditions, I observed that 90% of the flies could reach the top of the column in 12 seconds while ROT-induced flies could not. The higher the concentration of ROT, the fewer flies could climb.

In the early health phase fly (**Figure 3.4**), 500 µM concentration of ROT induces a clear mobility defect on the 5^{th} day but no mortality was observed. The mobility was significantly reduced by 30% by the selected concentration of 500 µM on the 5^{th} day. In the case of the late health phase fly (**Figure 3.5**), 25 µM ROT significantly affected the mobility on the 2^{nd} day (48 Hr) as it was lowered by 34% as compared to the control group. In the case of the transition phase fly (**Figure 3.6**), 10 µM ROT significantly induces mobility defects on the 2^{nd} day (48 Hr) as the climbing ability was reduced by 26% as compared to the control group. There was no observable mortality at all these time points. Hence, these concentrations and time points were selected for further assays.

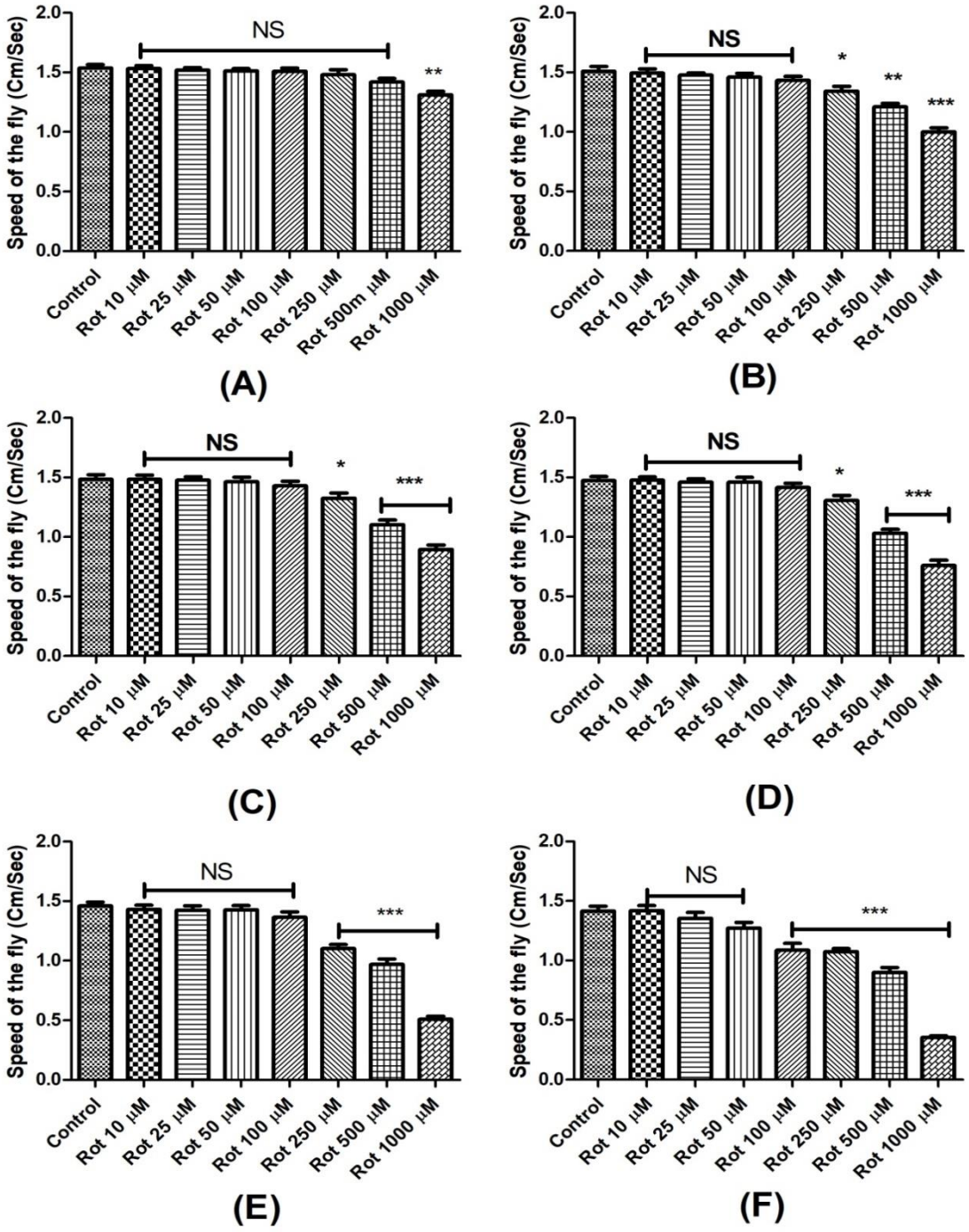

Figure 3.4: Mobility defects of the early health phase fly in multiple concentrations of ROT: Feeding the fly of the early health phase with ROT showed mobility defects as indicated by negative geotaxis assay after 1 day of exposure (A), 3 days of exposure (B), 4 days of exposure (C), 5 days of exposure (D), 7 days of exposure (E) and 10 days of exposure (F). 500 µM of ROT induced clear mobility defects in the adult male fly of the early health phase on the 5th day. Observation of mere mobility defects but not mortality of fly is the reason

behind selecting above mentioned toxin concentrations and durations of toxin exposure for the early health phase fly. (One-way ANOVA followed by the Newman-Keuls Multiple Comparison Test showed a significant difference in mobility. *p<0.05; **p<0.001; ***p<0.0001; NS- Not significant)

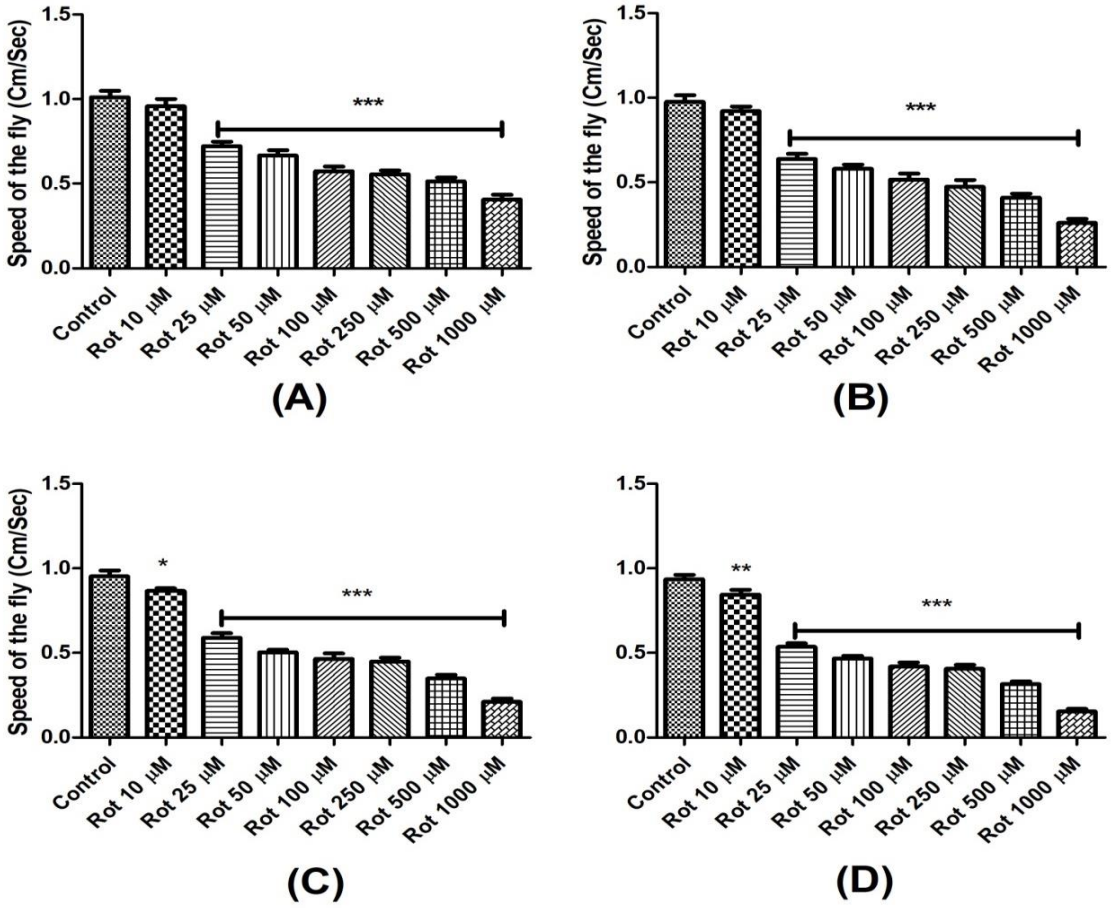

Figure 3.5: Mobility defects of the late health phase fly in multiple concentrations of ROT: Feeding the fly of the late health phase with ROT showed mobility defects as indicated by negative geotaxis assay after 1 day of exposure (A), 2 days of exposure (B), 3 days of exposure (C) and 4 days of exposure (D). There was no mortality up to the 3rd day for the late health phase fly. 25 µM of ROT induced clear mobility defects in the adult male fly of the late health phase on the 2nd day. Observation of mere mobility defects but not mortality of fly is the reason behind selecting above mentioned toxin concentrations and durations of

toxin exposure for the late health phase fly. (One-way ANOVA followed by the Newman-Keuls Multiple Comparison Test showed a significant difference in mobility. *p<0.05; **p<0.001; ***p<0.0001; NS- Not significant)

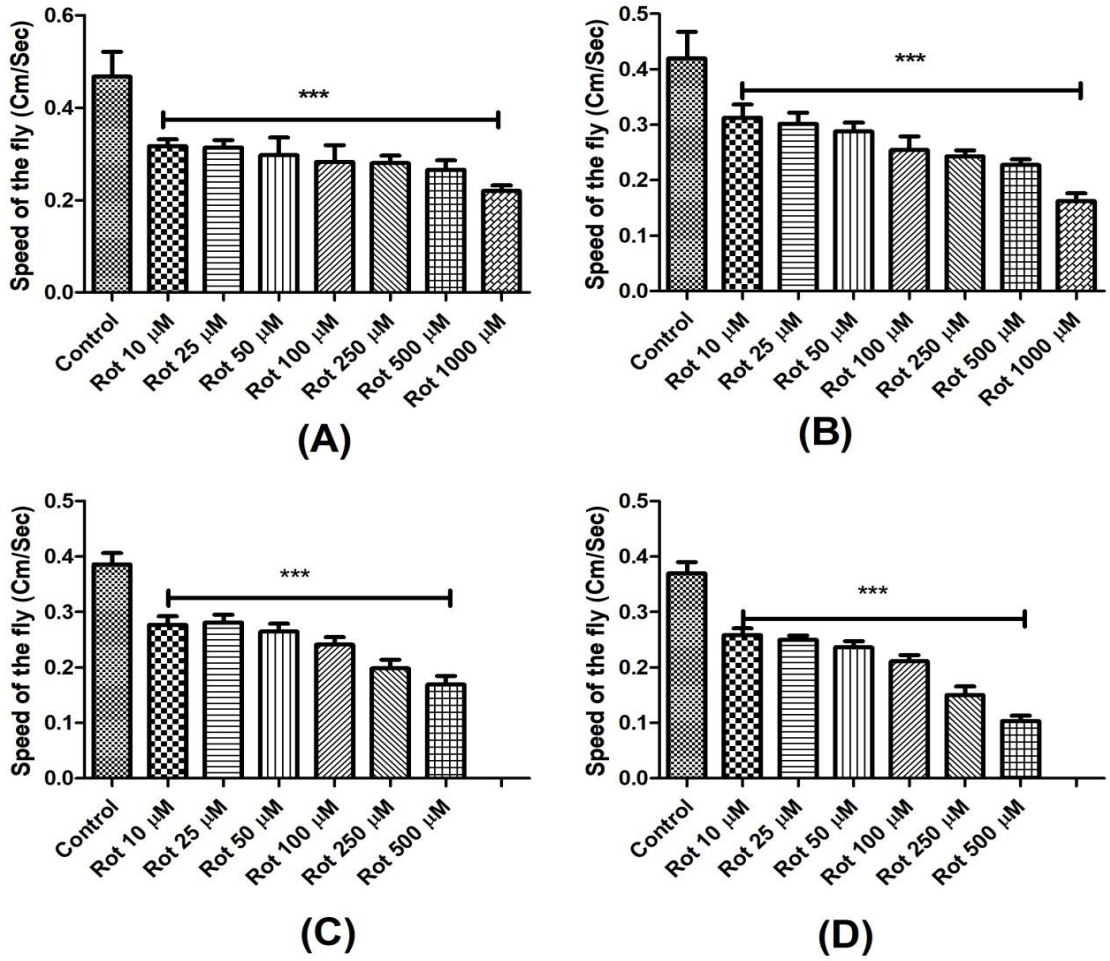

Figure 3.6: Mobility defects of the transition phase fly in multiple concentrations of ROT: Feeding the flies of the transition phase with ROT showed mobility defects as indicated by negative geotaxis assay after 1 day of exposure (A), 2 days of exposure (B), 3 days of exposure (C) and 4 days of exposure (D). There was no mortality up to the 3rd day for the transition phase fly. 10 µM of ROT induced clear mobility defects in the adult male fly of the transition phase on the 2nd day. Observation of mere mobility defects but not mortality of fly is the reason behind selecting above mentioned toxin concentrations and durations of

toxin exposure for the transition phase fly. (One-way ANOVA followed by the Newman-Keuls Multiple Comparison Test showed a significant difference in mobility. ***p<0.0001)

3.3. ROT mediated inhibition of mitochondrial complex I: Relevance of the fly model to human PD

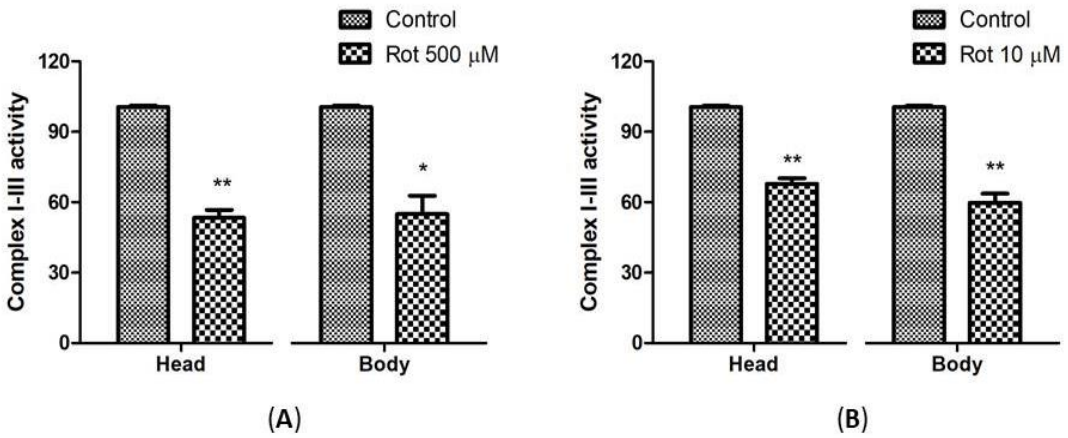

Figure 3.7: ROT inhibits mitochondrial Complex I activity. Upon feeding the early health phase fly with 500 μM ROT for 5 days (**A**) and 10 μM ROT for 2 days during the transition phase (**B**), there is a significant decrease of ~45% and ~35% respectively in the complex I-III activity of the respiratory chain in both the head and body parts of *Drosophila melanogaster*. (Statistical analysis was performed using a t-test. *p<0.05, **p<0.01; compared to control)

The mitochondrial complex I-III activity was assayed to explore the inhibition of mitochondrial complex I in ROT-treated flies. Mitochondrial complex I activity is shown to have been significantly reduced in substantia nigra, skeletal muscles and platelets of PD patients (Bose and Beal, 2016). A similar result is indicated in the present study. The complex I-III activity was significantly lowered by 45±4.77% in both the head and body parts of the flies during the early health phase (**Figure 3.7 A)** and a 35±5.46% reduction in

Complex I-III activity was observed during the transition phase (**Figure 3.7 B)** under ROT treated conditions. This reduction in complex I-III activity clearly indicates the impairment of complex I of the ETC.

3.4. Whole-brain immunostaining indicates that ROT doesn't cause a loss in the number of DA-ergic neurons but diminishes Tyrosine Hydroxylase (TH) synthesis

The adult *Drosophila* brain consists of six DA-ergic neuronal clusters in each brain hemisphere (**Figure 3.8 A**) (Whitworth *et al.,* 2006). To investigate DA-ergic neuronal dysfunction in ROT-administered fly, brains were dissected and immunostained for TH (the rate-limiting enzyme in the synthesis of dopamine) in the early health (**Figure 3.8 B**) and transition phases flies (**Figure 3.8 C**). Upon quantifying the number of DNs, no significant difference was observed in all the six clusters analyzed in PD brains as compared to control (**Figures 3.8 D, E**). There are slight variations in the number of neurons even in the control groups, which can be attributed to natural variation. This result is consistent with the earlier comprehensive study performed by Navarro *et al*. (2014). Then to understand if there is any variation in the level of synthesis of TH, I quantified the fluorescence intensity of the DNs (fluorescently labelled secondary antibody targets the primary antibody (anti-TH). Hence, fluorescence intensity is directly proportional to the level of TH protein synthesis). Upon exposure to ROT, the fluorescence intensity of DNs of the whole brain mount showed a significant reduction (40-50%) as compared to control groups (**Figures 3.8 F, G**). This reduction in fluorescence intensity (quantification of fluorescence intensity of GFP reporter), not the loss of neurons *per se* is termed "neuronal dysfunction" by Navarro *et al*. (2014).

This observation illustrates that DA neuronal structure is not degenerated (hence any loss in the number of neurons), but TH synthesis is diminished.

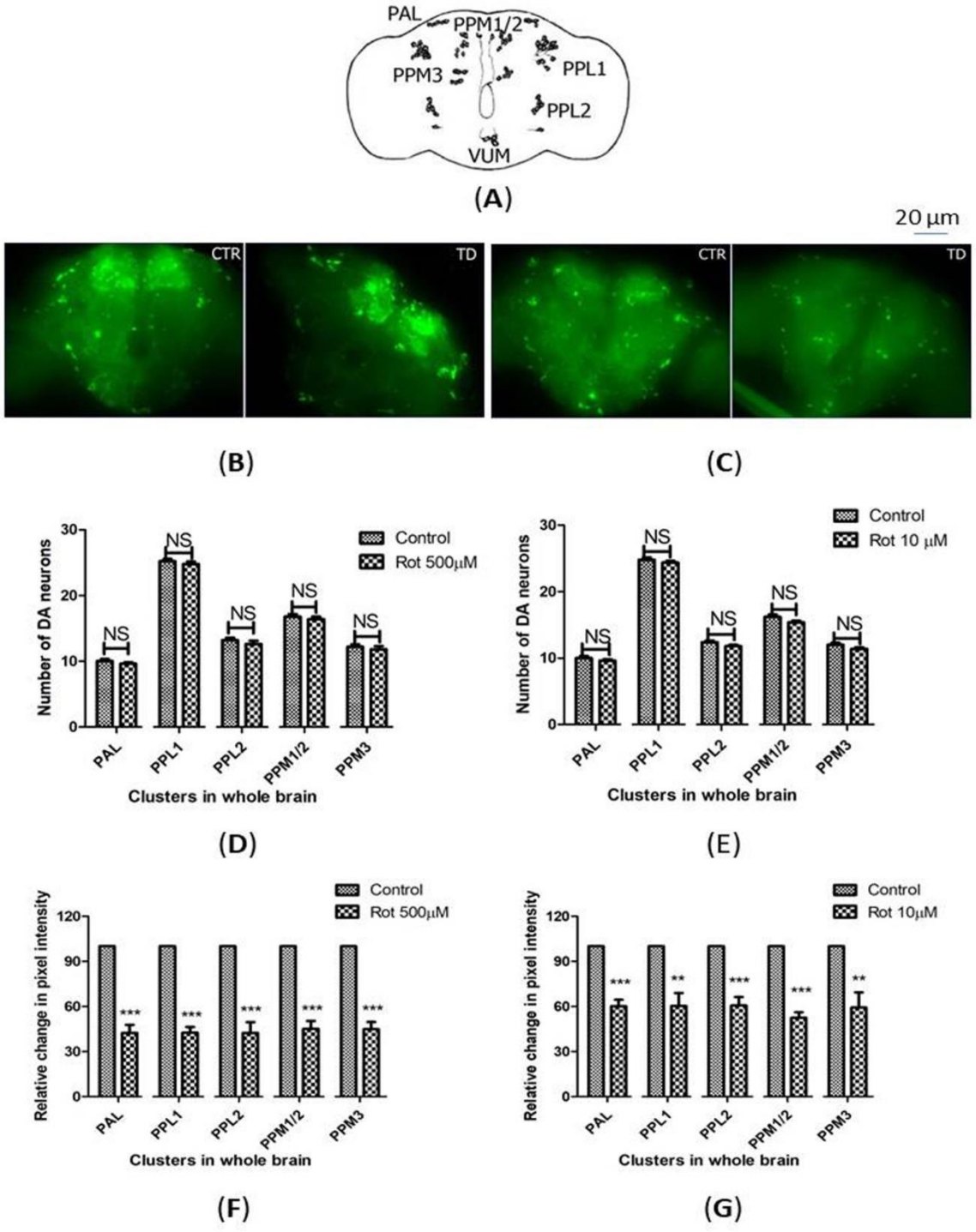

Figure 3.8: Characterization of DA-ergic neurodegeneration in the whole fly brain through anti-TH antibody immunostaining reveals that there is no loss in the number of DNs.

However, ROT leads to "neuronal dysfunction" as characterized by quantification of DA-ergic neuronal fluorescence intensity that is proportional to the amount of TH protein. Cartoon shows the position of DNs in the whole brain of *Drosophila melanogaster* (**A**). Brain image of normal and PD-induced condition during the early health phase (**B**) and transition phase (**C**). Quantification of DNs reveals that there is no loss of neuronal number *per se* in both life stages: early health phase (**D**) and transition phase (**E**) whereas the quantification of fluorescence intensity (of fluorescently labelled secondary antibody that targets anti-TH primary antibody) reveals a significant decrease in TH protein in both life stages, i.e., the health phase (**F**) and transition phase (**G**). (CTR- Control; TD- Treated with ROT; PAL- Protocerebral anterior lateral; PPL- Protocerebral posterior lateral; PPM- Protocerebral posterior medial). (Statistical analysis was performed using a t-test. **$p<0.01$, ***$p<0.0001$, NS- Not significant; compared to control)

3.5. ROT induces alteration in brain DA and its metabolites (DOPAC and HVA) in both health and transition phases:

To understand the role of ROT-induced neurotoxicity on DA metabolism, I quantified the level of brain DA and its metabolites (DOPAC and HVA) using HPLC with an electrochemical detector. Analysis reveals that the level of DA is significantly decreased by 38%, 28% and 26% under treated conditions in the early health phase (**Figure 3.9 C**), late health phase (**Figure 3.9 D**) and transition phase (**Figure 3.9 E**) flies respectively. The level of DOPAC is also significantly decreased in early health phase flies (38% compared to control), late health phase flies (20% as compared to control) and transition phase flies (13% as compared to control) as observed in human PD patients (Andersen *et al*., 2017) and *Drosophila* PD model exposed to PQ (Shukla *et al*., 2016). The level of HVA is significantly reduced (29%, 16% and 21% compared to control) during the early health phase, late health phase and transition phases of the fly life span. These results indicate

altered ROT-induced DA metabolism in the fly brain during early, late health and transition phases.

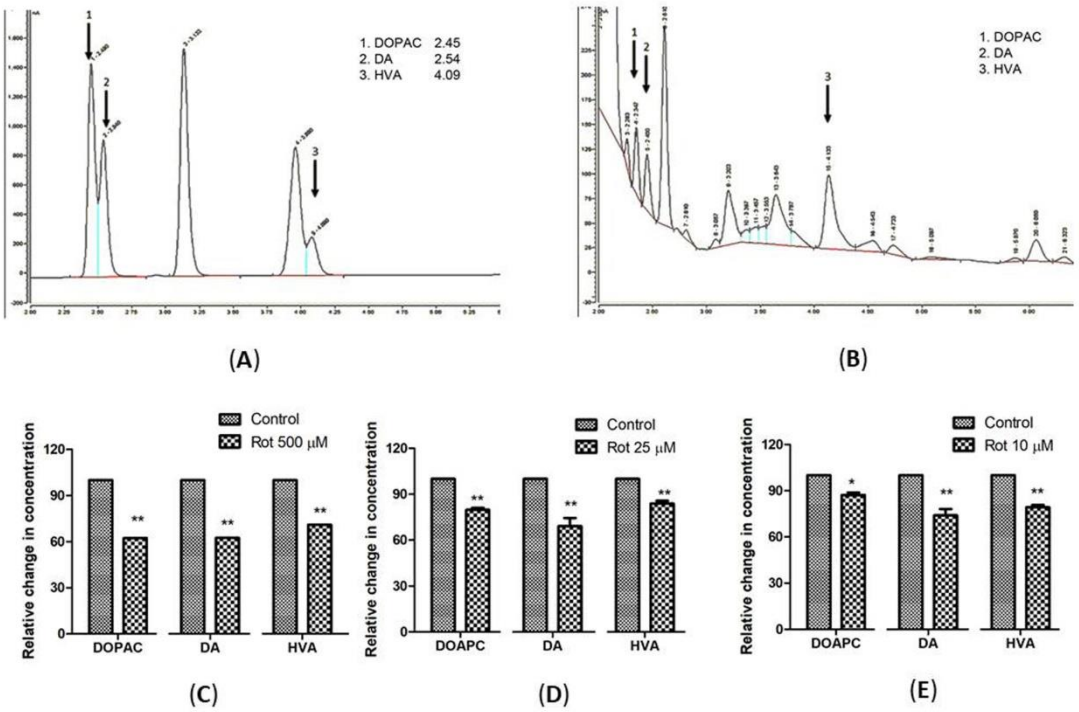

Figure 3.9: Quantification of DA and its metabolites, DOPAC and HVA using HPLC in fly brain homogenate: Chromatogram of standard DA, HVA and DOPAC (**A**) shows specific retention time and chromatogram for fly brain tissue extract (**B**). The relative level of DA and its metabolites at the selected time points in three stages of the life span i.e., the early health phase (**C**); late health phase (**D**); transition phase (**E**) indicates diminished levels of DA, HVA and DOPAC illustrating altered DA metabolism in brain-specific fashion in the PD model. (Statistical analysis was performed using a t-test *$p<0.05$; **$p<0.001$; compared to control).

3.4. Discussion:

The adult life of *Drosophila* was categorized by Arking *et al.* (2002) into health, transition and senescent stages. Our laboratory characterized these stages in OK flies as follows: health phase wherein there is no natural death occurs (0-30 days), transition phase (slight decline in the mortality curve showing 10% death; 31-60 days) and senescence phase (steady decline in mortality curve represented by the window between the end of transition phase till maximum life span of the fly; 61-120 days) (Phom *et al*., 2014). The review of the literature reveals that from 2004 to date, there are 50 research articles relating to ROT-mediated fly PD models (source: Pubmed). In all these works, the age of the *Drosophila* employed varies from 3-20 days (Maitra *et al*., 2021; Nguyen *et al*., 2018; Sur *et al*., 2018; Pandareesh *et al*., 2016; Cassar *et al*., 2015; Coulom and Birman, 2004), meaning all these animals belong to the adult health phase. But late-onset NDDs such as PD set in during the transition phase of adult life. It has been shown that gene expression profiles vary among different life stages and the observed variation is similar among flies, mice and humans (Pletcher *et al*., 2002). Hence, it is possible that molecular targets of genotropic nutraceuticals/therapeutic agents may not be present in all the life phases leading to the failure of young animal-based therapeutic strategies for late-onset NDDs such as PD (Phom *et al*., 2014). This critical aspect of the aging process is important to be taken into consideration while studying the pathophysiology of NDD such as PD. So, there is an immediate requirement of developing and characterizing life stage-specific animal models for PD.

Multiple epidemiological studies point toward a strong relationship between environmental toxin exposure and sporadic PD. Results from the present study reveal that *Drosophila* is susceptible to ROT in a time and dose-dependent manner (**Figure 3.3**) and ROT exposure

leads to mobility defects (**Figures 3.4, 3.5, 3.6**). The primary objective of the present study is to develop an adult life stage-specific *Drosophila* model to understand the pathophysiology associated with late-onset NDD such as PD. The present study shows that the ROT concentration of 1000 µM is toxic to early health phase flies while 50 µM and above concentrations are highly toxic in the case of late health phase and transition phase flies. While developing animal models of DA degeneration/PD, it is important to avoid acute concentrations of neurotoxicants. Acute concentrations lead to a systemic failure of an organism. Hence, observations made in such models may not throw light into the degeneration process of a specific set of neurons such as DA-ergic in the case of PD.

I aim to decipher the pathophysiology related to PD at such a time point wherein the organism exhibits disease phenotypes such as mobility defects well before the death of the organism. Hence, I chose 500 µM ROT for 5 days of exposure in case of the early health phase fly, 25 µM ROT for 2 days of exposure in case of the late health phase fly and 10 µM ROT for 2 days of exposure in case of the transition phase fly (all these concentrations and duration of exposures are carefully picked up after performing comprehensive longevity studies and characterizing mobility defects in such a way that though the fly exhibits mobility defects at these points, mortality due to systemic failure occurs much later.

It has been demonstrated that ROT-mediated DA-ergic neurodegeneration is due to the inhibition of mitochondrial complex I activity and subsequent failure of the energy-generating mechanism of the cells (Innos and Hickey, 2021; Coulom and Birman, 2004). Inhibited mitochondrial complex activities thereby causing oxidative damage to DNs have been demonstrated in PD patients (Carling *et al*., 2020; Zilocchi *et al*., 2018). The present study shows the reduced activity of complex I-III indicating the inhibition of complex I of

the ETC (**Figure 3.7**). The level of inhibition is lower in aged flies as seen in aged mice (Genova *et al*., 1997). This could be due to a significant decrease in sensitivity of NADH oxidation in old aged animals, as the ROT binding site encompasses a complex I subunit encoded by mt-DNA which is on the verge of cellular senescence (Genova *et al*., 1997). Inhibition of complex I disrupt electron flow thereby decreasing ATP production and increasing ROS production (Mizuno *et al*., 1987) leading to the death of the DNs. All these studies validate the present ROT-mediated fly PD model.

Upon analyzing the DNs, I found that the number of DNs remains unchanged in the PD model as compared to the control **(Figure 3.8).** My results are in agreement with the findings from other labs (Navarro *et al*., 2014; Meulener *et al*., 2005; Pesah *et al*., 2005). Loss of DA neuronal number has been an issue of controversy in fly models of PD (Navarro *et al*., 2014). By quantifying the fluorescence intensity of the nuclear GFP (driven by TH-gal4) in both genetic and toxin-based *Drosophila* models of PD, Navarro et al. (2014) re-evaluated the issue and clarified it. Though there was no loss of DNs, the level of TH protein synthesis was diminished and termed as "neuronal dysfunction" (Navarro *et al*., 2014). I quantified the fluorescence intensity of fluorescently labelled secondary antibody which is targeted against the primary antibody anti-TH. Results indicate that the fluorescence intensity is significantly reduced to 40-50% under induced PD conditions, which suggests the reduced levels of TH and the DA-ergic "neuronal dysfunction" (Navarro *et al*., 2014). Therefore, the present study illustrates that in the present model though there is no loss of DA neurons *per se*; there is a significant reduction in the TH synthesis. Hence, it is possible that DA synthesis is diminished which is further characterized using HPLC.

The oxidation of DA into its metabolites is a normal phenomenon to keep DNs intact in the *substantia nigra* (Segura-Aguilar *et al*., 2014). The effects of aldehyde dehydrogenases in three different life stages of mice (young (5–8 months); middle-aged (12–14 months) and old (18–27 months)) suggested that deletion of two isoforms of aldehyde dehydrogenase resulted in Parkinsonism like age-related reductions in monoamines and their metabolites and degeneration of DNs (Wey *et al*., 2012). Our laboratory has previously shown a significant reduction in the level of DA under PQ-induced PD conditions (Phom *et al*., 2014). The present study also showed a significant reduction in the level of DA ($p<0.001$) in all the life stages (**Figure 3.9**). This result validates the previous observation of diminished levels of TH as determined through quantification of fluorescence intensity of fluorescently labelled secondary antibodies (**Figure 3.8**). The level of DOPAC which is downstream of DA is significantly reduced in the early health phase ($P<0.001$), late health phase ($P<0.01$) and transition phase ($p<0.01$) flies. The level of HVA is significantly reduced during the health ($p<0.001$) and transition phases ($p<0.01$) of the fly life stages. There has been no study so far on the DA and its metabolites in three important stages of the life span of flies. I report here for the first time the effect of ROT on DA metabolism-related neurodegeneration in different life stages of *Drosophila*. Upon ROT treatment, the levels of DA are significantly diminished by 38 and 26% during the health and transition phases respectively. However, DA catabolism into HVA and DOPAC in the transition phase brain is higher compared to the levels in the health phase brain (DOPAC and HVA levels are close to the control brains) suggesting the differential influence of ROT on brain DA metabolism.

From the present study, I summarize that exposure of *Drosophila* to ROT demonstrates characteristic features of PD: concentration-dependent lethality, locomotor deficits, complex I inhibition, DA-ergic neuronal dysfunction and depletion in DA levels. By taking advantage

of the adult life stage-specific ROT-mediated sporadic PD model, I aim to screen potential neuroprotective small molecules. Life phase-specific models will further help to decipher underlying molecular mechanism(s) of neuroprotection/degeneration; knowledge of which is essential in developing novel therapeutic strategies for PD.

5. Conclusion:

The present study illustrates that exposure of *Drosophila* belonging to adult health and transition phases to neurotoxicant ROT exhibits characteristic features of PD: concentration-dependent lethality, locomotor deficits, complex I inhibition, DA-ergic neuronal dysfunction and depletion in DA levels. Importantly, life phase-specific animal models are crucial for understanding the progression and pathophysiology; deciphering the underlying molecular mechanism(s) of neurodegeneration and screening the potential neuroprotective efficacy of small molecules/nutraceuticals for late-onset NDDs such as PD.

CHAPTER 4

Adult Life Phase-Specific Dopaminergic Neuroprotective Efficacy of Curcumin in Rotenone-Mediated *Drosophila* Model of Parkinson's Disease: Inferences to Therapeutic Strategies for Late-Onset Neurodegenerative Disorders

4.1. Introduction:

Studies in the field of polyphenols and their potential benefits in modern medicine for their positive outcome on human health are becoming very common. In contemporary research, the application of natural products in aging and age-associated diseases is mainly focused on (Benameur *et al.,* 2021). In humans, healthy aging and longevity are complex processes affected by several environmental influences such as diet, exercise, health habits, psychosocial conditions and genetic factors as well. Promoting a healthy aging process is more effective and less expensive than treating particular age-related diseases. Diet and caloric restriction have a crucial role in healthy aging (Zia *et al.,* 2021). Therefore, natural products possessing diverse biological activities and drug-like properties are important resources for treating human diseases (Kashyap *et al.,* 2021). Researchers have suggested the efficacy of natural products by showing modulation of biochemical markers, antioxidant enzymes and phenotypes associated with rescue upon exposure to toxic agents in different disease models. Their varied natural role in organisms overlay the basis for their therapeutic prospect in presently non-treatable neurodegenerative disorders including PD. Hence, natural products present in our daily diet that could promote healthy aging are intensively studied.

Turmeric- a dietary spice, herbal supplement, medicine, cosmetic and fabric dye, has been widely used in traditional Indian and South Asian medicine for around 4000 years and has been recognized as a safe food ingredient by the US Food and Drug Administration (FDA). It is known to be highly rich in phytochemicals which imparts it a wide range of biological activity. Turmeric contains curcuminoids in several forms. The active components of turmeric notably exhibit countless pharmacological benefits due to its anti-inflammatory, antimutagenic, antioxidant, antimicrobial, immunoregulatory, chemopreventive and chemotherapeutic properties (Girisa *et al.,* 2021). Curcumin (CUR) is the most extensively studied compound extracted from turmeric. Diferuloylmethane or (1E, 6E)-1, 7-bis (4-hydroxy-3-methoxyphenyl)-1, 6-heptadiene-3, 5-dione, commonly known as curcumin, the main active, yellow-coloured natural polyphenolic compound along with curcuminoid accounts for 2-8% of turmeric (Sharma *et al.,* 2007). CUR is the most thoroughly investigated phytochemical with over 18000 PUBMED citations **(Figure. 4.1 A**) in the last two decades (among these, 253 studies are on PD (**Figure 4.1 B**)) and proved to possess powerful anti-inflammation, anti-virus, anti-oxidant, anti-biotic, anti-depressant, anti-arthritic, wound healing properties, anticancer, and anti-neurodegenerative characteristics (Fan *et al.,* 2021; Zia *et al.,* 2021). This "wonder molecule" has been employed in 438 clinical trials (120 trials in the USA only) for different human diseases (ClinicalTrial.gov; viewed on 11/6/2022).

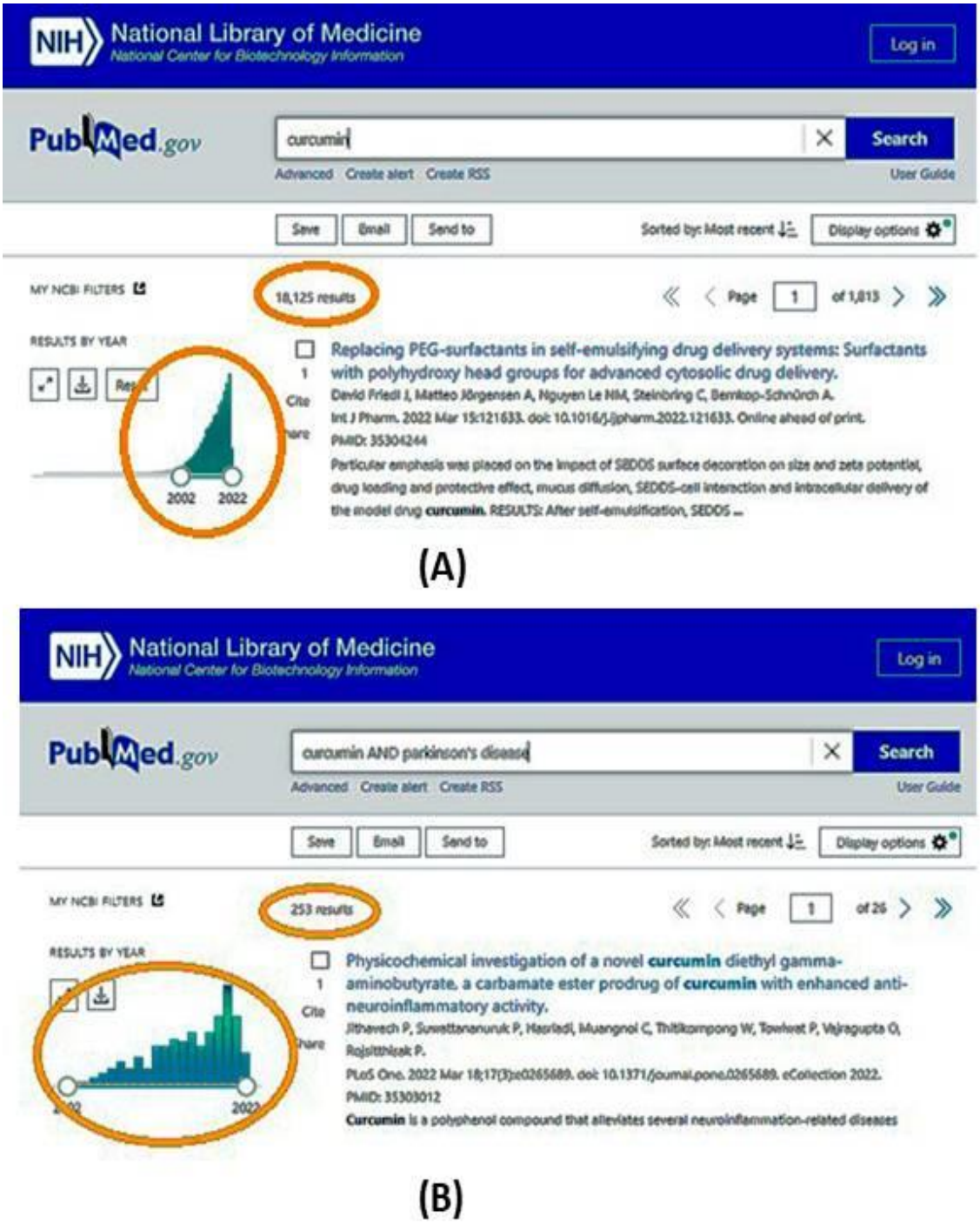

Figure 4.1: Screenshot of PUBMED search showing the number of studies on curcumin alone (A) and curcumin's efficacy with respect to Parkinson's disease (B) revealing that curcumin is one of the most extensively studied compounds for human health and disease in the last two decades.

4.1.1. Beneficial role of CUR in various diseases

Studies on aging and age-associated diseases revealed that CUR and its metabolites, prolong the mean life phase in model organisms such as *Caenorhabditis elegans, Drosophila melanogaster, Saccharomyces cerevisiae* and *Mus musculus via* increased superoxide dismutase (SOD) activity, and decreased malondialdehyde and lipofuscin levels. CUR is believed to modulate major signalling pathways mediated through insulin/insulin-like growth factor-1 (IGF-1), mammalian target of rapamycin (mTOR), protein kinase A (PKA), and FOXO (a subgroup of the Fork-head family of transcription factors) that influence the longevity of organisms (Zia *et al.*, 2021). CUR has also been shown to influence a variety of biological signalling pathways, including PI3K/Akt, JAK/STAT, MAPK, Wnt/-catenin, p53, NF-κB, and apoptosis (Deng *et al.,* 2019). CUR prevents neuroinflammation via CaMKKβ-dependent activation of the protein kinase signalling pathway (Qiao *et al.,* 2020). These biological activities pose great advantages to the development of CUR-based therapy for the treatment of chronic diseases (Laabbar *et al.,* 2019).

In humans, the therapeutic efficacy of CUR has been demonstrated in various diseases such as cancer (Tian *et al.,* 2021; Forouzanfar *et al.,* 2021), cardiovascular diseases (Sadoughi *et al.,* 2021), and various neurological disorders such as ALS (Chico *et al.,* 2018), anxiety (Esmaily *et al.,* 2015), depression (Kanchanatawan *et al.,* 2018), AD (Zou *et al.,* 2021; Maiti *et al.,* 2021), Schizophrenia (Miodownik *et al.,* 2019) and PD (Ramires Júnior *et al.,* 2021; El Nebrisi *et al.,* 2020). It has been reported to be a strong forager of a range of ROS including hydroxyl radicals, superoxide anion radicals and protection of oxidative damage to kidney cells by suppressing lipid degradation, lipid peroxidation and cellular breakdown (Cohly *et al.,* 1998). Randomized clinical trials comprising 631 patients with various

diseases have shown the beneficial role of CUR/turmeric (Bagherniya *et al.,* 2021). It is shown to be beneficial in skin diseases such as psoriasis, pruritic skin lesions, radiation dermatitis, vitiligo, etc (Zeng *et al.,* 2020). CUR is found to be beneficial in digestive disorders such as indigestion, heartburn, nausea, constipation, diarrhoea, abdominal pain, physical functioning, energy levels and sleep (Ried *et al.,* 2020). CUR is shown to have a beneficial role in several gynaecological disorders (Bahrami *et al.,* 2021). CUR is also shown to upregulate several genes in an *in vitro* human gingival fibroblast wound healing model suggesting its role as a therapeutic agent for gingival ulcers (Rujirachotiwat and Suttamanatwong, 2021). Due to its tremendous potential as a therapeutic agent, curcumin is now being tested in 438 human clinical trials for several chronic diseases. Thus, CUR is one such potential candidate that can be explored for a therapeutic approach to several human diseases including NDDs like PD.

4.1.2. Bioavailability and toxicity concerns of curcumin

There are concerns regarding the instability and poor absorption of CUR in the body fluids resulting in lower cellular uptake, rapid hepatic metabolism and faster elimination from the body (Gupta *et al.,* 2013). Moreover, low solubility and high hydrophobicity of CUR in water cause a major limitation in therapeutic applications (Sharma *et al.,* 2007). Nutraceutical CUR which is a beneficial phytochemical may also act as a toxin at higher concentrations and in aged animals including humans. Studies have indicated adverse side effects of high doses of CUR which include skin rashes, allergic reactions, swollen skin, gastrointestinal discomfort and chest tightness (Liddle *et al.,* 2006). Prolonged use of CUR for 1-4 months with doses of 0.9–3.6 g per day is shown to cause adverse effects by

increasing the lactate dehydrogenase and serum alkaline phosphatase causing nausea and diarrhoea in humans (Sharma *et al.,* 2004). Chronic intake of CUR is shown to cause a hepatotoxic effect by stimulating bile secretion. Therefore, a person with liver disease or one who is under medication for a hepatic problem is advised not to undergo CUR therapy (Dulbecco and Savarino, 2013). Supplementation of 20–40 mg CUR per day is shown to increase the contraction of the gallbladder in healthy individuals (Rasyid *et al.,* 2002). Furthermore, CUR therapy is not recommended for the individual who is taking any blood-thinning agents, non-steroidal anti-inflammatory drugs (NSAIDs) or Reserpine for the fear of its synergistic side effects (Begum *et al.,* 2008; Cole *et al.,* 2007). A higher dose of CUR may cause colon or lung cancer or other side effects like inhibition of proteasomal function. Oral administration of CUR among the individuals with chronic anterior uveitis, all the patients who received CUR alone improved but those who additionally received anti-tubercular therapy had developed complications in their eyes and lost vision over time (Lal *et al.,* 1999) suggesting that CUR may react with certain compounds resulting in a detrimental effect. In a clinical trial of CUR for the prevention of colorectal neoplasia it was found that, overall, 61% of participants showed toxicity, mainly the gastrointestinal disturbances, most prevalently diarrhoea, as well as swollenness and gastroesophageal reflux (Carroll *et al.,* 2011). Another experiment (that aimed to establish the linkage between exposures to mixed metals with child health outcomes due to the association of lead with environmental sources such as spices) has shown that most of the turmeric samples had a high level of lead which upon further study showed its increased bio-accessibility suggesting that turmeric powder upon contamination through environmental lead exposure can have potential lead toxicity and poisoning among some population (Gleason *et al.,* 2014).

Considering these reports, it is important to reconsider the safety doses of CUR therapy in various diseases including PD.

The studies concerning CUR safety under various experimental conditions are under-reported. Reports suggesting that CUR may cause toxicity under specific conditions are shown with the studies in mammalian cell lines on treatment with turmeric in which there is a dose and time-dependent induction of chromosome aberrations (Goodpasture and Arrighi, 1976). Another study on the effect of CUR on DNA has demonstrated that it induces DNA damage and chromosomal alterations (Cao *et al.,* 2006). An experiment testing the chelator action of CUR to cause iron deficiency *in vivo* showed that CUR suppressed the production of hepcidin, a peptide which plays an essential role in the regulation and balancing of systemic iron. It causes iron insufficiency leading to anaemia in mice that are fed with poor iron diets (Jiao *et al.,* 2009). CUR confers negative activity of enzymes such as glutathione-S-transferase and UDP-glucuronosyl transferase apart from hampering the action of drug-metabolizing enzymes such as cytochrome P450 (Appiah-Opong *et al.,* 2007). Such action of CUR may result in abnormal plasma flow of certain drugs that may lead to toxic action (Mancuso and Barone, 2009). Contradicting the reports that suggest beneficial properties of CUR, a study suggested both advantages and disadvantages of CUR in alcoholic liver injury. Concentration-dependent CUR toxicity was reported in animal models in which CUR was found to accelerate liver injury and liver cellular oedema (Zhao *et al.,* 2012).

In a study to assess the toxicity of CUR, it is shown that CUR induces dose-dependent lethality in which a concentration of 2.5 mM and above adversely affected the viability of *Drosophila* (Phom *et al.,* 2014). Another study showed that a concentration of 1 mg/L

aqueous extract of *Curcuma longa* induces an adverse effect on the viability of normal SH-SY5Y cells (Ma and Guo, 2017).

Hence, the use of CUR as a therapeutic agent must be moderated at an optimal dose to avoid its toxic side effects (Maiti and Dunbar, 2018). Therefore, while developing a therapeutic approach for a disease, it is important to thoroughly validate the toxicity as well as beneficial activity of drug/phytochemical *per se* in the model organism. Taking this important aspect into consideration, I used a wide range of CUR concentrations and assessed their possible toxicity in the adult life phase-specific *Drosophila* model and determined certain sub-lethal concentrations. These selected concentrations neither influence viability nor induce mobility defects in *Drosophila* and were employed for assessing the neuroprotective efficacy of CUR in further studies.

4.1.3. Neuroprotective role of CUR in mitigating PD pathology: Insights from animal models

CUR is shown to undergo a variety of molecular interactions inside the cell to inhibit the transcription of genes associated with OS and inflammatory responses thereby reducing the production of ROS (Qiao *et al.*, 2020; Deng *et al.*, 2019). Studies have shown the capability of CUR to slow down the key distinguishing features of PD like ROS accumulation, apoptosis, platelet assembly, cytokine production, cyclooxygenase lipoxygenase isoenzymes activities, repress oxidative injury and cognitive deficits in various models (Qiao *et al.*, 2020; Deng *et al.*, 2019). CUR can modulate the inflammation and OS induced by microglia in the brain by acting on different proteins (Benameur *et al.*, 2021). It is also suggested that

iron-induced primary cortical neuron toxicity is improved by CUR action through attenuating necroptosis (Dai *et al.,* 2013). Out of 87 genes found to be differentially expressed in CUR-treated wild type *Drosophila melanogaster*, 50 genes were markedly up-regulated and the rest 37 were down-regulated, suggesting that CUR can be explored as an alternative therapeutic approach to developing drugs for age-related disorders (Zhang *et al.*, 2015). Also when CUR was fed to developing larva, it triggers pathways that help to extend the health phase accompanied by a marked increase in median and maximum longevities in adult flies (Soh *et al.,* 2013). CUR treatment could significantly safeguard against G2385R-LRRK2-induced neurodegeneration by reducing mitochondrial ROS and caspase-3/7 activation, attenuating the toxicity of H_2O_2 in the cellular environment (Zhang *et al.,* 2021). The co-treatment of PC12 cells with 10 µM CUR exerted protective effects by reducing the levels of oxidized proteins, promoting proteasome activation and abolishing the inhibitory effect exerted by ROT (Buratta *et al.,* 2020). These findings provide an understanding of the role of CUR in therapeutic intervention against PD.

It is reported that CUR has gender and genotype-specific life phase extension and sequesters OS-mediated free radicals and enhances locomotor ability in *Drosophila*, suggesting its potential treatment applicability in higher organisms (Lee *et al.,* 2010). Co-feeding the fly with CUR could prevent mortality, inhibit AChE activity and restore DA levels in a Cu^{2+} mediated *Drosophila* PD model (Abolaji *et al.,* 2020). CUR inhibits OS and induces a strong modulatory effect on Transient Receptor Potential Melastatin-like 2- (TRPM2) mediated Ca^{2+} influx caused by ROS and caspase3/9 processes in SH-SY5Y human neuroblastoma cells (Öz and Celik, 2016). Transgenic fly expressing human α-syn when exposed to different concentrations of CUR was found to considerably delay the loss of activity pattern, decrease the level of OS and apoptosis and extend the life span (Siddique *et al.,* 2014).

Curcumin monoglucoside was also shown to mitigate the ROT-mediated neurotoxicity in cell and *Drosophila* models of PD (Pandareesh *et al*. 2016), suggesting its potential role in DA-ergic neuroprotection.

However, all these findings have shown the neuroprotective effects of CUR by employing young animal models of the adult health phase. It may be noted that the investigation of different phases of life in *Drosophila* has shown that each life stage is distinguished by a diverse pattern of gene expression (Pletcher *et al.,* 2002; Arking, 2005) (discussed in **Chapter 3**). This pattern is comparable to the corresponding life phase in mice and humans. Therefore, while screening nutraceuticals for their DA-ergic neuroprotective efficacy in animal models, it is important to follow the adult life stage/phase-specific studies for late-onset NDD such as PD. Considering this fact, I made an effort to understand the neuroprotective efficacy of CUR in ROT-mediated health and transition phase-specific *Drosophila* model of PD by employing four concentrations of CUR (100 µM, 250 µM, 500 µM and 1000 µM) in both the pre- and co-feeding regimen through assessing mobility phenotypes and further by characterizing the DA-ergic neurodegeneration/protection and modulation of DA metabolism under induced PD and possible rescue/no rescue conditions.

4.2. Materials and Methods:

4.2.1. Preparation of Curcumin stock

Refer to section 2.7 of chapter 2

4.2.2 Curcumin toxicity study

Refer to section 2.8 of chapter 2

4.2.3. Negative geotaxis assay

Refer to section 2.9 of chapter 2

4.2.4. Pre- and co-feeding regimens

Refer to section 2.13 of chapter 2

4.2.5. Quantification of dopaminergic neurons and fluorescence intensity using fluorescence microscopy

Refer to section 2.14 of chapter 2

4.2.6. Quantification of dopamine and its metabolites using High Performance Liquid Chromatography (HPLC)

Refer to section 2.15 of chapter 2

4.2.7. Statistical analysis

Refer to section 2.16 of chapter 2

4.3. Result:

4.3.1. *Drosophila* is susceptible to CUR in a time-dose-dependent manner

In order to understand the susceptibility of *Drosophila* to CUR, male OK flies of early health and transition phase were fed with eight different concentrations of CUR (25 µM, 50 µM, 100 µM, 250 µM, 500 µM, 1 mM, 1.5 mM and 2.5 mM) while the control flies remain on 5% sucrose only. The survivorship of flies was observed and recorded every 24 Hrs till all the flies were dead. A total of 100 flies were used for each concentration.

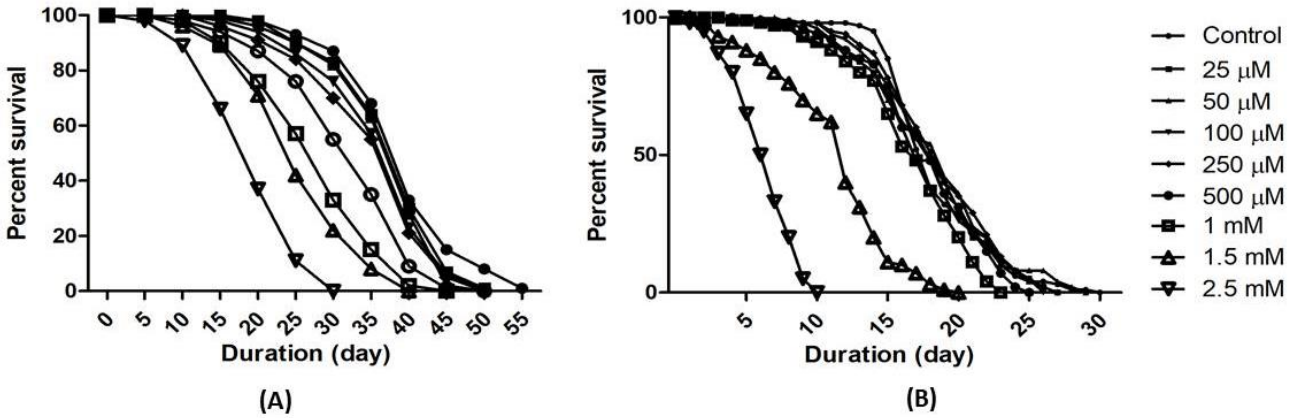

Figure 4.2: Dose- and time-dependent mortality of OK male fly exposed to CUR during different phases of adult life. Mortality pattern among adult male flies of early health phase (**A**) and transition phase (**B**), exposed to eight different concentrations of CUR (25 µM, 50 µM, 100 µM, 250 µM, 500 µM, 1 mM, 1.5 mM and 2.5 mM) showed concentration-dependent lethality. Mortality data were collected every 24 Hrs for each group till all the flies were dead. A comparison of survival curves showed a significant difference in response among different tested concentrations (log-rank [Mantel–Cox] test, $p<0.0001$).

CUR exerts concentration-dependent lethality on both the life stages of the fly. The survivability of the flies in the concentrations of 25 µM, 50 µM, 100 µM and 250 µM were

very close to the control group. The concentrations of CUR ranging from 25 µM to 1 mM showed no observable toxicity while concentrations of 1.5 mM and 2.5mM affect the viability of the transition phase fly showing that higher concentrations of CUR could be harmful to the fly. The flies in the lowest concentration of 25 µM could survive for 55 days (maximum life span) while they could survive for 30 days in the highest concentration of 2.5 mM in the case of the early health phase flies. In the case of the transition phase flies, they could survive for only 30 days in the lowest concentration of 25 µM and 10 days in the highest concentration of 2.5 mM. The median life span (LD_{50}) of the concentrations of 100 µM, 250 µM, 500 µM and 1 mM were 39 days, 38 days, 34 days and 30 days respectively for the early health phase flies (**Figure 4.2 A**) and 19 days, 18 days, 16 days and 15 days respectively for the transition phase flies (**Figure 4.2 B)**. A comparison of survival curves of early health phase and transition phase showed a significant difference in response among all the tested concentrations (Log-rank [Mantel-Cox] Test, $P < 0.0001$).

From this study, I carefully choose 100 µM, 250 µM, 500 µM and 1000 µM concentrations of CUR to understand the DA-ergic neuroprotective efficacy of CUR in the ROT-mediated life phase-specific fly PD model. All these concentrations of CUR did not affect the survival of the flies at the selected treatment windows. Care was also taken in such a way that selected CUR concentrations do not cause any mobility defects. Results of the negative geotaxis assay (NGA) illustrated that the selected CUR concentrations induced no mobility defects in the flies of the early health phase and transition phase (**Figure 4.3**).

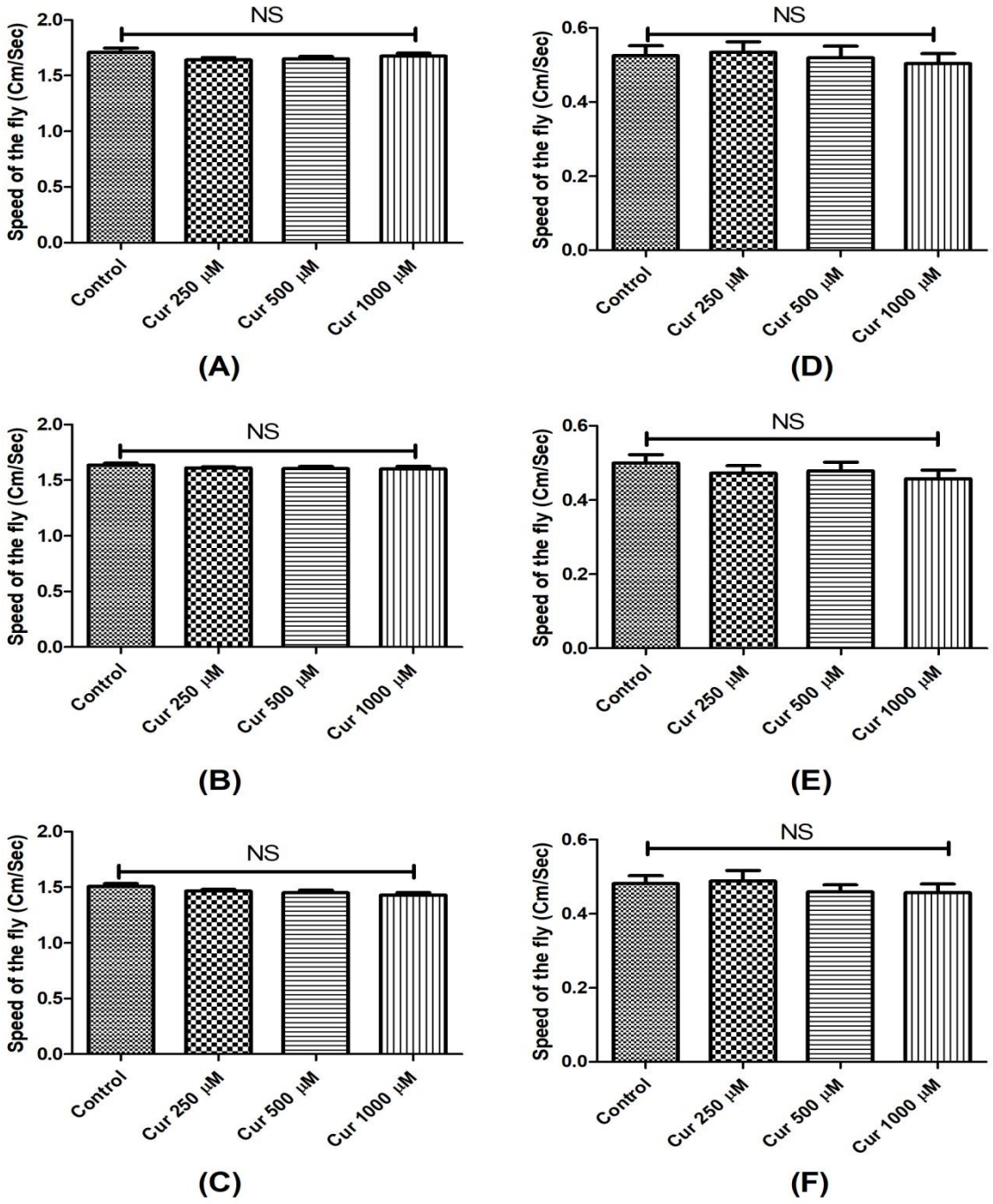

Figure 4.3: CUR does not cause perturbatons in mobility of *Drosophila* as determined thorugh assessing the climbing ability during early health and transition phases. Feeding with CUR concentrations of 250 µM, 500 µM and 1000 µM for 3 days (A), 5 days (B) and 7 days (C) of the early health phase flies resulted in no mobility perturbations. Feeding the flies of the transition phase with the same concentrations of CUR for 1 day (D), 3 days (E) and 5 days (F) resulted in no mobility defects too. There was no mortality at these time

points. (One-way ANOVA followed by the Newman-Keuls Multiple Comparison Test showed no significant difference in mobility. NS- Not Significant)

4.3.2. CUR rescues mobility defects mediated by ROT in both co- and pre-feeding regimens during the early health phase of *Drosophila*

I assessed the negative geotaxis ability of the ROT-mediated adult early health phase fly PD model to decipher the mobility alterations under both the CUR pre- and co-feeding conditions. The distance that the fly climbed in 12 sec was assayed after 4 days and 5 days of exposure to 500 µM ROT or ROT along with CUR (100 µM, 250 µM, 500 µM and 1000 µM). After 4 days of feeding the flies with ROT, they exhibited slowness in movement as indicated by a significant decrease in the speed (bradykinesia), which is the characteristic clinical feature of PD in humans. The speed of the flies were significantly improved when ROT was fed along with CUR (co-feeding regime) as compared to the flies fed with ROT alone (**Figure 4.4 A**). The mobility of ROT-fed flies were significantly reduced after 5 days whereas the CUR co-feeding rescues the phenotype as observed through the improved speed of the flies, suggesting the protective efficacy of curcumin (**Figure 4.4 B**). Pre-feeding the flies with CUR for 2 days (**Figures 4.4 C & D**), 3 days (**Figures 4.4 E & F**) and 5 days (**Figures 4.4 G & H**) and exposed to ROT for 4 days and 5 days also showed similar rescue (significant protective effect at lower concentrations i.e. 100 and 250 µM indicates the resilience provided by CUR pre-feeding comparing to the co-feeding regimen), suggesting that observed protective efficacy of CUR is not through physical interaction and sequestration of the toxin. CUR (500 µM) *per se* has no adverse influence on the mobility performance of the flies.

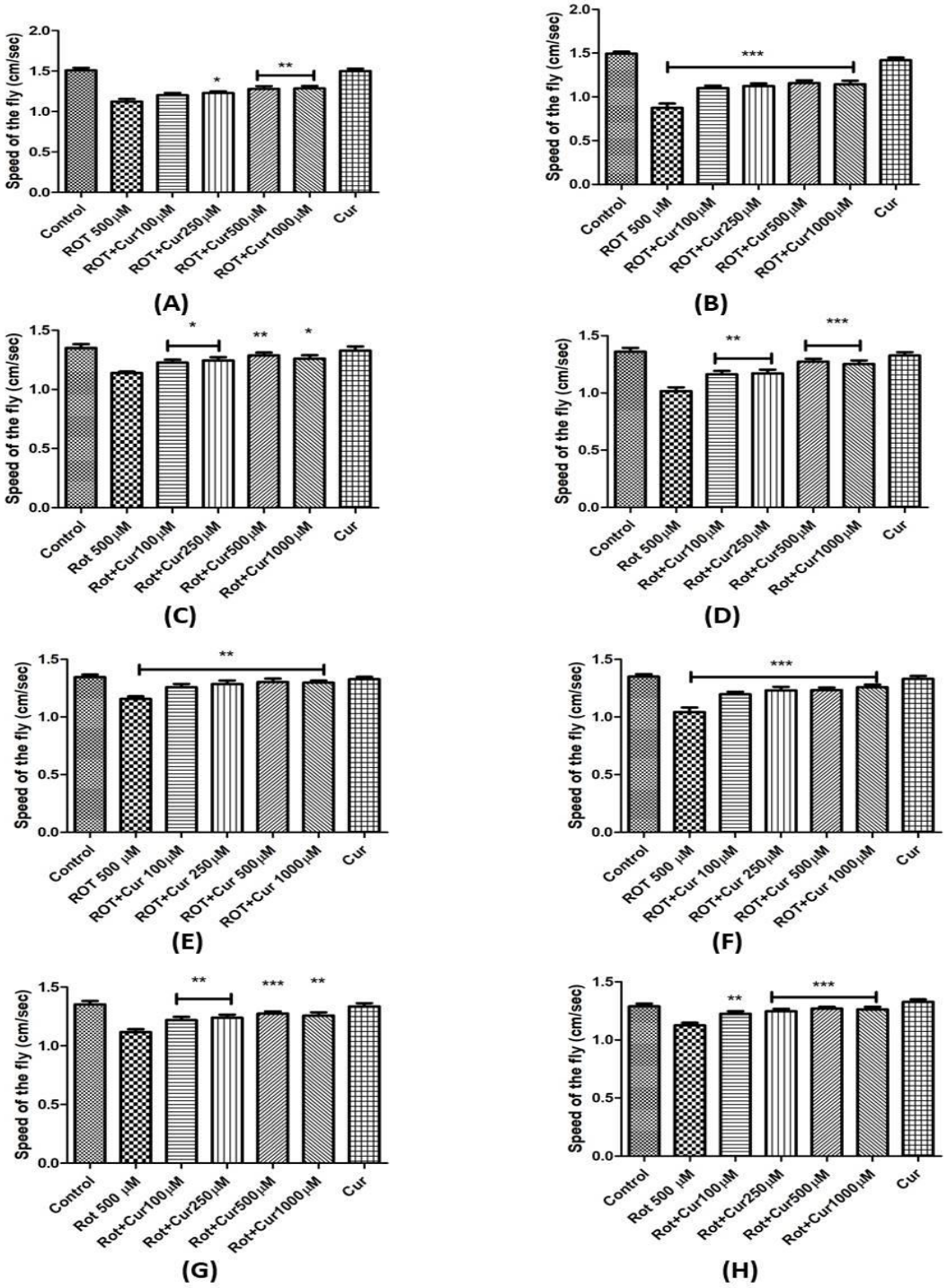

Figure 4.4: Curcumin rescues rotenone induced mobility defects during the early health phase of adult life in *Drosophila* model of PD. Negative geo-taxis assay of early health phase flies in co-feeding regime (A & B) and pre-feeding (C – H) regimens: In the co-feeding regimen, flies were fed with ROT alone or ROT along with CUR for 5 days the

mobility defect was assessed on 4th day (A) and 5th day (B). In the pre-feeding regimen, flies were pre-fed with CUR alone for 2 days (C & D), 3 days (E & F) and 5 days (G & H) and exposed to ROT for 5 days and the mobility defects were assessed on the 4th day (C, E & G) and 5th day (D, F and H). CUR rescues mobility defects during the adult early health phase in both the co-feeding and pre-feeding regimens in the fly model of ROT-mediated sporadic PD. (One way ANOVA followed by Newman-Keuls Multiple Comparison Test showed significant difference in mobility. * $P<0.05$; ** $P<0.001$; *** $P<0.0001$ compared with ROT-treated group)

4.3.3. CUR fails to rescue mobility defects mediated by ROT in both co- and pre-feeding regimens during the late health and the transition phases of *Drosophila*

The adult life span of *Drosophila* is categorized into a health phase, transition phase and senescent phase (Arking *et al.*, 2002). It has been shown that there is a significant variation (about 23%) in genome-wide transcript profiles with age in *Drosophila* (Pletcher *et al.*, 2002). The efficacy of genotropic drugs depends on the availability of the target molecules at that stage of the life cycle. Hence, there is a possibility that targets of genotropic compounds such as CUR may not be present in all life stages (Phom *et al.*, 2014).

To understand this paradigm, I tested CUR efficacy in the age groups of the late health phase (30 days old fly) and transition phase (50 days old fly). CUR could not improve the mobility defects induced by ROT in both the co- and pre-feeding regimens during the late health phase (**Figure 4.5**) and transition phase (**Figures 4.6**) of *Drosophila* as quantified with climbing ability. The distance that the fly climbed in 12 sec after one day and two days of exposure to 25 µM ROT or ROT along with CUR (100 µM, 250 µM, 500 µM and 1000 µM) was assayed. Feeding with ROT alone significantly impaired the mobility of the flies while feeding the flies with CUR (500 µM) *per se* did not show any effect on mobility. The

co-feeding of CUR could not improve the mobility defects induced by ROT in both the late health phase (**Figures 4.5 A & B**) and transition phase (**Figure 4.6 A & B).** Pre-feeding the flies of the late health phase with CUR for 2 days (**Figures 4.5 C & D**), 3 days (**Figures 4.5 E & F**) and 5 days (**Figures 4.5 G & H**) and exposed to ROT for 1 day and 2 days also could not rescue the mobility defects during late health phase. Pre-feeding the flies with CUR for 2 days (**Figures 4.6 C & D**), 3 days (**Figures 4.6 E & F**) and 5 days (**Figures 4.6 G & H**) and exposed to ROT for 1 day and 2 days also showed no improvement in mobility during the transition phase of the flies.

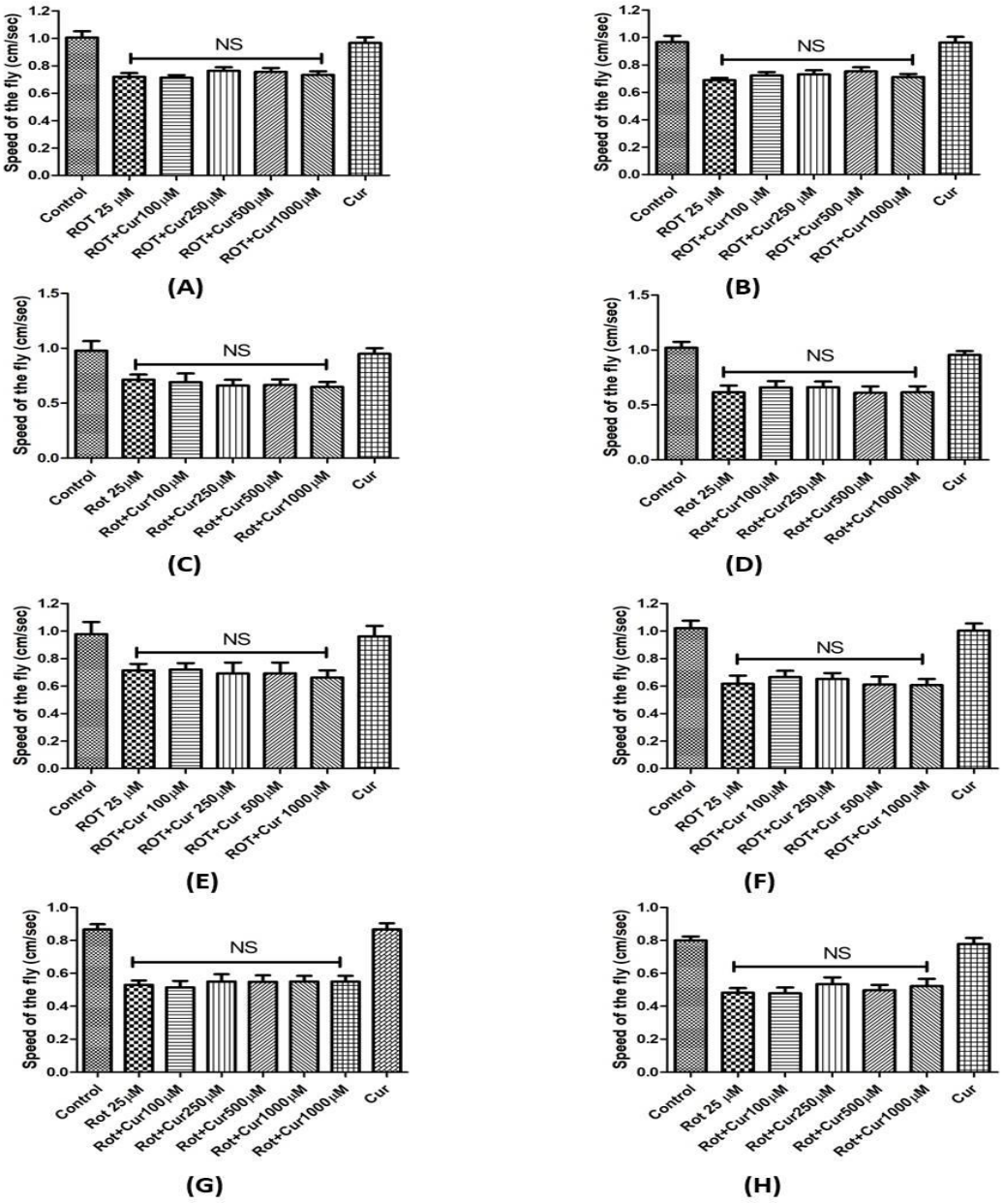

Figure 4.5: Curcumin fails to rescue rotenone induced mobility defects during the late health phase of adult life in *Drosophila* model of PD. Negative geo-taxis assay of the late health phase flies in co-feeding regime (A & B) and pre-feeding regimens (C – H): In the co-feeding regimen, flies were fed with ROT alone or ROT along with CUR for 2 days and the mobility defect was assessed on 1st day (24 Hr) (A) and 2nd day (48 Hr) (B). In the Pre-feeding regimen, flies were pre-fed with CUR alone for 2 days (C & D), 3 days (E & F) and 5 days (G & H) and exposed to ROT for 2 days and the mobility defects were assessed on 1st day (24 Hr) (C, E & G) and 2nd day (48 Hr) (D, F and H). CUR fails to rescues mobility defects during the late health phase in both the co-feeding and pre-feeding regimens in fly

model of ROT-mediated sporadic PD. (One way ANOVA followed by Newman-Keuls Multiple Comparison Test showed no significant difference in mobility. NS- Not significant)

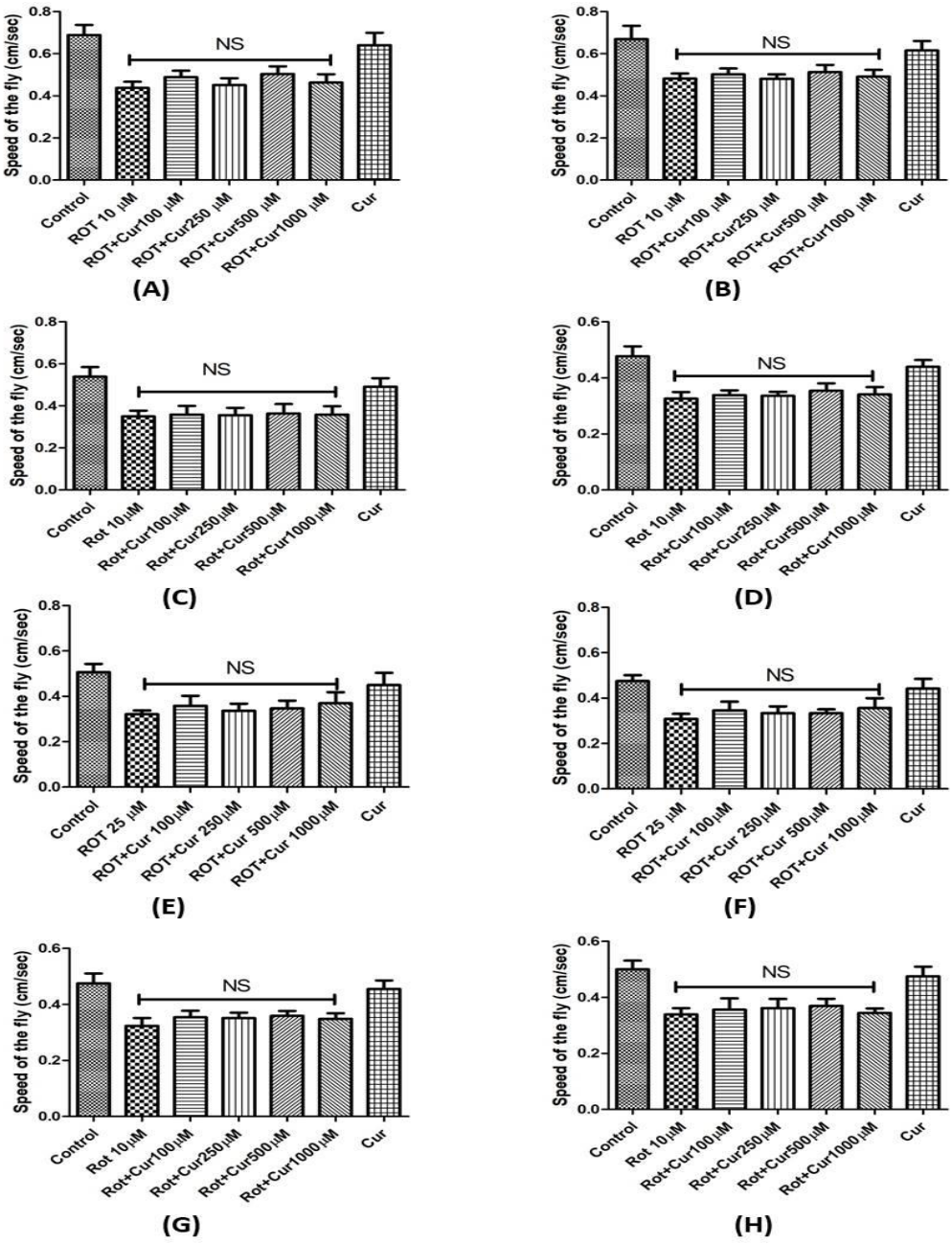

Figure 4.6: Curcumin fails to rescue rotenone induced mobility defects during the transition phase of adult life in *Drosophila* model of PD. Negative geo-taxis assay of the transition phase fly in co-feeding regime (A & B) and pre-feeding regimens (C – H): In the co-feeding regimen, fly was fed with ROT alone or ROT along with CUR for 2 days the mobility defect

was assessed on 1st day (24 Hr) (A) and 2nd day (48 Hr) (B). In the Pre-feeding regimen, fly was pre-fed with CUR alone for 2 days (C & D), 3 days (E & F) and 5 days (G & H) and exposed to ROT for 2 days and the mobility defects were assessed on 1st day (24 Hr) (C, E & G) and 2nd day (48 Hr) (D, F and H). CUR fails to rescues the mobility defects during the transition phase in both the co-feeding and pre-feeding regimens in fly model of ROT-mediated sporadic PD. (One way ANOVA followed by Newman-Keuls Multiple Comparison Test showed no significant difference in mobility. NS- Not significant)

With far-reaching limitations of therapeutic efficacy in NDDs like PD, which shows an average onset at 50 years (according to http: //www.ninds.nih.gov/disorders/parkinsons disease), CUR failed to rescue the mobility defects in both the pre- and co-feeding regimens during late health phase (**Figure 4.5**) and transition phase (**Figure 4.6**) as indicated by negative geotaxis assay. These results suggest the limitation of CUR as a therapeutic compound in late-onset NDDs such as PD. However, whether CUR can be a prophylactic agent is yet to be ascertained.

4.3.4. CUR rescues DA neuronal dysfunction during the health phase but not during the transition phase as determined through the quantification of DA neuronal number and the Tyrosine hydroxylase synthesis

In the *Drosophila* brain, the number of DNs in different clusters viz. PAL, PPL1, PPL2, PPM1/2 and PPM3 are 5, 12, 6/7, 8/9 and 6 respectively (**Figure 4.7**). The number of DNs was quantified by using fluorescently labelled secondary antibodies against the primary antibody targeting the rate-limiting enzyme in dopamine synthesis, tyrosine hydroxylase (TH). The image of the *Drosophila* brain during the early health phase and transition phase

captured through a fluorescence microscope is depicted in **Figure 4.8 A** and **Figure 4.9 A** respectively.

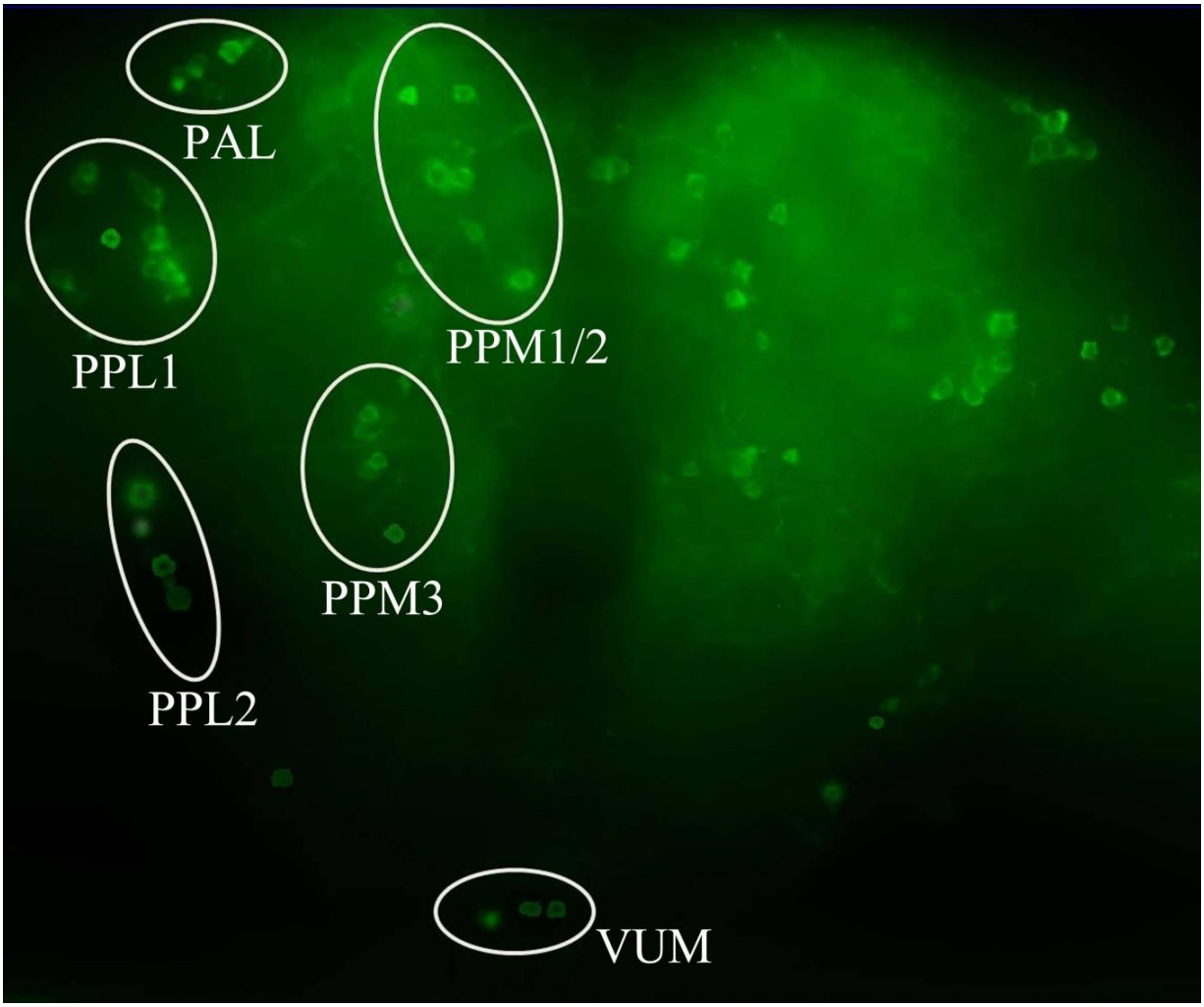

Figure 4.7: Image of whole-brain mount of *Drosophila* captured using ZEN software of Carl -Zeiss Fluorescence Microscope shows the position of different quantifiable clusters of the DNs in the whole fly brain. (PAL- Protocerebral anterior lateral; PPL- Protocerebral posterior lateral; PPM- Protocerebral posterior medial; VUM- Ventral Unpaired Medial)

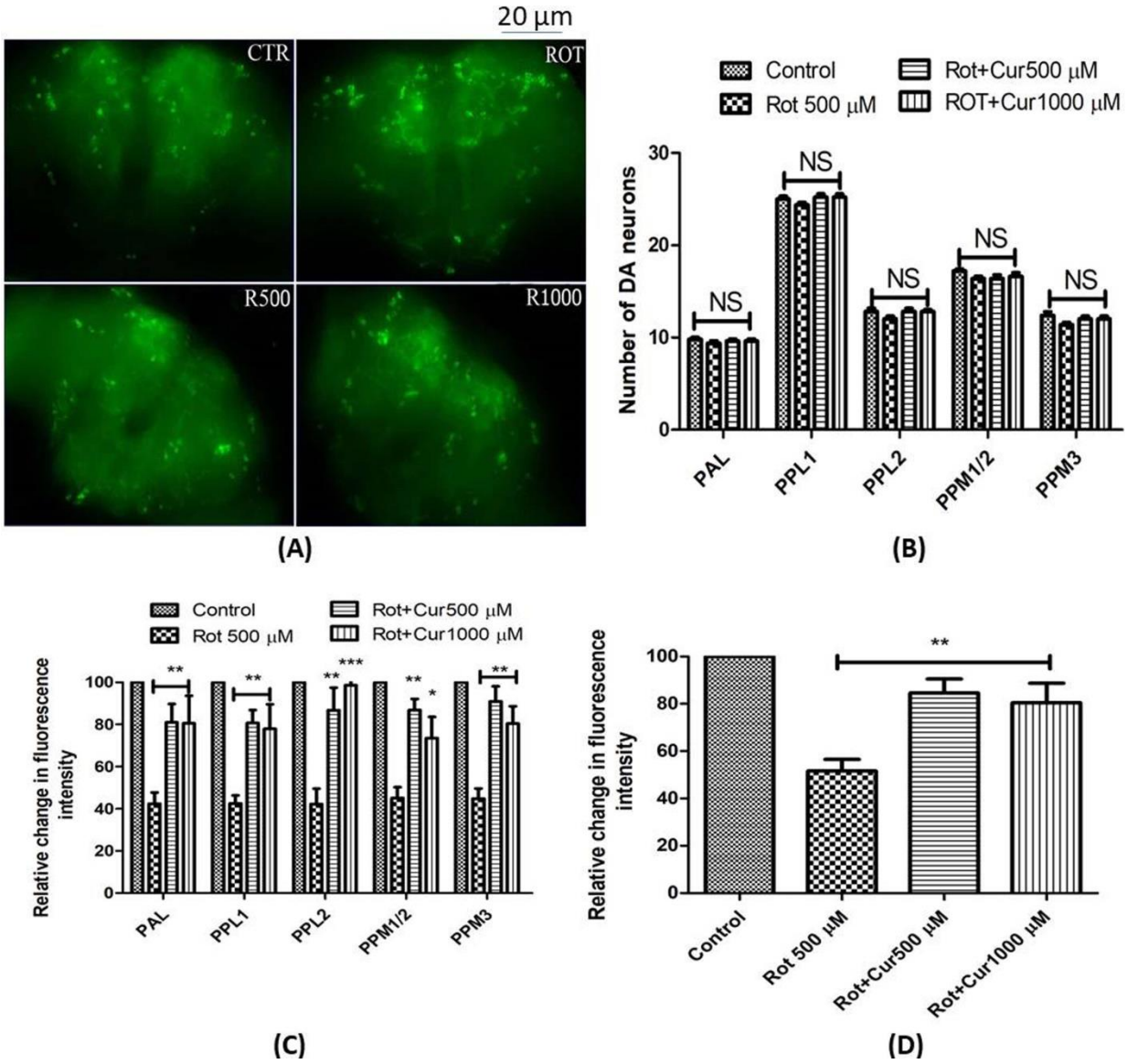

Figure 4.8: Characterization and quantification of DA-ergic neurodegeneration in the whole fly brain of the early health phase through anti-TH antibody immunostaining: Characterization of dopaminergic neurodegeneration in the fly brain of the early health phase **(A).** The scale bar of all the images in the panel is 20 µm. (CTR- Control; ROT- Treated with ROT only; R500- ROT along with CUR 500 µM concentration; R1000- ROT along with CUR 1000 µM concentration; Represented images are "merged" Z-stacking images; however, the quantification of DA-ergic neuronal number and fluorescence intensity is performed in 3D Z-stack images). Quantification of DNs reveals that there is no loss in the

number of DNs upon treatment with ROT alone or ROT along with multiple concentrations of CUR **(B)**. However, ROT leads to "neuronal dysfunction" as characterized by quantification of DA-ergic neuronal fluorescence intensity that is proportional to the amount of TH protein which could be rescued upon therapeutic intervention of CUR **(C)**. Further, a similar trend is observed upon pooling the fluorescence intensity sum of all the clusters in the fly brain **(D)** suggesting that CUR intervention can rescue the depleted levels of TH during the adult health phase of fly. (One way ANOVA followed by Newman-Keuls Multiple Comparison Test. *$p<0.05$; **$p<0.001$; ***$p<0.0001$; NS- Not significant).

Although there is a natural variation in the number of DNs of the same neuronal cluster, no significant difference is observed among the different treatment groups analyzed during the early health phase (**Figure 4.8 B**) and transition phase (**Figure 4.9 B**).

The fluorescence intensity of the secondary antibodies targeting the primary antibody (anti-TH) is an indicator of the amount of TH synthesis. Hence, the diminished fluorescence intensity can be an indicator of the level of DA-ergic neurodegeneration. During the early health phase of the fly, the fluorescence intensity of the fly fed with 500 µM ROT for 5 days was significantly reduced by 42.36%, 42.55%, 42.31%, 45.11% and 44.89% in PAL, PPL1, PPL2, PPM1/2 and PPM3 respectively when compared to control as observed under the fluorescence microscope (**Chapter 3**). Co-feeding the fly of the early health phase with CUR could significantly improve the fluorescence intensity (**Figures 4.8 C**). In the case of transition phase fly, feeding with ROT alone led to significant reduction in the fluorescence intensity by 55.20%, 57.83%, 55.70%, 47.49%, and 56.74% in PAL, PPL1, PPL2, PPM1/2 and PPM3 respectively after 48 hr (**Chapter 3**). Co-feeding the fly of the transition phase with CUR could not improve the reduction in fluorescence intensity (**Figure 4.9 C**).

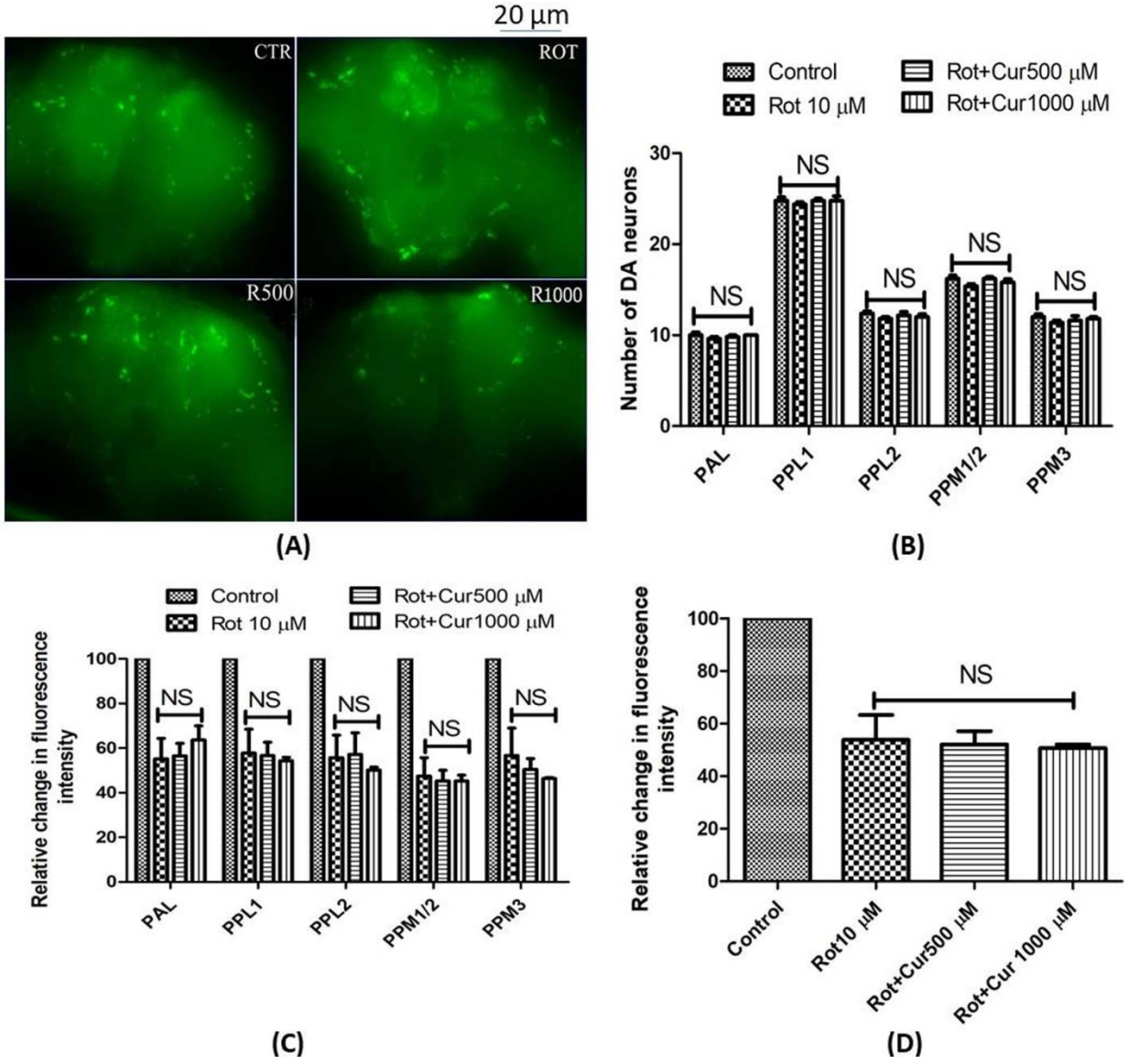

Figure 4.9: Characterization and quantification of DA-ergic neurodegeneration in the whole fly brain of the transition phase through anti-TH antibody immunostaining: Characterization of dopaminergic neurodegeneration in the fly brain of the transition phase **(A).** The scale bar of all the images in the panel is 20 µm. (CTR- Control; ROT- Treated with ROT only; R500- ROT along with CUR 500 µM concentration; R1000- ROT along with CUR 1000 µM concentration; Represented images are "merged" Z-stacking images; however, the quantification of DA-ergic neuronal number and fluorescence intensity is performed in 3D Z-stack images). Quantification of DNs reveals that there is no loss in the number of DNs

upon treatment with ROT alone or ROT along with multiple concentrations of CUR **(B)**. However, ROT leads to "neuronal dysfunction" as characterized by quantification of DA-ergic neuronal fluorescence intensity that is proportional to the amount of TH protein which could not be rescued upon therapeutic intervention of CUR **(C)**. Further, a similar trend is observed upon pooling the fluorescence intensity sum of all the clusters in the fly brain **(D)** suggesting that CUR intervention cannot rescue the depleted levels of TH during the transition phase of fly suggesting its limitation as a therapeutic agent in late-onset NDDs such as PD. (One way ANOVA followed by Newman-Keuls Multiple Comparison Test. NS-Not significant).

The cluster-wise analysis of DA-ergic neuronal fluorescence intensity showed significant rescue in neuronal dysfunction in all the clusters during the early health phase but not during the transition phase of life stages of *Drosophila*. The total intensity sum of all the DNs in the fly brain was clubbed together for further analysis. Results reveal that ROT significantly downregulates the fluorescence intensity (~50%) (Suggesting diminished levels of TH protein synthesis) which could be significantly altered upon co-feeding with CUR during early health phase of the fly (**Figure 4.8 D**). But the significantly reduced fluorescence intensity (~50%) of the DNs during the transition phase of the fly could not be improved upon co-feeding with CUR (**Figure 4.9 D**). These results indicate that CUR can rescue the neurodegeneration induced by ROT only during the early health phase but not during the transition phase of the fly.

The results from the present study support the findings of the negative geotaxis assay which indicated that CUR rescues mobility defects only during the early health phase but not during the transition phase. These results reveal that the synthesis of the rate-limiting

enzyme TH for DA synthesis is downregulated as the fluorescence intensity of the neuron is directly proportional to the level of TH. Hence, the level of dopamine synthesis may be reduced in the brain. This is ascertained by quantifying the level of DA and its metabolites using HPLC-ECD.

4.3.5. Life phase-specific dopaminergic neuroprotective efficacy of curcumin in rotenone mediated fly PD model is mediated through differential modulation of perturbations in dopamine metabolism

Reduced DA-ergic neuronal fluorescence intensity is directly proportional to the diminished TH synthesis. Quantification of fluorescence intensity revealed that the intensity was significantly reduced under ROT-mediated conditions revealing the neurodegeneration which could be improved upon co-feeding with CUR during the health phase but not during the transition phase of the fly. Also, CUR failed to improve the mobility defects induced by ROT in the transition phase fly (**Figure 4.6)**. Hence, I asked whether the failure in improving the climbing ability during this phase is due to CUR's failure in replenishing brain dopamine levels. To confirm this correlation, I estimated the levels of DA and its metabolites (DOPAC and HVA) in fly brain tissue extracts of different treatment groups under study using HPLC-ECD.

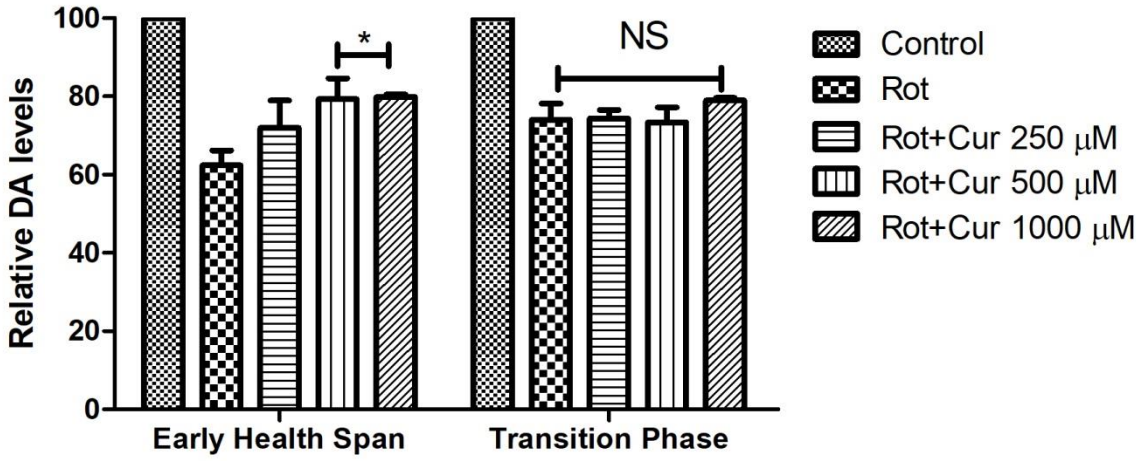

Figure 4.10: Curcumin replenishes diminished levels of brain DA only during the adult early health phase but not during the transition phase in the ROT-mediated *Drosophila* model of PD. Quantification of DA levels in the fly brain using HPLC: Feeding the fly with ROT alone led to a significant reduction in brain DA levels during the early health phase and transition phase but co-feeding with CUR could significantly alter the diminished DA levels only during the early health phase of the fly suggesting that CUR ameliorates DA neuronal degeneration only during the adult health phase; but fails during the transition phase of adult life (Two-way ANOVA followed by Bonferroni post-tests; *$p<0.05$; NS- Not significant; compared with ROT treated group).

Feeding the fly with ROT alone led to a significant decrease in DA levels by 38% and 26% during the early health phase and transition phase of the fly respectively. Co-feeding with 500 μM CUR and 1000 μM CUR could significantly increase the DA level by 17% as compared to ROT-mediated group whereas lowest concentration of 250 μM CUR showed no significant difference during the early health phase of the fly. Co-feeding the transition phase fly with CUR showed no improvement in the brain DA levels (**Figure 4.10**) as compared to ROT-induced group suggesting that efficacy of CUR is life stage-specific in fly

PD model. This observation highlights the limitation of CUR as a therapeutic agent in *Drosophila* PD model.

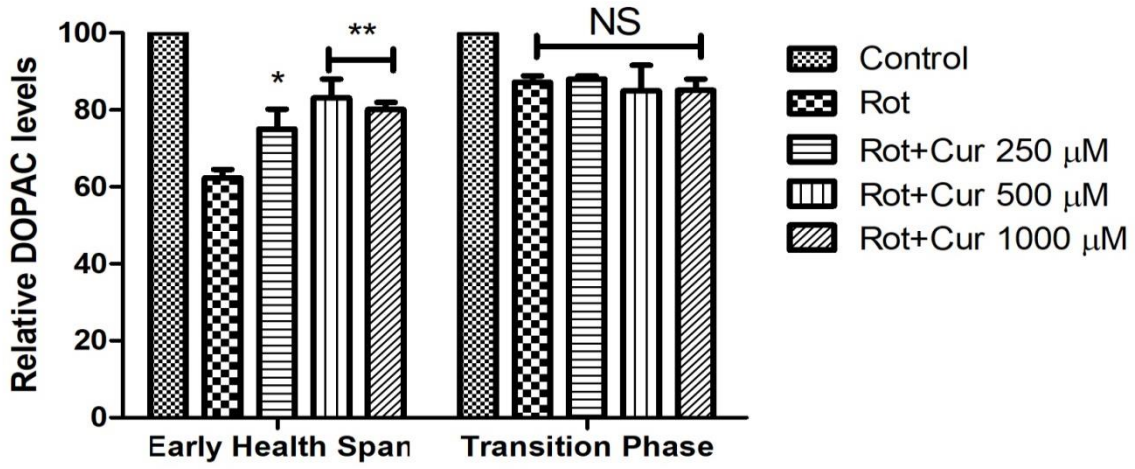

Figure 4.11: Curcumin corrects the reduced levels of brain DOPAC only during the adult early health phase but not during the transition phase in the ROT-mediated *Drosophila* model of PD. Quantification of DOPAC levels in the fly brain using HPLC: Feeding the fly with ROT alone led to a significant reduction in brain DOPAC levels during the early health and transition phases but co-feeding with CUR could significantly alter the diminished DOPAC levels only during the early health phase (Two-way ANOVA followed by Bonferroni post-tests; *$p<0.05$; **$p<0.01$; NS- Not significant; compared with ROT treated group).

Feeding the fly with ROT alone led to a significant decrease in DOPAC levels by 38% and 13% during the early health phase and transition phase of the fly respectively. Co-feeding with 250 μM CUR, 500 μM CUR and 1000 μM CUR could significantly increase the DOPAC levels by 13%, 21% and 18% respectively as compared to ROT-mediated group during the early health phase of the fly. Co-feeding the transition phase fly with similar concentrations of CUR as used in the early health phase fly showed no significant difference in the levels of DOPAC (**Figure 4.11**) as compared to ROT-mediated group. This result

indicates that CUR can rescue the DOPAC levels during the early health phase but fails during the transition phase of the fly.

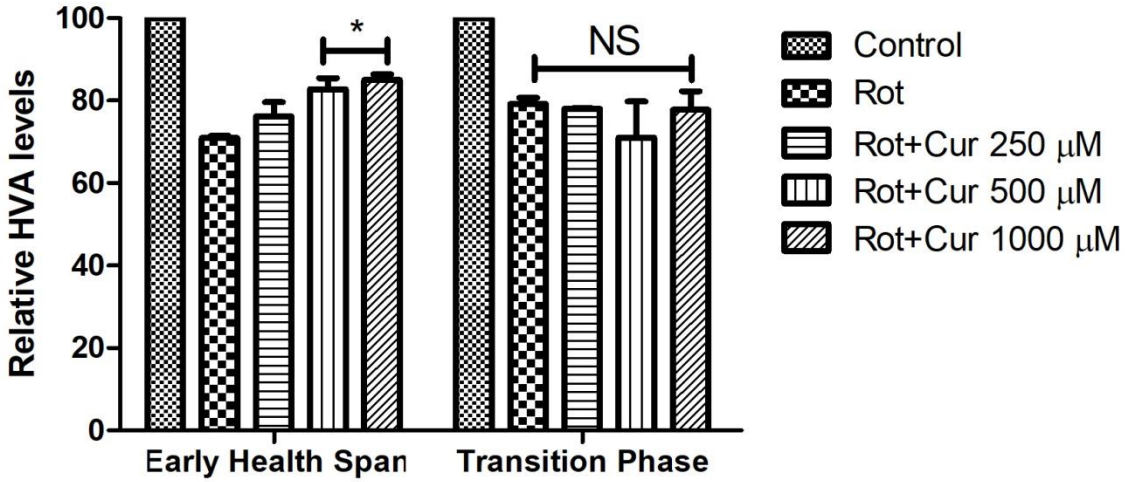

Figure 4.12: Curcumin corrects the reduced levels of brain HVA only during the adult early health phase but not during the transition phase in the ROT-mediated *Drosophila* model of PD. Quantification of HVA levels in the fly brain using HPLC: Feeding the fly with ROT alone led to a significant reduction in brain HVA levels during the early health phase and transition phase but co-feeding with CUR could significantly improve the diminished HVA levels only during the early health phase of the fly (Two-way ANOVA followed by Bonferroni post-tests; *$p<0.05$; compared with ROT treated group).

Feeding the fly with ROT alone led to a significant decrease in HVA levels by 29% and 21% during the early health phase and transition phase of the fly respectively. Co-feeding with 500 μM CUR and 1000 μM CUR could significantly increase the HVA levels by 12% and 14% respectively as compared to ROT-mediated group whereas the lowest concentration of 250 μM CUR showed no significant difference during the early health phase of the fly. Co-feeding the transition phase fly with similar concentrations of CUR as used in the early health phase fly showed no significant difference in the levels of HVA (**Figure 4.12**) as

compared to ROT-mediated group. This result indicates that CUR can rescue HVA level thereby rescuing the neurodegeneration during the early health phase but fails during transition phase of the fly. The present study suggests that CUR-mediated modulation of perturbations in DA metabolism is restricted to the adult health phase and not to the transition phase. This illustration suggests that the genetic targets and molecular networks of genotropic drug CUR-mediated correction process may not be active/expressive at optimum levels during later phases of the adult life. This critical observation underlines the limitations of CUR as a therapeutic agent in the late-onset NDDs such as PD.

To summarize the quantification of DA and its metabolites during the early health phase of the fly, treatment with 500 µM ROT leads to a significant decrease in brain-specific DA, DOPAC and HVA by 38%, 38% and 29% respectively when compared with control. Since mitochondria are involved in several metabolic pathways, it is possible that the inhibition of mitochondria by ROT also affects the metabolism of DA and downstream catecholamines. Upon co-feeding with CUR, the level of DA, DOPAC and HVA could be significantly rescued by 17%, 21% and 12% respectively during the early health phase of the fly (**Figure 4.13)**. In the case of the transition phase fly, the level of DA, DOPAC and HVA is significantly lowered by 26%, 13% and 21% under ROT-mediated conditions. Co-feeding the fly with multiple concentrations of CUR along with ROT could not rescue the depletion of DA and its metabolites. This could be due to the lack of targets of CUR during the transition phase of the fly. From this result, it can be hypothesized that CUR rescues the perturbations in brain DA metabolism in adult life stage specific fashion. However, trend shows a marginal slow-down in the catabolism of DOPAC to HVA during the transition phase of the fly (**Figure 4.13**).

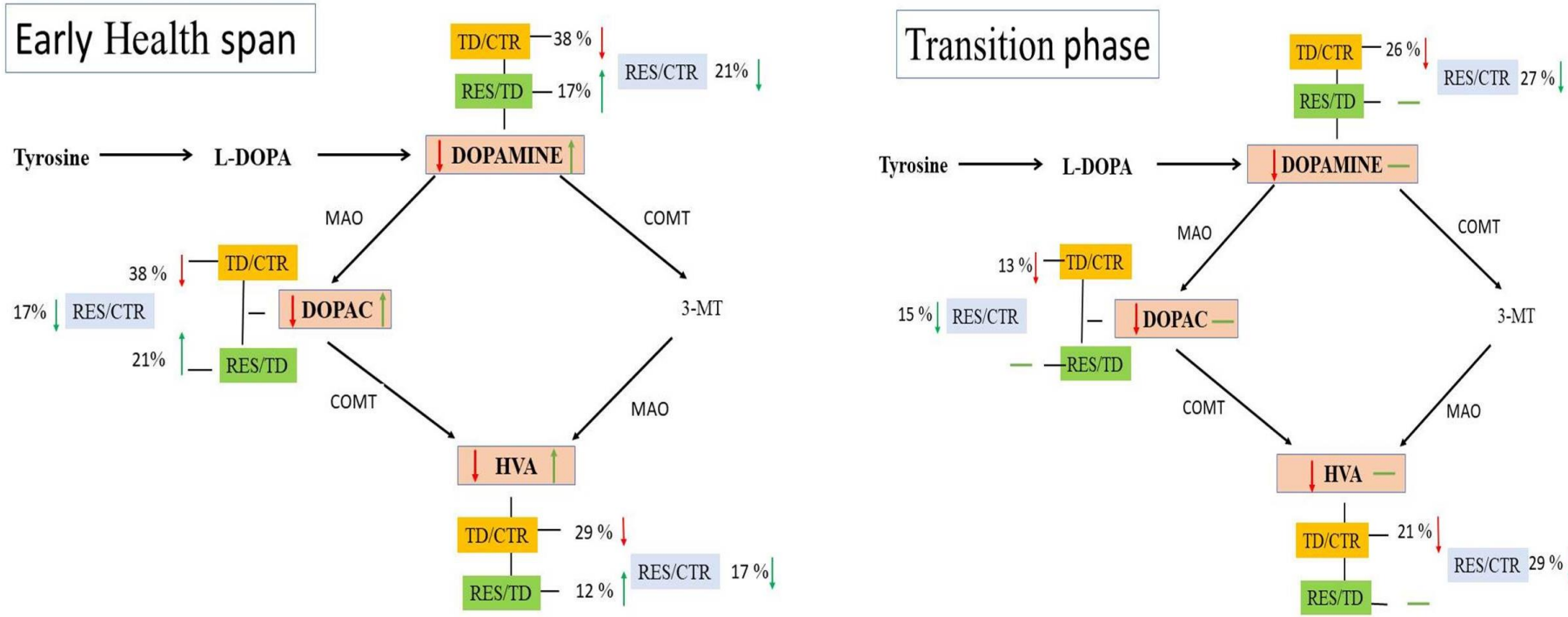

Figure 4.13. Schematic representation of alterations in levels of players involved in brain DA metabolism during the adult early health phase and transition phase in ROT-induced *Drosophila* model of PD and under nutraceutical curcumin mediated intervention strategy: DA and its metabolites- DOPAC and HVA are significantly reduced upon ROT-induced PD condition which could be altered upon co-feeding with CUR during the early health phase but not during the transition phase (CTR: Control; TD: Treated with ROT alone; RES: CUR mediated rescue, if any).

4.4. Discussion:

Epidemiological studies have shown a correlation between exposure to environmental toxins and the pathogenesis of PD. In most populations, 3–5% of PD is explained by genetic causes linked to known PD genes. However, the majority of patients (90-95%) have idiopathic or sporadic PD (Bloem *et al.*, 2021). Further, epidemiological studies indicate a relationship between various environmental factors such as pesticide exposure and the development of sporadic PD in later stages of life (Ascherio and Schwarzschild, 2016). **Chapter 3** illustrates that the mortality pattern and mobility defects of adult life phase-specific *Drosophila* male fly exposed to ROT were time- and concentration-dependent. These results suggest the relevance and importance of life phase-specific animal models for understanding the pathophysiology of PD and screening the small molecules/nutraceuticals with potential neuroprotective efficacy

Studies on animal models have shown the neuroprotective efficacy of CUR (Ramires Júnior *et al.,* 2021; El Nebrisi *et al.,* 2020). Contradictory reports of concentration-dependent CUR toxicity have been reported in animal models (Zhao *et al.,* 2012) and *Drosophila* model (Phom *et al.,* 2014). However, the toxicity of CUR in animal models is under-reported. Hence, I performed a comprehensive experiment with an array of CUR concentrations to identify the non-toxic concentrations of CUR in both the adult early health phase and transition phase of the *Drosophila*.

My experimental approach employing CUR was to expose the model animal to a range of concentrations to determine its detrimental effects and select a suitable range of non-toxic concentrations for further studies. I employed 8 concentrations ranging from 25 μM to 2.5 mM of CUR in both the adult health phase and transition phase male *Drosophila*. It was found that CUR concentrations of 2.5 mM had a deleterious effect on the viability

of the fly, whereas concentrations lower than 2.5 mM showed no observable toxicity in the adult health phase fly up to 10 days (**Figure 4.2 & 4.3**). In the highest concentration of 2.5 mM, all the flies employed in the experiment were dead by the 30^{th} day and 11^{th} day of CUR treatment in the case of the early health and transition phase respectively. The concentration below 1 mM did not show any mortality up to 10 days of exposure to CUR, indicating that there was no toxicity in all the lower concentrations. Concentration-dependent toxicity of CUR has been reported in pre-clinical models (Zhao *et al.,* 2012). In a study to assess the neuroprotective efficacy of CUR in the *Drosophila* model of PD, concentration-dependent lethality of CUR was demonstrated (Phom *et al.,* 2014). In humans, CUR toxicity has also been studied suggesting that it primarily causes gastrointestinal disturbances, diarrhoea, as well as distension and gastroesophageal reflux disease (Carroll *et al.*, 2011).

Therefore, it is essential to figure out the toxic concentrations of CUR before employing it as a neuroprotective agent in the fly model of PD. Hence, in order to decipher DA-ergic neuroprotective efficacy of CUR, after careful understanding and consideration, I have picked up sub-lethal concentrations of CUR (100 µM, 250 µM, 500 µM and 1 mM) and the same concentrations were employed in life phase-specific ROT-mediated *Drosophila* model of PD under pre- and co-feeding regimen.

To understand DA-ergic neurodegeneration and to decipher the effectiveness of therapeutic molecules, many laboratories either co-treat or pre-treat young PD fly models belonging to the health phase to screen small molecules/drugs/nutraceuticals and concluded about their DA-ergic neuroprotective efficiency (Maitra *et al*., 2021; Nguyen *et al*., 2018; Sur *et al*., 2018; Pandareesh *et al*., 2016; Cassar *et al*., 2015; Coulom and Birman, 2004). They determined the neuroprotective efficacy of the molecules by assessing behavioral markers such as mobility defects, biochemical markers such as anti-

oxidant enzyme levels and levels of brain DA and its metabolite levels, or cytological markers such as degeneration of DNs in the whole brain of young animals whereas late-onset NDDs such as PD onsets during the transition phase of adult life!!

The present study indicates that feeding the fly of the adult early health phase with ROT alone adversely decreases mobility (~30%) which could be improved upon co-feeding with CUR. Feeding the fly with CUR (500 µM) *per se* did not show any mobility defects (**Figures 4.4 A & B**). Results indicate that in both the co-feeding (**Figures 4.4 A & B**) and 2, 3, and 5 days pre-feeding regimens (**Figures 4.4 C-H**), CUR could confer neuroprotection during the early health phase. It has been reported that exposure to ROT induces severe mobility defects in *Drosophila* (Coulom and Birman, 2004) and the same can be rescued upon co-feeding with CUR (Nguyen *et al.,* 2018). In the case of the late health phase fly, CUR fails to rescue the mobility defects in both the co- and pre-feeding regimen (**Figure 4.5**). In the case of the transition phase fly also, CUR fails to rescue ROT-mediated mobility defects in both the co- and pre-feeding regimen as determined through the negative geotaxis assay (**Figure 4.6**). These results are in agreement with previous work from our lab, where CUR confers DA-ergic neuroprotection only during the health phase but not during the transition stage (Phom *et al.,* 2014). However in the present study, CUR fails even during the late health phase. This contradiction could be because of the ROT-specific toxicity, which specifically inhibits mitochondrial complex I. Previous studies demonstrated the neuroprotective efficacy of CUR in ROT-mediated neurotoxicity in cell culture, young adult *Drosophila* and rat models (Naser *et al*., 2022; Buratta *et al*., 2020; Pandareesh *et al*., 2016) and substantiated that CUR sequesters the intracellular and mitochondrial ROS levels and inhibits the caspase-3/caspase-9 activity (Liu *et al*., 2013). These results suggest that CUR may be a potential therapeutic compound for PD intervention. However, all these studies used young animals

belonging to the adult health stage. The results from the present study suggest that CUR can rescue ROT-mediated mobility defects in adult life phase-specific fashion; meaning CUR confers neuroprotection only during the early health phase and not in the late health phase and transition phase of the adult life.

The death of DNs is the characteristic pathological marker of PD. Hence in order to decipher the extent of DA-ergic neurodegeneration under induced PD conditions and possible rescue by CUR, I quantified the DNs in the whole fly brain followed by characterization of DA "neuronal dysfunction" by quantifying the fluorescence intensity emanated from the fluorescently labelled secondary antibody targeted against the primary anti-TH antibody using fluorescence microscopy. The results illustrate that there is no variation in the number of DNs between the control and PD brains of *Drosophila* in both the health and the transition phases of adult life (**Figures 4.8 B & 4.9 B**). This observation is consistent with the previous works from other laboratories (Navarro *et al.*, 2014; Pesah *et al.*, 2005; Meulener *et al.*, 2005). Here, I would like to mention that loss of DNs *per se* in fly PD models has been an issue of controversy in the field of *Drosophila* neurobiology

This issue has been thoroughly evaluated in multiple fly models of PD (both genetic and sporadic) and concluded that there is no structural loss of DA neurons, but only the synthesis of TH is diminished (Navarro *et al*., 2014). Hence, I went ahead with the quantification of the fluorescence intensity of TH-positive neurons. Results illustrate that the fly treated with ROT alone led to a significant decrease in fluorescence intensity to ~50% which could be significantly rescued by 25-30% upon co-feeding with CUR during the early health phase (**Figure 4.8 C**) while the diminished fluorescence intensity could not be rescued by CUR during the transition phase (**Figure 4.9 C**). I also tried to analyze the result by quantifying the fluorescence intensity of all the DNs present in the

fly brain of different treatment groups (**Figures 4.8 D & 4.9 D**). Similar result is obtained when analyzed in treatment group-wise also. As the fluorescence intensity of the neuronal cell body is directly proportional to the level of synthesis of the rate-limiting enzyme TH, diminished levels of fluorescence intensity suggest the decreased levels of TH. Hence, it is possible that the level of DA synthesis might be reduced in the fly brain. This approach allowed us to accurately assess the extent of neurodegeneration of DNs in the fly PD models. This result is further substantiated by quantifying the levels of the brain-specific DA and its metabolites (DOPAC and HVA) through HPLC-ECD.

The present study shows that feeding the fly with ROT alone led to a significant reduction in the levels of DA, DOPAC and HVA during the early health and the transition phases of *Drosophila* (**Figures 4.10, 4.11 & 4.12**). Similar results showing significant reduction in DA, DOPAC and HVA levels are indicated in 10 days old young fly (Pandareesh *et al.,* 2016), young mice (wang *et al.,* 2020), young wistar rat (Madiha and Haider, 2019; Moreira *et al.,* 2012). All these results indicate that ROT significantly downregulates the DA level under induced PD conditions.

The present study demonstrates that diminished levels of DA, DOPAC and HVA upon ROT treatment could be significantly rescued through co-feeding with CUR during the early health phase but not during the transition phase (**Figures 4.10, 4.11 & 4.12**) of the adult fly. Study on young 12 weeks old albino wistar rat showed a significant reduction in DA and DOPAC levels upon ROT-mediated conditions which could be significantly improved upon co-feeding with CUR (Madiha and Haider, 2019). Another study indicated that feeding the extract of the plant *Danshensu* (60 mg/kg for 28 days) could significantly improve the levels of DA, DOPAC and HVA in ROT-induced young 12 weeks old C57BL/6 mice indicating that the levels of DOPAC and HVA are proportional to DA content (Wang *et al.,* 2020). CUR is shown to restore the levels of DA, DOPAC

and HVA in neurodegeneration mediated by lipopolysaccharide in young Sprague-Dawley rats (Sharma *et al.,* 2017). All these results support the present study and indicate that CUR restores the levels of DA, DOPAC and HVA in ROT-mediated PD models. However, these studies are restricted to 5-20 days young fly (Pandareesh *et al.,* 2016; Coulom and Birman, 2004) and 10-12 weeks young mice and rat models (Wang *et al.,* 2020; Madiha and Haider, 2019) whose age is comparable with the health phase of adult life. There is no data available relating to the levels of DA and metabolites in PD models of the transition phase of adult life, during which PD sets in. This is the first of its kind to have shown the levels of DA and its metabolites in the transition phase of *Drosophila* model of ROT-mediated PD.

In humans, the levels of DA, DOPAC and HVA are significantly altered in the putamen, nucleus accumbens and caudate nucleus of the PD post-mortem brain (Gerlach *et al.,* 1996). Levels of DA, DOPAC and HVA are significantly reduced ($p<0.05$) in cerebrospinal fluid of human PD patients (Andersen *et al.,* 2017). A decrease in DOPAC and HVA in PD patients reflects the loss of DNs in the striatum and inhibition of MAO-B pathways (Parkinson Study Group, 1995). DOPAC is the principal metabolite of DA (Andersen *et al.,* 2017; Kopin, 1985). Hence, DOPAC is considered a more reliable marker than HVA for central DA deficiency (Andersen *et al.,* 2017). This is attributed because (a) HVA is a secondary metabolite mainly formed by actions of MAO and (b) DOPAC is produced in DNs after leakage of DA from synaptic neurons or following reuptake of extracellular DA *via* DAT in the presynaptic membrane (Goldstein *et al.,* 2012).

Research on DA metabolism gives an insight into the biochemical changes in DA-ergic system associated with PD. However, the biological significance of “turnover ratio” which denotes the level of metabolites (DOPAC and HVA) with respect to DA is not

discussed in many studies quantifying DA and metabolites. Pagan *et al.,* (2020) reported DA metabolites as "exploratory biomarkers" with reference to CSF levels of DOPAC and HVA. Though the compiled effect of the HVA in CSF along with xanthine improves its use as a biomarker (LeWitt *et al.,* 2011), the levels of HVA in CSF *per se* poorly correlate with PD severity or progression (Parkinson Study Group, 1995). Though DOPAC is the primary metabolite of DA (Andersen *et al*., 2017), LeWitt (2020) commented that representing the CSF level of DOPAC as a marker for the progression of PD is not valid though it shows severity. A significant amount of DOPAC and HVA, albeit lower DA levels, is seen in the human brain wherein DA-ergic innervation has not been implicated (Ebinger *et al.,* 1987). Furthermore, the levels of neurotransmitters in CSF partially implicate the metabolism indicating limited relevance to neurotransmission in the brain. Hence, quantitative analysis of brain-specific DA and its metabolites concentrations are unrelated to DA-ergic neurotransmission which could be due to the possible role of capillary walls and glial cells in the catabolism of DA that needs to be further investigated (Ebinger *et al.,* 1987). Hence, the notion "turnover" is not applicable with respect to the activity of DA-ergic system (Ebinger *et al.,* 1987).

These findings suggest that CUR-mediated sustenance of DA metabolism is restricted to the adult health phase and not to the transition phase. This illustration indicates that genetic targets and molecular networks of genotropic drug CUR-mediated correction process may not be active/expressive at optimum levels during later phases of the adult life. This critical observation underlines the limitation of CUR as a therapeutic agent in late-onset NDDs such as PD.

The present study provides insights into the underlying reasons for neuroprotective efficacy of CUR during the adult health phase of *Drosophila*. Further, it also provides insights into the probable cause for the inefficacy of CUR during the adult transition

phase of *Drosophila*. It is important to figure out why CUR is failing to sustain the activity of the TH during the transition phase, understanding of which will have critical implications in developing therapeutic strategies for late-onset neurodegenerative diseases such as PD. Figuring out the underlying molecular networks in an adult life stage-specific fashion will be a path-breaking contribution in addressing the pathophysiology of PD.

This is the first report to decipher the fact that CUR has limitations as a therapeutic molecule in the ROT-mediated idiopathic *Drosophila* model of PD, and its efficacy is restricted only to the early health phase of adult life. A schematic representation of the proposed model of study is depicted in **Figure 4.14**.

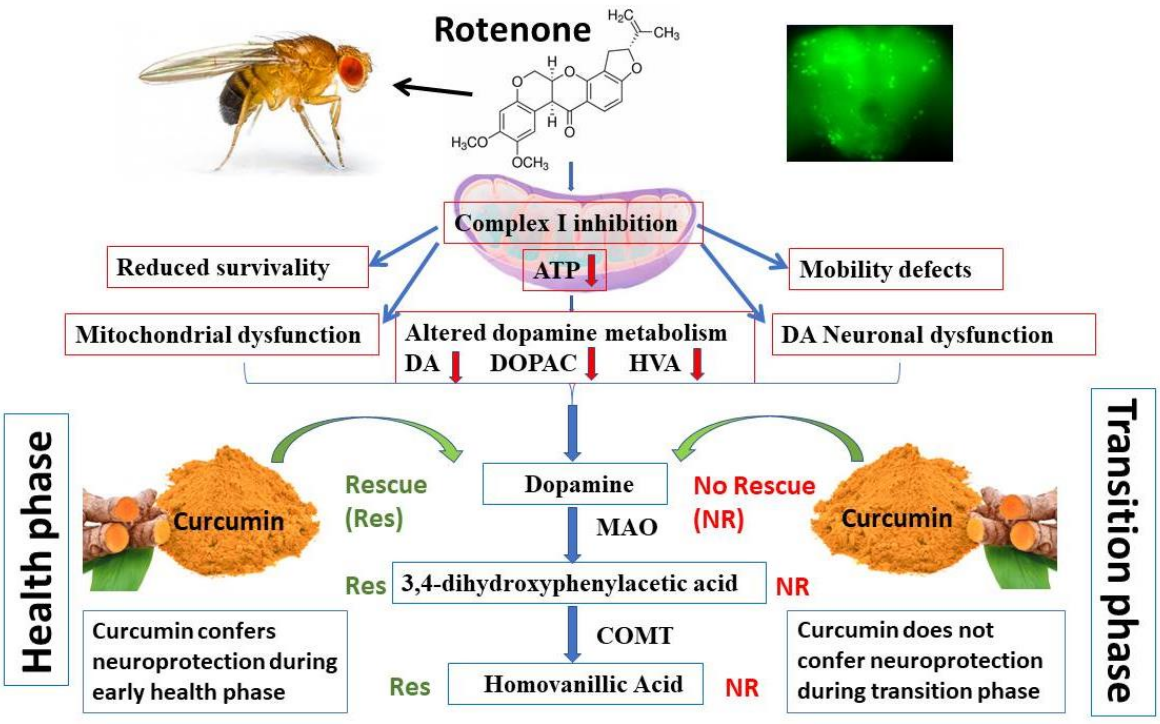

Figure 4.14: Proposed model of the study: Cartoon explains the adult life phase-specific DA-ergic neuroprotective efficacy of curcumin in rotenone-induced *Drosophila* model of PD. Rotenone inhibits mitochondrial complex I of the electron transport system leading to a reduced survivability, mobility defects, MD, neuronal dysfunction and reduced DA

and its metabolites. Therapeutic intervention with curcumin partially rescues the mobility defects, neuronal dysfunction and restores diminished brain DA, DOPAC and HVA levels during the health phase but not in the transition phase of adult *Drosophila*, suggesting curcumin's ability to modulate perturbed DA metabolism is constrained to the adult health phase only.

4.5. Conclusion:

The present study reveals that CUR mitigates the mobility defects induced by ROT during the early health phase but fails during the late health and transition phase in both the co- and pre-feeding regimens in the adult *Drosophila* model of sporadic PD. Analysis of DNs reveals that their number remains unchanged under ROT-induced PD conditions but the fluorescence intensity of the secondary antibody targeted against the primary anti-TH antibody is significantly reduced suggesting the diminished levels of TH synthesis, which could be improved upon co-feeding with CUR. Further analysis of the brain-specific DA and its metabolites reveals that CUR rescues DA and its metabolites during the health phase only. Observed contradictions can be attributed to the availability of genetic targets of genotropic nutraceutical curcumin in an adult life phase-specific fashion. The present study explains that curcumin's ability to modulate perturbed DA metabolism is constrained to the adult health phase. Hence, it confers DA-ergic neuroprotection in adult health phase but not in transition phase.

SUMMARY

Parkinson's disease (PD) is the most common neurodegenerative movement disorder prevalent in 1% of the worldwide population. The characteristic pathological feature of PD is the selective degeneration of DNs in the SNpc leading to motor dysfunction, bradykinesia, tremors and rigidity. Other non-motor symptoms of PD include depression, cognitive decline, sleep disturbances, constipation, fear, anxiety, fatigue, weight changes, hypotension, energy loss and sexual problems affecting the quality of their life.

Though the decisive cause of PD is yet to understand, the epidemiological studies indicate two major types of PD. In most populations, 3–5% of PD cases are known to be caused by genetic factors linked to known PD genes that signify monogenic PD whereas the remaining 90-95% cases are believed to be sporadic implicating the role of environment factors. Till date, treatment with Levodopa remains a main therapy of PD. Levodopa, the precursor of DA and currently in use as drug to treat PD, significantly lessens parkinsonian symptoms, improves quality of life and extends life expectancy. Despite all the beneficial role of the available therapeutic strategies of PD, there are limitations such as wearing out effect of oral drugs and narrow therapeutic strategies for advanced patients which led to instigate the researchers to review currently available methods.

PD is a late-onset NDD. However, several researchers developed PD models using young animals and studied the susceptibility genes and pathways.Most of the previous studies on the neuroprotective efficacy of phytochemicals/compounds were mainly based on young animals. No data are available on the later phases of life which is an important missing paradigm in finding the therapeutic strategies for PD.

Pre-clinical studies on NDDs should mimic the characteristic features of the disease, such as late-onset nature for developing therapeutic strategies. The adult life of *Drosophila* is categorized into health phase, transition phase and senescence phase (Arking *et al*., 2002). Analysis of these adult life stages has revealed that they are characterized by different gene expression profiles (Arking, 2015, 2009; Pletcher *et al*., 2002), which is similar to that of the corresponding life stages of humans. A transcriptomic analysis using microarrays to compare the gene expression profiles of different life stages of *Drosophila* has identified 1184 genes with marked differences in the expression levels between the young and old age groups (Bordet *et al*., 2021). The life stages of *Drosophila* are believed to have both common and unique complex processes and can be influenced independently by a relatively large number of stage associated pathways (Soh *et al*., 2013).

Hence, it is important to study the neuroprotective efficacy of phytochemicals in the later stages of life span of model organisms. Taking advantage of fly model system, I developed an adult life phase-specific rotenone (ROT)-mediated sporadic PD model at three different life stages of life span. Results reveal that ROT induces time- and dose-dependent effect on the survival and mobility. From this study, I selected different concentrations of ROT for the different life stages (5 days: early health phase; 30 days: late health phase and 50 days: transition phase) and different window of exposure wherein the fly started showing Parkinsonian symptoms like motor defects but did not affect the survival. This is very crucial in developing a model because the model organism may die out of systemic failure due to higher toxicity before the DNs degenerate. Hence, I selected sub-lethal concentrations of 500 µM concentration of ROT with an exposure window of 5 days for the early health phase fly; 25 µM concentration of ROT with an exposure window of 2 days for the late health phase fly and a

concentration of 10 µM ROT for a window of 2 days for the transition phase fly. These concentrations at the selected window of exposure showed reduced complex I-III activity indicating the inhibition of mitochondrial complex I of the electron transport chain (ETC). The DA-ergic neuronal fluorescence intensity was also significantly reduced indicating the reduced syntheis of tyrosine hydroxylase (TH) (primary antibody was targeted against the rate limiting enzyme of dopamine synthesis i.e. TH). Further, results showed reduced levels of DA, DOPAC and HVA under ROT-mediated conditions. These results denote the validity of the present PD model. This is the first study to develop an adult life phase-specific ROT-mediated *Drosophila* model of PD. Further, by utilizing this PD model system, I looked into the therapeutic propensity of DA-ergic neuroprotective efficacy of curcumin (CUR).

Using this life stage-specific *Drosophila* PD model, I made comprehensive effort to assess a wide range of CUR concentrations for its toxicity. Form this study, I selected certain sub-lethal concentrations (100 µM, 250 µM, 500 µM and 1000 µM) of CUR to deciper its DAergic neuroprotective efficacy in adult life stage specific fly PD model.

Results reveal that CUR can mitigate the mobility defects mediated by ROT only during the early health phase while it fails to alter the mobility defects during the late health phase and transition phase in both the co- and pre-feeding regimens. Further, I tried to analyze the DA-ergic neuronal dysfunction in fly PD model by looking into the number of neurons and fluorescence intensity of the neurons immunostained by using fluorescent dye against primary antibody anti-Tyrosine hydroxylase. Results revealed that there is no significant change in the DNs in all the treatment groups under study whereas fluorescence intensity varies. Feeding the fly with ROT alone led to a significant reduction in fluorescence intensity which could be rescued upon co-feeding with CUR during the early health phase but failed during transition phase of the fly. This result is

further substantiated by the reduced level of DA in ROT mediated fly which could be improved upon co-feeding with CUR during early health span stage but not during transition phase of the fly. These results illustrate that one of the possible mechanisms of DA replenishment is through upregulation of Tyrosine hydroxylase (as evident from fluorescence microscopy). Present study provides insights into the underlying mechanism of neuroprotective efficacy of CUR during the adult early health span of *Drosophila*. This study will provide an opportunity to understand the progression of neurodegeneration in the *Drosophila* model of Parkinson's disease.

Present study highlights the limitations of using young animal models (5-10 days old fly) to study late onset NDD such as PD. Further, the life stage-specific gene expression profiles can be one of the reasons for the efficacy/inefficacy of genotropic compounds such as CUR. Therefore, it is necessary to employ age-matched animal models (hence the importance of the transition phase animal models of PD) to screen the efficacy of nutraceuticals. This critical aspect has been overlooked by many research groups. Here, I demonstrate the efficacy/inefficacy of CUR during different life stages and provide insights into CUR-mediated modulation of TH synthesis and DA metabolism as possible targets of CUR efficacy during adult health phase.

Observed contradictions can be attributed to the availability of genetic targets of genotropic nutraceutical curcumin in an adult life phase-specific fashion. The present study explains that curcumin's ability to modulate perturbed DA metabolism is constrained to the adult health phase. Hence, it confers DA-ergic neuroprotection in adult health phase but not in transition phase.

REFERENCES

Aarsland D, Batzu L, Halliday GM, Geurtsen GJ, Ballard C, Ray Chaudhuri K, Weintraub D. Parkinson disease-associated cognitive impairment. *Nat Rev Dis Primers*. 2021;7(1):47. doi: 10.1038/s41572-021-00280-3.

Abdel-Sattar E, Mahrous EA, Thabet MM, Elnaggar DMY, Youssef AM, Elhawary R, Zaitone SA, Celia Rodríguez-Pérez, Segura-Carretero A, Mekky RH. Methanolic extracts of a selected Egyptian Vicia faba cultivar mitigate the oxidative/inflammatory burden and afford neuroprotection in a mouse model of Parkinson's disease. *Inflammopharmacol*. 2021;29(1):221-235.

Abdin AA, Hamouda HE. Mechanism of the neuroprotective role of coenzyme Q10 with or without l-dopa in rotenone-induced parkinsonism. *Neuropharmacol*. 2008;55(8):1340–1346.

Ablat N, Lv D, Ren R, Xiaokaiti Y, Ma X, Zhao X, Sun Y, Lei H, Xu J, Ma Y, Qi X, Ye M, Xu F, Han H, Pu X. Neuroprotective Effects of a Standardized Flavonoid Extract from Safflower against a Rotenone-Induced Rat Model of Parkinson's Disease. *Molecules*. 2016;21(9):1107. doi: 10.3390/molecules21091107.

Abolaji AO, Fasae KD, Iwezor CE, Aschner M, Farombi EO. Curcumin attenuates copper-induced oxidative stress and neurotoxicity in *Drosophila melanogaster*. *Toxicol Rep*. 2020;7:261-268.

Abrahams S, Miller HC, Lombard C, van der Westhuizen FH, Bardien S. Curcumin pre-treatment may protect against mitochondrial damage in LRRK2-mutant Parkinson's disease and healthy control fibroblasts. *Biochem Biophys Rep*. 2021;27:101035. doi: 10.1016/j.bbrep.2021.101035.

Aimaiti M, Wumaier A, Aisa Y, Zhang Y, Xirepu X, Aibaidula Y, Lei X, Chen Q, Feng X, Mi N. Acteoside exerts neuroprotection effects in the model of Parkinson's disease via inducing autophagy: Network pharmacology and experimental study. *Eur J Pharmacol*. 2021;903:174136. doi: 10.1016/j.ejphar.2021.174136.

Akinade TC, Babatunde OO, Adedara AO, Adeyemi OE, Otenaike TA, Ashaolu OP, Johnson TO, Terriente-Felix A, Whitworth AJ, Abolaji AO. Protective capacity of carotenoid trans-astaxanthin in rotenone-induced toxicity in *Drosophila melanogaster*. *Sci Rep*. 2022;12(1):4594. doi: 10.1038/s41598-022-08409-4.

Alam M, Mayerhofer A, Schmidt WJ. The neurobehavioral changes induced by bilateral rotenone lesion in medial forebrain bundle of rats are reversed by L-DOPA. *Behav Brain Res*. 2004;151(1-2):117-124.

Allen SA, Rednour S, Shepard S, Pond BB. A simple and sensitive high-performance liquid chromatography-electrochemical detection assay for the quantitative determination of monoamines and respective metabolites in six discrete brain regions of mice. *Biomed Chromatogr*. 2017;31(11). doi: 10.1002/bmc.3998.

Andersen AD, Blaabjerg M, Binzer M, Kamal A, Thagesen H, Kjaer TW, Stenager E, Gramsbergen JBP. Cerebrospinal fluid levels of catecholamines and its metabolites in Parkinson's disease: effect of l-DOPA treatment and changes in Levodopa-induced dyskinesia. *J Neurochem*. 2017;141(4):614-625.

Anichtchik OV, Kaslin J, Peitsaro N, Scheinin M, Panula P. Neurochemical and behavioural changes in zebrafish Danio rerio after systemic administration of 6-hydroxydopamine and 1-methyl-4-phenyl-1,2,3,6-tetrahydropyridine. *J Neurochem*. 2004;88(2):443-453.

Anusha C, Sumathi T, Joseph LD. Protective role of apigenin on rotenone induced rat model of Parkinson's disease: suppression of neuroinflammation and oxidative stress mediated apoptosis. *Chem Biol Interact*. 2017;269:67–79.

Appiah-Opong R, Commandeur JN, van Vugt-Lussenburg B, Vermeulen NP. Inhibition of human recombinant cytochrome P450s by curcumin and curcumin decomposition products. *Toxicol*. 2007;235(1-2):83-91.

Araujo SM, de Paula MT, Poetini MR, Meichtry L, Bortolotto VC, Zarzecki MS, Jesse CR, Prigol M. Effectiveness of γ-oryzanol in reducing neuromotor deficits, dopamine depletion and oxidative stress in a *Drosophila melanogaster* model of Parkinson's disease induced by rotenone. *Neurotoxicol*. 2015;51:96-105.

Arking R, Novoseltseva J, Hwangbo DS, Novoseltsev V, Lane M. Different age-specific demographic profiles are generated in the same normal-lived *Drosophila* strain by different longevity stimuli. *J Gerontol A Biol Sci Med Sci*. 2002;57(11):B390-398.

Arking R. Independent chemical regulation of health and senescent spans in *Drosophila* . *Invertebr Reprod Dev.* 2015;59(1):28-32.

Arking R. Multiple longevity phenotypes and the transition from health to senescence. *Ann N Y Acad Sci*. 2005;1057:16-27.

Arking R. Overview of the genomic architecture of longevity. In C. Sell, A. Lorenzini, and H.M. Brown-Borg (Eds.), Life span extension: single cell organisms to man . *Dordrecht: Humana Press.* 2009; pp 59–73.

Armstrong MJ, Okun MS. Diagnosis and Treatment of Parkinson Disease: A Review. *JAMA*. 2020;323(6):548-560.

Arnold B, Cassady SJ, VanLaar VS, Berman SB. Integrating multiple aspects of mitochondrial dynamics in neurons: agerelated differences and dynamic changes in a chronic rotenone model. *Neurobiol Dis.* 2011;41:189–200.

Ascherio A, Schwarzschild MA. The epidemiology of Parkinson's disease: risk factors and prevention. *Lancet Neurol*. 2016;15(12):1257-1272.

Auluck PK, Bonini NM. Pharmacological prevention of Parkinson disease in *Drosophila* . *Nat Med*. 2002;8(11):1185-1186.

Auluck PK, Chan HY, Trojanowski JQ, Lee VM, Bonini NM. Chaperone suppression of alpha-synuclein toxicity in a *Drosophila* model for Parkinson's disease. *Science*. 2002;295(5556):865-868.

Auluck PK, Meulener MC, Bonini NM. Mechanisms of Suppression of {alpha}-Synuclein Neurotoxicity by Geldanamycin in *Drosophila* . *J Biol Chem*. 2005;280(4):2873-2878.

Ayajuddin M, Das A, Phom L, Koza Z, Chaurasia R, Yenisetti SC. Quantification of dopamine and its metabolites in *Drosophila* brain using HPLC. In: Experiments with *Drosophila* for Biology Courses (eds: S.C. Lakhotia and H.A. Ranganath). *Ind Acad of Sci.* 2021;pp 433-440. ISBN: 978-81-950664-2-1

Ayajuddin M, Das A, Phom L, Modi P, Koza Z, Chaurasia R, Thepa A, Jamir N, Singh PR, Sentinungla, Lal P and Yenisetti SC. Parkinson's Disease: Insights from *Drosophila* Model In: *Drosophila melanogaster* - Model for Recent Advances in Genetics and Therapeutics. Farzana Khan Perveen (Ed). *InTechOpen*. 2018;pp 157-192. http://dx.doi.org/10.5772/intechopen.72021.

Bagherniya M, Soleimani D, Rouhani MH, Askari G, Sathyapalan T, Sahebkar A. The Use of Curcumin for the Treatment of Renal Disorders: A Systematic Review of Randomized Controlled Trials. *Adv Exp Med Biol*. 2021;1291:327-343.

Bahrami A, Zarban A, Rezapour H, Agha Amini Fashami A, Ferns GA. Effects of curcumin on menstrual pattern, premenstrual syndrome, and dysmenorrhea: A triple-blind, placebo-controlled clinical trial. *Phytother Res*. 2021. doi: 10.1002/ptr.7314.

Basil AH, Sim JPL, Lim GGY, Lin S, Chan HY, Engelender S, Lim KL. AF-6 Protects Against Dopaminergic Dysfunction and Mitochondrial Abnormalities in *Drosophila* Models of Parkinson's Disease. *Front Cell Neurosci*. 2017;11:241. doi: 10.3389/fncel.2017.00241.

Bayersdorfer F, Voigt A, Schneuwly S, Botella JA. Dopamine-dependent neurodegeneration in *Drosophila* models of familial and sporadic Parkinson's disease. *Neurobiol Dis*. 2010;40(1):113-119.

Bédard PJ, Di Paolo T, Falardeau P, Boucher R. Chronic treatment with L-DOPA, but not bromocriptine induces dyskinesia in MPTP-parkinsonian monkeys. Correlation with [3H]spiperone binding. *Brain Res.* 1986;379(2):294-299.

Begum AN, Jones MR, Lim GP, Morihara T, Kim P, Heath DD, Rock CL, Pruitt MA, Yang F, Hudspeth B, Hu S, Faull KF, Teter B, Cole GM, Frautschy SA. Curcumin structure-function, bioavailability, and efficacy in models of neuroinflammation and Alzheimer's disease. *J Pharmacol Exp Ther*. 2008;326(1):196-208.

Benameur T, Soleti R, Panaro MA, La Torre ME, Monda V, Messina G, Porro C. Curcumin as Prospective Anti-Aging Natural Compound: Focus on Brain. *Molecules.* 2021;26(16):4794. doi: 10.3390/molecules26164794.

Berry C, La Vecchia C, Nicotera P. Paraquat and Parkinson's disease. *Cell Death Differ*. 2010;17(7):1115-1125.

Bisbal M, Sanchez M. Neurotoxicity of the pesticide rotenone on neuronal polarization: a mechanistic approach. *Neural Regen Res*. 2019;14(5):762-766.

Blandini F, Armentero MT. Animal models of Parkinson's disease. *FEBS J*. 2012;279(7):1156-1166.

Blauwendraat C, Nalls MA, Singleton AB. The genetic architecture of Parkinson's disease. *Lancet Neurol*. 2020;19(2):170-178.

Blesa J, Phani S, Jackson-Lewis V, Przedborski S. Classic and new animal models of Parkinson's disease. *J Biomed Biotechnol*. 2012;2012:845618. doi: 10.1155/2012/845618.

Blesa J, Przedborski S. Parkinson's disease: animal models and dopaminergic cell vulnerability. *Front Neuroanat*. 2014;8:155. doi: 10.3389/fnana.2014.00155.

Blesa J, Trigo-Damas I, Quiroga-Varela A, del Rey NL. Animal Models of Parkinson's Disease. In: Jolanta Dorszewska and Wojciech Kozubski (Eds). Challenges in Parkinson's Disease. *InTechOpen*. 2016: https://www.intechopen.com/chapters/51004 doi: 10.5772/63328din

Bloem BR, Okun MS, Klein C. Parkinson's disease. *Lancet*. 2021;397(10291):2284-2303.

Blosser JA, Podolsky E, Lee D. L-DOPA-Induced Dyskinesia in a Genetic *Drosophila* Model of Parkinson's Disease. *Exp Neurobiol*. 2020;29(4):273-284.

Bonifati V, Rizzu P, Squitieri F, Krieger E, Vanacore N, van Swieten JC, Brice A, van Duijn CM, Oostra B, Meco G, Heutink P. DJ-1(PARK7), a novel gene for autosomal recessive, early onset parkinsonism. *Neurol Sci*. 2003;24(3):159-160.

Bordet G, Lodhi N, Kossenkov A, Tulin A. Age-Related Changes of Gene Expression Profiles in *Drosophila* . *Genes (Basel*). 2021;12(12):1982. doi: 10.3390/genes12121982

Bordoloi D, Roy NK, Monisha J, Padmavathi G, Kunnumakkara AB. Multi-Targeted Agents in Cancer Cell Chemosensitization: What We Learnt from Curcumin Thus Far. *Recent Pat Anticancer Drug Discov*. 2016;11(1):67-97.

Bose A, Beal MF. Mitochondrial dysfunction in Parkinson's disease. *J Neurochem*. 2016;139 Suppl 1:216-231. doi: 10.1111/jnc.13731.

Botella JA, Bayersdorfer F, Gmeiner F, Schneuwly S. Modelling Parkinson's disease in *Drosophila* . *Neuromolecular Med*. 2009;11(4):268-280.

Botella JA, Ulschmid JK, Gruenewald C, Moehle C, Kretzschmar D, Becker K, Schneuwly S. The *Drosophila* carbonyl reductase sniffer prevents oxidative stress-induced neurodegeneration. *Curr Biol*. 2004;14:782–786.

Bové J, Prou D, Perier C, Przedborski S. Toxin-induced models of Parkinson's disease. *NeuroRx*. 2005;2(3):484-494.

Braungart E, Gerlach M, Riederer P, Baumeister R, Hoener MC. Caenorhabditis elegans MPP+ model of Parkinson's disease for high-throughput drug screenings. *Neurodegener Dis*. 2004;1(4-5):175-183.

Breckenridge CB, Sturgess NC, Butt M, Wolf JC, Zadory D, Beck M, Mathews JM, Tisdel MO, Minnema D, Travis KZ, Cook AR, Botham PA, Smith LL. Pharmacokinetic, neurochemical, stereological and neuropathological studies on the potential effects of paraquat in the substantia nigra pars compacta and striatum of male C57BL/6J mice. *Neurotoxicol*. 2013;37:1-14.

Bretaud S, Lee S, Guo S. Sensitivity of zebrafish to environmental toxins implicated in Parkinson's disease. *Neurotoxicol Teratol*. 2004;26(6):857-864.

Bretaud S, Allen C, Ingham PW, Bandmann O. p53-dependent neuronal cell death in a DJ-1-deficient zebrafish model of Parkinson's disease. *J Neurochem*. 2007;100(6):1626-1635.

Briffa M, Ghio S, Neuner J, Gauci AJ, Cacciottolo R, Marchal C, Caruana M, Cullin C, Vassallo N, Cauchi RJ. Extracts from two ubiquitous Mediterranean plants ameliorate cellular and animal models of neurodegenerative proteinopathies. *Neurosci Lett*. 2017;638:12-20.

Buratta S, Chiaradia E, Tognoloni A, Gambelunghe A, Meschini C, Palmieri L, Muzi G, Urbanelli L, Emiliani C, Tancini B. Effect of Curcumin on Protein Damage Induced by Rotenone in Dopaminergic PC12 Cells. *Int J Mol Sci*. 2020;21(8):2761. doi: 10.3390/ijms21082761.

Burbulla LF, Song P, Mazzulli JR, Zampese E, Wong YC, Jeon S, Santos DP, Blanz J, Obermaier CD, Strojny C, Savas JN, Kiskinis E, Zhuang X, Krüger R, Surmeier DJ, Krainc D. Dopamine oxidation mediates mitochondrial and lysosomal dysfunction in Parkinson's disease. *Science*. 2017;357(6357):1255-1261.

Burns RS, Chiueh CC, Markey SP, Ebert MH, Jacobowitz DM, Kopin IJ. A primate model of parkinsonism: selective destruction of dopaminergic neurons in the pars compacta of the substantia nigra by N-methyl-4-phenyl-1,2,3,6-tetrahydropyridine. *Proc Natl Acad Sci USA*. 1983;80(14):4546-4550.

Butler EK, Voigt A, Lutz AK, Toegel JP, Gerhardt E, Karsten P, Falkenburger B, Reinartz A, Winklhofer KF, Schulz JB. The mitochondrial chaperone protein TRAP1 mitigates α-Synuclein toxicity. *PLoS Genet*. 2012;8(2):e1002488. doi: 10.1371/journal.pgen.1002488.

Cannon JR, Greenamyre JT. Neurotoxic in vivo models of Parkinson's disease recent advances. *Prog Brain Res*. 2010;184:17-33.

Cannon JR, Tapias V, Na HM, Honick AS, Drolet RE, Greenamyre JT. A highly reproducible rotenone model of Parkinson's disease. *Neurobiol Dis*. 2009;34(2):279-290.

Cao F, Souders CL II, Perez-Rodriguez V, Martyniuk CJ. Elucidating Conserved Transcriptional Networks Underlying Pesticide Exposure and Parkinson's Disease: A Focus on Chemicals of Epidemiological Relevance. *Front. Genet*. 2019; 9:701. doi: 10.3389/fgene.2018.00701

Cao J, Jia L, Zhou HM, Liu Y, Zhong LF. Mitochondrial and nuclear DNA damage induced by curcumin in human hepatoma G2 cells. *Toxicol Sci*. 2006;91(2):476-483.

Carling PJ, Mortiboys H, Green C, Mihaylov S, Sandor C, Schwartzentruber A, Taylor R, Wei W, Hastings C, Wong S, Lo C, Evetts S, Clemmens H, Wyles M, Willcox S, Payne T, Hughes R, Ferraiuolo L, Webber C, Hide W, Wade-Martins R, Talbot K, Hu MT, Bandmann O. Deep phenotyping of peripheral tissue facilitates mechanistic disease stratification in sporadic Parkinson's disease. *Prog Neurobiol*. 2020;187:101772. doi: 10.1016/j.pneurobio.2020.101772.

Carroll RE, Benya RV, Turgeon DK, Vareed S, Neuman M, Rodriguez L, Kakarala M, Carpenter PM, McLaren C, Meyskens FL Jr, Brenner DE. Phase IIa clinical trial of curcumin for the prevention of colorectal neoplasia. *Cancer Prev Res (Phila*). 2011;4(3):354-364.

Cassar M, Issa AR, Riemensperger T, Petitgas C, Rival T, Coulom H, Iché-Torres M, Han KA, Birman S. A dopamine receptor contributes to paraquat-induced neurotoxicity in *Drosophila* . *Hum Mol Genet*. 2015;24(1):197-212.

Cedarbaum JM. Elephants, Parkinson's Disease, and Proof-of-Concept Clinical Trials. *Mov Disord*. 2018;33(5):697-700.

Cha GH, Kim S, Park J, Lee E, Kim M, Lee SB, Kim JM, Chung J, Cho KS. Parkin negatively regulates JNK pathway in the dopaminergic neurons of *Drosophila* . *Proc Natl Acad Sci USA*. 2005;102(29):10345-10350.

Chaudhuri A, Bowling K, Funderburk C, Lawal H, Inamdar A, Wang Z, O'Donnell JM. Interaction of genetic and environmental factors in a *Drosophila* parkinsonism model. *J Neurosci*. 2007;27(10):2457-2467.

Chen L, Feany MB. Alpha-synuclein phosphorylation controls neurotoxicity and inclusion formation in a *Drosophila* model of Parkinson disease. *Nat Neurosci*. 2005;8(5):657-663.

Chico L, Ienco EC, Bisordi C, Lo Gerfo A, Petrozzi L, Petrucci A, Mancuso M, Siciliano G. Amyotrophic Lateral Sclerosis and Oxidative Stress: A Double-Blind Therapeutic Trial After Curcumin Supplementation. *CNS Neurol Disord Drug Targets*. 2018;17(10):767-779.

Chlebanowska P, Tejchman A, Sułkowski M, Skrzypek K, Majka M. Use of 3D Organoids as a Model to Study Idiopathic Form of Parkinson's Disease. *Int J Mol Sci*. 2020;21(3):694. doi: 10.3390/ijms21030694.

Chou AP, Li S, Fitzmaurice AG, Bronstein JM. Mechanisms of rotenone-induced proteasome inhibition. *Neurotoxicol*. 2010;31:367–372.

Choudhury GR, Daadi MM. Charting the onset of Parkinson-like motor and non-motor symptoms in nonhuman primate model of Parkinson's disease. *PLoS One*. 2018;13(8):e0202770. doi: 10.1371/journal.pone.0202770.

Cohly HH, Taylor A, Angel MF, Salahudeen AK. Effect of turmeric, turmerin and curcumin on H2O2-induced renal epithelial (LLC-PK1) cell injury. *Free Radic Biol Med*. 1998;24(1):49-54.

Cole GM, Teter B, Frautschy SA. Neuroprotective effects of curcumin. *Adv Exp Med Biol*. 2007;595:197-212.

Colle D, Farina M, Ceccatelli S, Raciti M. Paraquat and Maneb Exposure Alters Rat Neural Stem Cell Proliferation by Inducing Oxidative Stress: New Insights on Pesticide-Induced Neurodevelopmental Toxicity. *Neurotox Res*. 2018;34(4):820-833.

Condello S, Currò M, Ferlazzo N, Caccamo D, Satriano J, Ientile R. Agmatine effects on mitochondrial membrane potential and NF-κB activation protect against rotenone-induced cell damage in human neuronal-like SH-SY5Y cells. *J Neurochem*. 2011;116:67–75.

Cooke P, Janowitz H, Dougherty SE. Neuronal Redevelopment and the Regeneration of Neuromodulatory Axons in the Adult Mammalian Central Nervous System. *Front Cell Neurosci*. 2022;16:872501. doi: 10.3389/fncel.2022.872501.

Coulom H, Birman S. Chronic exposure to ROT models sporadic Parkinson’s disease in *Drosophila melanogaster*. *J Neurosci*. 2004; 24(48):10993–10998.

Dai MC, Zhong ZH, Sun YH, Sun QF, Wang YT, Yang GY, Bian LG. Curcumin protects against iron induced neurotoxicity in primary cortical neurons by attenuating necroptosis. *Neurosci Lett*. 2013;536:41-46.

Daimary UD, Parama D, Rana V, Banik K, Kumar A, Harsha C, Kunnumakkara AB. Emerging roles of cardamonin, a multitargeted nutraceutical in the prevention and treatment of chronic diseases. *Curr Res Pharmacol Drug Discov*. 2020;2:100008. doi: 10.1016/j.crphar.2020.100008.

Dawson V, Harman P, Schultz D, Allen, J. Rapid method for measuring rotenone in water at piscicidal concentrations. *Trans. Am. Fish. Soc*. 1983;112:725-727.

de Freitas Couto S, Araujo SM, Bortolotto VC, Poetini MR, Pinheiro FC, Santos Musachio EA, Meichtry LB, do Sacramento M, Alves D, La Rosa Novo D, Mesko MF, Prigol M. 7-chloro-4-(phenylselanyl) quinoline prevents dopamine depletion in a *Drosophila melanogaster* model of Parkinson's-like disease. *J Trace Elem Med Biol*. 2019;54:232-243.

Deng S, Shanmugam MK, Kumar AP, Yap CT, Sethi G, Bishayee A. Targeting autophagy using natural compounds for cancer prevention and therapy. *Cancer*. 2019;125(8):1228-1246.

Dhanraj V, Karuppaiah J, Balakrishnan R, Elangovan N. Myricetin attenuates neurodegeneration and cognitive impairment in Parkinsonism. *Front Biosci (Elite Ed*). 2018;10(3):481-494.

Dhillon AS, Tarbutton GL, Levin JL, Plotkin GM, Lowry LK, Nalbone JT, Shepherd S. Pesticide/environmental exposures and Parkinson's disease in East Texas. *J Agromedicine*. 2008;13(1):37-48.

Doktór B, Damulewicz M, Pyza E. Overexpression of Mitochondrial Ligases Reverses Rotenone-Induced Effects in a *Drosophila* Model of Parkinson's Disease. *Front Neurosci*. 2019;13:94. doi: 10.3389/fnins.2019.00094.

Dulbecco P, Savarino V. Therapeutic potential of curcumin in digestive diseases. *World J Gastroenterol*. 2013;19(48):9256-9270.

Ebinger G, Michotte Y, Herregodts P. The significance of homovanillic acid and 3,4-dihydroxyphenylacetic acid concentrations in human lumbar cerebrospinal fluid. *J Neurochem.* 1987;48(6):1725-1729.

Edvardson S, Cinnamon Y, Ta-Shma A, Shaag A, Yim YI, Zenvirt S, Jalas C, Lesage S, Brice A, Taraboulos A, Kaestner KH, Greene LE, Elpeleg O. A deleterious mutation in DNAJC6 encoding the neuronal-specific clathrin-uncoating co-chaperone auxilin, is associated with juvenile parkinsonism. *PLoS One*. 2012;7(5):e36458. doi: 10.1371/journal.pone.0036458.

El Nebrisi E, Javed H, Ojha SK, Oz M, Shehab S. Neuroprotective Effect of Curcumin on the Nigrostriatal Pathway in a 6-Hydroxydopmine-Induced Rat Model of Parkinson's Disease is Mediated by α7-Nicotinic Receptors. *Int J Mol Sci*. 2020;21(19):7329. doi: 10.3390/ijms21197329.

Elbaz A, Clavel J, Rathouz PJ, Moisan F, Galanaud JP, Delemotte B, Alpérovitch A, Tzourio C. Professional exposure to pesticides and Parkinson disease. *Ann Neurol*. 2009;66(4):494-504.

El-Horany HE, El-Latif RN, ElBatsh MM, Emam MN. Ameliorative Effect of Quercetin on Neurochemical and Behavioral Deficits in Rotenone Rat Model of Parkinson's Disease: Modulating Autophagy (Quercetin on Experimental Parkinson's Disease). *J Biochem Mol Toxicol*. 2016;30(7):360-369.

El-Sherbeeny NA, Soliman N, Youssef AM, Abd El-Fadeal NM, El-Abaseri TB, Hashish AA, Abdelbasset WK, El-Saber Batiha G, Zaitone SA. The protective effect of biochanin A against rotenone-induced neurotoxicity in mice involves enhancing of PI3K/Akt/mTOR signaling and beclin-1 production. *Ecotoxicol Environ Saf*. 2020;205:111344. doi: 10.1016/j.ecoenv.2020.111344.

Elsworth JD, Deutch AY, Redmond DE Jr, Sladek JR Jr, Roth RH. Effects of 1-methyl-4-phenyl-1,2,3,6-tetrahydropyridine (MPTP) on catecholamines and metabolites in primate brain and CSF. *Brain Res*. 1987;415(2):293-299.

EPA. Reregistration Eligibility Decision (RED) Facts for Ziram.Washington,DC: United States Environmental Protection Agency (EPA). 2015;PC Code:034805.

Esmaily H, Sahebkar A, Iranshahi M, Ganjali S, Mohammadi A, Ferns G, Ghayour-Mobarhan M. An investigation of the effects of curcumin on anxiety and depression in obese individuals: A randomized controlled trial. *Chin J Integr Med*. 2015;21(5):332-338.

Ethell DW, Fei Q. Parkinson-linked genes and toxins that affect neuronal cell death through the Bcl-2 family. *Antioxid Redox Signal*. 2009;11:529–540.

Fan C, Li Y, Lan T, Wang W, Mao X, Yu SY. Prophylactic treatment of curcumin in a rat model of depression by attenuating hippocampal synaptic loss. *Food Funct*. 2021;12(22):11202-11213.

Farombi EO, Abolaji AO, Farombi TH, Oropo AS, Owoje OA, Awunah MT. Garcinia kola seed biflavonoid fraction (Kolaviron), increases longevity and attenuates rotenone-induced toxicity in *Drosophila melanogaster*. *Pestic Biochem Physiol*. 2018;145:39-45.

Farombi EO, Awogbindin IO, Olorunkalu PD, Ogbuewu E, Oyetunde BF, Agedah AE, Adeniyi PA. Kolaviron protects against nigrostriatal degeneration and gut oxidative damage in a stereotaxic rotenone model of Parkinson's disease. *Psychopharmacology (Berl).* 2020;237(11):3225-3236.

Fawcett JW. The Struggle to Make CNS Axons Regenerate: Why Has It Been so Difficult? *Neurochem Res*. 2020;45(1):144-158.

Feany MB, Bender WW. A *Drosophila* model of Parkinson's disease. *Nature*. 2000;404(6776):394-398.

Fernandes EJ, Poetini MR, Barrientos MS, Bortolotto VC, Araujo SM, Santos Musachio EA, De Carvalho AS, Leimann FV, Gonçalves OH, Ramborger BP, Roehrs R, Prigol M, Guerra GP. Exposure to lutein-loaded nanoparticles attenuates Parkinson's model-induced damage in *Drosophila melanogaster*: Restoration of dopaminergic and cholinergic system and oxidative stress indicators. *Chem Biol Interact*. 2021;340:109431. doi: 10.1016/j.cbi.2021.109431.

Filaferro M, Codeluppi A, Brighenti V, Cimurri F, González-Paramás AM, Santos-Buelga C, Bertelli D, Pellati F, Vitale G. Disclosing the Antioxidant and Neuroprotective Activity of an Anthocyanin-Rich Extract from Sweet Cherry (Prunus avium L.) Using In Vitro and In Vivo Models. *Antioxidants (Basel*). 2022;11(2):211. doi: 10.3390/antiox11020211.

Flinn L, Mortiboys H, Volkmann K, Köster RW, Ingham PW, Bandmann O. Complex I deficiency and dopaminergic neuronal cell loss in parkin-deficient zebrafish (Danio rerio). *Brain*. 2009;132(Pt 6):1613-1623.

Fodor I, Hussein AA, Benjamin PR, Koene JM, Pirger Z. The unlimited potential of the great pond snail, Lymnaea stagnalis. *Elife*. 2020;9:e56962. doi: 10.7554/eLife.56962.

Forouzanfar F, Majeed M, Jamialahmadi T, Sahebkar A. Telomerase: A Target for Therapeutic Effects of Curcumin in Cancer. *Adv Exp Med Biol*. 2021;1286:135-143.

Franco-Iborra S, Vila M, Perier C. The Parkinson Disease Mitochondrial Hypothesis: Where Are We at? *Neuroscientist*. 2016;22(3):266-277.

Fricker M, Tolkovsky AM, Borutaite V, Coleman M, Brown GC. Neuronal Cell Death. *Physiol Rev*. 2018;98(2):813-880.

Furlong M, Tanner CM, Goldman SM, Bhudhikanok GS, Blair A, Chade A, Comyns K, Hoppin JA, Kasten M, Korell M, Langston JW, Marras C, Meng C, Richards M, Ross GW, Umbach DM, Sandler DP, Kamel F. Protective glove use and hygiene habits modify the associations of specific pesticides with Parkinson's disease. *Environ Int*. 2015;75:144-150.

Fuzzati-Armentero MT, Cerri S, Blandini F. Peripheral-Central Neuroimmune Crosstalk in Parkinson's Disease: What Do Patients and Animal Models Tell Us? *Front Neurol*. 2019;10:232. doi: 10.3389/fneur.2019.00232.

Gao F, Chen D, Si J, Hu Q, Qin Z, Fang M, Wang G. The mitochondrial protein BNIP3L is the substrate of PARK2 and mediates mitophagy in PINK1/PARK2 pathway. *Hum Mol Genet*. 2015;24(9):2528-2538.

Gao HM, Hong JS, Zhang W, Liu B. Distinct role for microglia in rotenone-induced degeneration of dopaminergic neurons. *J Neurosci*. 2002;22:782–790.

Garabadu D, Agrawal N. Naringin Exhibits Neuroprotection Against Rotenone-Induced Neurotoxicity in Experimental Rodents. *Neuromolecular Med*. 2020;22(2):314-330.

Gaspar P, Febvret A, Colombo J. Serotonergic sprouting in primate MTP-induced hemiparkinsonism. *Exp Brain Res*. 1993;96(1):100-106.

Genova ML, Bovina C, Marchetti M, Pallotti F, Tietz C, Biagini G, Pugnaloni A, Viticchi C, Gorini A, Villa RF, Lenaz G. Decrease of rotenone inhibition is a sensitive parameter of complex I damage in brain non-synaptic mitochondria of aged rats. *FEBS Lett*. 1997;410(2-3):467-469.

Gerlach M, Gsell W, Kornhuber J, Jellinger K, Krieger V, Pantucek F, Vock R, Riederer P. A post mortem study on neurochemical markers of dopaminergic, GABA-ergic and glutamatergic neurons in basal ganglia-thalamocortical circuits in Parkinson syndrome. *Brain Res*. 1996;741(1-2):142-152.

Ghatak S, Trudler D, Dolatabadi N, Ambasudhan R. Parkinson's disease: what the model systems have taught us so far. *J Genet*. 2018;97(3):729-751.

Giguère N, Burke Nanni S, Trudeau LE. On Cell Loss and Selective Vulnerability of Neuronal Populations in Parkinson's Disease. *Front Neurol*. 2018;9:455. doi: 10.3389/fneur.2018.00455.

Girisa S, Kumar A, Rana V, Parama D, Daimary UD, Warnakulasuriya S, Kumar AP, Kunnumakkara AB. From Simple Mouth Cavities to Complex Oral Mucosal Disorders-Curcuminoids as a Promising Therapeutic Approach. *ACS Pharmacol Transl Sci*. 2021;4(2):647-665.

Girish C, Muralidhara. Propensity of Selaginella delicatula aqueous extract to offset rotenone-induced oxidative dysfunctions and neurotoxicity in *Drosophila melanogaster*: Implications for Parkinson's disease. *Neurotoxicol*. 2012;33(3):444-456.

Gleason K, Shine JP, Shobnam N, Rokoff LB, Suchanda HS, Ibne Hasan MO, Mostofa G, Amarasiriwardena C, Quamruzzaman Q, Rahman M, Kile ML, Bellinger DC, Christiani DC, Wright RO, Mazumdar M. Contaminated turmeric is a potential source of lead exposure for children in rural Bangladesh. *J Environ Public Health*. 2014;2014:730636. doi: 10.1155/2014/730636.

Goldstein DS, Sullivan P, Cooney A, Jinsmaa Y, Sullivan R, Gross DJ, Holmes C, Kopin IJ, Sharabi Y. Vesicular uptake blockade generates the toxic dopamine metabolite 3,4-dihydroxyphenylacetaldehyde in PC12 cells: relevance to the pathogenesis of Parkinson's disease. *J Neurochem*. 2012;123(6):932-943.

Goodpasture CE, Arrighi FE. Effects of food seasonings on the cell cycle and chromosome morphology of mammalian cells in vitro with special reference to turmeric. *Food Cosmet Toxicol*. 1976;14(1):9-14.

Greene JC, Whitworth AJ, Kuo I, Andrews LA, Feany MB, Pallanck LJ. Mitochondrial pathology and apoptotic muscle degeneration in *Drosophila* parkin mutants. *Proc Natl Acad Sci USA*. 2003;100(7):4078-4083.

Guo Q, Wang B, Wang X, Smith WW, Zhu Y, Liu Z. Activation of Nrf2 in Astrocytes Suppressed PD-Like Phenotypes via Antioxidant and Autophagy Pathways in Rat and *Drosophila* Models. *Cells*. 2021;10(8):1850. doi: 10.3390/cells10081850.

Gupta SC, Patchva S, Aggarwal BB. Therapeutic roles of curcumin: lessons learned from clinical trials. *AAPS J*. 2013;15(1):195-218.

Haggerty DL, Grecco GG, Reeves KC, Atwood B. Adeno-Associated Viral Vectors in Neuroscience Research. *Mol Ther Methods Clin Dev*. 2020;17:69–82.

Ham S, Lee SV. Advances in transcriptome analysis of human brain aging. *Exp Mol Med*. 2020;52(11):1787-1797.

Han Y, Wang T, Li C, Wang Z, Zhao Y, He J, Fu L, Han B. Ginsenoside Rg3 exerts a neuroprotective effect in rotenone-induced Parkinson's disease mice via its anti-oxidative properties. *Eur J Pharmacol*. 2021;909:174413. doi: 10.1016/j.ejphar.2021.174413.

Hancock DB, Martin ER, Mayhew GM, Stajich JM, Jewett R, Stacy MA, Scott BL, Vance JM, Scott WK. Pesticide exposure and risk of Parkinson's disease: a family-based case-control study. *BMC Neurol*. 2008;8:6. doi: 10.1186/1471-2377-8-6.

Harkavyi A, Whitton PS. Glucagon-like peptide 1 receptor stimulation as a means of neuroprotection. *Br J Pharmacol*. 2010;159(3):495-501.

Harnack D, Meissner W, Jira JA, Winter C, Morgenstern R, Kupsch A. Placebocontrolled chronic high-frequency stimulation of the subthalamic nucleus preserves dopaminergic nigral neurons in a rat model of progressive Parkinsonism. *Exp Neurol*. 2008;210(1):257–260.

Harrington AJ, Hamamichi S, Caldwell GA, Caldwell KA. C. elegans as a model organism to investigate molecular pathways involved with Parkinson's disease. *Dev Dyn*. 2010;239(5):1282-1295.

Harrington AJ, Knight AL, Caldwell GA, Caldwell KA. Caenorhabditis elegans as a model system for identifying effectors of α-synuclein misfolding and dopaminergic cell death associated with Parkinson's disease. *Methods*. 2011;53(3):220-225.

Hasan W, Kori RK, Jain J, Yadav RS, Jat D. Neuroprotective effects of mitochondria-targeted curcumin against rotenone-induced oxidative damage in cerebellum of mice. *J Biochem Mol Toxicol*. 2020;34(1):e22416. doi: 10.1002/jbt.22416.

Heidari A, Yazdanpanah N, Rezaei N. The role of Toll-like receptors and neuroinflammation in Parkinson's disease. *J Neuroinflam*. 2022;19(1):135. doi: 10.1186/s12974-022-02496-w.

Herrera A, Muñoz P, Steinbusch HWM, Segura-Aguilar J. Are Dopamine Oxidation Metabolites Involved in the Loss of Dopaminergic Neurons in the Nigrostriatal System in Parkinson's Disease? *ACS Chem Neurosci*. 2017;8(4):702-711.

Hisahara S, Shimohama S. Toxin-induced and genetic animal models of Parkinson's disease. *Parkinsons Dis*. 2010;2011:951709. doi: 10.4061/2011/951709.

Höglinger GU, Féger J, Prigent A, Michel PP, Parain K, Champy P, Ruberg M, Oertel WH, Hirsch EC. Chronic systemic complex I inhibition induces a hypokinetic multisystem degeneration in rats. *J Neurochem*. 2003;84(3):491-502.

Hosamani R, Muralidhara. Neuroprotective efficacy of Bacopa monnieri against rotenone induced oxidative stress and neurotoxicity in *Drosophila melanogaster*. *Neurotoxicol*. 2009;30(6):977-985.

Hou L, Chen W, Liu X, Qiao D, Zhou FM. Exercise-Induced Neuroprotection of the Nigrostriatal Dopamine System in Parkinson's Disease. *Front Aging Neurosci*. 2017;9:358. doi: 10.3389/fnagi.2017.00358.

Hu LF, Lu M, Tiong CX, Dawe GS, Hu G, Bian JS. Neuroprotective effects of hydrogen sulfide on Parkinson’s disease rat models. *Aging Cell*. 2010;9:135–146.

Huang C, Ma J, Li BX, Sun Y. Wnt1 silencing enhances neurotoxicity induced by paraquat and maneb in SH-SY5Y cells. *Exp Ther Med*. 2019;18(5):3643-3649.

Huang J, Hao L, Xiong N, Cao X, Liang Z, Sun S, Wang T. Involvement of glyceraldehyde-3-phosphate dehydrogenase in rotenone-induced cell apoptosis: relevance to protein misfolding and aggregation. *Brain Res*. 2009;1279:1-8.

Hudry E, Vandenberghe LH. Therapeutic AAV gene transfer to the nervous system: a clinical reality. *Neuron*. 2019;101(5):839–862.

Huot P, Johnston TH, Lewis KD, Koprich JB, Reyes MG, Fox SH, Piggott MJ, Brotchie JM. Characterization of 3,4-methylenedioxymethamphetamine (MDMA) enantiomers in vitro and in the MPTP-lesioned primate: R-MDMA reduces severity of dyskinesia, whereas S-MDMA extends duration of ON-time. *J Neurosci*. 2011;31(19):7190-7198.

Hwang RD, Wiemerslage L, LaBreck CJ, Khan M, Kannan K, Wang X, Zhu X, Lee D, Fridell YW. The neuroprotective effect of human uncoupling protein 2 (hUCP2) requires cAMP-dependent protein kinase in a toxin model of Parkinson's disease. *Neurobiol Dis*. 2014;69:180-191.

Inden M, Kitamura Y, Takeuchi H, Yanagida T, Takata K, Kobayashi Y, *et al*. Neurodegeneration of mouse nigrostriatal dopaminergic system induced by repeated oral administration of rotenone is prevented by 4-phenylbutyrate, a chemical chaperone. *J Neurochem*. 2007;101(6):1491-1504.

Innos J, Hickey MA. Using Rotenone to Model Parkinson's Disease in Mice: A Review of the Role of Pharmacokinetics. *Chem Res Toxicol*. 2021;34(5):1223-1239.

Isenberg JS, Klaunig JE. Role of the mitochondrial membrane permeability transition (MPT) in rotenone-induced apoptosis in liver cells. *Toxicol Sci*. 2000;53:340–351.

Islam R, Yang L, Sah M, Kannan K, Anamani D, Vijayan C, Kwok J, Cantino ME, Beal MF, Fridell YW. A neuroprotective role of the human uncoupling protein 2 (hUCP2) in a *Drosophila* Parkinson's disease model. *Neurobiol Dis*. 2012;46(1):137-146.

Javed H, Azimullah S, Meeran MFN, Ansari SA, Ojha S. Neuroprotective Effects of Thymol, a Dietary Monoterpene Against Dopaminergic Neurodegeneration in Rotenone-Induced Rat Model of Parkinson's Disease. *Int J Mol Sci*. 2019b;20(7):1538. doi: 10.3390/ijms20071538.

Javed H, Kamal MA, Ojha S. An Overview on the Role of α -Synuclein in Experimental Models of Parkinson's Disease from Pathogenesis to Therapeutics. *CNS Neurol Disord Drug Targets*. 2016;15(10):1240-1252.

Javed H, Meeran MFN, Azimullah S, Bader Eddin L, Dwivedi VD, Jha NK, Ojha S. α-Bisabolol, a Dietary Bioactive Phytochemical Attenuates Dopaminergic Neurodegeneration through Modulation of Oxidative Stress, Neuroinflammation and Apoptosis in Rotenone-Induced Rat Model of Parkinson's disease. *Biomolecules*. 2020;10(10):1421. doi: 10.3390/biom10101421.

Javed H, Nagoor Meeran MF, Azimullah S, Adem A, Sadek B, Ojha SK. Plant Extracts and Phytochemicals Targeting α-Synuclein Aggregation in Parkinson's Disease Models. *Front Pharmacol*. 2019a;9:1555. doi: 10.3389/fphar.2018.01555.

Jayaraj R, Megha P, Sreedev P. Organochlorine pesticides, their toxic effects on living organisms and their fate in the environment. *Interdiscip Toxicol*. 2016;9(3-4):90-100.

Jayaraj RL, Beiram R, Azimullah S, Meeran MFN, Ojha SK, Adem A, Jalal FY. Lycopodium Attenuates Loss of Dopaminergic Neurons by Suppressing Oxidative Stress and Neuroinflammation in a Rat Model of Parkinson's Disease. *Molecules*. 2019;24(11):2182. doi: 10.3390/molecules24112182.

Jenner P, Rupniak NM, Rose S, Kelly E, Kilpatrick G, Lees A, Marsden CD. 1-Methyl-4-phenyl-1,2,3,6-tetrahydropyridine-induced parkinsonism in the common marmoset. *Neurosci Lett*. 1984;50(1-3):85-90.

Jeon YM, Lee S, Kim S, Kwon Y, Kim K, Chung CG, Lee S, Lee SB, Kim HJ. Neuroprotective Effects of Protein Tyrosine Phosphatase 1B Inhibition against ER Stress-Induced Toxicity. *Mol Cells*. 2017;40(4):280-290.

Jiang P, Dickson DW. Parkinson's disease: experimental models and reality. *Acta Neuropathol*. 2018;135(1):13-32.

Jiao Y, Wilkinson J 4th, Di X, Wang W, Hatcher H, Kock ND, D'Agostino R Jr, Knovich MA, Torti FM, Torti SV. Curcumin, a cancer chemopreventive and chemotherapeutic agent, is a biologically active iron chelator. *Blood*. 2009;113(2):462-469.

Jin J, Davis J, Zhu D, Kashima DT, Leroueil M, Pan C, Montine KS, Zhang J. Identification of novel proteins affected by rotenone in mitochondria of dopaminergic cells. *BMC Neurosci*. 2007;8:67. doi: 10.1186/1471-2202-8-67.

Jinsmaa Y, Sharabi Y, Sullivan P, Isonaka R, Goldstein DS. 3,4-Dihydroxyphenylacetaldehyde-Induced Protein Modifications and Their Mitigation by N-Acetylcysteine. *J Pharmacol Exp Ther*. 2018;366(1):113-124.

Johnson ME, Bobrovskaya L. An update on the rotenone models of Parkinson's disease: their ability to reproduce the features of clinical disease and model gene-environment interactions. *Neurotoxicol*. 2015;46:101-116.

Johnson SL, Park HY, DaSilva NA, Vattem DA, Ma H, Seeram NP. Levodopa-Reduced Mucuna pruriens Seed Extract Shows Neuroprotective Effects against Parkinson's Disease in Murine Microglia and Human Neuroblastoma Cells, Caenorhabditis elegans, and *Drosophila melanogaster*. *Nutrients*. 2018;10(9):1139. doi: 10.3390/nu10091139.

Johnston TH, Huot P, Fox SH, Wakefield JD, Sykes KA, Bartolini WP, Milne GT, Pearson JP, Brotchie JM. Fatty acid amide hydrolase (FAAH) inhibition reduces L-3,4-dihydroxyphenylalanine-induced

hyperactivity in the 1-methyl-4-phenyl-1,2,3,6-tetrahydropyridine-lesioned non-human primate model of Parkinson's disease. *J Pharmacol Exp Ther*. 2011;336(2):423-430.

Kamel F, Tanner C, Umbach D, Hoppin J, Alavanja M, Blair A, Comyns K, Goldman S, Korell M, Langston J, Ross G, Sandler D. Pesticide exposure and self-reported Parkinson's disease in the agricultural health study. *Am J Epidemiol*. 2007;165(4):364-374.

Kanchanatawan B, Tangwongchai S, Sughondhabhirom A, Suppapitiporn S, Hemrunrojn S, Carvalho AF, Maes M. Add-on Treatment with Curcumin Has Antidepressive Effects in Thai Patients with Major Depression: Results of a Randomized Double-Blind Placebo-Controlled Study. *Neurotox Res*. 2018;33(3):621-633.

Kashyap D, Tuli HS, Yerer MB, Sharma A, Sak K, Srivastava S, Pandey A, Garg VK, Sethi G, Bishayee A. Natural product-based nanoformulations for cancer therapy: Opportunities and challenges. *Semin Cancer Biol*. 2021;69:5-23.

Kasture AS, Hummel T, Sucic S, Freissmuth M. Big Lessons from Tiny Flies: *Drosophila melanogaster* as a Model to Explore Dysfunction of Dopaminergic and Serotonergic Neurotransmitter Systems. *Int J Mol Sci*. 2018;19(6):1788. doi: 10.3390/ijms19061788.

Khairnar RC, Parihar N, Prabhavalkar KS, Bhatt LK. Emerging targets signaling for inflammation in Parkinson's disease drug discovery. *Metab Brain Dis*. 2022. doi: 10.1007/s11011-022-00999-2.

Khatri DK, Juvekar AR. Kinetics of Inhibition of Monoamine Oxidase Using Curcumin and Ellagic Acid. Pharmacogn Mag. 2016;12(2):S116-120.

Kim H, Park HJ, Choi H, Chang Y, Park H, Shin J, Kim J, Lengner CJ, Lee YK, Kim J. Modeling G2019S-LRRK2 Sporadic Parkinson's Disease in 3D Midbrain Organoids. *Stem Cell Reports*. 2019;12(3):518-531.

Kishore Kumar SN, Deepthy J, Saraswathi U, Thangarajeswari M, Yogesh Kanna S, Ezhil P, Kalaiselvi P. Morinda citrifolia mitigates rotenone-induced striatal neuronal loss in male Sprague-Dawley rats by preventing mitochondrial pathway of intrinsic apoptosis. *Redox Rep*. 2017;22(6):418-429.

Kitada T, Asakawa S, Hattori N, Matsumine H, Yamamura Y, Minoshima S, Yokochi M, Mizuno Y, Shimizu N. Mutations in the parkin gene cause autosomal recessive juvenile parkinsonism. *Nature*. 1998;392(6676):605-608.

Kopin IJ. Catecholamine metabolism: basic aspects and clinical significance. *Pharmacol Rev*. 1985;37(4):333-364.

Koprich JB, Fox SH, Johnston TH, Goodman A, Le Bourdonnec B, Dolle RE, DeHaven RN, DeHaven-Hudkins DL, Little PJ, Brotchie JM. The selective mu-opioid receptor antagonist ADL5510 reduces Levodopa-induced dyskinesia without affecting antiparkinsonian action in MPTP-lesioned macaque model of Parkinson's disease. *Mov Disord*. 2011;26(7):1225-1233.

Kotake Y, Ohta S. MPP+ analogs acting on mitochondria and inducing neuro-degeneration. *Curr Med Chem.* 2003;0:2507–2516.

Krebs CE, Karkheiran S, Powell JC, Cao M, Makarov V, Darvish H, Di Paolo G, Walker RH, Shahidi GA, Buxbaum JD, De Camilli P, Yue Z, Paisán-Ruiz C. The Sac1 domain of SYNJ1 identified mutated in a family with early-onset progressive Parkinsonism with generalized seizures. *Hum Mutat*. 2013;34(9):1200-1207.

Krüger R, Kuhn W, Müller T, Woitalla D, Graeber M, Kösel S, Przuntek H, Epplen JT, Schöls L, Riess O. Ala30Pro mutation in the gene encoding alpha-synuclein in Parkinson's disease. *Nat Genet*. 1998;18(2):106-108.

Kujawska M, Jourdes M, Kurpik M, Szulc M, Szaefer H, Chmielarz P, Kreiner G, Krajka-Kuźniak V, Mikołajczak PŁ, Teissedre PL, Jodynis-Liebert J. Neuroprotective Effects of Pomegranate Juice against Parkinson's Disease and Presence of Ellagitannins-Derived Metabolite-Urolithin A-In the Brain. *Int J Mol Sci*. 2019;21(1):202. doi: 10.3390/ijms21010202.

Kuwahara T, Koyama A, Gengyo-Ando K, Masuda M, Kowa H, Tsunoda M, Mitani S, Iwatsubo T. Familial Parkinson mutant alpha-synuclein causes dopamine neuron dysfunction in transgenic Caenorhabditis elegans. *J Biol Chem*. 2006;281(1):334-340.

La Forge FB, Haller HL, Smith LE. The Determinationof the Structure of Rotenone. *Chem. Rev*. 1933;12:181–213

Laabbar W, Elgot A, Elhiba O, Gamrani H. Curcumin prevents the midbrain dopaminergic innervations and locomotor performance deficiencies resulting from chronic aluminum exposure in rat. *J Chem Neuroanat*. 2019;100:101654. doi: 10.1016/j.jchemneu.2019.101654.

Lakkappa N, Krishnamurthy PT, M D P, Hammock BD, Hwang SH. Soluble epoxide hydrolase inhibitor, APAU, protects dopaminergic neurons against rotenone induced neurotoxicity: Implications for Parkinson's disease. *Neurotoxicol*. 2019;70:135-145.

Lakkappa N, Krishnamurthy PT, Yamjala K, Hwang SH, Hammock BD, Babu B. Evaluation of antiparkinson activity of PTUPB by measuring dopamine and its metabolites in *Drosophila melanogaster*: LC-MS/MS method development. *J Pharm Biomed Anal*. 2018;149:457-464.

Lal B, Kapoor AK, Asthana OP, Agrawal PK, Prasad R, Kumar P, Srimal RC. Efficacy of curcumin in the management of chronic anterior uveitis. *Phytother Res*. 1999;13(4):318-322.

Lane EL. L-DOPA for Parkinson's disease-a bitter-sweet pill. *Eur J Neurosci* 2019;49(3):384-398.

Langston JW, Ballard P, Tetrud JW, Irwin I. Chronic Parkinsonism in humans due to a product of meperidine-analog synthesis. *Science*. 1983;219(4587):979-980.

Langston JW, Forno LS, Rebert CS, Irwin I. Selective nigral toxicity after systemic administration of 1-methyl-4-phenyl-1,2,5,6-tetrahydropyrine (MPTP) in the squirrel monkey. *Brain Res*. 1984;292(2):390-4.

Langston JW. The MPTP Story. *J Parkinsons Dis*. 2017;7(s1):S11-S19. doi: 10.3233/JPD-179006.

Laurent St R, O'Brien LM, Ahmad ST. Sodium butyrate improves locomotor impairment and early mortality in a rotenone-induced *Drosophila* model of Parkinson's disease. *Neuroscience*. 2013;246:382-390.

Lawal HO, Chang HY, Terrell AN, Brooks ES, Pulido D, Simon AF, Krantz DE. The *Drosophila* vesicular monoamine transporter reduces pesticide-induced loss of dopaminergic neurons. *Neurobiol Dis*. 2010;40(1):102-112.

Lee KS, Lee BS, Semnani S, Avanesian A, Um CY, Jeon HJ, Seong KM, Yu K, Min KJ, Jafari M. Curcumin extends life span, improves health span, and modulates the expression of age-associated aging genes in *Drosophila melanogaster*. *Rejuvenation Res*. 2010;13(5):561-570.

Lesage S, Anheim M, Letournel F, Bousset L, Honoré A, Rozas N, Pieri L, Madiona K, Dürr A, Melki R, Verny C, Brice A; French Parkinson's Disease Genetics Study Group. G51D α-synuclein mutation causes a novel parkinsonian-pyramidal syndrome. *Ann Neurol*. 2013;73(4):459-571.

Lessing D, Bonini NM. Maintaining the brain: insight into human neurodegeneration from *Drosophila melanogaster* mutants. *Nat Rev Genet*. 2009;10(6):359-370.

Lev N, Ickowicz D, Melamed E, Offen D. Oxidative insults induce DJ-1 upregulation and redistribution: implications for neuroprotection. *Neurotoxicol*. 2008;29(3):397-405.

LeWitt P, Schultz L, Auinger P, Lu M; Parkinson Study Group DATATOP Investigators. CSF xanthine, homovanillic acid, and their ratio as biomarkers of Parkinson's disease. *Brain Res*. 2011;1408:88-97.

LeWitt PA. Dopamine Metabolite Biomarkers and Testing for Disease Modification in Parkinson Disease. *JAMA Neurol*. 2020;77(8):1038-1039

Liao J, Morin LW, Ahmad ST. Methods to characterize spontaneous and startle-induced locomotion in a rotenone-induced Parkinson's disease model of *Drosophila* . *J Vis Exp*. 2014;(90):51625. doi: 10.3791/51625.

Liddle M, Hull C, Liu C, Powell D. Contact urticaria from curcumin. *Dermatitis*. 2006;17(4):196-197.

Lindholm D, Mäkelä J, Di Liberto V, Mudò G, Belluardo N, Eriksson O, Saarma M. Current disease modifying approaches to treat Parkinson's disease. *Cell Mol Life Sci*. 2016;73(7):1365-1379.

Linhart R, Wong SA, Cao J, Tran M, Huynh A, Ardrey C, Park JM, Hsu C, Taha S, Peterson R, Shea S, Kurian J, Venderova K. Vacuolar protein sorting 35 (Vps35) rescues locomotor deficits and shortened

lifespan in *Drosophila* expressing a Parkinson's disease mutant of Leucine-Rich Repeat Kinase 2 (LRRK2). *Mol Neurodegener*. 2014;9:23. doi: 10.1186/1750-1326-9-23.

Liu CB, Wang R, Pan HB, Ding QF, Lu FB. Effect of lycopene on oxidative stress and behavioral deficits in rotenone induced model of Parkinson's disease. *Zhongguo Ying Yong Sheng Li Xue Za Zhi*. 2013;29(4):380-384.

Liu G, Yu J, Ding J, Xie C, Sun L, Rudenko I, Zheng W, Sastry N, Luo J, Rudow G, Troncoso JC, Cai H. Aldehyde dehydrogenase 1 defines and protects a nigrostriatal dopaminergic neuron subpopulation. *J Clin Invest*. 2014;124(7):3032-3046.

Liu LF, Song JX, Lu JH, Huang YY, Zeng Y, Chen LL, Durairajan SS, Han QB, Li M. Tianma Gouteng Yin, a Traditional Chinese Medicine decoction, exerts neuroprotective effects in animal and cellular models of Parkinson's disease. *Sci Rep*. 2015;5:16862. doi: 10.1038/srep16862.

Liu M, Yu S, Wang J, Qiao J, Liu Y, Wang S, Zhao Y. Ginseng protein protects against mitochondrial dysfunction and neurodegeneration by inducing mitochondrial unfolded protein response in *Drosophila melanogaster* PINK1 model of Parkinson's disease. *J Ethnopharmacol*. 2020;247:112213. doi: 10.1016/j.jep.2019.112213.

Liu Z, Wang X, Yu Y, Li X, Wang T, Jiang H, Ren Q, Jiao Y, Sawa A, Moran T, Ross CA, Montell C, Smith WW. A *Drosophila* model for LRRK2-linked parkinsonism. *Proc Natl Acad Sci USA*. 2008;105(7):2693-2698.

Lohr KM, Stout KA, Dunn AR, Wang M, Salahpour A, Guillot TS, Miller GW. Increased Vesicular Monoamine Transporter 2 (VMAT2; Slc18a2) Protects against Methamphetamine Toxicity. *ACS Chem Neurosci.* 2015;6(5):790-799.

Ma XW, Guo RY. Dose-dependent effect of Curcuma longa for the treatment of Parkinson's disease. *Exp Ther Med*. 2017;13(5):1799-1805.

Madiha S, Haider S. Curcumin restores rotenone induced depressive-like symptoms in animal model of neurotoxicity: assessment by social interaction test and sucrose preference test. *Metab Brain Dis*. 2019;34(1):297-308.

Maiti P, Bowers Z, Bourcier-Schultz A, Morse J, Dunbar GL. Preservation of dendritic spine morphology and postsynaptic signaling markers after treatment with solid lipid curcumin particles in the 5xFAD mouse model of Alzheimer's amyloidosis. *Alzheimers Res Ther*. 2021;13(1):37. doi: 10.1186/s13195-021-00769-9.

Maiti P, Dunbar GL. Use of Curcumin, a Natural Polyphenol for Targeting Molecular Pathways in Treating Age-Related Neurodegenerative Diseases. *Int J Mol Sci*. 2018;19(6):1637. doi: 10.3390/ijms19061637.

Maitra U, Harding T, Liang Q, Ciesla L. GardeninA confers neuroprotection against environmental toxin in a *Drosophila* model of Parkinson's disease. *Commun Biol*. 2021;4(1):162. https://doi.org/10.1038/s42003-021-01685-2

Mancuso C, Barone E. Curcumin in clinical practice: myth or reality? *Trends Pharmacol Sci*. 2009;30(7):333-334.

Manjunath MJ, Muralidhara. Standardized extract of Withania somnifera (Ashwagandha) markedly offsets rotenone-induced locomotor deficits, oxidative impairments and neurotoxicity in *Drosophila melanogaster*. *J Food Sci Technol*. 2015;52(4):1971-1981.

Marino BLB, de Souza LR, Sousa KPA, Ferreira JV, Padilha EC, da Silva CHTP, Taft CA, Hage-Melim LIS. Parkinson's Disease: A review from pathophysiology to treatment. *Mini Rev Med Chem*. 2020;20(9):754-767.

Martí Y, Matthaeus F, Lau T, Schloss P. Methyl-4-phenylpyridinium (MPP+) differentially affects monoamine release and re-uptake in murine embryonic stem cell-derived dopaminergic and serotonergic neurons. *Mol Cell Neurosci*. 2017;83:37-45.

Masato A, Plotegher N, Boassa D, Bubacco L. Impaired dopamine metabolism in Parkinson's disease pathogenesis. *Mol Neurodegener*. 2019;14(1):35. doi: 10.1186/s13024-019-0332-6.

McCormack AL, Di Monte DA. Effects of L-dopa and other amino acids against paraquat-induced nigrostriatal degeneration. *J Neurochem*. 2003;85(1):82-86.

Mei M, Zhou Y, Liu M, Zhao F, Wang C, Ding J, Lu M, Hu G. Antioxidant and anti-inflammatory effects of dexrazoxane on dopaminergic neuron degeneration in rodent models of Parkinson's disease. *Neuropharmacol*. 2019;160:107758. doi: 10.1016/j.neuropharm.2019.107758.

Menzies FM, Yenisetti SC, Min KT. Roles of *Drosophila* DJ-1 in survival of dopaminergic neurons and oxidative stress. *Curr Biol*. 2005;15(17):1578-1582.

Meredith GE, Rademacher DJ. MPTP mouse models of Parkinson's disease: an update. *J Parkinsons Dis*. 2011;1(1):19-33.

Meulener M, Whitworth AJ, Armstrong-Gold CE, Rizzu P, Heutink P, Wes PD, Pallanck LJ, Bonini NM. *Drosophila* DJ-1 mutants are selectively sensitive to environmental toxins associated with Parkinson's disease. *Curr Biol*. 2005;15(17):1572-1577.

Mingazov ER, Khakimova GR, Kozina EA, Medvedev AE, Buneeva OA, Bazyan AS, Ugrumov MV. MPTP Mouse Model of Preclinical and Clinical Parkinson's Disease as an Instrument for Translational Medicine. *Mol Neurobiol*. 2018;55(4):2991-3006.

Miodownik C, Lerner V, Kudkaeva N, Lerner PP, Pashinian A, Bersudsky Y, Eliyahu R, Kreinin A, Bergman J. Curcumin as Add-On to Antipsychotic Treatment in Patients With Chronic Schizophrenia: A Randomized, Double-Blind, Placebo-Controlled Study. *Clin Neuropharmacol*. 2019;42(4):117-122.

Miyazaki I, Isooka N, Wada K, Kikuoka R, Kitamura Y, Asanuma M. Effects of Enteric Environmental Modification by Coffee Components on Neurodegeneration in Rotenone-Treated Mice. *Cells*. 2019;8(3). pii: E221. doi: 10.3390/cells8030221.

Mizuno Y, Sone N, Saitoh T. Effects of 1-methyl-4-phenyl-1,2,3,6-tetrahydropyridine and 1-methyl-4-phenylpyridinium ion on activities of the enzymes in the electron transport system in mouse brain. *J Neurochem*. 1987;48(6):1787-1793.

Modi P*, **Ayajuddin M***, Phom L, Koza Z, Das A, Chaurasia R, Samadder S, Achumi B, Muralidhara, Singh PR and Yenisetti SC. Understanding pathophysiology of sporadic Parkinson's disease in *Drosophila* model: Potential opportunities and notable limitations. In: Jolanta Dorszewska and Wojciech Kozubski (Eds). Challenges in Parkinson's Disease. *InTechOpen*. 2016:pp.217-244. doi: 10.5772/63767.

Moon Y, Lee KH, Park JH, Geum D, Kim K. Mitochondrial membrane depolarization and the selective death of dopaminergic neurons by rotenone: protective effect of coenzyme Q10. *J Neurochem*. 2005;93:1199–1208.

Moors T, Paciotti S, Chiasserini D, Calabresi P, Parnetti L, Beccari T, van de Berg WD. Lysosomal Dysfunction and α-Synuclein Aggregation in Parkinson's Disease: Diagnostic Links. *Mov Disord*. 2016;31(6):791-801.

Moreadith RW, Fiskum G. Isolation of mitochondria from ascites tumor cells permeabilized with digitonin. *Anal Biochem*. 1984;137(2):360-367.

Moreira CG, Barbiero JK, Ariza D, Dombrowski PA, Sabioni P, Bortolanza M, Da Cunha C, Vital MA, Lima MM. Behavioral, neurochemical and histological alterations promoted by bilateral intranigral rotenone administration: a new approach for an old neurotoxin. *Neurotox Res*. 2012;21(3):291-301.

Morin N, Grégoire L, Gomez-Mancilla B, Gasparini F, Di Paolo T. Effect of the metabotropic glutamate receptor type 5 antagonists MPEP and MTEP in parkinsonian monkeys. *Neuropharmacol*. 2010;58(7):981-986.

Nalls MA, Blauwendraat C, Vallerga CL, Heilbron K, Bandres-Ciga S, Chang D, Tan M, Kia DA, Noyce AJ, Xue A, Bras J, Young E, von Coelln R, Simón-Sánchez J, Schulte C, Sharma M, Krohn L, Pihlstrøm L, Siitonen A, Iwaki H, Leonard H, Faghri F, Gibbs JR, Hernandez DG, Scholz SW, Botia JA, Martinez M, Corvol JC, Lesage S, Jankovic J, Shulman LM, Sutherland M, Tienari P, Majamaa K, Toft M, Andreassen OA, Bangale T, Brice A, Yang J, Gan-Or Z, Gasser T, Heutink P, Shulman JM, Wood NW, Hinds DA, Hardy JA, Morris HR, Gratten J, Visscher PM, Graham RR, Singleton AB; 23andMe Research Team; System Genomics of Parkinson's Disease Consortium; International Parkinson's Disease Genomics

Consortium. Identification of novel risk loci, causal insights, and heritable risk for Parkinson's disease: a meta-analysis of genome-wide association studies. *Lancet Neurol*. 2019;18(12):1091-1102.

Naser AFA, Aziz WM, Ahmed YR, Khalil WKB, Hamed MAA. Parkinsonism-like Disease Induced by Rotenone in Rats: Treatment Role of Curcumin, Dopamine Agonist and Adenosine A2A Receptor Antagonist. *Curr Aging Sci*. 2022;15(1):65-76.

Nass R, Hall DH, Miller DM 3rd, Blakely RD. Neurotoxin-induced degeneration of dopamine neurons in Caenorhabditis elegans. *Proc Natl Acad Sci USA*. 2002;99(5):3264-3269.

Nässel DR, Elekes K. Aminergic neurons in the brain of blowflies and *Drosophila* : dopamine- and tyrosine hydroxylase-immunoreactive neurons and their relationship with putative histaminergic neurons. *Cell Tissue Res*. 1992;267(1):147-167.

Navarro A, Gomez C, López-Cepero JM, Boveris A. Beneficial effects of moderate exercise on mice aging: survival, behavior, oxidative stress, and mitochondrial electron transfer. *Am J Physiol Regul Integr Comp Physiol.* 2004;286(3):R505-11.

Navarro JA, Heßner S, Yenisetti SC, Bayersdorfer F, Zhang L, Voigt A, Schneuwly S, Botella JA. Analysis of dopaminergic neuronal dysfunction in genetic and toxin-induced models of Parkinson's disease in *Drosophila* . *J Neurochem*. 2014;131(3):369-382.

Nguyen M, Wong YC, Ysselstein D, Severino A, Krainc D. Synaptic, Mitochondrial, and Lysosomal Dysfunction in Parkinson's Disease. *Trends Neurosci*. 2019;42(2):140-149.

Nguyen TT, Vuu MD, Huynh MA, Yamaguchi M, Tran LT, Dang TPT. Curcumin Effectively Rescued Parkinson's Disease-Like Phenotypes in a Novel *Drosophila melanogaster* Model with dUCH Knockdown. *Oxid Med Cell Longev*. 2018;2018:2038267. doi: 10.1155/2018/2038267.

Norazit A, Meedeniya AC, Nguyen MN, Mackay-Sim A. Progressive loss of dopaminergic neurons induced by unilateral rotenone infusion into the medial forebrain bundle. *Brain Res.* 2010;1360:119–129.

Ntetsika T, Papathoma PE, Markaki I. Novel targeted therapies for Parkinson's disease. *Mol Med*. 2021;27(1):17. doi: 10.1186/s10020-021-00279-2.

Ojha S, Javed H, Azimullah S, Abul Khair SB, Haque ME. Neuroprotective potential of ferulic acid in the rotenone model of Parkinson's disease. *Drug Des Devel Ther*. 2015;9:5499-5510.

Öz A, Çelik Ö. Curcumin inhibits oxidative stress-induced TRPM2 channel activation, calcium ion entry and apoptosis values in SH-SY5Y neuroblastoma cells: Involvement of transfection procedure. *Mol Membr Biol*. 2016;33(3-5):76-88.

Pagan FL, Hebron ML, Wilmarth B, Torres-Yaghi Y, Lawler A, Mundel EE, Yusuf N, Starr NJ, Anjum M, Arellano J, Howard HH, Shi W, Mulki S, Kurd-Misto T, Matar S, Liu X, Ahn J, Moussa C. Nilotinib

Effects on Safety, Tolerability, and Potential Biomarkers in Parkinson Disease: A Phase 2 Randomized Clinical Trial. *JAMA Neurol*. 2020;77(3):309-317.

Paisán-Ruíz C, Bhatia KP, Li A, Hernandez D, Davis M, Wood NW, Hardy J, Houlden H, Singleton A, Schneider SA. Characterization of PLA2G6 as a locus for dystonia-parkinsonism. *Ann Neurol*. 2009;65(1):19-23.

Paisán-Ruíz C, Jain S, Evans EW, Gilks WP, Simón J, van der Brug M, López de Munain A, Aparicio S, Gil AM, Khan N, Johnson J, Martinez JR, Nicholl D, Martí Carrera I, Pena AS, de Silva R, Lees A, Martí-Massó JF, Pérez-Tur J, Wood NW, Singleton AB. Cloning of the gene containing mutations that cause PARK8-linked Parkinson's disease. *Neuron*. 2004;44(4):595-600.

Pal GD, Ouyang B, Serrano G, Shill HA, Goetz C, Stebbins G, Metman LV, Driver-Dunckley E, Mehta SH, Caviness JN, Sabbagh MN, Adler CH, Beach TG, Arizona Study of Aging Neurodegenerative Disorders. Comparison of neuropathology in Parkinson's disease subjects with and without deep brain stimulation. *Mov Disord*. 2017;32(2):274-277.

Palle S, Neerati P. Improved neuroprotective efect of resveratrol nanoparticles as evinced by abrogation of rotenoneinduced behavioral defcits and oxidative and mitochondrial dysfunctions in rat model of Parkinson's disease. *Naunyn-Schmiedeberg's Arch Pharmacol*. 2018;391(4):445–453.

Pan T, Kondo S, Le W, Jankovic J. The role of autophagy-lysosome pathway in neurodegeneration associated with Parkinson's disease. *Brain*. 2008;131:1969–1978.

Pan T, Rawal P, Wu Y, Xie W, Jankovic J, Le W. Rapamycin protects against rotenone-induced apoptosis through autophagy induction. *Neuroscience*. 2009;164:541–551.

Pandareesh MD, Shrivash MK, Naveen Kumar HN, Misra K, Srinivas Bharath MM. Curcumin Monoglucoside Shows Improved Bioavailability and Mitigates Rotenone Induced Neurotoxicity in Cell and *Drosophila* Models of Parkinson's Disease. *Neurochem Res*. 2016;41(11):3113-3128.

Pandey UB, Nichols CD. Human disease models in *Drosophila melanogaster* and the role of the fly in therapeutic drug discovery. *Pharmacol Rev*. 2011;63(2):411-436.

Pan-Montojo F, Anichtchik O, Dening Y, Knels L, Pursche S, Jung R, Jackson S, Gille G, Spillantini MG, Reichmann H, Funk RH. Progression of Parkinson's disease pathology is reproduced by intragastric administration of rotenone in mice. *PLoS One*. 2010;5(1):e8762. doi: 10.1371/journal.pone.0008762.

Parama D, Boruah M, Yachna K, Rana V, Banik K, Harsha C, Thakur KK, Dutta U, Arya A, Mao X, Ahn KS, Kunnumakkara AB. Diosgenin, a steroidal saponin, and its analogs: Effective therapies against different chronic diseases. *Life Sci*. 2020;260:118182. doi: 10.1016/j.lfs.2020.118182.

Parenti I, Rabaneda LG, Schoen H, Novarino G. Neurodevelopmental Disorders: From Genetics to Functional Pathways. *Trends Neurosci*. 2020;43(8):608-621.

Park A, Stacy M. Disease-Modifying Drugs in Parkinson's Disease. *Drugs*. 2015;75(18):2065-2071.

Park J, Kim SY, Cha GH, Lee SB, Kim S, Chung J. *Drosophila* DJ-1 mutants show oxidative stress-sensitive locomotive dysfunction. *Gene*. 2005;361:133-139.

Park J, Lee SB, Lee S, Kim Y, Song S, Kim S, Bae E, Kim J, Shong M, Kim JM, Chung J. mitochondrial dysfunction in *Drosophila* PINK1 mutants is complemented by parkin. *Nature*. 2006;441(7097):1157-1161.

Parkhe A, Parekh P, Nalla LV, Sharma N, Sharma M, Gadepalli A, Kate A, Khairnar A. Protective effect of alpha mangostin on rotenone induced toxicity in rat model of Parkinson's disease. *Neurosci Lett.* 2020;716:134652. doi: 10.1016/j.neulet.2019.134652.

Parkinson Study Group. Cerebrospinal fluid homovanillic acid in the DATATOP study on Parkinson's disease. *Arch Neurol*. 1995;52(3):237-245.

Pasanen P, Myllykangas L, Siitonen M, Raunio A, Kaakkola S, Lyytinen J, Tienari PJ, Pöyhönen M, Paetau A. Novel α-synuclein mutation A53E associated with atypical multiple system atrophy and Parkinson's disease-type pathology. *Neurobiol Aging*. 2014;35(9):2180.e1-5. doi: 10.1016/j.neurobiolaging.2014.03.024.

Perlbarg V, Lambert J, Butler B, Felfli M, Valabrègue R, Privat AL, Lehéricy S, Petiet A. Alterations of the nigrostriatal pathway in a 6-OHDA rat model of Parkinson's disease evaluated with multimodal MRI. *PLoS One*. 2018;13(9):e0202597. doi: 10.1371/journal.pone.0202597.

Pesah Y, Burgess H, Middlebrooks B, Ronningen K, Prosser J, Tirunagaru V, Zysk J, Mardon G. Whole-mount analysis reveals normal numbers of dopaminergic neurons following misexpression of alpha-Synuclein in *Drosophila* . *Genesis*. 2005;41(4):154-159.

Pesah Y, Pham T, Burgess H, Middlebrooks B, Verstreken P, Zhou Y, Harding M, Bellen H, Mardon G. *Drosophila* parkin mutants have decreased mass and cell size and increased sensitivity to oxygen radical stress. *Development*. 2004;131(9):2183-2194.

Pest Management Regulatory Agency-Canada. Re-evaluation Note: Rotenone (REV2008-01), Consumer Product Safety, Health Canada. 2008: Available online at: http://publications.gc.ca/collections/collection_2008/pmra-arla/H113-5-2008-1E.pdf

Phom L, Achumi B, Alone DP, Muralidhara, Yenisetti SC: Curcumin's neuroprotective efficacy in *Drosophila* model of idiopathic Parkinson's disease is phase specific: implication of its therapeutic effectiveness. *Rejuvenation Res*. 2014;17(6):481–489.

Phom L, **Ayajuddin** M, Koza Z, Modi P, Jamir N, Yenisetti SC. A primary screening assay to characterize mobility defects in *Drosophila* model. . In: Experiments with *Drosophila* for Biology Courses (eds: S.C. Lakhotia and H.A. Ranganath). *Ind Acad of Sci.* 2021;pp 477-480. ISBN: 978-81-950664-2-1

Pletcher SD, Macdonald SJ, Marguerie R, Certa U, Stearns SC, Goldstein DB, Partridge L. Genome-wide transcript profiles in aging and calorically restricted *Drosophila melanogaster*. *Curr Biol*. 2002;12(9):712-723.

Plotegher N, Berti G, Ferrari E, Tessari I, Zanetti M, Lunelli L, Greggio E, Bisaglia M, Veronesi M, Girotto S, Dalla Serra M, Perego C, Casella L, Bubacco L. DOPAL derived alpha-synuclein oligomers impair synaptic vesicles physiological function. *Sci Rep*. 2017;7:40699. doi: 10.1038/srep40699.

Poirier AA, Aubé B, Côté M, Morin N, Di Paolo T, Soulet D. Gastrointestinal Dysfunctions in Parkinson's Disease: Symptoms and Treatments. *Parkinsons Dis*. 2016;2016:6762528. doi: 10.1155/2016/6762528.

Polymeropoulos MH, Lavedan C, Leroy E, Ide SE, Dehejia A, Dutra A, Pike B, Root H, Rubenstein J, Boyer R, Stenroos ES, Chandrasekharappa S, Athanassiadou A, Papapetropoulos T, Johnson WG, Lazzarini AM, Duvoisin RC, Di Iorio G, Golbe LI, Nussbaum RL. Mutation in the alpha-synuclein gene identified in families with Parkinson's disease. *Science*. 1997;276(5321):2045-2047.

Porter CC, Totaro JA, Stone CA. Effect of 6-hydroxydopamine and some other compounds on the concentration of norepinephrine in the hearts of mice. *J Pharmacol Exp Ther*. 1963;140:308-316.

Pouchieu C, Piel C, Carles C, Gruber A, Helmer C, Tual S, Marcotullio E, Lebailly P, Baldi I. Pesticide use in agriculture and Parkinson's disease in the AGRICAN cohort study. *Int J Epidemiol*. 2018;47(1):299-310.

Pramod Kumar P, Prashanth HKV. Diet with Low Molecular Weight Chitosan exerts neuromodulation in Rotenone induced *Drosophila* model of Parkinson's disease. *Food Chem Toxicol*. 2020;146:111860. doi: 10.1016/j.fct.2020.111860.

Prasad V, Wasser Y, Hans F, Goswami A, Katona I, Outeiro TF, Kahle PJ, Schulz JB, Voigt A. Monitoring α-synuclein multimerization in vivo. *FASEB J*. 2019;33(2):2116-2131.

Proukakis C, Dudzik CG, Brier T, MacKay DS, Cooper JM, Millhauser GL, Houlden H, Schapira AH. A novel α-synuclein missense mutation in Parkinson disease. *Neurology*. 2013;80(11):1062-1064.

Qiao J, Zhao Y, Liu Y, Zhang S, Zhao W, Liu S, Liu M. Neuroprotective effect of Ginsenoside Re against neurotoxin-induced Parkinson's disease models via induction of Nrf2. *Mol Med Rep*. 2022;25(6):215. doi: 10.3892/mmr.2022.12731.

Qiao P, Ma J, Wang Y, Huang Z, Zou Q, Cai Z, Tang Y. Curcumin Prevents Neuroinflammation by Inducing Microglia to Transform into the M2-phenotype via CaMKKβ-dependent Activation of the AMP-Activated Protein Kinase Signal Pathway. *Curr Alzheimer Res*. 2020;17(8):735-752.

Quadri M, Fang M, Picillo M, Olgiati S, Breedveld GJ, Graafland J, Wu B, Xu F, Erro R, Amboni M, Pappatà S, Quarantelli M, Annesi G, Quattrone A, Chien HF, Barbosa ER; International Parkinsonism Genetics Network, Oostra BA, Barone P, Wang J, Bonifati V. Mutation in the SYNJ1 gene associated with autosomal recessive, early-onset Parkinsonism. *Hum Mutat*. 2013;34(9):1208-1215.

Rai SN, Singh P. Advancement in the modelling and therapeutics of Parkinson's disease. *J Chem Neuroanat*. 2020;104:101752. doi: 10.1016/j.jchemneu.2020.101752.

Ramachandiran S, Hansen JM, Jones DP, Richardson JR, Miller GW. Divergent mechanisms of paraquat, MPP+, and rotenone toxicity: oxidation of thioredoxin and caspase-3 activation. *Toxicol Sci.* 2007;95:163–171.

Ramires Júnior OV, Alves BDS, Barros PAB, Rodrigues JL, Ferreira SP, Monteiro LKS, Araújo GMS, Fernandes SS, Vaz GR, Dora CL, Hort MA. Nanoemulsion Improves the Neuroprotective Effects of Curcumin in an Experimental Model of Parkinson's Disease. *Neurotox Res*. 2021;39(3):787-799.

Ramirez A, Heimbach A, Gründemann J, Stiller B, Hampshire D, Cid LP, Goebel I, Mubaidin AF, Wriekat AL, Roeper J, Al-Din A, Hillmer AM, Karsak M, Liss B, Woods CG, Behrens MI, Kubisch C. Hereditary parkinsonism with dementia is caused by mutations in ATP13A2, encoding a lysosomal type 5 P-type ATPase. *Nat Genet*. 2006;38(10):1184-1191.

Ramkumar M, Rajasankar S, Swaminathan Johnson WM, Prabu K, Venkatesh Gobi V. Demethoxycurcumin ameliorates rotenone-induced toxicity in rats. *Front Biosci (Elite Ed)*. 2019;11:1-11.

Rao SV, Muralidhara, Yenisetti SC, Rajini PS. Evidence of neuroprotective effects of saffron and crocin in a *Drosophila* model of parkinsonism. *Neurotoxicol*. 2016;52:230-242.

Rasyid A, Rahman AR, Jaalam K, Lelo A. Effect of different curcumin dosages on human gall bladder. *Asia Pac J Clin Nutr*. 2002;11(4):314-318.

Rees JN, Florang VR, Anderson DG, Doorn JA. Lipid peroxidation products inhibit dopamine catabolism yielding aberrant levels of a reactive intermediate. *Chem Res Toxicol*. 2007;20:1536–1542.

Reiter LT, Potocki L, Chien S, Gribskov M, Bier E. A systematic analysis of human disease-associated gene sequences in *Drosophila melanogaster*. *Genome Res*. 2001;11(6):1114-1125.

Ren Y, Zhao J, Feng J. Parkin binds to alpha/beta tubulin and increases their ubiquitination and degradation. *J Neurosci*. 2003;23:3316–3324.

Ried K, Travica N, Dorairaj R, Sali A. Herbal formula improves upper and lower gastrointestinal symptoms and gut health in Australian adults with digestive disorders. *Nutr Res*. 2020;76:37-51.

Ritz BR, Manthripragada AD, Costello S, Lincoln SJ, Farrer MJ, Cockburn M, Bronstein J. Dopamine transporter genetic variants and pesticides in Parkinson's disease. *Environ Health Perspect*. 2009;117(6):964-969.

Rujirachotiwat A, Suttamanatwong S. Curcumin upregulates transforming growth factor-β1, its receptors, and vascular endothelial growth factor expressions in an in vitro human gingival fibroblast wound healing model. *BMC Oral Health*. 2021;21(1):535. doi: 10.1186/s12903-021-01890-9.

Sadoughi F, Hallajzadeh J, Mirsafaei L, Asemi Z, Zahedi M, Mansournia MA, Yousefi B. Cardiac fibrosis and curcumin: a novel perspective on this natural medicine. *Mol Biol Rep. 2021;48(11):7597-7608.*

Saha S, Guillily MD, Ferree A, Lanceta J, Chan D, Ghosh J, Hsu CH, Segal L, Raghavan K, Matsumoto K, Hisamoto N, Kuwahara T, Iwatsubo T, Moore L, Goldstein L, Cookson M, Wolozin B. LRRK2 modulates vulnerability to mitochondrial dysfunction in Caenorhabditis elegans. *J Neurosci.* 2009;29(29):9210-9218.

Santo GD, de Veras BO, Rico E, Magro JD, Agostini JF, Vieira LD, Calisto JFF, Mocelin R, de Sá Fonseca V, Wanderley AG. Hexane extract from SpoSndias mombin L. (Anacardiaceae) prevents behavioral and oxidative status changes on model of Parkinson's disease in zebrafish. *Comp Biochem Physiol C Toxicol Pharmacol*. 2021;241:108953. doi: 10.1016/j.cbpc.2020.108953.

Sawin ER, Ranganathan R, Horvitz HR. C. elegans locomotory rate is modulated by the environment through a dopaminergic pathway and by experience through a serotonergic pathway. *Neuron*. 2000;26(3):619-631.

Schildknecht S, Di Monte DA, Pape R, Tieu K, Leist M. Tipping Points and Endogenous Determinants of Nigrostriatal Degeneration by MPTP. *Trends Pharmacol Sci*. 2017;38(6):541-555.

Segura-Aguilar J, Kostrzewa RM. Neurotoxin mechanisms and processes relevant to Parkinson's disease: an update. *Neurotox Res*. 2015;27(3):328-354.

Segura-Aguilar J, Paris I, Muñoz P, Ferrari E, Zecca L, Zucca FA. Protective and toxic roles of dopamine in Parkinson's disease. *J Neurochem*. 2014;129(6):898-915.

Selvaraj S, Piramanayagam S. Impact of gene mutation in the development of Parkinson's disease. *Genes Dis*. 2019;6(2):120-128.

Sharma N, Sharma S, Nehru B. Curcumin protects dopaminergic neurons against inflammation-mediated damage and improves motor dysfunction induced by single intranigral lipopolysaccharide injection. *Inflammopharmacol*. 2017;25(3):351-368.

Sharma PA, Steward WP, Gescher AJ. Pharmacokinetics and pharmacodynamics of curcumin. *Adv Exp Med Biol.* 2007;595:453-470.

Sharma RA, Euden SA, Platton SL, Cooke DN, Shafayat A, Hewitt HR, Marczylo TH, Morgan B, Hemingway D, Plummer SM, Pirmohamed M, Gescher AJ, Steward WP. Phase I clinical trial of oral curcumin: biomarkers of systemic activity and compliance. *Clin Cancer Res*. 2004;10(20):6847-6854.

Sherer TB, Betarbet R, Stout AK, Lund S, Baptista M, Panov AV, Cookson MR, Greenamyre JT. An in vitro model of Parkinson’s disease: linking mitochondrial impairment to altered alpha-synuclein metabolism and oxidative damage. *J Neurosci*. 2002;22:7006–7015.

Sherer TB, Betarbet R, Testa CM, Seo BB, Richardson JR, Kim JH, Miller GW, Yagi T, Matsuno-Yagi A, Greenamyre JT. Mechanism of toxicity in rotenone models of Parkinson's disease. *J Neurosci.* 2003;23(34):10756-10764.

Shojaee S, Sina F, Banihosseini SS, Kazemi MH, Kalhor R, Shahidi GA, Fakhrai-Rad H, Ronaghi M, Elahi E. Genome-wide linkage analysis of a Parkinsonian-pyramidal syndrome pedigree by 500 K SNP arrays. *Am J Hum Genet*. 2008;82(6):1375-1384.

Shukla AK, Ratnasekhar C, Pragya P, Chaouhan HS, Patel DK, Chowdhuri DK, Mudiam MKR. Metabolomic Analysis Provides Insights on Paraquat-Induced Parkinson-Like Symptoms in *Drosophila melanogaster*. *Mol Neurobiol*. 2016;53(1):254-269.

Siddique YH, Naz F, Jyoti S, Ali F, Rahul. Effect of Genistein on the Transgenic *Drosophila* Model of Parkinson's Disease. *J Diet Suppl*. 2019;16(5):550-563.

Siddique YH, Naz F, Jyoti S. Effect of curcumin on lifespan, activity pattern, oxidative stress, and apoptosis in the brains of transgenic *Drosophila* model of Parkinson's disease. *Biomed Res Int*. 2014;2014:606928. doi: 10.1155/2014/606928.

Siima AA, Stephano F, Munissi JJE, Nyandoro SS. Ameliorative effects of flavonoids and polyketides on the rotenone induced *Drosophila* model of Parkinson's disease. *Neurotoxicol*. 2020;81:209-215.

Smith TS, Parker WD Jr, Bennett JP Jr. L-dopa increases nigral production of hydroxyl radicals in vivo: potential L-dopa toxicity? *Neuroreport*. 1994;5(8):1009-1011.

Soh JW, Marowsky N, Nichols TJ, Rahman AM, Miah T, Sarao P, Khasawneh R, Unnikrishnan A, Heydari AR, Silver RB, Arking R. Curcumin is an early-acting stagespecific inducer of extended functional longevity in *Drosophila* . *Exp Gerontol*. 2013;48(2):229–239.

Spieles-Engemann AL, Behbehani MM, Collier TJ, Wohlgenant SL, Steece-Collier K, Paumier K, Daley BF, Gombash S, Madhavan L, Mandybur GT, Lipton JW, Terpstra BT, Sortwell CE. Stimulation of the rat subthalamic nucleus is neuroprotective following significant nigral dopamine neuron loss. *Neurobiol Dis*. 2010;39(1):105-115.

Stephano F, Nolte S, Hoffmann J, El-Kholy S, von Frieling J, Bruchhaus I, Fink C, Roeder T. Impaired Wnt signaling in dopamine containing neurons is associated with pathogenesis in a rotenone triggered *Drosophila* Parkinson's disease model. *Sci Rep*. 2018;8(1):2372. doi: 10.1038/s41598-018-20836-w.

Sudati JH, Vieira FA, Pavin SS, Dias GR, Seeger RL, Golombieski R, Athayde ML, Soares FA, Rocha JB, Barbosa NV. Valeriana officinalis attenuates the rotenone-induced toxicity in *Drosophila melanogaster*. *Neurotoxicol*. 2013;37:118-126.

Sulthana AS, Balakrishnan R, Renuka M, Mohankumar T, Manimaran D, Arulkumar K, Namasivayam E. PIASA, a novel peptide, prevents SH-SY5Y neuroblastoma cells against rotenone-induced toxicity. *Curr Mol Pharmacol*. 2022. doi: 10.2174/1874467215666220427103045.

Sulzer D, Alcalay RN, Garretti F, Cote L, Kanter E, Agin-Liebes J, Liong C, McMurtrey C, Hildebrand WH, Mao X, Dawson VL, Dawson TM, Oseroff C, Pham J, Sidney J, Dillon MB, Carpenter C, Weiskopf D, Phillips E, Mallal S, Peters B, Frazier A, Lindestam Arlehamn CS, Sette A. T cells from patients with Parkinson's disease recognize α-synuclein peptides. *Nature*. 2017;546(7660):656-661.

Sur M, Dey P, Sarkar A, Bar S, Banerjee D, Bhat S, Mukherjee P. Sarm1 induction and accompanying inflammatory response mediates age-dependent susceptibility to rotenone-induced neurotoxicity. *Cell Death Discov*. 2018;4:114. doi: 10.1038/s41420-018-0119-5.

Swarnkar S, Singh S, Mathur R, Patro IK, Nath C. A study to correlate rotenone induced biochemical changes and cerebral damage in brain areas with neuromuscular coordination in rats. *Toxicol*. 2010;272(1-3):17-22.

Tambasco N, Romoli M, Calabresi P. Levodopa in Parkinson's Disease: Current Status and Future Developments. *Curr Neuropharmacol*. 2018;16(8):1239-1252.

Tanner CM, Kamel F, Ross GW, Hoppin JA, Goldman SM, Korell M, Marras C, Bhudhikanok GS, Kasten M, Chade AR, Comyns K, Richards MB, Meng C, Priestley B, Fernandez HH, Cambi F, Umbach DM, Blair A, Sandler DP, Langston JW. Rotenone, paraquat, and Parkinson's disease. *Environ Health Perspect*. 2011;119(6):866-872.

Tanner CM, Ross GW, Jewell SA, Hauser RA, Jankovic J, Factor SA, Bressman S, Deligtisch A, Marras C, Lyons KE, Bhudhikanok GS, Roucoux DF, Meng C, Abbott RD, Langston JW. Occupation and risk of parkinsonism: a multicenter case-control study. *Arch Neurol*. 2009;66(9):1106-1113.

Tantucci M, Mariucci G, Taha E, Spaccatini C, Tozzi A, Luchetti E, Calabresi P, Ambrosini MV. Induction of heat shock protein 70 reduces the alteration of striatal electrical activity caused by mitochondrial impairment. *Neuroscience*. 2009;163:735–740.

Teerapattarakan N, Benya-Aphikul H, Tansawat R, Wanakhachornkrai O, Tantisira MH, Rodsiri R. Neuroprotective effect of a standardized extract of Centella asiatica ECa233 in rotenone-induced parkinsonism rats. *Phytomedicine*. 2018;44:65-73.

Tello JA, Williams HE, Eppler RM, Steinhilb ML, Khanna M. Animal models of neurodegenerative disease: Recent advances in fly highlight innovative approaches to drug discovery. *Front. Mol. Neurosci*. 2022;15:883358. doi: 10.3389/fnmol.2022.883358

Testa CM, Sherer TB, Greenamyre JT. Rotenone induces oxidative stress and dopaminergic neuron damage in organotypic substantia nigra cultures. *Brain Res Mol Brain Res*. 2005;134:109–118.

Thao DTP. Targeting UCH in *Drosophila melanogaster* as a model for Parkinson's disease. *Front Biosci (Landmark Ed)*. 2020;25:159-167.

Thiruchelvam M, Richfield EK, Baggs RB, Tank AW, Cory-Slechta DA. The nigrostriatal dopaminergic system as a preferential target of repeated exposures to combined paraquat and maneb: implications for Parkinson's disease. *J Neurosci*. 2000;20(24):9207-9214.

Thompson MD, Zhang XF. Response to: Neurotoxicity of paraquat and paraquat-induced Parkinson's disease. *Lab Invest*. 2016;96(9):1030-1034.

Tian S, Liao L, Zhou Q, Huang X, Zheng P, Guo Y, Deng T, Tian X. Curcumin inhibits the growth of liver cancer by impairing myeloid-derived suppressor cells in murine tumor tissues. *Oncol Lett*. 2021;21(4):286. doi: 10.3892/ol.2021.12547.

Tio M, Wen R, Lim YL, Zukifli ZHB, Xie S, Ho P, Zhou Z, Koh TW, Zhao Y, Tan EK. Varied pathological and therapeutic response effects associated with CHCHD2 mutant and risk variants. *Hum Mutat*. 2017;38(8):978-987.

Todd RD, Carl J, Harmon S, O'Malley KL, Perlmutter JS. Dynamic changes in striatal dopamine D2 and D3 receptor protein and mRNA in response to 1-methyl-4-phenyl-1,2,3,6-tetrahydropyridine (MPTP) denervation in baboons. *J Neurosci*. 1996;16(23):7776-7782.

Trounce IA, Kim YL, Jun AS, Wallace DC. Assessment of mitochondrial oxidative phosphorylation in patient muscle biopsies, lymphoblasts, and transmitochondrial cell lines. *Methods Enzymol*. 1996;264:484-509.

Tseng HC, Wang MH, Chang KC, Soung HS, Fang CH, Lin YW, Li KY, Yang CC, Tsai CC. Protective Effect of (-)Epigallocatechin-3-gallate on Rotenone-Induced Parkinsonism-like Symptoms in Rats. *Neurotox Res*. 2020;37(3):669-682.

Vaccari C, El Dib R, de Camargo JLV. Paraquat and Parkinson's disease: a systematic review protocol according to the OHAT approach for hazard identification. *Syst Rev*. 2017;6(1):98. doi: 10.1186/s13643-017-0491-x.

Valente EM, Salvi S, Ialongo T, Marongiu R, Elia AE, Caputo V, Romito L, Albanese A, Dallapiccola B, Bentivoglio AR. PINK1 mutations are associated with sporadic early-onset parkinsonism. *Ann Neurol*. 2004;56(3):336-341.

van Vliet SA, Blezer EL, Jongsma MJ, Vanwersch RA, Olivier B, Philippens IH. Exploring the neuroprotective effects of modafinil in a marmoset Parkinson model with immunohistochemistry, magnetic resonance imaging and spectroscopy. *Brain Res*. 2008;1189:219-228.

Varga SJ, Qi C, Podolsky E, Lee D. A new *Drosophila* model to study the interaction between genetic and environmental factors in Parkinson's disease. *Brain Res*. 2014;1583:277-286.

Ved R, Saha S, Westlund B, Perier C, Burnam L, Sluder A, Hoener M, Rodrigues CM, Alfonso A, Steer C, Liu L, Przedborski S, Wolozin B. Similar patterns of mitochondrial vulnerability and rescue induced by

genetic modification of alpha-synuclein, parkin, and DJ-1 in Caenorhabditis elegans. *J Biol Chem*. 2005;280(52):42655-42668.

Vehovszky A, Szabó H, Hiripi L, Elliott CJ, Hernádi L. Behavioural and neural deficits induced by rotenone in the pond snail Lymnaea stagnalis. A possible model for Parkinson's disease in an invertebrate. *Eur J Neurosci*. 2007;25(7):2123-2130.

Venderova K, Kabbach G, Abdel-Messih E, Zhang Y, Parks RJ, Imai Y, Gehrke S, Ngsee J, Lavoie MJ, Slack RS, Rao Y, Zhang Z, Lu B, Haque ME, Park DS. Leucine-Rich Repeat Kinase 2 interacts with Parkin, DJ-1 and PINK-1 in a *Drosophila melanogaster* model of Parkinson's disease. *Hum Mol Genet.* 2009;18(22):4390-4404.

Veyres N, Hamadjida A, Huot P. Predictive Value of Parkinsonian Primates in Pharmacologic Studies: A Comparison between the Macaque, Marmoset, and Squirrel Monkey. *J Pharmacol Exp Ther*. 2018;365(2):379-397.

Wan Z, Xu J, Huang Y, Zhai Y, Ma Z, Zhou B, Cao Z. Elevating bioavailable iron levels in mitochondria suppresses the defective phenotypes caused by PINK1 loss-of-function in *Drosophila melanogaster*. *Biochem Biophys Res Commun*. 2020;532(2):285-291.

Wang B, Su CJ, Liu TT, Zhou Y, Feng Y, Huang Y, Liu X, Wang ZH, Chen LH, Luo WF, Liu T. The Neuroprotection of Low-Dose Morphine in Cellular and Animal Models of Parkinson's Disease Through Ameliorating Endoplasmic Reticulum (ER) Stress and Activating Autophagy. *Front Mol Neurosci.* 2018;11:120. doi: 10.3389/fnmol.2018.00120.

Wang C, Lu R, Ouyang X, Ho MW, Chia W, Yu F, Lim KL. *Drosophila* overexpressing parkin R275W mutant exhibits dopaminergic neuron degeneration and mitochondrial abnormalities. *J Neurosci*. 2007;27(32):8563-8570.

Wang D, Qian L, Xiong H, Liu J, Neckameyer WS, Oldham S, Xia K, Wang J, Bodmer R, Zhang Z. Antioxidants protect PINK1-dependent dopaminergic neurons in *Drosophila* . *Proc Natl Acad Sci USA*. 2006;103(36):13520-13525.

Wang D, Tang B, Zhao G, Pan Q, Xia K, Bodmer R, Zhang Z. Dispensable role of *Drosophila* ortholog of LRRK2 kinase activity in survival of dopaminergic neurons. *Mol Neurodegener*. 2008;3:3. doi: 10.1186/1750-1326-3-3.

Wang HS, Toh J, Ho P, Tio M, Zhao Y, Tan EK. In vivo evidence of pathogenicity of VPS35 mutations in the *Drosophila* . *Mol Brain*. 2014;7:73. doi: 10.1186/s13041-014-0073-y.

Wang T, Li C, Han B, Wang Z, Meng X, Zhang L, He J, Fu F. Neuroprotective effects of Danshensu on rotenone-induced Parkinson's disease models in vitro and in vivo. *BMC Complement Med Ther*. 2020;20(1):20. doi: 10.1186/s12906-019-2738-7.

Wang X, Qin ZH, Leng Y, Wang Y, Jin X, Chase TN, Bennett MC. Prostaglandin A1 inhibits rotenone-induced apoptosis in SH-SY5Y cells. *J Neurochem*. 2002;83:1094–1102.

Wang Y, Gulis G, Buckner S, Johnson PC, Sullivan D, Busenlehner L, Marcus S. The MAP kinase Pmk1 and protein kinase A are required for rotenone resistance in the fission yeast, Schizosaccharomyces pombe. *Biochem Biophys Res Commun.* 2010;399:123–128.

Watabe M, Nakaki T. Mitochondrial complex I inhibitor rotenone-elicited dopamine redistribution from vesicles to cytosol in human dopaminergic SH-SY5Y cells. *J Pharmacol Exp Ther*. 2007;323(2):499-507.

Wen L, Wei W, Gu W, Huang P, Ren X, Zhang Z, Zhu Z, Lin S, Zhang B. Visualization of monoaminergic neurons and neurotoxicity of MPTP in live transgenic zebrafish. *Dev Biol*. 2008;314(1):84-92.

Wey MC, Fernandez E, Martinez PA, Sullivan P, Goldstein DS, Strong R. Neurodegeneration and motor dysfunction in mice lacking cytosolic and mitochondrial aldehyde dehydrogenases: implications for Parkinson's disease. *PLoS One*. 2012;7(2):e31522. doi: 10.1371/journal.pone.0031522.

Whitworth AJ, Theodore DA, Greene JC, Benes H, Wes PD, Pallanck LJ. Increased glutathione S-transferase activity rescues dopaminergic neuron loss in a *Drosophila* model of Parkinson's disease. *Proc Natl Acad Sci USA*. 2005;102(22):8024-8029.

Whitworth AJ, Wes PD, Pallanck LJ. *Drosophila* models pioneer a new approach to drug discovery for Parkinson's disease. *Drug Discov Today*. 2006;11(3-4):119-126.

Whitworth AJ. *Drosophila* models of Parkinson's disease. *Adv Genet*. 2011;73:1-50.

Witkamp RF, van Norren K. Let thy food be thy medicine….when possible. *Eur J Pharmacol*. 2018;836:102-114.

Xi Y, Ryan J, Noble S, Yu M, Yilbas AE, Ekker M. Impaired dopaminergic neuron development and locomotor function in zebrafish with loss of pink1 function. *Eur J Neurosci*. 2010;31(4):623-633.

Xicoy H, Wieringa B, Martens GJ. The SH-SY5Y cell line in Parkinson's disease research: a systematic review. *Mol Neurodegener*. 2017;12(1):10. doi: 10.1186/s13024-017-0149-0.

Xiong N, Huang J, Chen C, Zhao Y, Zhang Z, Jia M, Zhang Z, Hou L, Yang H, Cao X, Liang Z, Zhang Y, Sun S, Lin Z, Wang T. Dl-3-n-butylphthalide, a natural antioxidant, protects dopamine neurons in rotenone models for Parkinson's disease. *Neurobiol Aging*. 2011;33(8):1777-1791.

Xiong N, Zhang Z, Huang J, Chen C, Zhang Z, Jia M, Xiong J, Liu X, Wang F, Cao X, Liang X, Sun S, Lin Z, Wang T. Vegf-expressing human umbilical cord mesenchymal stem cells, an improved therapy strategy for parkinson’s disease. *Gene Ther.* 2010;18:394–402

Xiong Y, Ding H, Xu M, Gao J. Protective effects of Asiatic acid on ROT- or H2O2-induced injury in SH-SY5Y cells. *Neurochem Res*. 2009;34:746–754.

Xiong Y, Yu J. Modeling Parkinson's Disease in *Drosophila* : What Have We Learned for Dominant Traits? *Front Neurol*. 2018;9:228. doi: 10.3389/fneur.2018.00228.

Xu Y, Xie M, Xue J, Xiang L, Li Y, Xiao J, Xiao G, Wang HL. EGCG ameliorates neuronal and behavioral defects by remodeling gut microbiota and TotM expression in *Drosophila* models of Parkinson's disease. *FASEB J*. 2020;34(4):5931-5950.

Xue J, Wang HL, Xiao G. Transferrin1 modulates rotenone-induced Parkinson's disease through affecting iron homeostasis in *Drosophila melanogaster*. *Biochem Biophys Res Commun*. 2020;531(3):305-311.

Yamamoto S, Seto ES. Dopamine dynamics and signaling in *Drosophila*: an overview of genes, drugs and behavioral paradigms. *Exp Anim*. 2014;63(2):107-119.

Yang L, Beal MF. Determination of neurotransmitter levels in models of Parkinson's disease by HPLC-ECD. *Methods Mol Biol*. 2011;793:401-415.

Yang Y, Gehrke S, Haque ME, Imai Y, Kosek J, Yang L, Beal MF, Nishimura I, Wakamatsu K, Ito S, Takahashi R, Lu B. Inactivation of *Drosophila* DJ-1 leads to impairments of oxidative stress response and phosphatidylinositol 3-kinase/Akt signaling. *Proc Natl Acad Sci USA*. 2005;102(38):13670-13675.

Yang Y, Nishimura I, Imai Y, Takahashi R, Lu B. Parkin suppresses dopaminergic neuron-selective neurotoxicity induced by Pael-R in *Drosophila* . *Neuron*. 2003;37(6):911-924.

Yuan H, Ma Q, Ye L, Piao G. The Traditional Medicine and Modern Medicine from Natural Products. *Molecules*. 2016;21(5):559. doi: 10.3390/molecules21050559.

Yun JW, Ahn JB, Kang BC. Modeling Parkinson's disease in the common marmoset (Callithrix jacchus): overview of models, methods, and animal care. *Lab Anim Res*. 2015;31(4):155-165.

Zarranz JJ, Alegre J, Gómez-Esteban JC, Lezcano E, Ros R, Ampuero I, Vidal L, Hoenicka J, Rodriguez O, Atarés B, Llorens V, Gomez Tortosa E, del Ser T, Muñoz DG, de Yebenes JG. The new mutation, E46K, of alpha-synuclein causes Parkinson and Lewy body dementia. *Ann Neurol. 2004;55(2):164-173.*

Zeng XS, Geng WS, Jia JJ. Neurotoxin-Induced Animal Models of Parkinson Disease: Pathogenic Mechanism and Assessment. *ASN Neuro*. 2018;10:1759091418777438. doi: 10.1177/1759091418777438.

Zeng Y, Zhao H, Zhang T, Zhang C, He Y, Du L, Zuo F, Wang W. Curcumin against imiquimod-induced psoriasis of mice through IL-6/STAT3 signaling pathway. *Biosci Rep*. 2020:BSR20192842. doi: 10.1042/BSR20192842.

Zhang J, Li K, Wang X, Smith AM, Ning B, Liu Z, Liu C, Ross CA, Smith WW. Curcumin Reduced H2O2- and G2385R-LRRK2-Induced Neurodegeneration. *Front Aging Neurosci*. 2021;13:754956. doi: 10.3389/fnagi.2021.754956.

Zhang ZG, Niu XY, Lu AP, Xiao GG. Effect of curcumin on aged *Drosophila melanogaster*: a pathway prediction analysis. *Chin J Integr Med*. 2015;21(2):115-122.

Zhang ZN, Zhang JS, Xiang J, Yu ZH, Zhang W, Cai M, Li XT, Wu T, Li WW, Cai DF. Subcutaneous rotenone rat model of Parkinson's disease: Dose exploration study. *Brain Res*. 2017;1655:104-113.

Zhao HL, Song CH and Chai OH. Negative effects of curcumin on liver injury induced by alcohol. *Phytother Res* 2012;26(12):1857–1863.

Zhao X, Kong D, Zhou Q, Wei G, Song J, Liang Y, Du G. Baicalein alleviates depression-like behavior in rotenone- induced Parkinson's disease model in mice through activating the BDNF/TrkB/CREB pathway. *Biomed Pharmacother*. 2021;140:111556. doi: 10.1016/j.biopha.2021.111556.

Zhu B, Yin D, Zhao H, Zhang L. The immunology of Parkinson's disease. *Semin Immunopathol*. 2022. doi: 10.1007/s00281-022-00947-3.

Zia A, Farkhondeh T, Pourbagher-Shahri AM, Samarghandian S. The role of curcumin in aging and senescence: Molecular mechanisms. *Biomed Pharmacother*. 2021;134:111119. doi: 10.1016/j.biopha.2020.111119.

Zilocchi M, Finzi G, Lualdi M, Sessa F, Fasano M, Alberio T. Mitochondrial alterations in Parkinson's disease human samples and cellular models. *Neurochem Int*. 2018;118:61-72.

Zou X, Himbert S, Dujardin A, Juhasz J, Ros S, Stöver HDH, Rheinstädter MC. Curcumin and Homotaurine Suppress Amyloid-β25-35 Aggregation in Synthetic Brain Membranes. *ACS Chem Neurosci*. 2021;12(8):1395-1405.

CONFERENCES/SEMINARS/WORKSHOPS

International

- "4th International Conference on Neurology and Brain Disorders" supported by International Brain Research Organization (IBRO) held in Rome, Italy during 9-11 September 2021.
- "Fourth International Conference on Nutraceuticals and Chronic Diseases" held at Indian Institute of Technology, Guwahati, Assam, India during 23-25 September 2019.

National

- National Conference on "Contemporary Excitement in New Biology" held at Department of Zoology, Nagaland University, India during 30-31 October, 2018.
- National Seminar on "Recent Advances in Applied Biological Sciences" held at North East Hill University, Shillong, Meghalaya India during 4-5 May, 2018.
- National Seminar on "Climate Change and Sustainable Development with Special Focus on North East India" held at Nagaland University, Nagaland, India during 17-18 May, 2017.

International Workshops

- "Global Engagement Workshop on Neurodegenerative Diseases" supported by International Brain Research Organization (IBRO) held at Department of Biomedical Engineering, NEHU, Shillong during 1-5 October, 2021.
- "Anti-inflammatory Life Style for Prevention and Treatment of Cancer and Neurodegeneration: Facts and fiction" organized under "Global Initiative on Academic Network (GIAN) program" in collaboration with foreign faculty from USA held at Department of Zoology, Nagaland University during 1-5 October, 2019.

HONORS/AWARDS

- Awarded and availed **International Travel Grant** from **International Brain Research Organization (IBRO), France** to attend the **4th International Conference on Neurology and Brain Disorder** held in Rome, Italy on 9-11th September 2021.
- Awarded and availed **Senior Research Fellowship** from **Indian Council of Medical Research, Government of India, New Delhi** from 10th Sept. 2018 to 9th September 2020
- Awarded and availed **Junior Research Fellowship** from **Department of Biotechnology, Government of India, New Delhi**
- Awarded and availed **Non-NET fellowship** from **University Grant Commission** (**UGC**) through **Nagaland University**

PUBLICATIONS

- **Ayajuddin M**, Phom L, Koza Z, Modi P, Das A, Chaurasia R, Thepa A, Jamir N, Neikha K and Yenisetti S C. (2022) Adult health and transition stage-specific rotenone-mediated *Drosophila* model of Parkinson'sdisease: Impact on late-onset neurodegenerative disease models. *Front. Mol. Neurosci*. 15:896183. doi: 10.3389/fnmol.2022.896183

- **Ayajuddin M,** Das A, Phom L, Koza Z, Chaurasia R, Yenisetti SC. (2021) Quantification of dopamine and its metabolites in *Drosophila* brain using HPLC. In: *Experiments with Drosophila for Biology Courses* (Eds: S.C. Lakhotia and H.A. Ranganath). *Indian Academy of Sciences,* pp. 433-440. ISBN: 978-81-950664-2

- Phom L, **Ayajuddin M**, Koza Z, Modi P, Jamir N, Yenisetti SC. (2021) A primary screening assay to characterize mobility defects in *Drosophila* model. In: *Experiments with Drosophila for Biology Courses* (Eds: S.C. Lakhotia and H.A. Ranganath). *Indian Academy of Sciences.* pp. 477-480. ISBN: 978-81-950664-2-1

- Phom L, **Ayajuddin M**, Achumi B, Longkumer I, Koza Z, Modi P, Yenisetti SC. (2021) Extraction of Genomic DNA from single *Drosophila* fly. In: *Experiments with Drosophila for Biology Courses* (Eds: S.C. Lakhotia and H.A. Ranganath). *Indian Academy of Sciences.* pp. 337-340. ISBN: 978-81-950664-2-1

- **Ayajuddin M**, Das A, Phom L, Modi P, Chaurasia R, Koza Z, Thepa A, Jamir N, Singh PR, Sentinungla, Lal P and Yenisetti SC. (2018) Parkinson's Disease: Insights from *Drosophila* Model. In: *Drosophila melanogaster - Model for Recent Advances in Genetics and Therapeutics* (Ed: Farzana Khan Perveen). *InTechOpen* pp. 157-192. http://dx.doi.org/10.5772/intechopen.72021. ISBN: 978-953-51-3854-9

- **Ayajuddin M**, Modi P, Achumi B, Muralidhara and Yenisetti SC. (2016) Plant products and fermented foods as nutrition and medicine in Manipur state of North-East India: Pharmacological authenticity. In: *Bioprospecting of Indigenous Bioresources of North-East India* (Ed: Jubilee Purkayastha). *Springer Science.* 10; 165-179.

- Achumi B, **Ayajuddin M**, Phom L, Hegde SN, Lal P, Singh OP, Yenisetti SC (2016) Drosophilid (Insecta, Diptera: Drosophilidae) Biodiversity of North-East India. In: *Bioprospecting of Indigenous Bioresources of North East India*. (Ed: Jubilee Purkayastha) *Springer Science* 14; 231-251.

- Modi P, **Ayajuddin M***, Phom L, Koza Z, Das A, Chaurasia R, Samadder S, Achumi B, Muralidhara, Pukhrambam RS, Yenisetti SC (2016) Understanding Pathophysiology of Sporadic Parkinson's Disease in *Drosophila* Model: Potential Opportunities and Notable Limitations. In: *Challenges in Parkinson's Disease.* (Eds: Jolanta Dorszewska and Wojciech Kozubski) *InTechOpen.* pp. 217-244 *DOI: 10.5772/63767*. ISBN: 978-953-51-2464-1 (*equal contribution).

- Achumi B, Phom L, Koza Z, **Ayajuddin M**, Lal P, Yenisetti SC (2014) Eco-geopraphic Pattern of Genus *Drosophila* (Insecta, Diptera: Drosophilidae) in Nagaland State, India. *Nagaland University Research Journal*. 7; 320-337.

Sub-editor of Book:

- Dopamine: Health and Disease (2018) Editor: Sarat Chandra Yenisetti, sub-editors: Limamanen Phom and **Ayajuddin M**, *InTechOpen, UK.* http://dx.doi.org/10.5772/intechopen.74360

Manuscript under preparation:

- Adult Life Phase Specific Dopaminergic Neuroprotective Efficacy of Curcumin is Mediated through Differential Modulation of Dopamine Metabolism: Insights from *Drosophila* Model of Parkinson’s Disease